ZooKeys 1009: 1–28 (2021)
doi: 10.3897/zookeys.1009.59205
https://zookeys.pensoft.net

RESEARCH ARTICLE

A peer-reviewed open-access journal
ZooKeys
Launched to accelerate biodiversity research

Three new species of *Cataglyphis* Foerster, 1850 (Hymenoptera, Formicidae) from Iran

Arsalan Khalili-Moghadam[1], Sebastian Salata[2,3], Lech Borowiec[2]

1 *Plant Protection Department, Agricultural College, Shahrekord University, Shahrekord, Iran* **2** *Department of Biodiversity and Evolutionary Taxonomy, University of Wrocław, Przybyszewskiego 65, 51–148 Wrocław, Poland* **3** *California Academy of Sciences, 55 Music Concourse Dr, San Francisco, CA 94118, USA*

Corresponding author: Sebastian Salata (sdsalata@gmail.com)

Academic editor: B.L. Fisher | Received 1 October 2020 | Accepted 10 December 2020 | Published 4 January 2021

http://zoobank.org/535597AB-2281-45E9-BF99-4E72EB225A54

Citation: Khalili-Moghadam A, Salata S, Borowiec L (2021) Three new species of *Cataglyphis* Foerster, 1850 (Hymenoptera, Formicidae) from Iran. ZooKeys 1009: 1–28. https://doi.org/10.3897/zookeys.1009.59205

Abstract

Cataglyphis bazoftensis **sp. nov.**, *C. fritillariae* **sp. nov.**, and *C. dejdaranensis* **sp. nov.** are described from the Koohrang county of central-west Iran (Chaharmahal va Bakhtiari Province). All new species belong to the *C. altisquamis* complex and are characterized by presence of the thick, black, and decumbent setae on lateral and posterior surfaces of tibiae. Additionally, a key to Asian *Cataglyphis* was updated to accommodate the new species.

Keywords

Central-western Iran, eastern Mediterranean, key to species, taxonomy

Introduction

Cataglyphis Foerster, 1850 is a moderately large ant genus comprising 94 valid species and 18 valid subspecies divided into nine species groups (Agosti 1990; Bolton 2020). Its representatives are distributed mostly in the Palearctic Region's semideserts and deserts (Agosti 1990; Brown 2000). However, *Cataglyphis* species were also recorded from other arid habitats, such as high altitude, mountain steppes, and forest steppes

(Agosti 1990; Brown 2000). Members of the genus are among the commonest ants of the arid ecosystems of North Africa, Arabian Peninsula, and Central Asia, where they build crater nests directly in the ground (Agosti 1990; Collingwood and Agosti 1996; Brown 2000) and feed on dead insects (Lenoir et al. 2010). They have been reported as flower pollinators (Herrera et al. 1984) and as contributors in myrmecochorous seed dispersal (Hulme 1997; Boulay et al. 2007; Wehner 2020).

Many *Cataglyphis* species are polymorphic what causes challenges in their determination. Additionally, distinct polymorphism makes it necessary to prepare descriptions of new species based on nest samples. This approach should ensure comprehensive descriptions based on a detailed overview of infraspecific variability of studied samples. One should remember that genetic studies of some species did not confirm their homogeneity and suggested the presence of cryptic species and a high level of hybridization (Ionescu and Eyer 2016; Eyer et al. 2017).

The worldwide revision of the genus by Santschi (1929) is outdated, and the only relatively modern and global review of *Cataglyphis* was published three decades ago (Agosti 1990). On the regional level, the genus was studied for Arabian Peninsula (Collingwood and Agosti 1996; Sharaf et al. 2015), Armenia (Arakelian 1994), Bulgaria (Atanasov and Dlussky 1992), Northwest China (Chang and He 2002), Iraq (Pisarski 1965), Kingdom of Saudi Arabia (Collingwood 1985), Morocco (Cagniant 2009), Portugal (Collingwood and Prince 1998), Turkmenistan (Dlussky et al. 1992), former European U.S.S.R. (Arnol'di and Dlussky 1978), Asia (Radchenko 1997, 1998), Iberian Peninsula (Collingwood 1978), and Central and North Europe (Seifert 2018). Recent publications, which include changes in taxonomic status of some species and descriptions of new ones, show that the diversity of *Cataglyphis* is underestimated (Radchenko and Paknia 2010; Collingwood et al. 2011; Amor and Ortega 2014; Sharaf et al. 2015; Ionescu and Eyer 2016; Salata and Borowiec 2018).

Due to its location, geography, and predominance of open and arid habitats, Iran hosts the highest number of *Cataglyphis* worldwide (Paknia et al. 2008, Janicki et al. 2016). So far, there are 32 species of the genus known from the county, but some records need verification and confirmation (Paknia et al. 2008, 2009; Moradloo et al. 2015; Rad et al. 2018). The present work is a contribution to the understanding of the Iranian *Cataglyphis*. We describe three new species of the *C. altisquamis* species group (sensu Agosti 1990): *C. bazoftensis* sp. nov., *C. fritillariae* sp. nov., and *C. dejdaranensis* sp. nov. based on the worker caste. The *C. altisquamis* species group is characterized by the following combination of characters in the worker caste: relatively large (WL up to 5 mm); body dull, uniformly yellow-black to black or bicolored with black gaster, petiole cuneiform or pseudo-nodiform, head finely reticulate with punctulate frons. The geographic range of this group extends from Portugal and Morocco to Central Asia. Members of this group were included in Radchenko's key (1998) to the Asian *Cataglyphis*. Herein, we modify the key to accommodate the new species. Additionally, we also included in the key *C. asiriensis* Collingwood, 1985, a member of the *altisquamis* species group known from Saudi Arabia, which was omitted by Radchenko (1998).

Materials and methods

Investigated specimens were collected from five sites in the Koohrang County, located in the northern part of the Chaharmahal va Bakhtiari Province of Iran. All sites were placed at altitude from 1738 to 2778 m. a.s.l. The county is surrounded by the Zagros Mountains, one of the two largest mountain ranges of Iran, and is characterized by an alpine climate. The only exception is the Bazoft region, which is warmer than other parts of the Koohrang County and covered by deciduous oak forests.

The dominant sampling method was a direct sampling (hand collecting). Individual specimens were collected on the ground or from nests under stones. All specimens were preserved in 75% EtOH. Photos were taken using a Nikon SMZ 1500 stereomicroscope, Nikon D5200 photo camera, and Helicon Focus software. All given label data are in the original spelling, only the geographic coordinates are given in decimal notation, instead of the degrees, minutes, seconds on the labels; a vertical bar (|) separates data on different rows and double vertical bars (||) separate labels. Type specimens' photographs are available online on AntWeb (www.AntWeb.org) and are accessible using the unique CASENT identifying specimen code.

Museum abbreviations (Evenhuis 2020):

MNHW Museum of Natural History, University of Wrocław, Poland, in temporary deposit in Department of Biodiversity and Evolutionary Taxonomy, University of Wrocław, Poland;
MHNG Muséum d'Historie Naturelle, Genève, Switzerland;
USMB Upper Silesian Museum, Bytom, Poland.

Pilosity inclination degree follows that used in Wilson (1955). Adpressed (0–5°) hairs run parallel or nearly parallel to the body surface. Decumbent hairs stand 10–40°, subdecumbent hair stands ~45° from the surface, suberect hairs bend about 10–20° from vertical, and erect hairs stand vertical or nearly vertical.

Measurements: all measurements are given in mm.

HFL hind femur length; measured on dorsal side from trochanter to apex of femur;
HL head length; measured in a straight line from mid-point of anterior clypeal margin to mid-point of posterior margin in full-face view;
HW head width; measured in full-face view directly behind the eyes;
PRL propodeum length; measured in lateral view, from metanotal groove to posterior-most point of propodeum;
PRW propodeal width; maximum width of propodeum in dorsal view;
PTH petiole height; the chord of ventral petiolar profile at node level is the reference line perpendicular to which the maximum height of petiole is measured, measured in lateral view;
PTW petiole width; maximum width of the petiolar node in lateral view;
PW pronotum width; maximum width of pronotum in dorsal view;

SL scape length; maximum straight-line length of scape excluding the basal condylar bulb;
WL Weber's length; measured as diagonal length from the anterior end of the neck shield to the posterior margin of the propodeal lobe.

Ratios

CI cephalic index, HL/HW;
FI femur index, HFL/WL;
PI petiole index, PTH/PTW;
SI scape index, SL/HL.

Results

Synoptic list of *Cataglyphis* of Iran

The list is created based on data from Paknia et al. (2008) and Janicki et al. (2016), while the species-group divisions follows Agosti (1990) and Radchenko and Paknia (2010).

***Cataglyphis albicans* species group**
Cataglyphis albicans (Roger, 1859)
First record from Iran: Ghahari et al. (2011).
Cataglyphis alibabae Pisarski, 1965
First record from Iran: Rad et al. (2018).
Cataglyphis aurata Menozzi, 1932
First record from Iran: Ghahari et al. (2009).
Cataglyphis cinnamomea (Karavaiev, 1910)
First record from Iran: Paknia et al. (2010).
Cataglyphis cuneinodis Arnol'di, 1964
First record from Iran: Radchenko (1998).
Cataglyphis elegantissima Arnol'di, 1968
First record from Iran: Radchenko (1998).
Cataglyphis livida (André, 1881)
First record from Iran: Forel (1904).
Cataglyphis rubra (Forel, 1903)
First record from Iran: Radchenko (1998).
Cataglyphis semitonsa Santschi, 1929
First record from Iran: Ghahari et al. (2009).
Cataglyphis viaticoides (André, 1881)
First record from Iran: Rad et al. (2018).

***Cataglyphis alitisquamis* species group**
Cataglyphis altisquamis (André, 1881)
First record from Iran: Paknia et al. (2008).

Cataglyphis bazoftensis sp. nov.
Cataglyphis bucharica Emery, 1925
First record from Iran: Radchenko (1998).
Cataglyphis dejdaranensis sp. nov.
Cataglyphis foreli (Ruzsky, 1903)
First record from Iran: Forel (1904).
Cataglyphis fritillariae sp. nov.
Cataglyphis kurdistanica Pisarski, 1965
First record from Iran: Paknia et al. (2010).

***Cataglyphis bicolor* species group**
Cataglyphis abyssinica (Forel, 1904)
First record from Iran: Ghahari and Collingwood (2011).
Cataglyphis bellicosa (Karavaiev, 1924)
First record from Iran: Karavaiev (1924).
Cataglyphis bergiana Arnol'di, 1964
First record from Iran: Paknia et al. (2010).
Cataglyphis diehlii (Forel, 1902)
First record from Iran: Ghahari and Collingwood (2011).
Cataglyphis isis (Forel, 1913)
First record from Iran: Crawley (1920).
Cataglyphis longipedem (Eichwald, 1841)
First record from Iran: Forel (1904).
Cataglyphis nigra (André, 1881)
First record from Iran: Forel (1904).
Cataglyphis nodus (Brullé, 1833)
First record from Iran: Radchenko (1998).
Cataglyphis oasium Menozzi, 1932
First record from Iran: Ionescu and Eyer (2016).
Cataglyphis setipes (Forel, 1894)
First record from Iran: Radchenko (1998).
Cataglyphis stigmata Radchenko & Paknia, 2010
First record from Iran: Radchenko and Paknia (2010).

***Cataglyphis cursor* species group**
Cataglyphis aenescens (Nylander, 1849)
First record from Iran: Forel (1904).
Cataglyphis cugiai Menozzi, 1939
First record from Iran: Paknia et al. (2010).
Cataglyphis frigida (André, 1881)
First record from Iran: Emery (1906).
Cataglyphis frigida persica (Emery, 1906)
First record from Iran: Emery (1906).

Cataglyphis pubescens Radchenko & Paknia, 2010
First record from Iran: Radchenko and Paknia (2010).

***Cataglyphis nigripes* species group**
Cataglyphis nigripes Arnol'di, 1964
First record from Iran: Radchenko (1998).

***Cataglyphis pallida* species group**
Cataglyphis emeryi (Karavaiev, 1911)
First record from Iran: Radchenko (1998).

Taxonomy

***Cataglyphis bazoftensis* sp. nov.**
http://zoobank.org/A586710F-F2AE-496E-91F3-93A454CF641E
Figs 1–8, 27

Type material. ***Holotype*:** major worker (CASENT0872262): IRAN, Chaharmahal Va | Bakhtiari, Koohrang (Bazoft) | 1 VII 2017, 1754 m | leg. Khalili-Moghadam | 32.2969 / 49.9358 || LBC || LBC-IR00083 (MNHW); ***paratypes*:** 12 major, 2 medium and 9 minor workers (CASENT0872263–CASENT0872285): the same data as holotype (MNHW, MHNG, USMB); 3 major, 2 medium and 4 minor workers (CASENT0872286–CASENT0872294): IRAN, Chaharmahal Va | Bakhtiari, Koohrang (Bazoft) | 1 VII 2017, 1798 m | leg. Khalili-Moghadam | 32.2927 / 49.9391 || Collection L. Borowiec || LBC-IR00082 (MNHW, MHNG); three major workers (CASENT0872295–CASENT0872297): IRAN, Chaharmahal Va | Bakhtiari, Koohrang (Bazoft) | 1 VII 2017, 1886 m | leg. Khalili-Moghadam | 32.4855 / 49.7472 || LBC | Formicidae | LBC-IR00079 (MNHW, MHNG); major worker (CASENT0872298): IRAN, Chaharmahal Va | Bakhtiari, Koohrang (Bazoft) | 1 VII 2017, 1738 m | leg. Khalili-Moghadam | 32.3766 / 49.8594 || LBC | Formicidae | LBC-IR00079 (MNHW).

Diagnosis. Bicolored body combined with thick, dense, black, decumbent setae on femora and tibiae resemble characters typical for species of the *Cataglyphis setipes* complex. *Cataglyphis bazoftensis* distinctly differs from them in the cuneiform petiolar node, which is distinctly nodiform among members of the *setipes* complex. At first glance, large species of the *Cataglyphis bucharica* complex, with cuneiform petiole, resemble *C. bazoftensis,* but most of these species differ in femora and tibiae lacking thick, black, decumbent setae. Members of the *bucharica* complex with setose femora and tibiae differ in the presence of black, erect setae on the posterior part of the head. *Cataglyphis kurdistanica* Pisarski is the most similar to *C. bazoftensis*, but differs in the presence of the major soldier caste, and posterior part of head and propodeum covered with long, black and erect setae. *Cataglyphis altisquamis* (André) and *C. foreli* (Ruzsky) differ from *C. bazoftensis* in major workers with reddish brown to brownish black head

Figures 1, 2. Major worker of *Cataglyphis bazoftensis* sp. nov. **1** dorsal **2** lateral. Scale bar 2 mm.

and mesosoma; while *C. bazoftensis* has major workers with uniformly red head and mesosoma (only the smallest majors of *C. bazoftensis* can be sometimes reddish brown).

Description. Major worker (n = 10): ***Measurements.*** HL: 2.945 (2.72–3.04); HW: 2.738 (2.42–2.88); SL: 3.600 (3.39–3.80); PW: 1.923 (1.77–2.05); PRL: 1.732 (1.59–1.78); PRW: 1.457 (1.27–1.58); PTH: 0.955 (0.81–1.05); PTW: 0.945 (0.87–

Figure 3. Major worker of *Cataglyphis bazoftensis* sp. nov., head and antennae. Scale bar 2 mm.

1.00); WL: 4.580 (4.25–4.78); HFL: 5.308 (5.12–5.58); CI: 1.077 (1.056–1.124); SI: 1.223 (1.184–1.246); PI: 1.011 (0.931–1.114); FI: 1.160 (1.105–1.205). ***Color.*** Head, mesosoma, and petiolar node red in the largest major workers; the percentage of brown in body coloration increases in smaller major workers with the smallest major workers reddish brown. Legs most often black or black with brownish black coxa; in the largest major workers coxa and trochanters mostly reddish brown to brown with darker brown spots of diffused borders; in the palest specimens femora brownish black with reddish iridescence, tibiae sometimes reddish brown apically, and tarsi reddish brown to brown. Antennal scapus red to red-brown; only in the darkest major workers brown; funicles darker than scapus, from brown to almost black, only in the palest specimens red-brown (Fig. 3). ***Head.*** Square; approximately 1.05× as long as wide; sides below eyes almost parallel, above eyes gently convex; posterior margin of head almost straight (Fig. 3). Anterior clypeal margin convex; without central impression; clypeal plate with three or four long black central setae and a pair of moderately long basal setae; anterior clypeal margin with a row of short black setae, and 8–10 long black setae, the longest as long as 0.75 length of clypeus; some workers have long setae often worn off or broken. Clypeus shiny and densely microreticulate; covered with very sparse and short, appressed pubescence. Eyes large and oval; approximately 1.3–1.4× as long as wide. Frontal carinae short; not extending beyond frontal lobes; interocular area with thin and shiny line and a pair of long black setae. Antennal fossa shallow; opalescent and densely microreticulated. Head shiny and densely microreticulate; mostly without

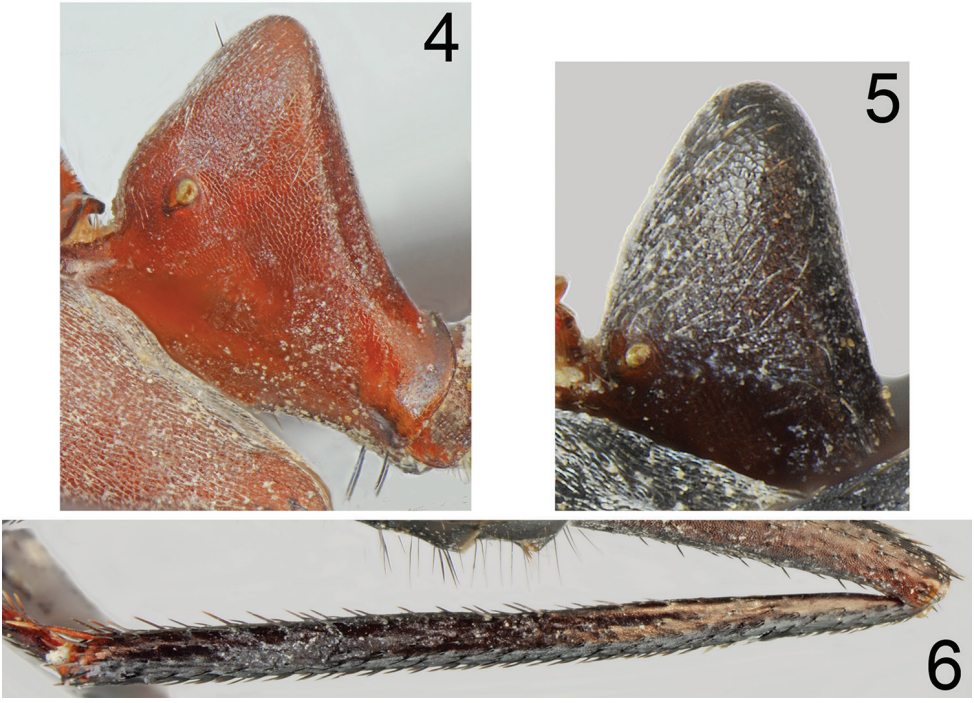

Figures 4–6. *Cataglyphis bazoftensis* sp. nov. **4** petiole of major worker **5** petiole of minor worker **6** hind tibia (not to scale).

appressed pubescence; only antennal fossa, posterior margin of head, and gular parts covered with sparse, short, adpressed hairs. Ocellar region with 2–4 moderately long and black setae; posterior angles without black setae; rest of frontal and lateral faces of head without erect setae; ventral side with a dozen yellowish to brown setae; interocular and ocular setae often broken. Antennal scape long; in frontal view almost straight, 1.3× as long as width of the head; base without tooth; apex slightly and gradually widening; funiculus long; pedicel elongated, approximately 0.82× as long as segments II and III combined, 1.6× as long as segment II (Fig. 3). Surface of scape densely microsculptured; distinctly to moderately shiny; covered with thick, moderately dense and decumbent setae. Mandibles rounded; basally smooth and shiny; apical ¾ length with deep grooves; surface shiny with several long yellow setae; masticatory margin with four large teeth. ***Mesosoma.*** Long; 2.4× as long as wide; metanotal groove shallow (Fig. 2). Pronotum convex on sides (Fig. 1). In lateral view promesonotum slightly arched in profile; propodeum positioned lower than promesonotum, moderately convex in lateral view (Fig. 2). Mesosoma shiny and densely microreticulated; covered with sparse, short, appressed pubescence; lateral sides of pronotum and mesonotum almost hairless; anterior part of pronotum, posterior angles of both mesonotum and propodeum with indistinct vestiture. Pronotum and mesonotum without erect setae; propodeum without or with one or two short, black, erect setae. ***Petiole.*** Cuneiform; in lateral view almost

Figures 7, 8. Minor worker of *Cataglyphis bazoftensis* sp. nov. **7** dorsal **8** lateral. Scale bar 2 mm.

triangular with very short peduncle. Anterior face in front of spiracle distinctly convex; posterior face almost flat; top of petiole in lateral view obtusely angulate, lacking erect setae; sometimes frontal face apically with a single short seta. In anterior or posterior view petiolar dorsum emarginated. Surface of petiole distinctly microreticulated; shiny to slightly opalescent. ***Gaster.*** Dull and distinctly microreticulate. Whole surface of

gaster with indistinct, sparse, appressed pubescence; tergites I and II without erect setae; tergite III with 2–4 long, black, central setae placed close to anterior margin, and none or one seta at lateral margin; tergite IV in with 6–8 long black setae; setosity in older specimens usually broken (Fig. 2). Each of gastral sternites with three or four long, black, erect setae. ***Legs.*** Dorsal and lateral surfaces of femora and tibiae covered with thick, dense, black, decumbent setae; interspaces between setae hairless. Ventral surfaces of femora and tibiae with numerous long, black, suberect to erect, spiniform setae.

Minor worker (n = 10): ***Measurements.*** HL: 1.308 (1.27–1.41); HW: 1.138 (1.09–1.22); SL: 1.270 (1.20–1.43); PW: 0.815 (0.76–0.88); PRL: 0.738 (0.68–0.82); PRW: 0.593 (0.55–0.65); PTH: 0.507 (0.47–0.56); PTW: 0.363 (0.34–0.40); WL: 1.957 (2.02–2.48); HFL: 1.697 (1.59–1.86); CI: 1.151 (1.142–1.174); SI: 0.970 (0.930–1.014); PI: 1.396 (1.342–1.559); FI: 0.867 (0.834–0.883).

Color. Head and mesosoma uniformly brown to black or brown with diffused red-brown parts; gaster, petiole, femora, and tibiae brown; trochanters and tarsi yellow-brown. Younger specimens often paler than older specimens, with large areas of body yellowish brown. Antennae bright brown, only in younger specimens mostly yellowish to yellowish brown (Figs 7, 8). ***Head.*** More elongated than in major workers; 1.2× as long as wide; below eyes parallel sided, behind eyes regularly rounded; posterior margin of head convex. Anterior clypeal margin convex with shallow impression in central part. Eyes large and oval; 1.3–1.4× as long as wide. Sculpture and setation of head and legs same as in major worker. ***Mesosoma.*** Same as in major worker. ***Petiole.*** More conical than cuneiform; dorsum more rounded, anterior face slightly convex (Fig. 5). ***Gaster.*** Strongly microreticulated and dull. Tergites I and II without erect setae; tergite III with only a pair of black setae centrally; tergite IV with two long, and two short black setae; in older specimens, setae usually partially broken (Fig. 8). Each of gastral sternites with 2–4 long, black, erect setae.

Biology. Little known, nests were found under stones inside a deciduous, oak forest surrounded by a grazing area. All collecting sites were in alpine zone, from 1738 to 1886 m a.s.l.

Etymology. The species name *bazoftensis* is a feminine Latin adjective in the nominative case and refers to the Bazoft region of the Koohrang County, the type locality for this species.

Cataglyphis fritillariae sp. nov.

http://zoobank.org/25117B97-D60C-4746-98AA-816D3C1259C3
Figs 9–16, 28

Type material. ***Holotype*****:** major worker (CASENT0872299): IRAN, Chaharmahal Va | Bakhtiari, Koohrang | Dashte laleh, 2400 m || 32.5884 / 50.2002 | 25 V 2017 | A. Khalili-Moghadam || Collection L. Borowiec | Formicidae | LBC-IR00069 (MNHW); ***paratypes*****:** 16 major, 11 medium and 43 minor workers (CASENT0872300-CASENT0872369): the same data as holotype (MNHW, MHNG, USMB).

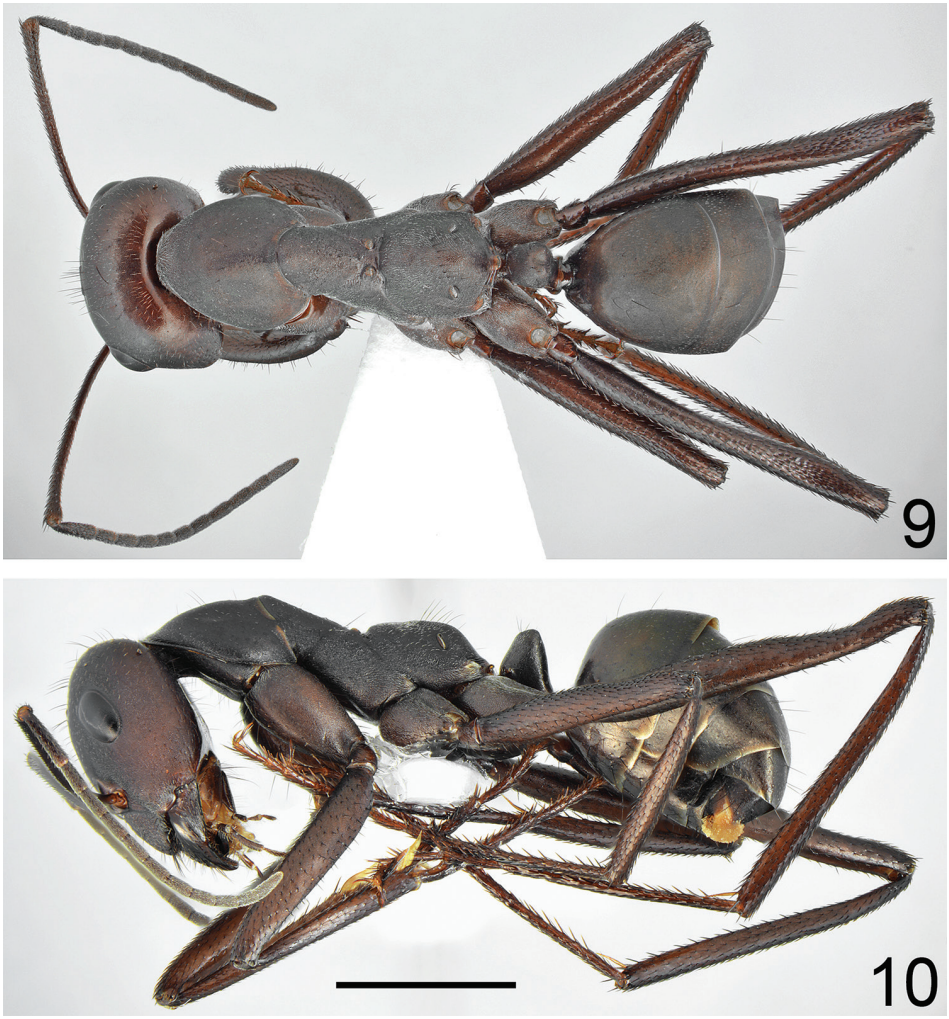

Figures 9, 10. Major worker of *Cataglyphis fritillariae* sp. nov. **9** dorsal **10** lateral. Scale bar 2 mm.

Other material. Two major and two minor workers: IRAN, Chaharmahal Va | Bakhtiari, Koohrang (Dashte | laleh), 25 IV 2017, 2400 m | leg. Khalili-Moghadam | 32.5886 / 50.2002 || Collection L. Borowiec | Formicidae | LBC-IR00084 (MNHW); 7 major workers: IRAN, Chaharmahal Va | Bakhtiari, Koohrang (Dashte | laleh), 25 IV 2017, 2391 m | leg. Khalili-Moghadam | 32.5875 / 50.2002 || Collection L. Borowiec | Formicidae | LBC-IR00086 (MNHW); two major workers: IRAN, Chaharmahal Va | Bakhtiari, Koohrang (Soodejan) | 25 IV 2017, 2143 m | leg. Khalili-Moghadam | 32.5425 / 50.3505 || Collection L. Borowiec | Formicidae | LBC-IR00087 (MNHW); major worker: IRAN, Chaharmahal Va | Bakhtiari, Koohrang (Dashte | laleh), 25 IV 2017, 2400 m | leg. Khalili-Moghadam | 32.5886 / 50.2002 || Collection L. Borowiec | Formicidae | LBC-IR00078 (MNHW).

Figure 11. Major worker of *Cataglyphis fritillariae* sp. nov., head and antennae. Scale bar 1 mm.

Diagnosis. *Cataglyphis fritillariae* belongs to a group of large species with well-developed and dull body sculpture. Femora and tibiae covered with thick, dense, black, decumbent setae cluster this species with the *Cataglyphis setipes* complex, while the shape of the petiolar node groups it with the *C. altisquamis* complex. At first glance, *C. foreli* appears similar to *C. fritillariae*, but it differs by the trapezoidal profile of petiole, larger eyes, and lack of thick, black, decumbent setae on femora and tibia. *Cataglyphis kurdistanica* Pisarski has similar petiole and black decumbent setae on legs, but it can be separated by the bicolored body and the presence of a soldier caste. *Cataglyphis bucharica* also appears similar to *C. fritillariae,* but it is readily recognized by reddish head and mesosoma, presence of numerous erect setae on propodeum, longer propodeal spiracle, and absence of thick, black, decumbent setae on femora. *Cataglyphis asiriensis* Collingwood, known from the Asir Mountains (Kingdom of Saudi Arabia), has a similar petiole shape and the legs covered with black decumbent setae but it differs from *C. fritillariae* by the presence of long, black, erect setae also present on the dorsal side of femora and tibiae, and more numerous black erect setae on the mesosoma. *Cataglyphis dejdaranensis* sp. nov. is the most similar to *C. fritillariae*, but it differs by the weakly sculptured gaster that has moderately shiny sides of gastral tergite I, petiolar node of major workers knob-shaped in profile, and more convex propodeum.

Description. Major worker (n = 15): ***Measurements.*** HL: 2.435 (2.31–2.55); HW: 2.203 (2.10–2.33); SL: 2.732 (2.63–2.90); PW: 1.582 (1.50–1.69); PRL: 1.430 (1.35–1.52); PRW: 1.155 (1.07–1.260); PTH: 0.878 (0.78–1.11); PTW: 0.715 (0.66–0.78); WL: 3.777 (3.63–3.92); HFL: 4.050 (3.76–4.27); CI: 1.105 (1.064–1.123); SI: 1.122 (1.113–1.137); PI: 1.292 (1.164–1.423); FI: 1.072 (1.019–1.109). ***Color.*** Head, mesosoma and gaster uniformly black or black with indistinct brownish black spots with diffused borders. Legs uniformly black to brownish black. Antennae completely black or black with brownish black scape (Figs 9–11). ***Head.*** Square; approximately 1.13× as long as wide; sides below eyes almost parallel, above eyes gently convex, posterior margin almost straight (Fig. 11). Anterior clypeal margin convex; without central impression; with a row of short black setae, and eight additional long black setae, the longest approximately as long as 0.6 length of clypeus; clypeal plate with a pair of long and black setae close to basal margin, and two pairs of similar setae close to anterior margin; sometimes clypeal plate with 1–3 additional short setae. Clypeus opalescent and densely microreticulated; covered with very sparse, short and adpressed hairs. Eyes large and oval, 1.3–1.4× as long as wide. Frontal carinae short; not extending beyond frontal lobes; interocular area with thin shiny line and 1–3 long black setae placed along each side of the line. Antennal fossa shallow, opalescent, densely microreticulated. Head opalescent and densely microreticulated; covered with sparse, short, adpressed hairs (Fig. 11). Ocellar region with three or four moderately long and black setae and often additional two or three shorter black setae; a transverse row of 4–8 black setae present above ocelli; area behind eyes with three or four yellowish to brown short setae; rest of frontal and lateral faces of head without erect setae; ventral side of the head with a dozen white to brown setae. Antennal scape long; in frontal view straight; 1.3× as long as width of the head; from base to apex slightly and gradually widened; its base without tooth; funiculus long; pedicel elongated, approximately 0.96× as long as segments II+III combined and 1.9× as long as segment II (Fig. 11). Surface of scape densely microsculptured and opalescent; covered with thick, dense, decumbent setae. Mandibles rounded; basally smooth and shiny; apical ¾ length with deep grooves; surface shiny with several long, white to brown setae; masticatory margin with four large teeth. ***Mesosoma.*** Long; 2.4× as long as wide; metanotal groove shallow (Fig. 10). Pronotum convex on sides. In lateral view promesonotum slightly arched in profile; propodeum positioned lower than promesonotum, moderately convex in lateral view (Fig. 10). Mesosoma opalescent and densely microreticulated; covered with sparse, short and adpressed hairs. Pronotum with 2–5 moderately long and black setae medially, sometimes with one or two short black setae close to its anterior and posterior margins; mesonotum with one or two moderately long and black setae in front of spiracles, sometimes with one or two short, black setae medially and anteriorly; propodeum dorsally with 4–7 long and black setae, and often two or three additional short setae; older specimens sometimes with setae completely to partly broken (Fig. 10). ***Petiole.*** Trapezoidal in profile; its anterior face mostly flat with only basal part convex; posterior face straight to slightly concave; dorsum flat; peduncle very short. Surface opalescent and microreticulated; covered with sparse, short and

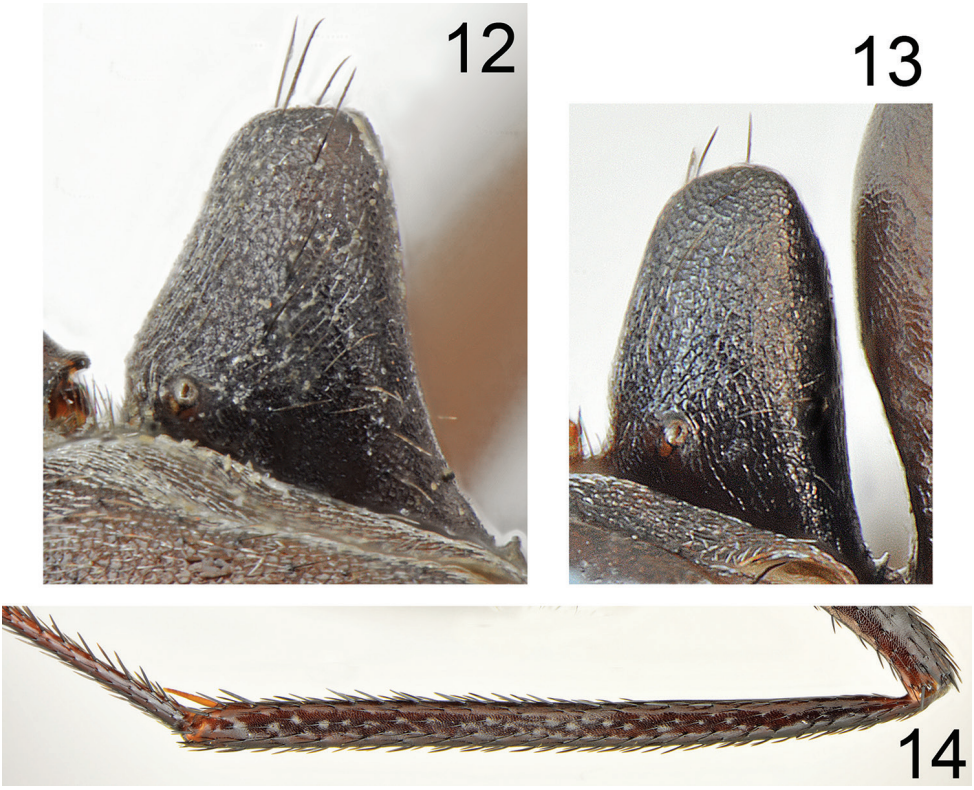

Figures 12–14. *Cataglyphis fritillariae* sp. nov. **12** petiole of major worker **13** petiole of minor worker **14** hind tibia (not in scale).

adpressed hairs; top of knob with 3–6 moderately long, black, erect setae (Fig. 12). In anterior view petiolar dorsum with distinct emargination medially. ***Gaster.*** Dull and distinctly microreticulated. Whole surface of gaster with short, sparse, adpressed hairs; tergite I in anterior part with 2–4 long, black setae; tergite II without a pair of black setae anteriorly; tergite III with 2–4 long and black setae centrally; in older specimens, setae usually broken (Fig. 16). Each of gastral sternites with three or four long, black, erect setae. ***Legs.*** Dorsal and lateral surfaces of femora and tibiae covered with thick, dense, black, decumbent setae; no white, adpressed setae on surface between black setae. Ventral surfaces of femora and tibiae with numerous long, black, suberect to erect, spiniform setae (Fig. 14).

Minor worker (n=15): ***Measurements.*** HL: 1.240 (0.98–1.52); HW: 1.083 (0.87–1.32); SL: 1.168 (0.84–1.57); PW: 0.753 (0.59–0.92); PRL: 0.692 (0.51–0.88); PRW: 0.552 (0.44–0.69); PTH: 0.518 (0.40–0.61); PTW: 0.330 (0.27–0.45); WL: 1.818 (1.39–2.34); HFL: 1.573 (1.10–2.20); CI: 1.145 (1.126–1.173); SI: 0.935 (0.857–1.033); PI: 1.606 (1.356–2.000); FI: 0.858 (0.791–0.940).

Color. Uniformly yellowish brown to brownish black. Antennae and legs yellowish brown to bright brown (Figs 15, 16). ***Head.*** Almost square; 1.15–1.17× as long as

Figures 15, 16. Minor worker of *Cataglyphis fritillariae* sp. nov. **15** dorsal **16** lateral. Scale bar 2 mm.

wide; sides below eyes almost parallel, behind eyes regularly convex, posterior margin of head convex. Sculpture and setation of the head similar as in major worker but with lower number of long setae. ***Mesosoma.*** Long; 2.4–2.5× as long as wide; metanotal groove shallow. Pronotum convex on sides. In lateral view promesonotum slightly arched in profile; propodeum positioned lower than promesonotum, its dorsum and posterior side slightly convex (Fig. 16). Whole mesosoma opalescent and densely microreticulated (Figs 15, 16). Whole mesosoma covered with dense, short, adpressed hair; pronotum with additional two or three black and erect setae; mesonotum and propodeum with additional one or two black and erect setae. ***Petiole.*** In form of thick

scale; its anterior surface slightly convex; apex rounded and posterior surface almost flat; surface microreticulated and covered by sparse, short, adpressed hairs; dorsum with 1–3 black, moderately elongated and erect setae (Fig. 13). ***Gaster.*** Dull and distinctly microreticulated; tergites I and II with up to two black and erect setae; tergite III without or with a pair of black and erect setae close to its anterior margin; tergite IV with 2–4 erect setae; sternites with two or three black and erect setae; whole surface of gaster with short, adpressed hairs (Figs 15, 16). ***Legs.*** Dorsal and lateral surfaces of femora and tibiae covered with thick, dense, black, decumbent setae; no white, adpressed setae on surface between black setae. Ventral surfaces of femora and tibiae with numerous long, black, suberect to erect, spiniform setae.

Biology. Little known, in Dashte laleh a nest was found under rocks in a grazing area (Fig. 25). The site was located on a small plateau (3600 hectares), between 2100–2600 m above sea level, and in May was predominantly overgrown by Snake's head (*Fritillaria imperialis* L.). Other common plants recorded from this locality were Milkvetch (*Astragalus* spp.), Persian shallot (*Allium stipitatum* Regel), and kheshk (*Daphne mucronata* Royle). The species appears to be alpine, as all its collecting sites were placed on high altitude from 2143 to 2400 m.

Etymology. The species name *fritillariae* is named after the genitive singular case of the generic name of the Snake's head *Fritillaria imperialis* L., the dominant flower in Dashte laleh, the type locality of this ant species.

***Cataglyphis dejdaranensis* sp. nov.**
http://zoobank.org/31D1EF27-49CB-4218-8A8A-AD5706CF4421
Figs 17–26

Type material. ***Holotype*:** major worker (CASENT0872370): IRAN, Chaharmahal Va | Bakhtiari, Koohrang (Cheri) | 2 VI 2017, 2778 m | leg. Khalili-Moghadam | 32.1686 / 50.1752 || Collection L. Borowiec | Formicidae | LBC-IR00088 (MNHW); ***paratypes*:** one major and two minor workers (CASENT0872371–CASENT0872373): the same data as holotype (MHNG, MNHW); ***paratypes*:** four major and two minor workers (CASENT0872374–CASENT0872379): IRAN, Chaharmahal Va | Bakhtiari, Koohrang (Dejdaran | valley) 2 VI 2017, 2319 m | leg. Khalili-Moghadam | 32.1955 / 50.2075 || Collection L. Borowiec | Formicidae | LBC-IR00076 (MNHW).

Diagnosis. *Cataglyphis dejdaranensis* belongs to the group of large species with well-developed and dull body sculpture. Femora and tibiae covered with thick, dense, black, decumbent setae cluster this species with the *Cataglyphis setipes* complex, and the shape of the petiolar node groups it with the *C. altisquamis* complex. From all species of the *C. setipes* complex, *C. dejdaranensis* differs in a knob-shaped petiole, which is not forming a spherical node; from all species of the *C. altisquamis* complex, *C. dejdaranensis* differs in a weak microsculpture of gaster of which at least sides are visibly shiny. *Cataglyphis dejdaranensis* has the least sculpted gaster within all large species with well-developed body microsculpture. At first glance, *C. foreli* appears

Figures 17, 18. Major worker of *Cataglyphis dejdaranensis* sp. nov. **17** dorsal **18** lateral. Scale bar 2 mm.

similar to *C. dejdaranensis*, but it differs in larger eyes, and femora and tibia lacking thick, black, decumbent setae. *Cataglyphis kurdistanica* Pisarski has similarly shaped petiole and legs with black decumbent setae, but it differs in bicolored body and presence of the soldier caste. *Cataglyphis bucharica* also appears similar to *C. dejdaranensis* but it differs in reddish head and mesosoma, numerous erect setae on propodeum, longer propodeal spiracle, and femora and tibia lacking thick, black, decumbent setae. *Cataglyphis fritillariae* sp. nov. is the most similar to *C. dejdaranensis*, but differs in strongly sculptured gaster, petiolar node of major workers trapezoidal in profile, and less convex propodeum.

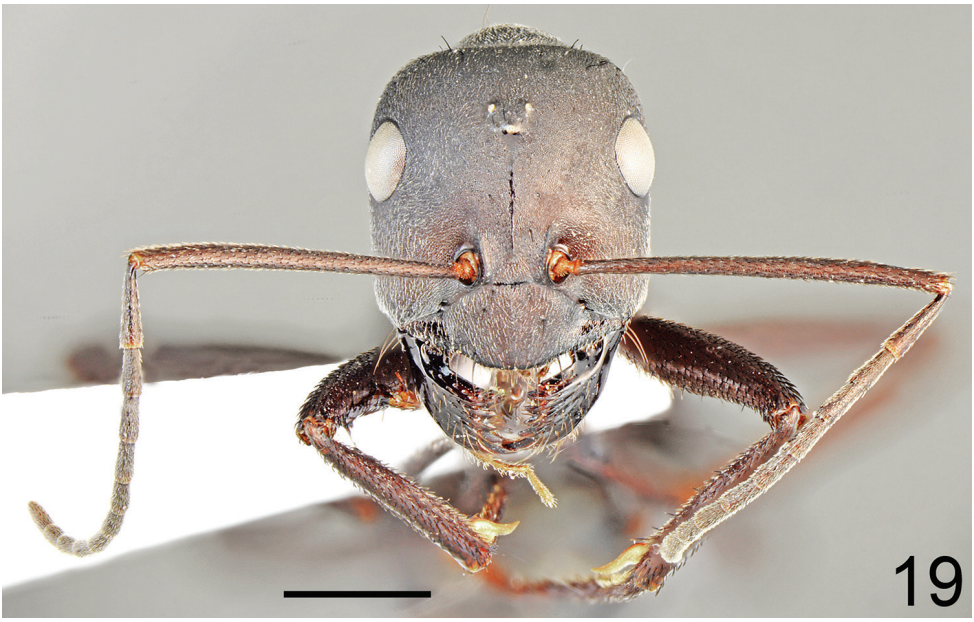

Figure 19. Major worker of *Cataglyphis dejdaranensis* sp. nov., head and antennae. Scale bar 1 mm.

Description. Major worker (n = 6): ***Measurements.*** HL: 2.197 (2.07–2.14); HW: 1.970 (1.85–2.12); SL: 2.413 (2.25–2.64); PW: 1.350 (1.25–1.46); PRL: 1.178 (1.08–1.32); PRW: 0.998 (0.93–1.09); PTH: 0.877 (0.78–0.94); PTW: 0.452 (0.42–0.49); WL: 3.263 (3.05–3.48); HFL: 3.402 (3.13–3.69); CI: 1.117 (1.085–1.141); SI: 1.098 (1.064–1.131); PI: 1.945 (1.694–2.163); FI: 1.042 (1.024–1.098). ***Color.*** Head, mesosoma and gaster completely black or head anteriorly, and pronotum and mesosoma on lateral sides with indistinct brownish black spots of diffused borders. Legs completely black or black-brown with tarsi sometimes slightly paler than femora and tibiae. Antennae completely black (Figs 17–19, 23, 24). ***Head.*** Square; approximately 1.12× as long as wide; sides below eyes almost parallel, above eyes gently convex, posterior margin almost straight (Fig. 19). Anterior margin of the clypeus convex; without central impression; with a row of short black setae, and eight longer black setae, the longest as long as 0.6 length of clypeus; clypeal plate with a pair of long and black setae centrally and a pair of similar setae basally. Clypeus opalescent and densely microreticulated; covered with sparse, short and adpressed hairs. Eyes large and oval; approximately 1.2× as long as wide. Frontal carinae short, not extending beyond frontal lobes; interocular area with thin shiny line and two or three long black setae along each of its sides. Antennal fossa shallow, opalescent, densely microreticulated. Head opalescent and densely microreticulated; covered with sparse, short, adpressed hairs (Fig. 19). Ocellar region with group of 2–4 moderately long black setae; posterior angles with two or three long and 1–3 short black setae; rest of frontal and lateral faces of head without erect setae; ventral side of the head with a dozen white to brown setae.

Figures 20–22. *Cataglyphis dejdaranensis* sp. nov. **20** petiole of major worker **21** petiole of minor worker **22** hind tibia (not in scale).

Antennal scape long; in frontal view straight; 1.1× as long as width of the head; its base without tooth; from base to apex slightly and gradually widening; funiculus long; pedicel elongated, approximately 0.85× as long as segments II and III combined and 1.7× as long as segment II (Fig. 19). Surface of scape densely microsculptured, opalescent; covered with thick, dense, decumbent setae. Mandibles rounded; basally smooth and shiny; apical half with deep grooves; surface shiny with several long white setae; masticatory margin with four large teeth. ***Mesosoma.*** Long, 2.2× as long as wide; metanotal groove shallow. Pronotum convex on sides. In lateral view promesonotum slightly arched in profile, propodeum positioned lower than promesonotum; distinctly convex in lateral view (Figs 24, 25). Mesosoma opalescent and densely microreticulated; covered with sparse, short and adpressed hairs. Pronotum posteriorly with 2–4 moderately long and black setae; and anteriorly with 2–4 short black setae; sometimes setae broken or missing; mesonotum with up to two moderately long and black setae close to the anterior margin and usually two black setae close to the median groove; propodeum apically with 1–4 short, black setae; sometimes mesonotal and propodeal setae broken. ***Petiole.*** In form of knob; its anterior face distinctly convex; posterior face only slightly convex and dorsum regularly rounded; peduncle short. Surface opalescent and densely microreticulated; covered with dense, short, adpressed hairs; dorsum of knob with 3–5

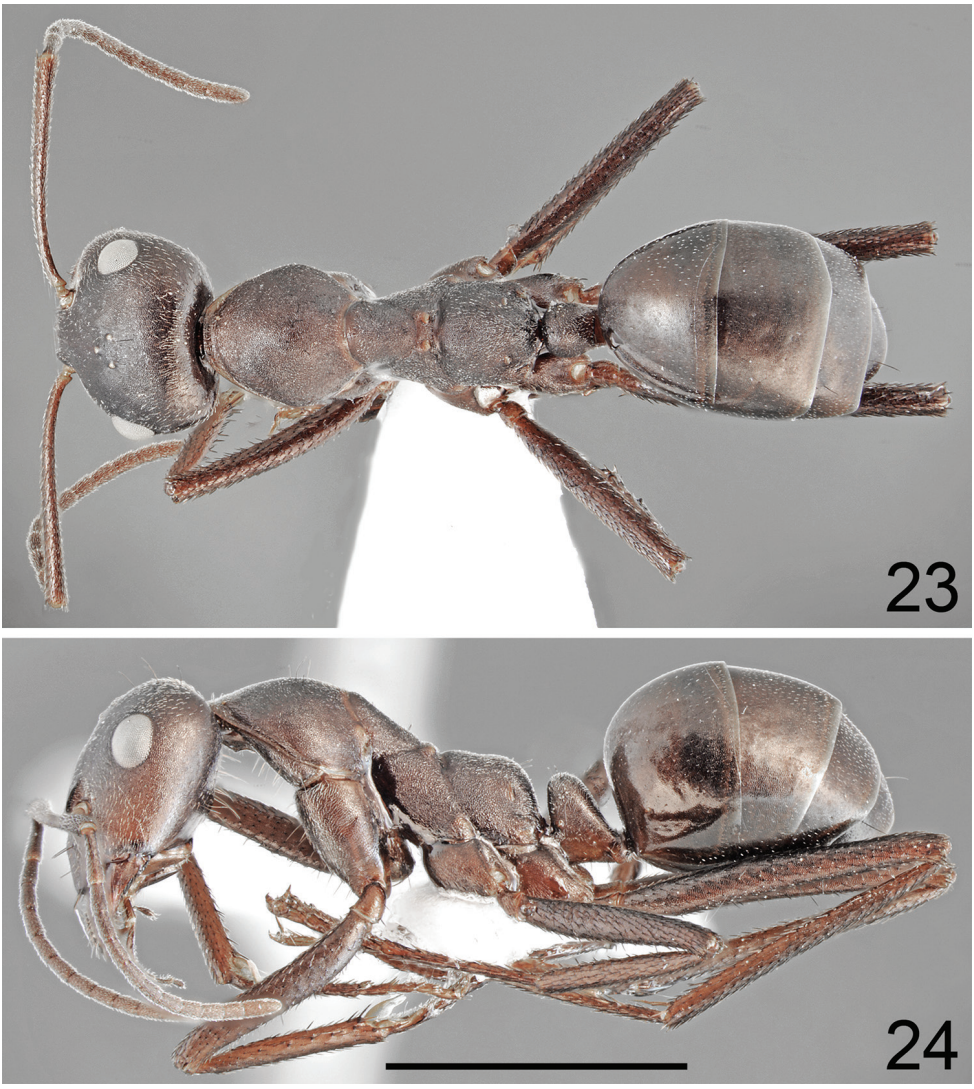

Figures 23, 24. Minor worker of *Cataglyphis dejdaranensis* sp. nov. **23** dorsal **24** lateral. Scale bar 2 mm.

very short, black, erect setae. ***Gaster.*** Finely microreticulated and moderately shiny; gastral segment I and lateral sides of remaining segments appear distinctly shinier than remaining parts of gaster. Whole surface of gaster with short, sparse, adpressed hairs; tergites I and II without erect setae; tergite III with one or two long black setae centrally and close to anterior margin, and up to one setae at lateral margin; tergite IV in younger specimens with four long black setae on each side; in older specimens setae usually broken (Fig. 24). Each of gastral sternites with three or four long, black, erect setae. ***Legs.*** Dorsal and lateral surfaces of femora and tibiae covered with thick, dense, black decumbent setae; no white adpressed setae on surface between black setae. Ventral surfaces of femora and tibiae with numerous long, black, suberect to erect setae.

25

26

Figures 25, 26. Nest of *Cataglyphis fritillariae* under a large stone at the Dashte laleh site (**25**) Locality Cheri (**26**).

Minor worker (n = 4): ***Measurements.*** HL: 1.575 (1.39–1.71); HW: 1.373 (1.19–1.53); SL: 1.593 (1.35–1.85); PW: 0.948 (0.83–1.04); PRL: 0.860 (0.76–0.96); PRW: 0.700 (0.62–0.77); PTH: 0.595 (0.54–0.65); PTW: 0.330 (0.28–0.35); WL: 2.303 (2.02–2.48); HFL: 2.185 (1.81–2.53); CI: 1.149 (1.118–1.168); SI: 1.009 (0.971–1.082); PI: 1.808 (1.647–1.929); FI: 0.946 (0.896–1.020).

Color. Slightly paler than major workers; head, mesosoma and gaster mostly brown to dark brown; upper part of head, propodeum and gaster usually blackish brown but never black; transition from brown to blackish brown diffused. Antennae and legs brown to almost black, legs brown to dark brown (Figs 23, 24). ***Body.*** Morphological characters similar to these of major worker except petiole which appears as a very thick scale; approximately 2× as high as broad, with anterior surface only slightly convex and posterior surface flat, and with only rudiment of peduncle (Fig. 21). Dorsal surface of gastral tergites I and II without erect setae; tergite III without or with only a pair of erect setae; tergite IV with two or four setae. Sternites setose as in major worker. Legs generally similarly setose as in major workers except fewer suberect and erect black setae on ventral sides of femora and tibiae. Head slightly longer and scape slightly shorter than in major workers.

Biology. Little known. On the locality Cheri, specimens were collected in a mountain grazing area overgrown by grass, and on the locality Dejdaran Valley ants were found on mountain pastures with scant vegetation (Fig. 26). Nests were located under large stones. Both collecting sites were placed on high altitude: 2319 m and 2778 m.

Etymology. The species name *dejdaranensis* is a feminine Latin adjective in the nominative case and refers to Dejdaran Valley, where one of the specimens of this species was collected.

Comments

All three new Iranian species belong to the group of large, polymorphic *Cataglyphis*. Based on their morphology, they should be assigned to the *Cataglyphis altisquamis* group, sensu Agosti (1990). Herein, we present a modified version of the key to the Asian *Cataglyphis* (Radchenko 1998). The key was modified to accommodate the three new species and *C. asiriensis*, which was not included in the original version. We also decided not to refer to figures available in Radchenko's paper but provide photographs of type specimens of species which are included in the key (except photographs of *C. oxiana* Arnol'di and *C. piligera* Arnol'di that were not available).

In the key to the Asian *Cataglyphis altisquamis* species group proposed by Radchenko (1998) all four species run to couplet 39 and the key is modified as follow:

1 [39 in Radchenko 1998]. Petiole wide-cuneiform or conical; if petiole slightly node-shaped, then eyes large, as long as, or 0.8× as long as genae, and body uniformly black or black-brown **2**

– Petiole node-shaped, eyes small less than 0.8× as long as genae, and body never uniformly black to black-brown ..... 18 [in Radchenko 1998]

2 Surface of femora and tibiae covered with black, thick, and decumbent setae....**3**
– Surface of femora and tibiae not covered with a black, thick, and decumbent setae....**7**
3 Soldier caste present, soldiers have saber-shaped mandibles with blunt denticles along their inner margin. Head and mesosoma yellowish red, gaster red-brown to dark brown, posterior margin of head with black, erect setae (Figs 33, 34). Turkey, Iraq....***C. kurdistanica*** **Pisarski, 1965**
– Soldier caste absent. Head, mesosoma and gaster brown to black, if red- brown then posterior margin of head without black, erect setae (Figs 1, 2, 9, 10, 15–18, 22, 24)....**4**
4 Mesonotum in major workers distinctly bicolored, head, mesosoma and petiole reddish (Figs 1, 2), petiole in both, major and minor workers conical (Figs 4, 5). Iran....***C. bazoftensis*** **sp. nov.**
– Mesonotum in both major and minor workers uniformly brown to black (Figs 9, 10, 15–18, 22, 24), petiole in major workers trapezoidal or knob-shaped, in minor workers in form of a thick squama (Figs 12, 13, 20, 21)....**5**
5 Both dorsal and ventral surfaces of femora and tibiae with a row of long, black, and spiniform setae, mesosoma with thick and black setae (Figs 27, 28) Saudi Arabia ....***C. asiriensis*** **Collingwood, 1985**
– Only ventral surfaces of femora and tibiae with row of long, black, and spiniform setae, mesosoma with fewer and thinner setae (Figs 9, 15, 17, 24) **6**
6 Gaster dull (Figs 9, 15). Petiole in major worker trapezoidal in profile (Fig. 12). Iran....***C. fritillariae*** **sp. nov.**
– At least sides of gastral tergite I with relatively shiny area (Figs 17, 24). Petiole in major worker knob-shaped in profile (Fig. 20). Iran....***C. dejdaranensis*** **sp. nov.**
7 Mesosoma and posterior margin of head with numerous erect setae (Figs 29, 30)...**8**
– Mesosoma and posterior margin of head without or with sparse erect hairs (Figs 31, 32). Body black or black-brown....**9**
8 Propodeal dorsum distinctly longer than its declivity in profile. Petiole high, narrow-cuneiform, with weakly convex anterior surface, about as high as propodeum. Head and mesosoma red to red-brown (posterior half of thorax sometimes dark brown); gaster dark brown to black. Mountains of Uzbekistan and Tajikistan; Afghanistan and N Iran ....***C. bucharica*** **Emery**
– Propodeal dorsum as long as its declivity in profile. Petiole cuneiform, with strongly convex anterior surface, clearly lower than propodeum. Body uniformly dark brown to black. Turkmenistan and Uzbekistan ..... ***C. piligera*** **Arnol'di, 1964**
9 Eyes small, 0.6–0.5× length of genae. Middle East.... ***C. altisquamis*** **(André, 1881)**
– Eyes large, 0.8–1× as long as genae....**10**
10 Petiole low, nearly node-shaped, posterior margin of head strongly convex, rounded. Turkmenistan and Uzbekistan....***C. oxiana*** **Arnol'di, 1964**
– Petiole comparatively higher, broad- cuneiform. In large workers, posterior margin of head straight or slightly concave. Turkmenistan, Iran ..... ***C. foreli*** **(Ruzsky, 1903)**

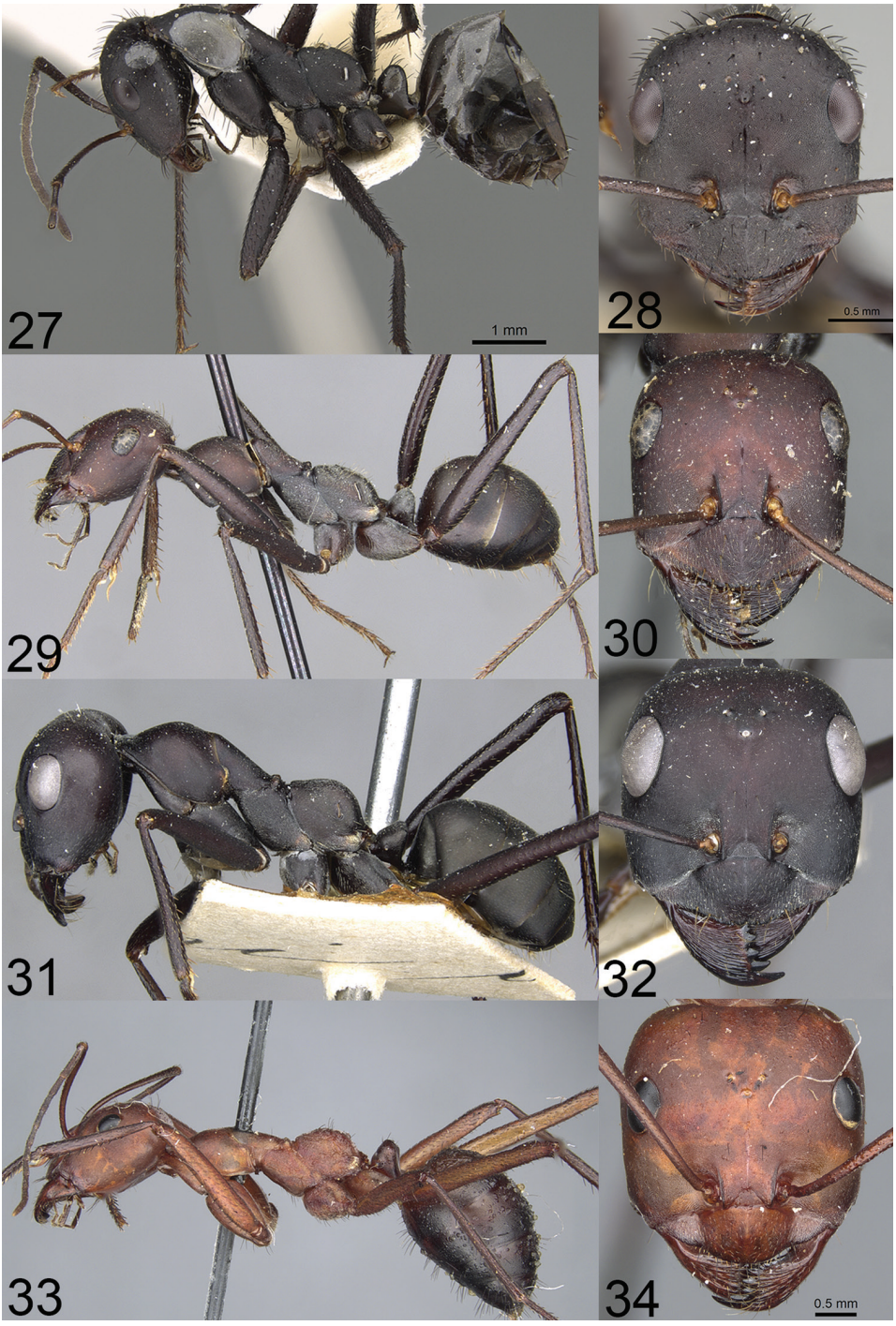

Figures 27–34. Photographs of members of the *Cataglyphis altisquamis* species group. *C. asiriensis* Collingwood **27** lateral **28** head (Michele Esposito, from www.antweb.org), *C. bucharica* Emery **29** lateral **30** head (Zach Lieberman, from www.antweb.org), *C. foreli* (Ruzsky) **31** lateral **32** head (Zach Lieberman, from www.antweb.org), *C. kurdistanica* Pisarski **33** lateral **34** head (Kate Martynova, from www.antweb.org).

Acknowledgements

Arsalan Khalili-Moghadam thanks Shahrekord University, Iran for supporting his scientific project on biodiversity of ants of Chaharmahal va Bakhtiari Province. The authors would like to thank to Mostafa Sharaf and Brian L. Fisher for their comments on the manuscript of this publication.

References

Agosti D (1990) Review and reclassification of *Cataglyphis* (Hymenoptera, Formicidae). Journal of Natural History 24: 1457–1506. https://doi.org/10.1080/00222939000770851

Amor F, Ortega P (2014) *Cataglyphis tartessica* sp. n., a new ant species (Hymenoptera: Formicidae) in south-western Spain. Myrmecological News 19: 125–132. https://doi.org/10.5281/zenodo.16346

Arakelian GR (1994) Fauna of the Republic of Armenia. Hymenopterous insects. Ants (Formicidae). Gitutium, Erevan, 153 pp. [In Russian]

Arnol'di KV, Dlussky GM (1978) Superfam. Formicoidea. 1. Fam. Formicidae – ants. In: Medvedev GS (Ed.) Keys to the insects of the European part of the USSR. Vol. 3. Hymenoptera. Part 1. Opredeliteli Faune SSSR 119: 519–556. [In Russian]

Atanassov N, Dlussky GM (1992) Fauna of Bulgaria. Hymenoptera, Formicidae. Fauna of Bulgaria 22: 1–310.

Bolton B (2020) An online catalog of the ants of the world. https://antcat.org [accessed 06 September 2020]

Boulay R, Carro F, Soriguer RC, Cerdá X (2007) Synchrony between fruit maturation and effective dispersers' foraging activity increases seed protection against seed predators. Proceedings of the Royal Society of London B 274: 2515–2522. https://doi.org/10.1098/rspb.2007.0594

Brown Jr WL (2000) Diversity of ants. In: Agosti D, Majer J, Alonso E, Schultz TR (Eds) Ants: standard methods for measuring and monitoring biodiversity. Biological diversity hand book series. Smithsonian Institution Press, Washington, DC, 280 pp.

Cagniant H (2009) Le genre *Cataglyphis* Foerster, 1850 au Maroc (Hyménoptères Formicidae). Orsis 24: 41–71. https://www.antwiki.org/wiki/images/c/ca/Cagniant_Cataglyphis_2009.pdf

Chang YD, He DH (2002) Three new species of the genus *Cataglyphis* Foerster from Northwest China (Hymenoptera: Formicidae: Formicinae). Zoological Research 23: 61–64. [In Chinese]

Collingwood CA (1978) A provisional list of Iberian Formicidae with a key to the worker caste (Hym. Aculeata). EOS. Revista Española de Entomología 52: 65–95. https://doi.org/10.5281/zenodo.26690

Collingwood CA, Agosti D (1996) Formicidae (Insecta: Hymenoptera) of Saudi Arabia (Part 2). Fauna of Saudi Arabia 15: 300–385. https://antcat.org/references/130931

Collingwood C, Prince A (1998) A guide to ants of continental Portugal (Hymenoptera: Formicidae). Boletim da Sociedade Portuguesa de Entomologia. Suplemento 5: 1–49. https://doi.org/10.5281/zenodo.1244612

Collingwood C, Agosti D, Sharaf MR, van Harten A (2011) Order Hymenoptera, family Formicidae. Arthropod fauna of the UAE 4: 405–474. https://doi.org/10.5281/zenodo.1168586

Crawley WC (1920) Ants from Mesopotamia and north-west Persia (concluded). The Entomologist's Record and Journal of Variation 32: 177–179. https://doi.org/10.5281/zenodo.15001

Dlussky GM, Soyunov OS, Zabelin SI (1990) Ants of Turkmenistan. Ylym Press, Ashkabad, 273 pp. [In Russian]

Emery C (1906) Rassegna critica delle specie paleartiche del genere Myrmecocystus. Memorie della Reale Accademia delle Scienze dell'Istituto di Bologna (6)3: 47–61. https://doi.org/10.5281/zenodo.25506

Evenhuis N (2020) The insect and spider collections of the world website. http://hbs.bishopmuseum.org/codens/ [accessed 10 Augst 2020]

Eyer PA, Seltzer R, Reiner-Brodetzki, Hefetz A (2016) An integrative approach to untangling species delimitation in the *Cataglyphis bicolor* desert ant complex in Israel. Molecular Phylogenetics and Evolution 115: 128–139. https://doi.org/10.1016/j.ympev.2017.07.024

Forel A (1904) Note sur les fourmis du Musée Zoologique de l'Académie Impériale des Sciences à St. Pétersbourg. Ezhegodnik Zoologicheskago Muzeya Imperatorskoi Akadernii Nauk 8: 368–388. https://doi.org/10.5281/zenodo.25586

Ghahari H, Collingwood CA (2011) A study on the ants (Hymenoptera: Formicidae) of southern Iran. Calodema 176: 1–5.

Ghahari H, Collingwood CA, Havaskary M, Ostovan H, Samin N (2011) A contribution to the knowledge of ants (Hymenoptera: Formicidae) from the Arasbaran biosphere reserve and vicinity, Northwestern Iran. Jordan Journal of Agricultural Sciences 7(3): 558–563. https://www.antwiki.org/wiki/images/1/11/Ghahari_et_al_2011.pdf

Ghahari H, Collingwood CA, Tabari M, Ostovan H (2009) Faunistic notes on Formicidae (Insecta: Hymenoptera) of rice fields and surrounding grasslands in northern Iran. Munis Entomology & Zoology Journal 4(1): 184–189. https://www.munisentzool.org/yayin/vol4/issue1/184–189.pdf

Herrera CM, Herrera J, Espadaler X (1984) Nectar thievery by ants from southern Spanish insect-pollinated flowers. Insectes Sociaux 31: 142–154. https://doi.org/10.1007/BF02232711

Hulme PE (1997) Post-dispersal seed predation and the establishment of vertebrate dispersed plants in Mediterranean scrublands. Oecologia 111: 91–98. https://doi.org/10.1007/s004420050212

Ionescu A, Eyer P-A (2015) Notes on *Cataglyphis* Foerster, 1850 of the bicolor species group in Israel, with description of a new species (Hymenoptera: Formicidae). Israel Journal of Entomology 46: 109–131. https://doi.org/10.5281/zenodo.221456

Janicki J, Narula N, Ziegler M, Guénard B, Economo EP (2016) Visualizing and interacting with large-volume biodiversity data using client-server web-mapping applications: The design and implementation of antmaps.org. Ecological Informatics 32: 185–193. https://doi.org/10.1016/j.ecoinf.2016.02.006

Karavaiev V (1924) Zur Systematik der paläarktischen Myrmecocystus (Formicidae), nebst einigen biologischen Notizen. Konowia 3: 301–308. https://doi.org/10.5281/zenodo.25958

Lenoir A, Aron S, Cerdá X, Hefetz A (2010) *Cataglyphis* desert ants: a good model for evolutionary biology in Darwin's anniversary year—a review. Israel Journal of Entomology 39: 1–32. http://digital.csic.es/bitstream/10261/65135/1/israel.pdf

Moradloo S, Fard RN, Rad SP, Taylor B (2015) Records of ants (Hymenoptera: Formicidae) from Northern Iran. Zoology in the Middle East 2015: 1–6. https://doi.org/10.1080/09397140.2015.1020611

Paknia O, Radchenko A, Alipanah H, Pfeiffer M (2008) A preliminary check list of the ants (Hymenoptera: Formicidae) of Iran. Myrmecological News 151–159. http://antbase.org/ants/publications/21820/21820.pdf

Paknia O, Radchenko A, Pfeiffer M (2009) New records of ants (Hymenoptera, Formicidae) from Iran. Asian Myrmecology 3: 29–38.

Pisarski B (1965) Les fourmis du genre *Cataglyphis* Foerst. en Irak (Hymenoptera, Formicidae). Bulletin de l'Académie Polonaise des Sciences. Série des Sciences Biologiques 13: 417–422. https://doi.org/10.5281/zenodo.25692

Rad SP, Taylor B, Torabi R, Aram E, Abolfathi, Afshari, Borjali F, Ghatei M, Hediary F, Jazini F, Kiah VH, Mahmoudi Z, Sararyan F, Seiri M (2018) Further records of ants (Hymenoptera: Formicidae) from Iran. Zoology in the Middle East 2015: 1–15.

Radchenko AG (1997) Review of ants of the genus *Cataglyphis* Foerster (Hymenoptera, Formicidae) of Asia. Entomologicheskoe Obozrenie 76: 424–442. [In Russian]

Radchenko AG (1998) A key to the ants of the genus *Cataglyphis* Foerster (Hymenoptera, Formicidae) of Asia. Entomologicheskoe Obozrenie 77: 502–508. [In Russian]

Radchenko AG, Paknia O (2010) Two new species of the genus *Cataglyphis* Foerster, 1850 (Hymenoptera: Formicidae) from Iran. Annales Zoologici 60: 69–76. https://doi.org/10.3161/000345410X499533

Salata S, Borowiec L (2018) Taxonomic and faunistic notes on Greek ants (Hymenoptera: Formicidae). Annals of the Upper Silesian Museum in Bytom Entomology 27(online 008): 1–51. http://doi.org/10.5281/zenodo.2199191

Santschi F (1929) Étude sur les *Cataglyphis*. Revue Suisse de Zoologie 36: 25–70. https://doi.org/10.5962/bhl.part.117626

Seifert B (2018) The ants of Central and North Europe. lutra Verlags- und Vertriebsgesellschaft, Tauer, Germany, 407 pp.

Sharaf MR, Collingwood CA, Aldawood AS (2015) Notes on the ant genus *Cataglyphis* Foerster, 1850 (Hymenoptera, Formicidae) in the Arabian Peninsula with description of a new species and a key to species of the *C. pallida*-group. ZooKeys 545: 101–117. https://doi.org/10.3897/zookeys.545.6308

Wehner R (2020) Desert navigator. The journey of an ant. The Belknap press of Harvard University Press, Cambridge, Massachusetts, 392 pp. https://doi.org/10.4159/9780674247918

Wilson EO (1955) A monographic revision of the ant genus *Lasius*. Bulletin of the Museum of Comparative Zoology 113:1–201. https://doi.org/10.5281/zenodo.25290

ZooKeys 1009: 29–43 (2021)
doi: 10.3897/zookeys.1009.59693
https://zookeys.pensoft.net

RESEARCH ARTICLE

A peer-reviewed open-access journal
ZooKeys
Launched to accelerate biodiversity research

New record of the genus *Manipuria* Jacoby (Chrysomelidae, Criocerinae) from China, with description of a new species

Yuan Xu[1,3], Wenxuan Bi[2], Hongbin Liang[3]

1 *College of Life Sciences, Anhui Normal University, Anhui 241000, China* **2** *Room 401, No. 2, Lane 155, Lianhua South Road, Shanghai, 201100, China* **3** *Key Laboratory of Zoological Systematics and Evolution, Institute of Zoology, Chinese Academy of Sciences, Beijing 100101, China*

Corresponding author: Hongbin Liang (lianghb@ioz.ac.cn)

Academic editor: A. Konstantinov | Received 15 October 2020 | Accepted 10 December 2020 | Published 4 January 2021

http://zoobank.org/A5C16285-1A31-4847-9C2D-810FE7AE42EC

Citation: Xu Y, Bi W, Liang H (2021) New record of the genus *Manipuria* Jacoby (Chrysomelidae, Criocerinae) from China, with description of a new species. ZooKeys 1009: 29–43. https://doi.org/10.3897/zookeys.1009.59693

Abstract

After a century since the erection of the genus *Manipuria* from India, its type species *M. dohertyi* Jacoby was discovered in Yunnan Province of China. A new *Manipuria* species, *M. yuae* **sp. nov.**, is described from Tibet and Yunnan, China. The new species differs from *M. dohertyi* by its larger size, unicolored elytra, and absence of a tooth-like prolongation in front of the mandible. Additional data is provided for *M. dohertyi* based on new material from China.

Keywords

Coleoptera, Crioceris, Smilacaceae, taxonomy, Tibet

Introduction

The monotypic genus *Manipuria* Jacoby was erected in 1908 based on *Manipuria dohertyi* Jacoby, 1908 from Manipur, India. This particular species is characterized by an elongate and subcylindrical body; the head longer than wide, not strongly constricted posteriorly, with a tooth-like prolongation on the under surface in front of the mandible

(Jacoby 1908). For more than a century, no other species of the genus have been found, and no other distribution records are known except for the type locality, Manipur.

During an expedition to southeastern Tibet in August 2011, three large specimens of Criocerinae were discovered on a host plant belonging to Smilacaceae. Based on the keys of Jacoby (1908) and Monrós (1960), these specimens were readily keyed out as members of the genus *Manipuria*. In the insect collection of Kunming Institute of Zoology, Kunming, China, we found another specimen of *Manipuria* collected from Ruili City of Yunnan Province. Subsequent morphological comparisons of the specimens with the type of *M. dohertyi* have convinced us that they represent another *Manipuria* species previously unknown to science. A description of this new species follows.

In August 2019, we made an expedition to Tibet and Yunnan to survey Criocerinae. When walking on a road in Maku village of Dulongjiang township, we saw a "*Lilioceris*" beetle flying quickly in front of us and then resting on a plant. We caught it with an insect net and recognized it as *M. dohertyi* from four ocular patches on the elytra. In fact, Dulongjiang represented a new distribution area, because the second author (BWX) caught this species in July 2015 from Qinlangdang, another village of Dulongjiang ca 10 km south of Maku.

The purpose of this paper is to describe the new species discovered in Tibet and Yunnan, and to provide additional data on *M. dohertyi* based on our new material from Yunnan.

Materials and methods

This study is based on the examination of the type specimen and those collected from Tibet and Yunnan, China. The methods of specimen observation and preparation followed previous publications (Tishechkin et al. 2011; Li et al. 2013; Shi and Liang 2015). Morphological terminology follows Chou et al. (1993), Matsumura et al. (2013) and Li and Liang (2018).

Body length (**BL**) was measured from the anterior margin of labrum to the apex of elytra; body width (**BW**) was measured along the greatest elytral width **(EW)**; head length (**HL**) was measured along the anterior margin of labrum to the posterior margin tumid gena; head width (**HW**) was measured along the widest part of head including eyes; pronotum length (**PL**) was measured along the median line of pronotum; pronotum width (**PW**) was measured across the widest part of the pronotum; elytra length (**EL**) was measured along the suture from base of scutellum to the elytral apex.

Dry specimens were soaked in hot water for 1–2 hours to soften the body. The abdomen was opened at its lateroapical margin and genitalia were pulled out using forceps. Genitalia were soaked in warm 10% KOH for 1 hour, and dyed in Chlorazol Black E. The basal orifice of the aedeagus was injected with 100% ethanol by using a microinjector until the internal sac was fully everted. The aedeagus with its everted internal sac was photographed by a Canon D450 camera fitted to a Nikon SMZ1500 stereomicroscope or a Nikon D610 digital camera fitted to a Nikon SMZ18 stereomi-

croscope. The photographs were combined with Helicon Focus software to obtain one synthesized photograph, and finally edited in Photoshop (CC). A microvial with genitalia was pinned to the specimen from which the genitalia were removed for storage. Collections cited in this article are indicated by the following abbreviations:

CBWX Collection of Bi Wenxuan, Shanghai, China.
IZCAS Institute of Zoology, Chinese Academy of Sciences, Beijing, China.
KIZ Kunming Institute of Zoology, Chinese Academy of Sciences, Kunming, China.
NHMUK The Natural History Museum, London, UK.

Taxonomy

Genus *Manipuria* Jacoby, 1908

Manipuria Jacoby, 1908: 84; Monrós 1960: 153.

Type species. *Manipuria dohertyi* Jacoby, 1908: 84 (type locality: Manipur; holotype in NHMUK), by monotypy.

Diagnosis. Body elongate and subcylindrical. Head obviously longer than width; eye small; gena elongate, lateral sides behind eyes almost parallel; vertex smooth in the center, sparsely punctate in lateral area, with a longitudinal groove in the middle; occipit punctate, with a longitudinal groove medially; frontal tubercle glabrous, raised; clypeo-frontal area triangular, area near the anterior margin raised, disc with punctures and setae; labrum transverse, with setae on both apical angles. Antenna filiform, more than half BL. Pronotum wider than head, lateral constriction impunctate; posterior transverse impression distinct. Elytra unicolored or with yellow patches; striae with punctures regularly arranged, punctures weakened posteriorly and disappeared apically. Legs slender, with punctures and pubescence. Two claws asymmetrical. Abdominal sternite with pubescence and punctures.

BL. 9.0–14.0 mm.

Distribution. China (Yunnan, Tibet); India (Manipur).

Manipuria yuae sp. nov.

http://zoobank.org/1C8831C4-A2E8-484F-B356-B004BEFA86E1
Figures 1–3, 5–10, 15–16, 18–19, 21, 22

Type locality. China, Tibet, Mêdog, Baibung, Gelin village, altitude 1171 m.

Type material. ***Holotype*:** male (IZCAS), China, Tibet, Mêdog, Baibung, Gelin village, 29.40322N, 95.18435E/1171 m, 2011.VIII.13, Wenxuan Bi coll./HOLOTYPE *Manipuria yuae* sp. nov., des. by Xu, Bi & Liang, 2020 [red label]. ***Paratype***

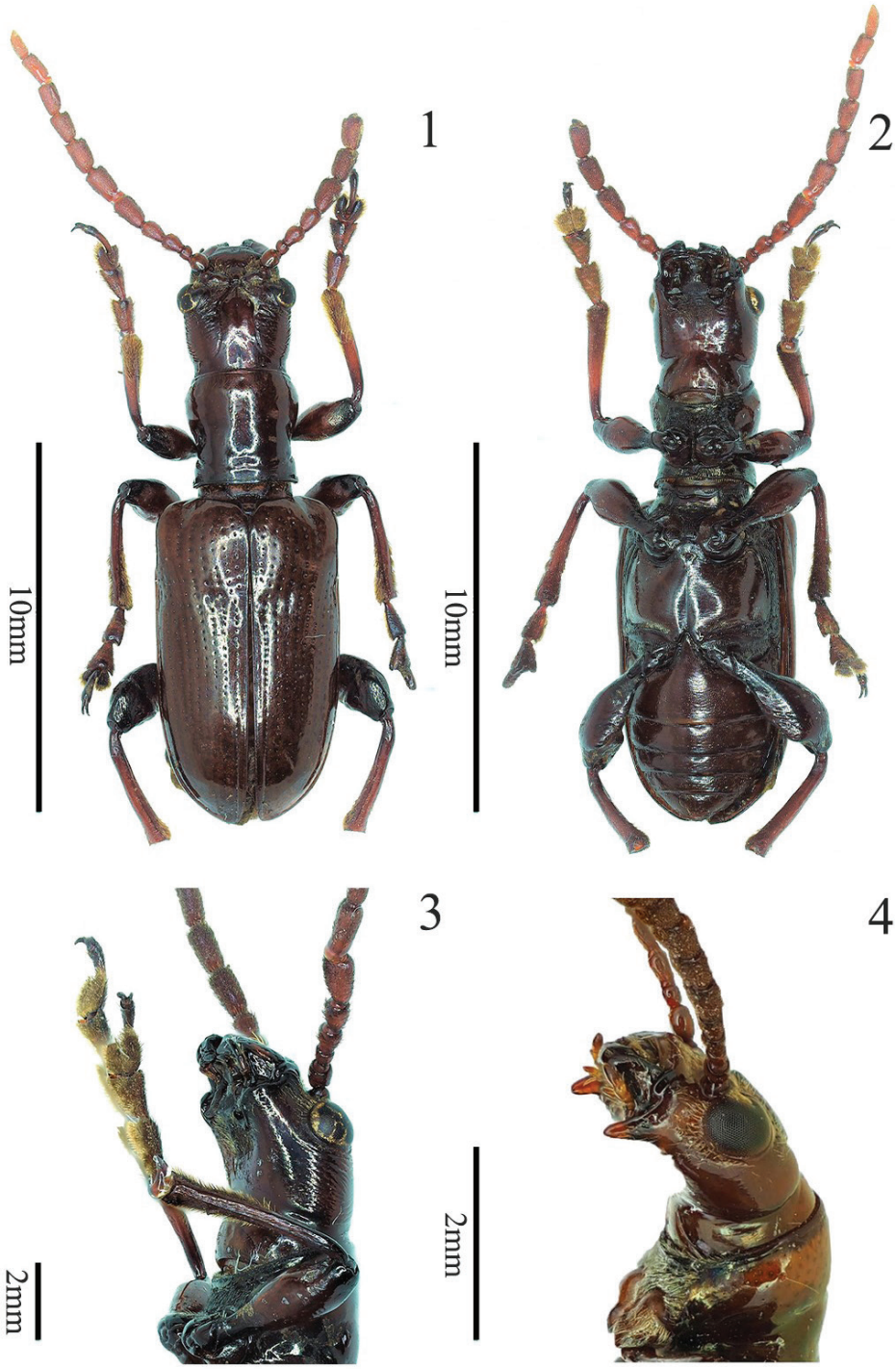

Figures 1–4. *Manipuria* spp. **1** holotype of *M. yuae* sp. nov., dorsal view **2** holotype of *M. yuae* sp. nov., ventral view **3** head of holotype of *M. yuae* sp. nov., ventro-lateral view **4** head of *M. dohertyi*, male, ventro-lateral view.

(two males and one female): one male (IZCAS), the same collecting data as holotype but labeled as paratype; one female (IZCAS), China, Tibet, Mêdog, Baibung, Gelin village, 29.40322°N, 95.18435°E/1171 m, 2011.VIII.11, Xiaodong Yang coll./PARATYPE *Manipuria yuae* sp. nov., des. by Xu, Bi & Liang, 2020; one male (KIZ), China, Yunnan, Ruili, 1981.X.16, Dazhi Dong coll./PARATYPE *Manipuria yuae* sp. nov., des. by Xu, Bi & Liang, 2020 [yellow label].

Diagnosis. Body brownish red. Head longer than wide; gena elongate with wrinkles and setae, lateral sides behind eyes almost parallel, slightly constricted behind gena; antennae more than half of BL, 5–11 antennomeres cylindrical. Pronotal disc with fine punctures, lateral sides constricted after the middle. Scutellum triangular. Elytra with punctures regularly arranged, punctures absent apically.

Comparisons. This species can be distinguished from *M. dohertyi* by the following combination of characters: lateral sides of head without prolongation in front of mandible, elytral unicolored (lateral sides of head with a tooth-like prolongation in front of mandible, elytra with four yellow patches in *M. dohertyi*).

Description. BL = 12.4–14.0 mm, BW = 4.2–4.5 mm. Head, pronotum, elytra, antennae, tibia, metasternum, abdominal sternite brownish red; prosternum, mesosternum, metepisternum black; ventral surface of femora brown, dorsal surface black; basal three tarsomeres brown, apical tarsomere black.

Head (Figs 1, 3, 5, 9). HL/HW = 1.5–1.6; gena elongate, lateral sides behind eyes almost parallel, head slightly constricted after gena, area behind eyes with wrinkles and setae; vertex smooth in the center, punctate in lateral area, with a deep groove in the middle, with apex pointed dorsally before groove (Fig. 9); occipit with a shallow furrow medially, sparsely punctate; frontal tubercle glabrous, raised; clypeo-frontal area triangular, area near the anterior margin raised, disc with punctures and setae; labrum transverse, with 3–5 long setae on each outer apical angle; antennae filiform, more than half of BL, antennomeres 1 and 2 nearly globular, shiny, antennomere 1 twice as long as antennomere 2, antennomeres 3 and 4 pubescent and punctate, length almost equal, antennomeres 5–11 cylindrical, with punctures and pubescence, antennomeres 5–7 twice as long as wide, antennomeres 8–11 three times as long as wide.

Pronotum. PW/HW =1.0–1.1, PL/PW = 1.1–1.2; anterior angle protruding, posterior angle not protruding; lateral side constricted behind the middle; areas near anterior and posterior margins with a few fine punctures, middle areas of disc with four rows of irregular fine punctures; posterior transverse impression distinct, basal transverse groove weak. Scutellum triangular, posterior angles round, lateral area of base sparsely pubescent.

Elytra narrowed posteriorly. EL/EW = 1.7; suture angle rounded; humeri protruding, humeral groove shallow, basal impression distinct; striae with punctures regularly arranged, punctures in basal impression larger, remaining punctures smaller, and punctures disappeared apically, intervals with a few fine punctures; scutellar stria composed of 8–11 punctures; epipleura raised, with a row of small punctures; underside of the hind sutural angles with plectrum.

Mesosternum pubescent; mesosternal process short, narrow, densely pubescent, pointed ventrally. metasternal disc with very sparse setae; metepisternum densely pubescent.

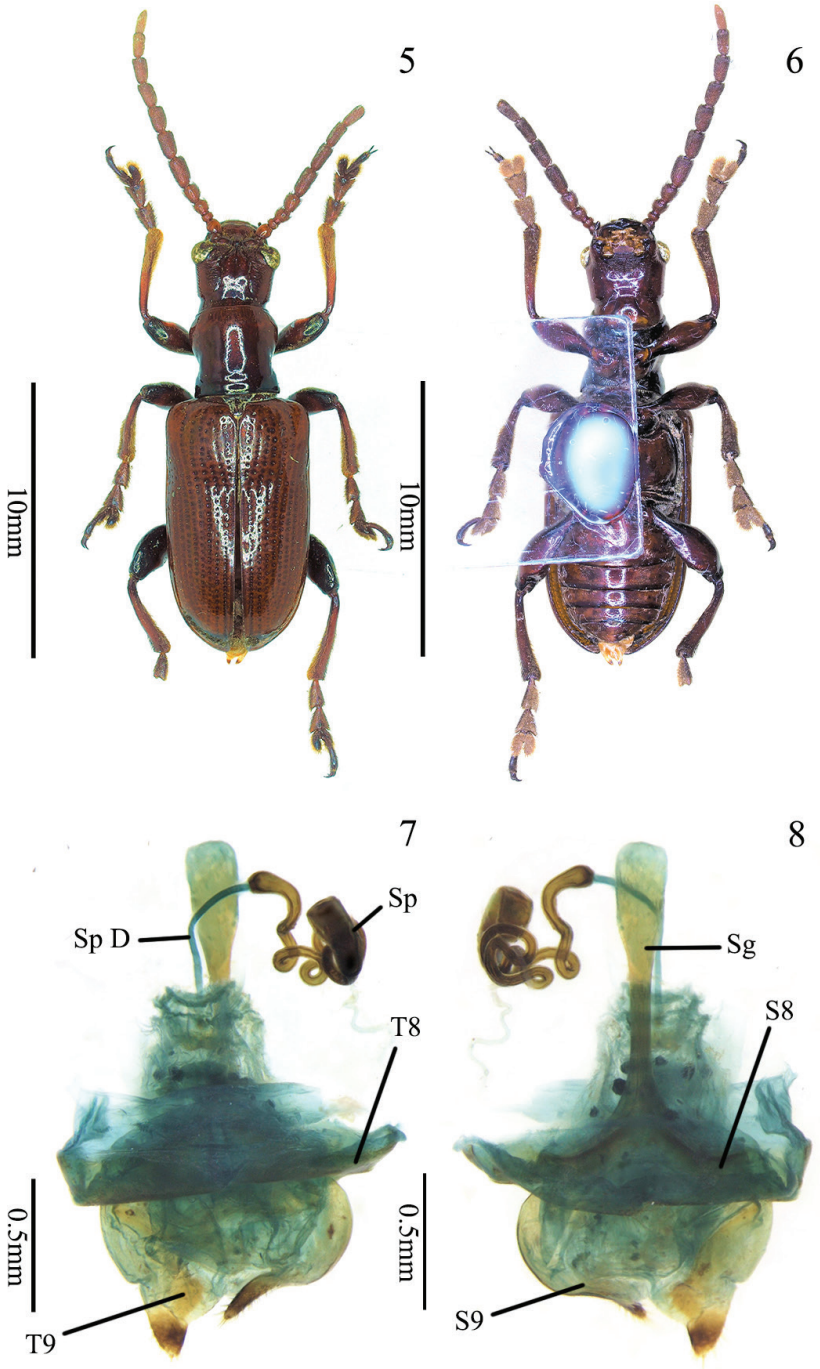

Figures 5–8. Paratype of *Manipuria yuae* sp. nov., female **5** habitus, dorsal view **6** habitus, ventral view **7** female genitalia and reproductive organs, dorsal view **8** genitalia and reproductive organs, ventral view. Abbreviations: Sg spiculum gastrale; S8 sternite 8; S9 sternite 9; T8 tergite 8; T9 tergite 9; Sp D spermathecal duct; Sp spermatheca.

Figures 9, 10. *Manipuria yuae* sp. nov. **9** head, dorsal view **10** spermatheca and spermathecal gland.

Abdominal sternite with sparse setae and punctures, transverse impressions distinct in both lateral areas of each sternite; the eighth visible abdominal tergite with pars stidens.

Legs slender; tibia with dense punctures and pubescence; metafemur with dense setae in dorsal surface, with sparse setae in ventral surface, middle area with a large triangular denticle.

Male genitalia. Median lobe strongly sclerotized, tubular, curved, apical portion gradually narrowed, median foramen occupying 1/5 length of aedeagus (Figs 15, 16); apex truncated in the middle (Figs 18, 19); tegmen Y-shaped and slender, basal piece of tegmen triangular and relatively broad, lateral lobes narrow and combined with second connecting membrane; internal sac membranous, with dorsal, median, and ventral strongly scleritized (Figs 21A–C, 22A–C).

Female reproductive organs (Figs 7, 8, 10). Tergites 8 and 9, sternites 8 and 9 of female sclerotized, posterior areas of tergite 8 and sternite 8 with sparse setae and apodemes, spiculum gastrale Y-shaped and expanded in the end, distal part of spiculum gastrale squared, margin curved; ovipositor with dense setae, distal part of ovipositor conical, short; spermatheca strongly sclerotized, complicatedly folded and curved; spermathecal duct relatively long, connected with spermatheca and bursa copulatrix; spermathecal gland curved, long.

Distribution. China (Tibet, Yunnan).

Etymology. The specific name *yuae* is proposed in memory of Professor Peiyu Yu, who contributed greatly to the taxonomy on Chinese Criocerinae.

Host plant. This species lived on *Smilax* sp. (Smilacaceae) according to observations of the second author (BWX).

Habitat. The locality of the new species in Mêdog county is situated at the northernmost part of tropics in Asia. The vegetation is tropical seasonal rainforest. The climate is characteristic of high temperature, plentiful precipitation, and high humidity. The biodiversity is rich in this region. The forests are composed of tall trees, woody

vines and epiphytes. The host plant of new species is *Smilax* sp. (Smilacaceae). It shares its habitat with plants such as *Hedychium* sp. (Zingiberaceae), *Musa* sp. (Musaceae), *Epipremnum* sp. (Araceae), *Lysionotis* spp. (Gesneriaceae), *Alsophila* sp. (Cyatheaceae), and *Dryopteris* sp. (Dryopteridaceae).

Remarks. The specimen from Yunnan differs slightly from those from Tibet in having a lighter color (yellow-red), a shorter head (HL/HW = 1.5), and weaker sclerites (yellow) of the male genitalia.

When this new species is included, the concept of the genus *Manipuria* is expanded slightly by the absence of a projection on front of the mandible. The genus *Manipuria* differs from the genus *Lilioceris* mainly in having elongate gena, a less constricted neck, and small eyes.

Some characters of the new species suggest its intermediate position between *Lilioceris* and *Manipuria* as the head is only slightly enlarged and the ventral teeth on the head only weakly developed. It appears to occupy a position nearer to *Lilioceris* than to *Crioceris* as the pronotum is strongly narrowed in the middle. The relationship between *Manipuria* and *Lilioceris* needs further investigation.

Manipuria dohertyi Jacoby, 1908

Figures 4, 11–14, 17, 20, 23

Manipuria dohertyi Jacoby, 1908: 84; Monrós 1960: 153.

Material examined. Types. One female (NHMUK), Type / Doherty / India Or, Manipur / Fry Coll. 1905-100 / Manipuria Dohertyi Jac. / Syntype. **Non-types.** one male (IZCAS), China, Yunnan, Gongshan, Dulongjiang, Maku village, 27.68936°N, 98.30804°E/1692 m, 2019.8.22, Liang HB & Xu Y coll. one female (CBWX), China, Yunnan, Gongshan, Dulongjiang, Maku village / 1250 m, 2015.7.25, Bi WX coll.

Diagnosis. Body brownish black, elytra with yellow patches, each patch surrounded with a black circle. Head longer than wide; lateral sides of head with a tooth-like prolongation in front of mandible; gena elongate, with fine wrinkles and setae; lateral sides behind eyes almost parallel; antenna more than half BL. Pronotal disc with fine punctures; lateral sides constricted behind the middle. Scutellum triangular.

Redescription. BL = 8.7–9.0 mm, BW = 3.0–3.2 mm. Brown or brownish black, with coppery metallic luster, each elytron with two yellow patches, one patch behind the shoulders slightly transverse, and another near the apex rounded, each surrounded by a black circle.

Head (Figs 4, 11, 13). HL/HW = 1.1; lateral sides of head with a tooth-like prolongation in front of mandible, gena elongate with fine wrinkles and setae, lateral sides behind eyes almost parallel, then constricted behind gena; vertex smooth, with a shallow longitudinal groove in the middle, apex pointed dorsally before the groove; occipit sparsely punctate, with a shallow longitudinal groove medially; frontal tubercle glabrous, raised; clypeo-frontal area triangular, area near anterior margin raised, disc

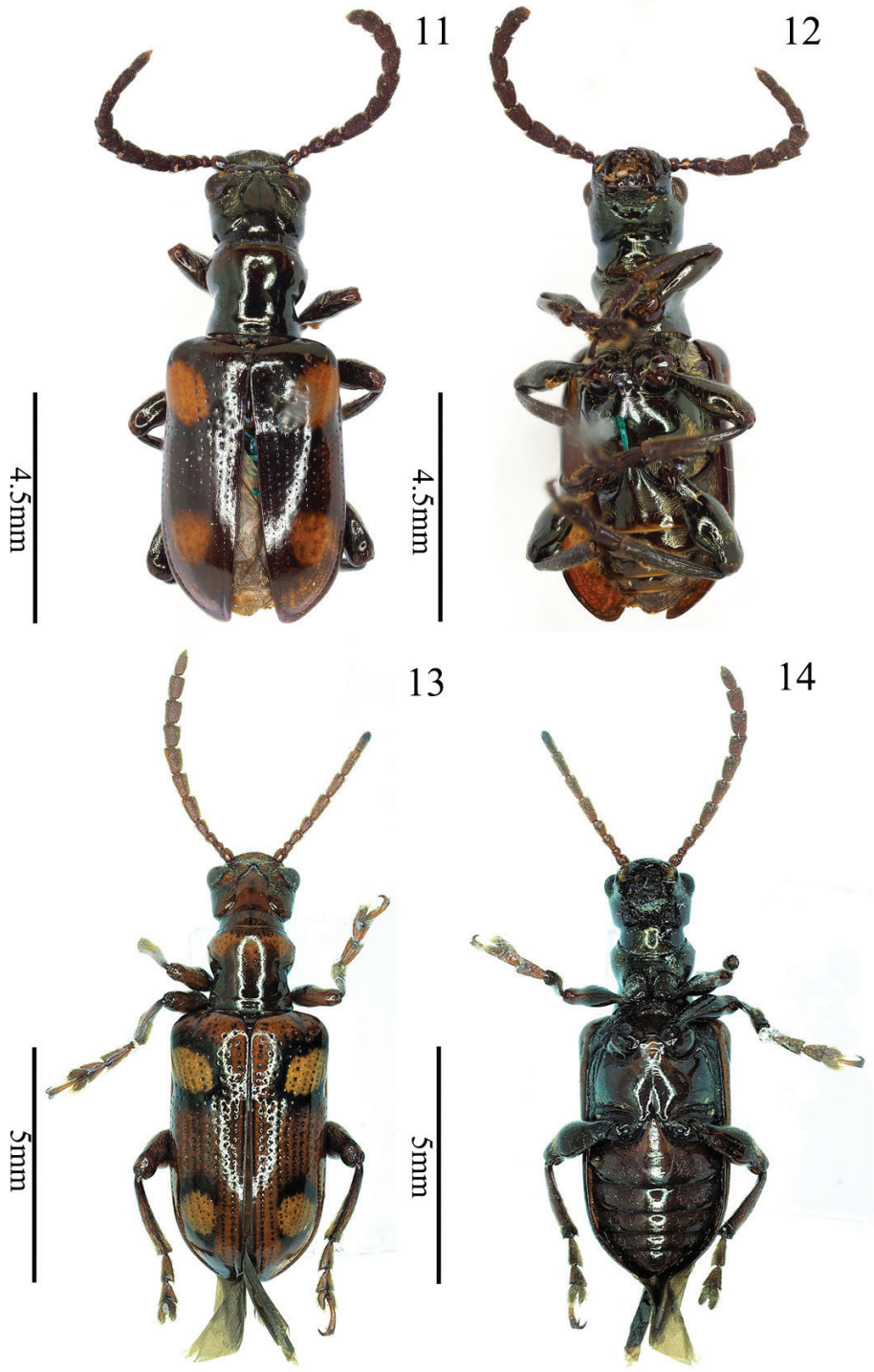

Figures 11–14. *Manipuria dohertyi* Jacoby **11** type, female, dorsal view **12** type, female, ventral view **13** specimen from Yunnan, male, dorsal view **14** specimen from Yunnan, male, ventral view.

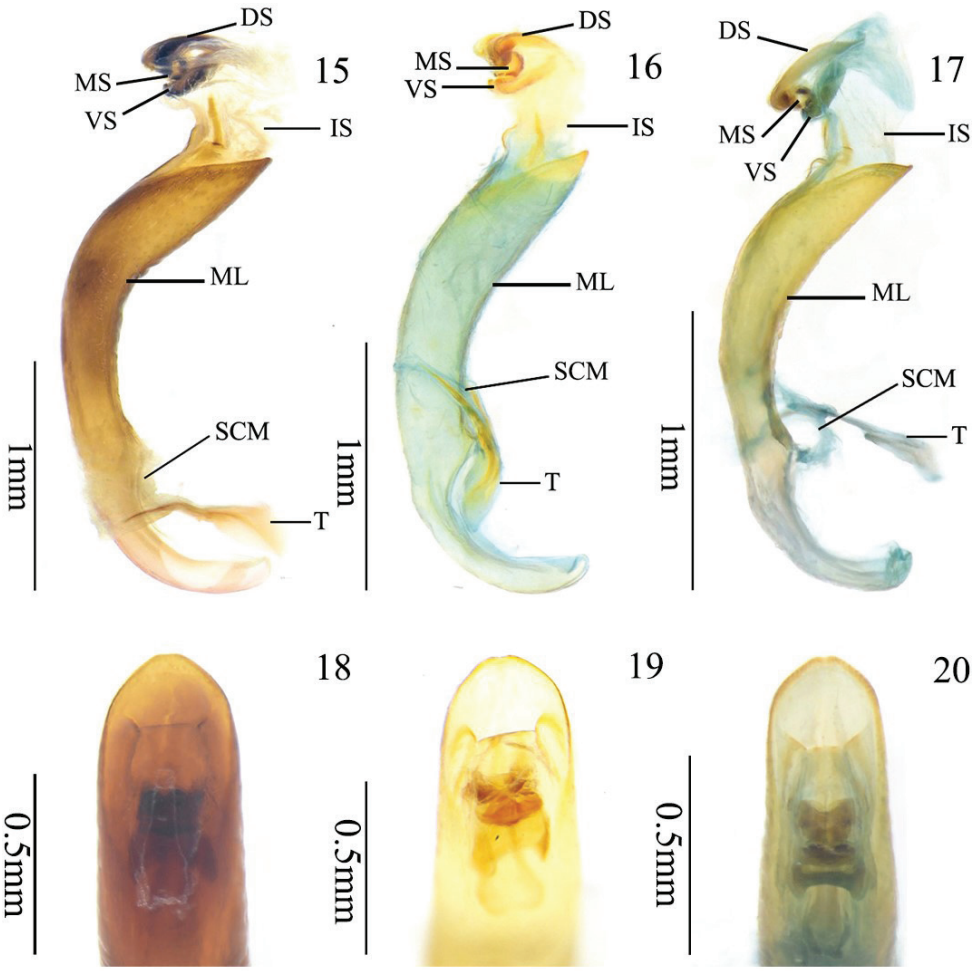

Figures 15–20. Aedeagus and internal sac of *Manipuria* spp. **15** holotype of *M. yuae* sp. nov., lateral view **16** paratype of *M. yuae* from Yunnan, lateral view **17** *M. dohertyi* from Yunnan, lateral view **18** holotype of *M. yuae* sp. nov., dorsal view **19** paratype of *M. yuae* sp. nov. from Yunnan in dorsal view **20** *M. dohertyi* from Yunnan, dorsal view. Abbreviations: DS dorsal sclerite; MS dorsal sclerite; VS dorsal sclerite; IS internal sac; ML median lobe; SCM second connecting membrane; T tegmen.

with punctures and setae; labrum transverse, with 3–5 long setae on both apical angles; antenna filiform, more than half BL, antennomeres 1 and 2 nearly globular and shiny, antennomere 1 twice as long as antennomere 2, antennomeres 3 and 4 pubescent and punctate, length almost equal, antennomeres 5–11 cylindrical, with punctures and pubescence, antennomeres twice as long as wide.

Pronotum. PW/HW = 1.1–1.3, PL/PW = 0.9–1.0; anterior angle protruding, posterior angle not protruding; lateral side constricted just behind the middle; middle region of disc with two rows of fine punctures and a longitudinal fovea; posterior transverse impression distinct; basal transverse groove weak. Scutellum triangular, lateral sides of base with pubescence.

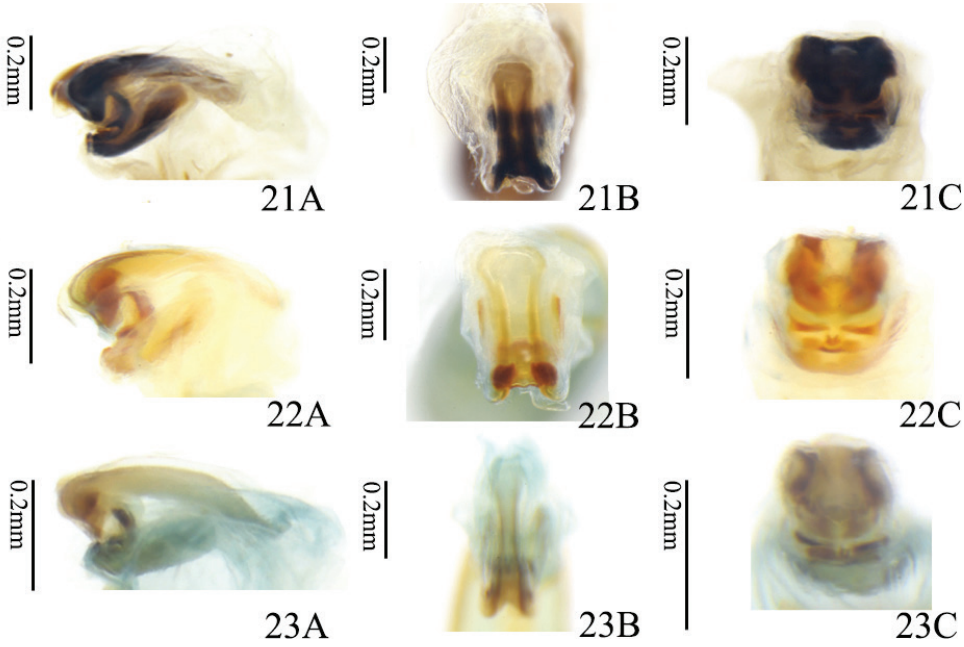

Figures 21–23. Sclerites in internal sac **21** holotype of *Manipuria yuae* **22** paratype of *M. yuae* from Yunnan **23** *M. dohertyi* from Yunnan **A** lateral view **B** dorsal view **C** ventral view.

Figure 24. Habitat of *Manipuria dohertyi* in Maku village of Yunnan, China.

Elytra narrowed posteriorly, EL/EW =1.7; suture angle rounded; humeri protruding, humeral groove shallow; basal impression distinct; punctures in basal impression large, remaining punctures small, apical punctures disappeared, intervals with few fine punctures; scutellar stria composed of 3–6 punctures; epipleura raised, with a single row of small punctures; underside of the hind sutural angles with plectrum.

Mesosternum pubescent, mesosternal process short, narrow, densely pubescent, pointed ventrally. Outer metasternal disc with an oblique setose area, extending from posterior angle to the middle of disc (setae partially fell off in Fig. 14, but their pores still visible); metepisternum densely pubescent.

Abdominal sternite with dense pubescence and punctures, middle area of sternite less pubescent than both sides, transverse impressions distinct in both lateral areas; the eighth visible abdominal tergite with pars stidens.

Legs slender; tibia with punctures and pubescence; femora with dense setae in dorsal surface, with sparse setae in ventral surface, middle area with a triangular denticle.

***Genitalia*.** Median lobe sclerotized, tubular, curved, median foramen occupying 1/4 length of aedeagus; medial portion slightly broader than basal and apical portion in ventral view (Fig. 17); middle of apex truncated in dorsal view (Fig. 20); tegmen Y-shaped and weak, basal piece of tegmen triangle and relatively small, lateral lobes slender and combined with second connecting membrane; internal sac membranous, with three sclerotized sclerites, dorsal, median, and ventral sclerites (Fig. 23A–C).

Distribution. China (Yunnan), India (Manipur).

Host plant. This species lived on *Smilax ferox* Wall. ex Kunth (Smilacaceae) according to photos (Figs 25, 26) taken by the second author (BWX).

Habitat. The habitats are shown in Fig. 24. It is similar to those of *M. yuae* sp. nov. in Mêdog, but with some patches of cultivated field.

Remarks. The specimens from Yunnan, China differ slightly from the type specimen in having: 1) body color brown (brownish black in type); 2) sides behind eyes and outer area of metasternal disc with sparser setae (denser in type); 3) antennomeres 3 and 4 longer (shorter in types); 4) anterior yellow patches more distant from shoulder and each of four patches surrounded by a distinct blackish circle (anterior yellow patches closer to shoulder and patches surrounded by a weak blackish circle in type). These external variations indicate that the specimens from Yunnan might represent another new species, but we only checked two specimens from Yunnan and tentatively treated them as members of *M. dohertyi*. These new records extend the distribution of *M. dohertyi* northwards by ca 500 km.

We also compared the differences in the internal sac between *M. dohertyi* and *M. yuae*, and they differ significantly in the shape of the dorsal sclerite (Figs 21–23). In lateral view, the dorsal sclerite of *M. dohertyi* is obviously enlarged backwards but *M. yuae* does not have such a sclerite; in dorsal view, the dorsal sclerite of *M. dohertyi* is slender and narrowed in the middle, and the sides of the dorsal sclerite of *M. yuae* are nearly parallel; in ventral view, the horn of the dorsal sclerite of *M. yuae* is bent downwards, but in *M. dohertyi* it is bent forwards.

Figure 25. *Manipuria dohertyi* Jacoby standing on leaf of *Smilax*.

Figure 26. *Smilax ferox* Wall. ex Kunth (host plant of *Manipuria dohertyi*).

Acknowledgements

We thank Mr Changchin Chen (Tianjin, Wuqing) and Mr Xiaodong Yang (Sichuan, Yibin) for presenting us with the specimens; Professor Rong Li (Kunming Institute of Botany) for identification the host plant; Professor Hong Liu (South-Central University for Nationalities) for providing data of plant assemblage in Mêdog; Professor Peiyu Yu (IZCAS), Dr Qiaozhe Lou (Hebei, Shijiazhuang), and Ms Kaiqin Li (KIZ) for their advice and suggestions on this paper; Dr Beulah Garner and Dr Michael Geiser for hosting third author (LHB) at NHMUK. This study was supported by the Second Tibetan Plateau Scientific Expedition and Research (STEP) program (Grant No. 2019QZKK0501), and National Natural Science Foundation of China (Grant No. 31970400).

References

Berti N, Rapilly M (1976) Faune d'Iran. Liste d'espèces et révision du genre *Liliоceris* Reitter [Col. Chrysomelidae]. Annales de la Société Entomologique de France (N.S.) 12(1): 31–73.

Bezděk J, Schmitt M (2017) Subfamily Criocerinae. In: Löbl I, Smetana A (Eds) Catalogue of Palaearctic Coleoptera (Vol. 6) Corrigenda et Addenda. Entomologische Blätter und Coleoptera 113(2): 113–135.

Chou I, Liu SK, Xie WP (1993) Taxonomist's Glossary of Genitalia in Insects. Tianze Eldonejo, Hong Kong, 82–88. [In Chinese]

Chûjô M (1951) A taxonomic study on the Chrysomelidae (Insecta-Coleoptera) of Formosa. I. Subfamily Criocerinae. Technical Bulletin of the Kagawa Agricultural College 2: 71–120.

Fabricius J (1798) Supplementum entomologiae systematicae. C.G. Proft et Storch, Hafniae, 572 pp.

Geoffroy E (1762) Histoire abrégée des insectes qui se trouvent aux environs de Paris; dans laquelle ces animaux sont rangés suivant un ordre méthodique. Tome premier. Durand, Paris, [4] + xxxviii + 523 + 1 pp. [11 pls.] https://doi.org/10.5962/bhl.title.154767

Gressitt J, Kimoto S (1961) The Chrysomelidae (Coleopt.) of China and Korea, Part 1. Pacific Insects Monograph 1A: 1–299.

Heinze E (1943) Über australische Criocerinen. Entomologische Blätter 39: 22–28.

Jacoby M (1908) The Fauna of British India, including Ceylon and Burma. Coleoptera, Chrysomelidae. Taylor & Francis, London, 534 pp.

Kimoto S (2005) Systematic Catalog of the Chrysomelidae (Coleoptera) from Nepal and Bhutan. Bulletin of the Kitakyushu Museum of Natural History and Human History Series A, 3: 13–114.

Lawrence J, Newton A (1995) Families and subfamilies of Coleoptera (with selected genera, notes, references and data on family-group names). In: Pakaluk J, Ślipiński SA (Eds) Biology, Phylogeny, and Classification of Coleoptera: Papers Celebrating the 80th Birthday of Roy A. Crowson. Muzeum Instytut Zoologii PAN, Warszawa, 779–1006.

Lee CF, Matsumura Y (2013) On newly and recently recorded species of the genus *Lema* Fabricius (Coleoptera, Chrysomelidae, Criocerinae) from Taiwan. ZooKeys 262 (262): 17–38. https://doi.org/10.3897/zookeys.262.4152

Li KQ, Liang HB (2018) A comparative study of external female genitalia (including the 8th and 9th abdominal segments) in the family Megalopodidae and other related families of Chrysomeloidea. ZooKeys (762): 69–104. https://doi.org/10.3897/zookeys.762.22163

Li KQ, Liang ZL, Liang HB (2013) Two new species of the genus *Temnaspis* Lacordaire, 1845, (Coleoptera: Chrysomeloidea: Megalopodidae) from China and Myanmar, with notes on the biology of the genus. Zootaxa 3737(4): 379–398. https://doi.org/10.11646/zootaxa.3737.4.3

Matsumura Y, Machida R, Wipfler B, Beutel R, Yoshizawa K (2013) Parallel evolution of novelties: extremely long intromittent organs in the leaf beetle subfamily Criocerinae. Evolution and Development 15(4): 305–315. https://doi.org/10.1111/ede.12036

Matsumura Y, Yoshizawa K (2012) Homology of the Internal Sac Components in the Leaf Beetle Subfamily Criocerinae and Evolutionary Novelties Related to the Extremely Elongated Flagellum. Journal of Morphology 273: 507–518. https://doi.org/10.1002/jmor.11037

Monrós F (1960) Los géneros de Chrysomelidae (Chrysomelidae). Opera Lilloana (Tucumán) 3(1959): 1–337. [3 pls.]

Reitter E (1913) Fauna Germanica. Die Käfer des Deutschen Reiches. Band IV. K.G. Lutz' Verlag, Stuttgart [1912], 236 pp. [+ 22 pls.]

Sharp D, Muir F (1912) The comparative anatomy of the male genitalia tube in Coleoptera. Transactions of the Entomological Society of London 1912: 477–642. https://doi.org/10.5962/bhl.title.11474

Shi HL, Liang HB (2015) The genus *Pterostichus* in China II: the subgenus *Circinatus* Sciaky, a species revision and phylogeny (Carabidae, Pterostichini). ZooKeys 536: 1–92. https://doi.org/10.3897/zookeys.536.5982

Snodgrass R (1935) Principles of Insect Morphology. McGraw-Hill Book Company, New York, 667 pp.

Suzuki K (1988) Comparative morphology of the internal reproductive system of Chrysomelidae (Coleoptera). In: Jolivet P, Petitpierre E, Hsiao TH (Eds) Biology of Chrysomelidae. Kluwer Academic Publishers, Dordrecht, Boston, and London, 317–355. https://doi.org/10.1007/978-94-009-3105-3_19

Tishechkin A, Konstantinov A, Bista S, Pemberton R, Center T (2011) Review of the continental Oriental species of *Lilioceris* Reitter (Coleoptera, Chrysomelidae, Criocerinae) closely related to *Lilioceris impressa* (F.). ZooKeys 103: 63–83. https://doi.org/10.3897/zookeys.103.983

Warchałowski A (2010) The Palaearctic Chrysomelidae: identification keys (Vol. 1). Natura optima dux Foundation, Warszawa, 629 pp. https://doi.org/10.1649/072.065.0210

Warchałowski A (2011) An attempt on a review of *Lilioceris* Reitter,1913-species from continental part of south-eastern Asia (Coleoptera: Chrysomelidae: Criocerinae). Wroclaw 22(1): 95–122.

ZooKeys 1009: 45–66 (2021)
doi: 10.3897/zookeys.1009.54554
https://zookeys.pensoft.net

RESEARCH ARTICLE

A peer-reviewed open-access journal
ZooKeys
Launched to accelerate biodiversity research

A new species of *Rangabradya* (Copepoda, Harpacticoida, Ectinosomatidae) from a cave in Satun Province, southern Thailand

Chaichat Boonyanusith[1], Sujeephon Athibai[2]

1 *School of Biology, Faculty of Science and Technology, Nakhon Ratchasima Rajabhat University, Nakhon Ratchasima 30000, Thailand* **2** *Applied Taxonomic Research Center and Department of Biology, Faculty of Science, Khon Kaen University, Khon Kaen 40002, Thailand*

Corresponding author: Chaichat Boonyanusith (chaichat.b@nrru.ac.th)

Academic editor: Kai Horst George | Received 21 May 2020 | Accepted 5 November 2020 | Published 4 January 2021

http://zoobank.org/5400526C-94CA-4E73-B738-57427B8635DD

Citation: Boonyanusith C, Athibai S (2021) A new species of *Rangabradya* (Copepoda, Harpacticoida, Ectinosomatidae) from a cave in Satun Province, southern Thailand. ZooKeys 1009: 45–66. https://doi.org/10.3897/zookeys.1009.54554

Abstract

A representative of the family Ectinosomatidae was discovered in a temporary pool in a cave in the Satun Province, southern Thailand. Based on the characteristics of the antennary exopod, armature of the female fifth leg, and configuration of the male sixth leg, a new species of the genus *Rangabradya* was identified, representing the first record of the genus in the continental waters of Thailand and in Southeast Asia. The new species can be distinguished from *Rangabradya indica* by the configurations of the fifth and the sixth legs in both sexes, the body ornamentation of the urosomite, and the armature of the mouthparts. These structures show a more primitive state in the new species. Accordingly, a new subgeneric rank in the genus *Rangabradya*, *Siamorangabradya* **subgen. nov**, was established to accommodate the Thai species and *Rangabradya* (*Siamorangabradya*) *wongkamhaengae* **subgen. et sp. nov.** was described. Also, the key to all 23 genera of the family was updated.

Keywords

Anchialine caves, cave-dwelling copepods, Satun Geopark, Satun Province, Southeast Asia

Introduction

Satun Province is located in southern Thailand and is part of the continental area of the Sunda Subregion (Fig. 1A). Evidence for an Australian affinity of Late Cambrian fossils on Tarutao Island (a part of the province in the Andaman Sea) has suggested an eastern Gondwana origin of the Sibumasu Terrane (Shergold et al. 1988; Metcalfe 1998). A karst topography dominates the north and east of the province characterized by limestone mountains with sharp blade-like tips, sinkholes, caves, and a network of underground water channels. The west of the province is represented by a lowland area covered by sediments of the ancient shallow sea. A rich diversity of fauna endemic to the country is expected for Satun Province, where several new taxa have recently been discovered from karstic areas (e.g., Sumontha et al. 2014; Liu et al. 2017; Nilsai et al. 2017; Promdam et al. 2017). To date, two new copepod species from this province have been described, namely, *Onychocamptus satunensis* Boonyanusith, Saetang, Wongkamhaeng & Maiphae, 2018 and *Boholina laorsriae* Boonyanusith, Wongkamhaeng & Athibai, 2020 (Boonyanusith et al. 2018, 2020). The latter is the first record of the subterranean Calanoida in Thailand.

The family Ectinosomatidae Sars, 1903 is speciose, encompassing 325 valid species from 23 genera (George and Schwabe 2019). Representatives of the family occupy a wide array of habitats. Most species are known from the fine sediments of the sublittoral marine environments (Kihara and Huys 2009), although, many species inhabit the abyssal plains (Bodin 1968; Seifried et al. 2007), and a few have been described from the surface and subterranean freshwater habitats (Karanovic and Pesce 2001). Additionally, a few species are symbionts (Boxshall and Halsey 2004; George and Schwabe 2019).

Among the genera currently known as members of the family Ectinosomatidae, the genus *Rangabradya* Karanovic & Pesce, 2001 is a subterranean freshwater representative. The only known species of the genus is *Rangabradya indica* Karanovic & Pesce, 2001, previously described from a freshwater bore-well in India (Fig. 1A). Morphologically, the genus is distinguished from all other Ectinosomatidae by the presence of a single seta on the endopodal lobe of the male fifth leg and the characteristics of the antennary exopod (Karanovic and Pesce 2001).

Five years ago**,** a representative of the family Ectinosomatidae was encountered in samples of cave-dwelling copepods from a cave in the La-Ngu District of Satun Province, southern Thailand. The morphology of body shape, maxilla, and swimming legs indicates the close relatedness of the Thai specimens and the genus *Rangabradya*, but a detailed examination revealed a more primitive state in the mouthparts, fifth and sixth swimming legs, and ornamentation of the urosomites. However, there is no apomorphic character to distinguish it as a new genus. For this reason, a new subgeneric rank was created within the genus *Rangabradya*, and the new cave-dwelling Harpacticoida from southern Thailand was named *Rangabradya* (*Siamorangabradya*) *wongkamhaengae* subgen. et sp. nov. In this paper, descriptions and illustrations of the new species are presented. Furthermore, an updated key to all 23 genera of the family is provided.

Materials and methods

Samples were collected from a temporary pool in Khay Cave of Satun Province, southern Thailand, using a hand net with a mesh size of 60 μm, and stored in a solution of 4% formaldehyde. Specimens were sorted under a stereomicroscope and stored in 70% ethanol. Before the morphological examination, the specimens were placed in a mixture of glycerol and 70% ethanol (ratio ~1:10 v/v) for 30 minutes. They were subsequently completely dissected and mounted on slides in glycerol and covered with coverslips.

The examination of body parts and ornamentations was performed under a Nikon ECLIPSE E200 compound light microscope at 1000× magnification. The habitus and body appendages were drawn using a drawing tube attached to the compound microscope, and the final versions of the illustrations were prepared in Adobe Illustrator CC 2020. For a detailed examination, additional material was dehydrated in ethanol in a series of concentrations increasing from 70% to 100% and dried in a critical point dryer. Afterwards, they were mounted on stubs, coated with gold, and examined using a scanning electron microscope (Leo 1450VP).

Morphological descriptions were made following the terminology used in Huys and Boxshall (1991). The terms 'pars incisiva' and 'lacinia' were retained for the descriptions of the mandible. The following descriptive abbreviations are used in the description and figures:

Endp endopod; **ae** aesthetasc;
Exp exopod; **I** spine;
Endp/Exp-1 (2, 3) proximal (middle, distal) segment of endopod and exopod; **P1–P6** swimming legs 1–6.

The type material has been deposited at the Princess Maha Chakri Sirindhorn Natural History Museum, Prince of Songkla University, Songkhla, Thailand (**PSUNHM**).

Taxonomy

Order Harpacticoida Sars, 1903
Family Ectinosomatidae Sars, 1903
Genus *Rangabradya* Karanovic & Pesce, 2001

Subgenus *Siamorangabradya* subgen. nov.
http://zoobank.org/33D0FA48-E799-409E-84B0-F546BED6BC2A

Diagnosis. Ectinosomatidae, with fusiform habitus. Urosomite with spinule ornamentation. Antennule six-segmented in both male and female; third segment longest. Distal segment of antennary Exp elongate, with two apical setae; longest seta normally

developed; shortest one as long as segment bearing it. Mandible with additional spine at dorsal site of pars incisiva. Coxa of maxillule free. Maxilla straight, with three setae on distal endite of syncoxa and allobasis with two medial setae. Maxilliped three-segmented, with four setae on Endp. Armature formula of Exp-3, from P1–P4: 5.6.6.6. Female P5 Exp partly fused with baseoendopod, with three marginal setae; endopodal lobe of baseoendopod with two apical elements. Female P6 reduced to small protuberance with one apical seta on peduncle. Male P5 Exp completely fused to baseoendopod, with two apical setae on endopodal lobe. Male P6 reduced to simple plate and unarmed.

Type species. *Rangabradya* (*Siamorangabradya*) *wongkamhaengae* subgen. et sp. nov.

Etymology. The subgenus is named after Siam, Thailand's former name, prefixed to the existing generic name *Rangabradya*. The name is a feminine noun in the nominative singular.

Rangabradya (*Siamorangabradya*) *wongkamhaengae* sp. nov.

http://zoobank.org/17517BF1-EA91-46A4-98C5-66F8144065DF
Figures 2–6, 7A, 9 (female); 7B, 8, 10 (male)

Material examined. ***Holotype*:** Thailand • 1 ♀ (adult), 485 μm long; Satun Province, Khay Cave; 6°53'40"N, 99°46'44"E, 17 m a.s.l.; 17 Dec. 2014; C. Boonyanusith leg.; hand net; completely dissected and mounted on a slide in glycerol and sealed with nail polish; PSUZC-PK2005-01. ***Allotype*:** Thailand • 1 ♂ (adult), 428 μm long, collection data as for holotype; PSUZC-PK2005-02. ***Paratypes*:** Thailand • 1 ♀ (adult) and 1 ♂ (adult); same data as for holotype; PSUZC-PK2005-03 and PSUZC-PK2005-04, respectively.

Additional material. Thailand • 3 ♂♂ (adult), 1 ♀ (adult), 3 copepodids; same data as for holotype; preserved in 70% ethanol; retained in collection of the first author (CB).

Type locality. Khay Cave in La-Ngu District, Satun Province, Thailand. The cave's geography and morphology have previously been described in Boonyanusith et al. (2020) (Fig. 1).

Description of female. Total body length, excluding caudal setae, 485–489 μm (mean = 487; *N* = 3). Preserved specimens colourless. Habitus fusiform, gradually tapering posteriorly, with maximum width at posterior margin of cephalothorax (Figs 2A, 9A). Rostrum (Fig. 2B) well developed, broadly rounded, completely fused with cephalothorax, with two lateral sensilla near base. Prosome ca 1.6× as long as urosome (including caudal rami), comprising cephalothorax and three free pedigerous somites. Cephalothorax ca 1.1× as long as wide and ca 0.5× as long as length of prosome; posterior margin smooth. Distribution of sensilla and cuticular pores as illustrated (Figs 2A, 9B). All free pedigerous somites dorsally with a pair of pores on anterior margin; finely spinulated hyaline frill incised on posterior margin.

Urosome comprising fifth pedigerous somite, genital double-somite, and three free abdominal somites (Fig. 2A). Posterior margin of all urosomites with finely spinulated hyaline frill, except anal somite; hyaline frill on genital double-somite and

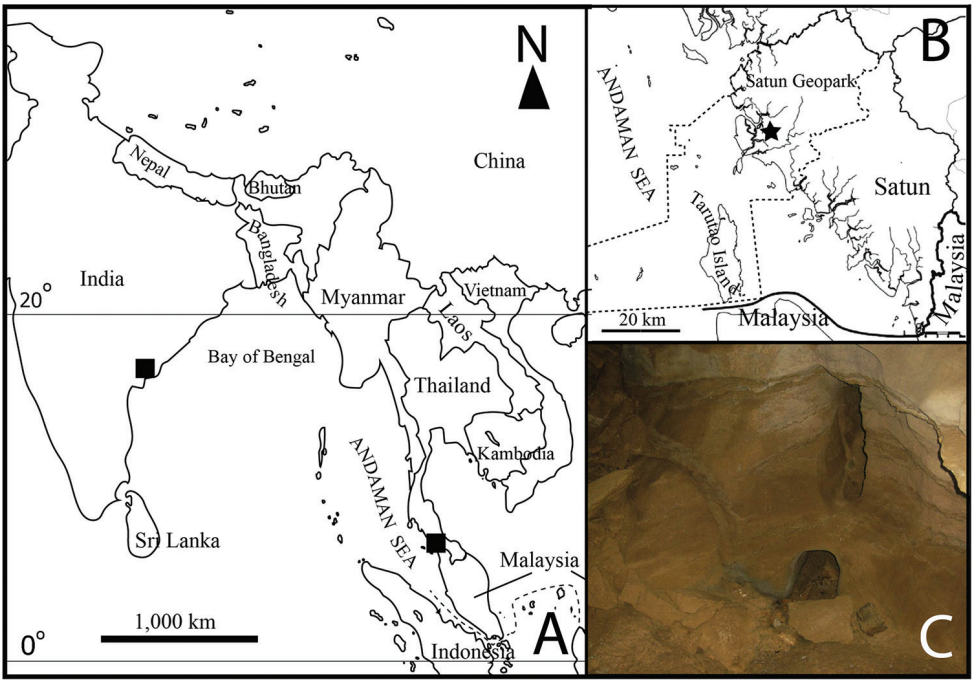

Figure 1. Geographical location and details of a sampling site **A** distribution of the representatives of the genus *Rangabradya* (black squares) **B** location of the Khay Cave in Satun Province, Thailand (star) **C** sampling point in the cave.

subsequent somite uniform in width dorsally and laterally, and central part wider than outer parts ventrally (Fig. 3A, B). Ornamentation as illustrated (Figs 2A, 3A, B). Fifth pedigerous somite wider than long, dorsally with pair of cuticular pores near anterior margin plus continuous row of minute spinules and four sensilla along posterior margin (Fig. 2A). Two rows of spinules lateroventrally, positioned next to implantation of P5, with one pore close to tip of proximal row (Figs 7A, 9G). Genital double-somite slightly wider than long, with three pores dorsally, arranged in triangle. Two sensilla near posterior margin and three rows of minute spinules dorsally on anterior half of double-somite; distal row with short gap medially (Fig. 3B). Ventrally a pore on either side of copulatory pore and two transverse rows of minute spinules along medial margin. Antero-laterally with three additional rows of relatively strong spinules, continuing into rows of spinules dorsally. Genital field (Fig. 3B) with small copulatory pore medially, at 1/3 of the double-somite length. Short seta representing P6 on peduncle. Second and third abdominal somites, with one single pore middorsally, near anterior margin plus pair of sensilla dorsally, near posterior margin and row of minute spinules, next to cuticular pore. Ventrally pair of cuticular pores present in second abdominal segment, but absent in the subsequent one, with lateral and lateroventral row of spinules anteriorly. Additional row of spinules ventrally, near posterior margin. Third abdominal somite with cuticular bell-shaped flap dorsally,

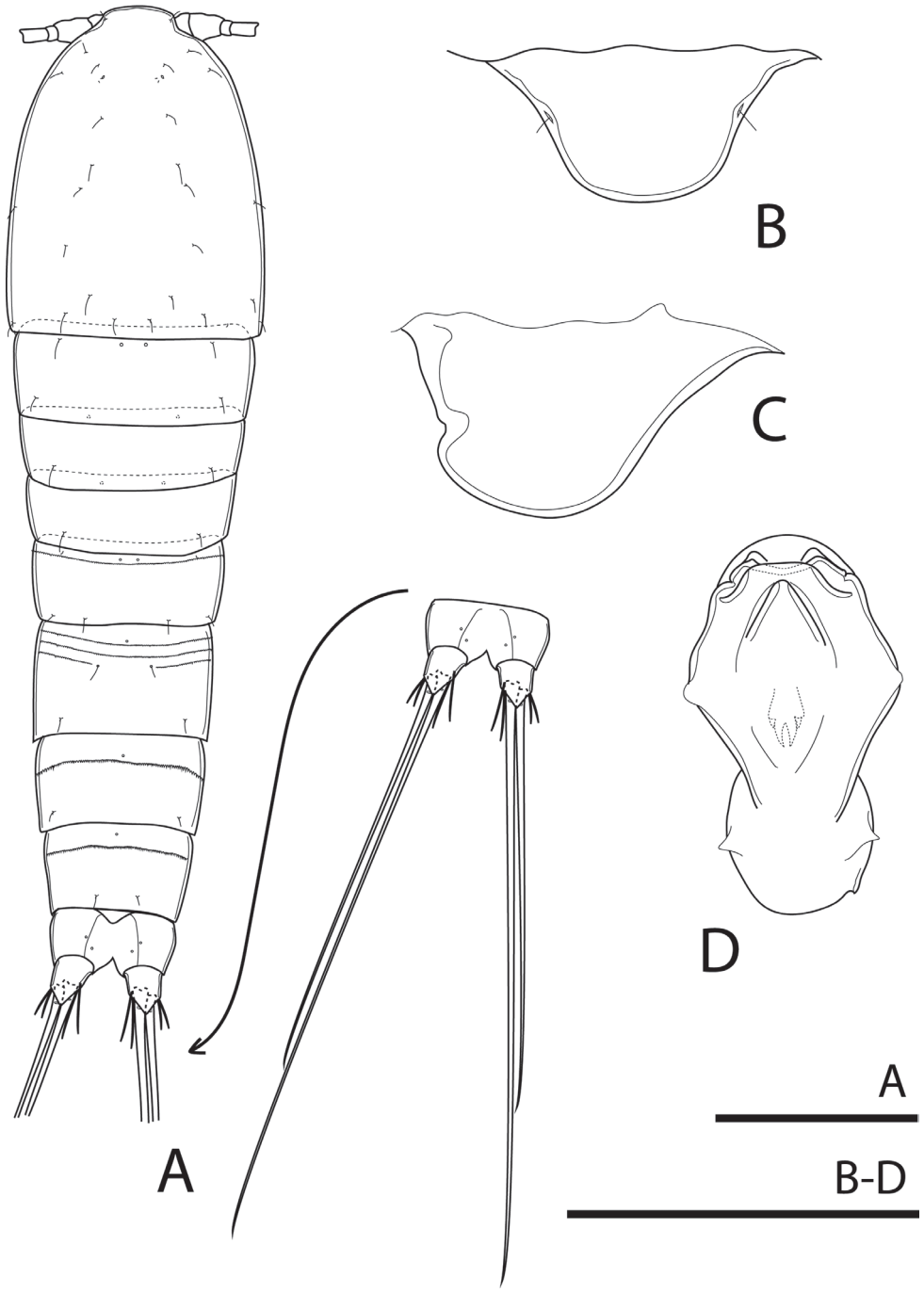

Figure 2. *Rangabradya* (*Siamorangabradya*) *wongkamhaengae* subgen. et sp. nov. female **A** habitus, dorsal view **B** rostrum, frontal view **C** labrum, lateral view **D** labrum, ventral view. Scale bars: 100 μm (**A**); 50 μm (**B–D**).

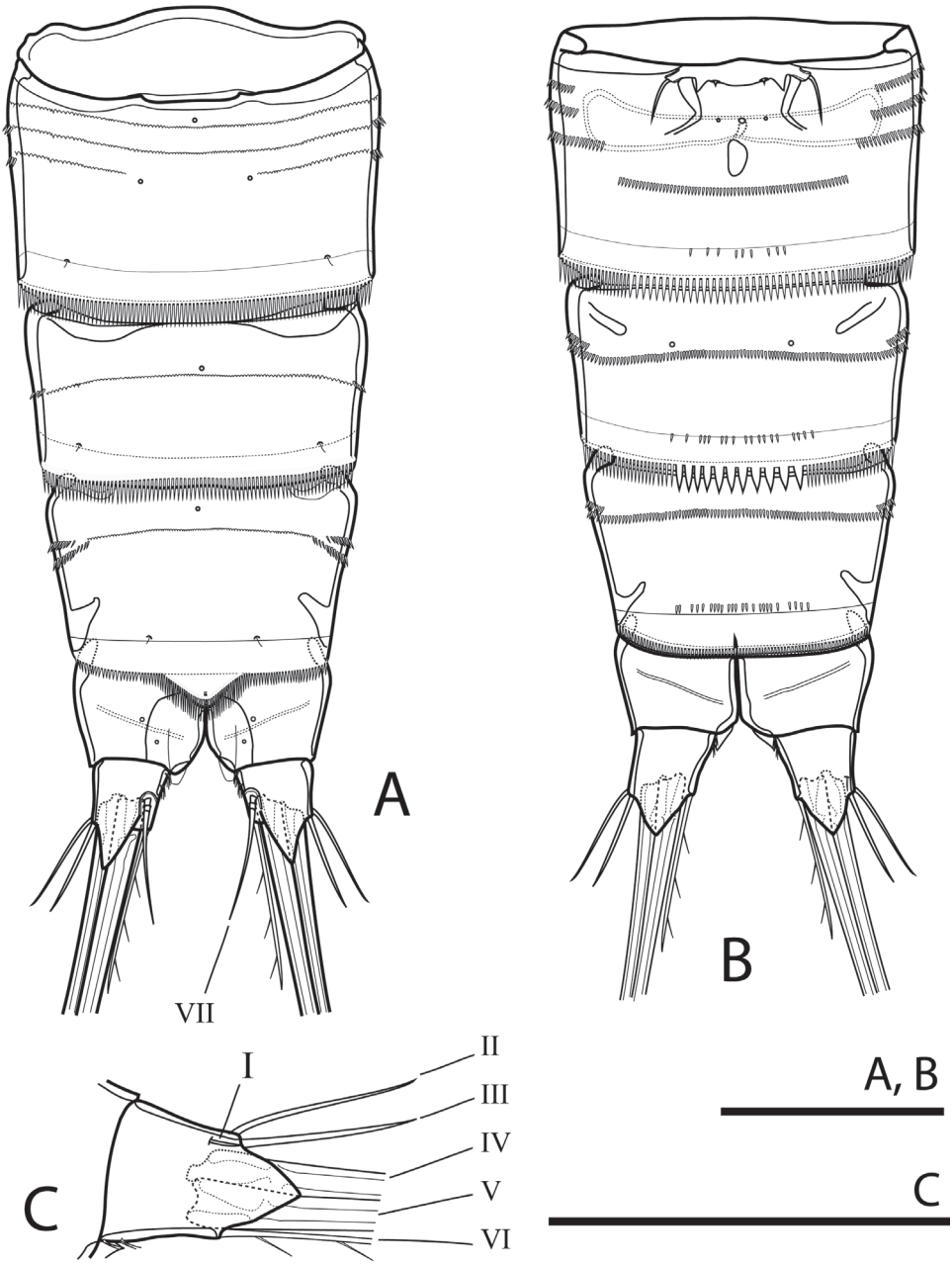

Figure 3. *Rangabradya* (*Siamorangabradya*) *wongkamhaengae* subgen. et sp. nov. female **A** urosome, dorsal view **B** urosome, ventral view **C** caudal ramus, ventral view. Scale bars: 50 μm. Roman numerals correspond to setal number.

representing pseudoperculum. Anal somite with cleft medially, with two pairs of cuticular pores dorsally.

Caudal rami (Figs 2A, 3A, C) slightly divergent, as long as anal somite, ca 1.3× as long as wide, with transparent triangular lappets dorsally and ventrally, reaching beyond fracture plane of inner apical seta (V); each ramus armed with seven setae. Lateral accessory seta (I) minute (Figs 3A, 10D). Lateral seta (II) and outermost apical seta (III) subequal in length. Outer apical seta (IV) and inner apical seta (V) well developed, with fracture plane; seta V longest, ca 1.3× as long as seta IV. Innermost apical seta (VI) ornamented with spinules on inner margin, ca 1.5× as long as seta II. Dorsal seta (VII) biarticulate, inserted at ½ length of ramus on medial margin, ca 1.5× as long as seta II.

Antennule (Figs 4A, 9C) short, six-segmented. Third segment longest, with robust and curved aesthetasc, reaching well beyond tip of antennule. Ultimate segment incompletely separated from preceding one, with remnant of ancestral articulation and aesthetasc on tip of segment. Both aesthetascs combined as acrothec (common base of seta and aestetasc). Armature formula: 1-[1], 2-[8], 3-[5 + 1 pinnate + (1 + ae)], 4-[2], 5-[2], 6-[5 + (1 + ae)].

Antenna (Figs 4B, 9D, E) biramous. Coxa short, without ornamentation. Basis with transverse row of long spinules at ½ length of medial margin and set of long setules on distal medial corner. Exp three-segmented. Exp-1 bare, Exp-2 ca 0.5× as long as Exp-1, with seta subapically. Exp-3 elongate, as long as Endp-2, ca ⅗ of length of Exp, with two apical setae; shorter one as long as segment bearing it, longer one ca 2.2× as long as shorter one and ca 2× as long as segment bearing it. Row of long setules subapically. Endp two-segmented. Endp-1 bare. Endp-2 with short seta accompanied by two groups of strong spinules on proximal lateral corner. Two strong spiniform setae at ½ length of Endp-2, and six spiniform apical setae, one very short. All spiniform setae on Endp-2 robust, with spinules along margins.

Labrum (Fig. 2D) large, rhomboidal in ventral view, strongly bulging, without beak on posterior margin.

Mandible (Figs 4C, D, 9E) comprising sclerotized coxal gnathobase and mandibular palp. Coxal gnathobase with two spines at ventral base. One spine at dorsal site of tridentate pars incisiva; lacinia unidentate. Mandibular palp comprising basis, one-segmented Exp and one-segmented Endp. Basis large, armed with three setae on distal medial corner. Exp small, armed with lateral and apical seta; lateral seta plumose. Endp armed with four setae laterally. Three setae apically, and one robust, plumose seta subapically.

Maxillule (Figs 5A, B, 9E, F) with large praecoxa. Praecoxal arthrite mobile, bearing slender seta at base plus three spines apically and one spine subapically. Anterior apical and subapical spines on praecoxal arthrite with row of curved long spinules, two other spines armed with few setules. Coxa small, one-segmented, bare. Basis and Endp completely fused, with two endites and endopodal lobe. Proximal endite with three subequal setae; distal endite with two setae. Endopodal lobe with two lateral and four apical setae, each seta fused with neighbouring one at its base. Exp free, one-segmented, with two plumose setae.

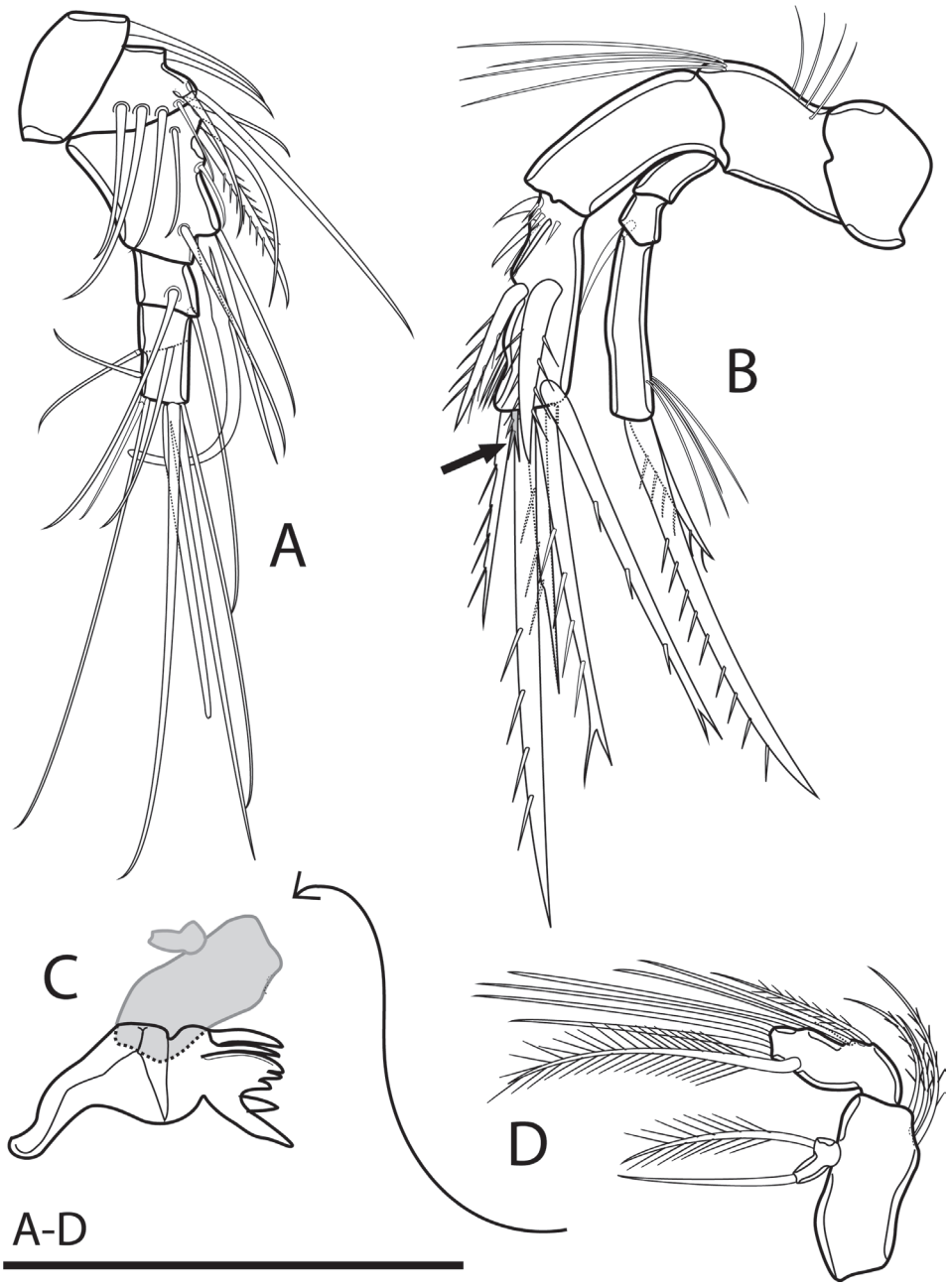

Figure 4. *Rangabradya* (*Siamorangabradya*) *wongkamhaengae* subgen. et sp. nov. female **A** antennule **B** antenna **C** praecoxa of mandible **D** mandibular pulp. Scale bars: 50 μm.

Maxilla (Figs 5C, 9F) non-prehensile, with slight angle between syncoxa and allobasis. Syncoxa with rows of spinules laterally and three endites along medial margin. Proximal endite at ⅓ of syncoxa length, with three setae apically; one robust and

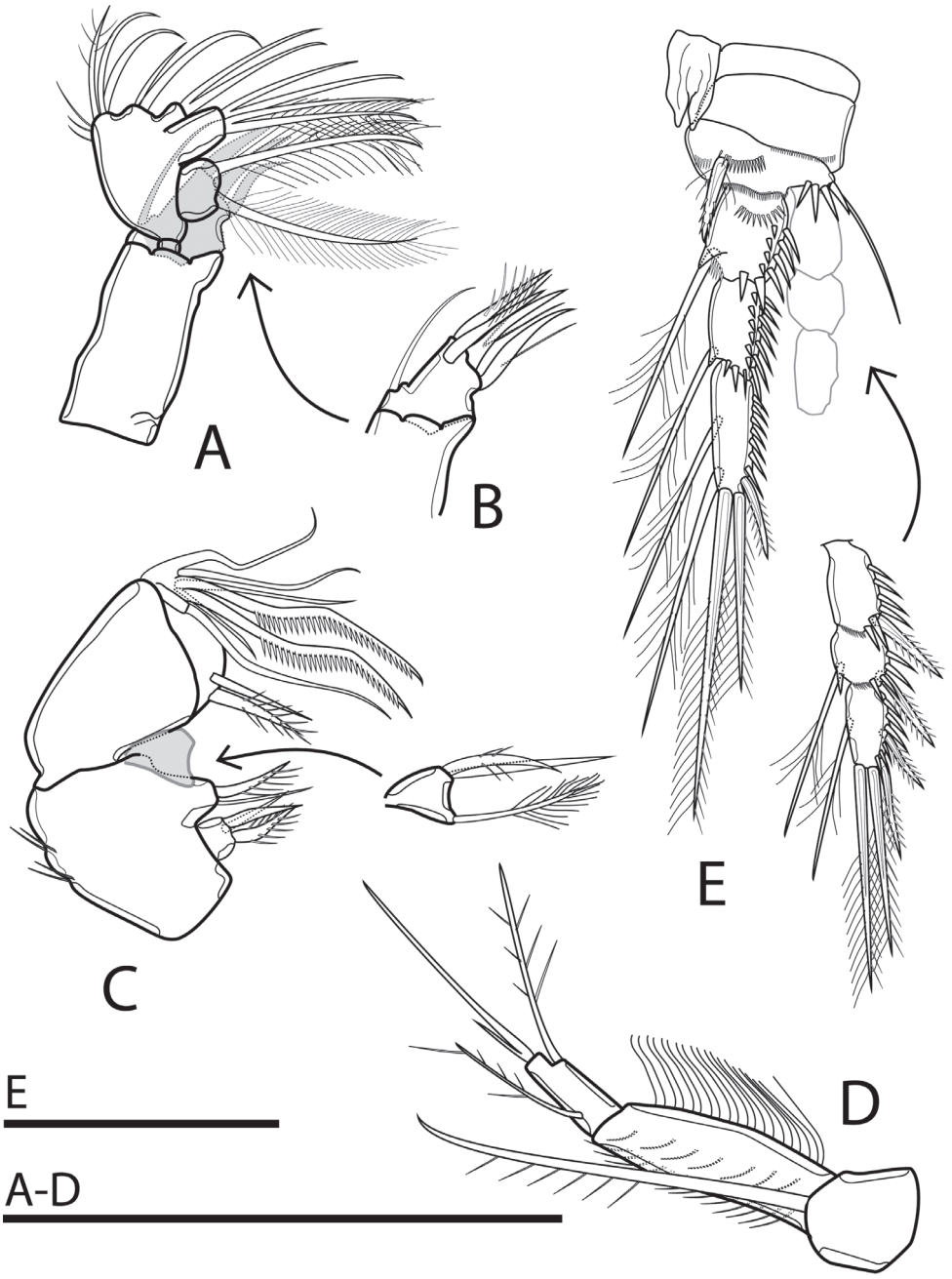

Figure 5. *Rangabradya* (*Siamorangabradya*) *wongkamhaengae* subgen. et sp. nov. female **A** maxillule **B** maxillular praecoxal arthrite **C** maxilla **D** maxilliped **E** P1. Scale bars: 50 μm.

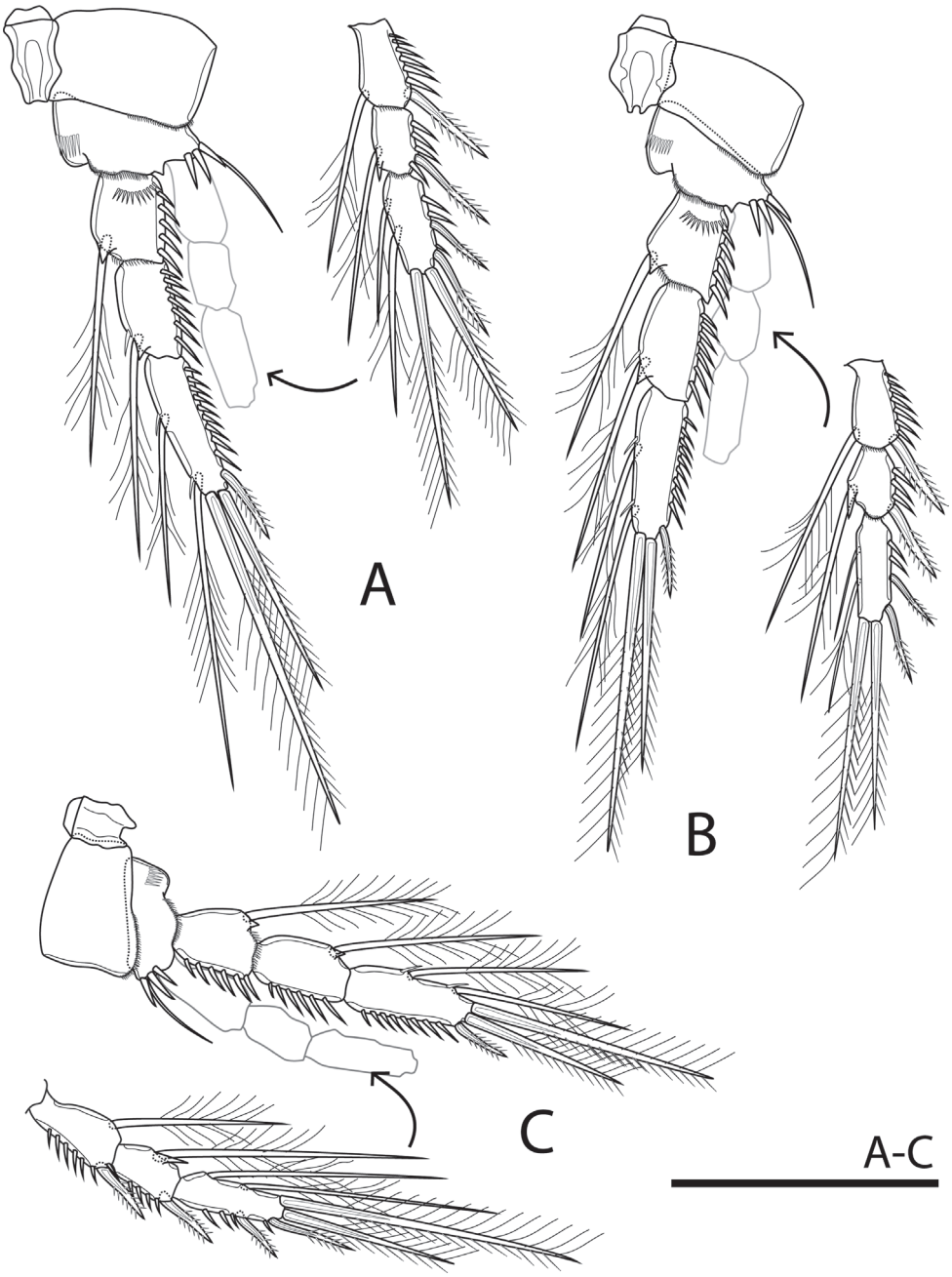

Figure 6. *Rangabradya* (*Siamorangabradya*) *wongkamhaengae* subgen. et sp. nov. female: **A** P2 **B** P3 **C** P4. Scale bars: 50 μm.

pinnate, other two smooth. Middle endite situated at ½ length of syncoxa, with one robust, pinnate seta and one smooth, slender seta apically. Distal endite triangular, mobile, with three elements; one plumose, one smooth, and one curved and pinnate. Medial margin of allobasis with one bare and one pinnate seta, at ½ length of segment. Distal endite small, with long smooth seta apically. Endp short, inconspicuous, with four bare setae, unequal in length and two robust, uni-pinnate setae.

Maxilliped (Fig. 5D) three-segmented, comprising syncoxa, basis, and one-segmented Endp. Syncoxa with one long, robust, uni-pinnate seta at distal medial corner. Basis long, with two rows of long spinules anteriorly and one row of long setules on outer margin. Endp with seta at ⅓ of segment length, with bipinnate seta subapically. Two setae apically fused at base, longer one ca 4× as long as shorter one.

P1–P4 with three-segmented Exp and Endp. Endp always longer than Exp. Segments with rows of strong spinules on outer margins and without ornamentations on inner margins. Armature formula as follows (legend: inner-outer element; inner-apical-outer; Arabic numerals representing setae; Roman numerals representing spines):

Legs	Basis	Exopod			Endopod		
		1	2	3	1	2	3
P1	I-1	0-I	1-I	1-II-II	1-0	1-0	2-II-I
P2	0-1	1-I	1-I	2-II-II	1-0	1-0	2-II-I
P3	0-1	1-I	1-I	2-II-II	1-0	1-0	2-II-I
P4	0-1	1-I	1-I	2-II-II	1-0	1-0	2-II-I

P1 (Fig. 5E). Coxa rectangular, with continuous row of spinules at distal lateral corner on anterior surface. Intercoxal sclerite narrow, elongate, free margin with obtuse lobes, without surface ornamentation. Basis with row of spinules at base of insertion of inner spine. Row of three or four spinules on distal lateral corner, near insertion of outer seta. Exp reaching just midlength of Endp-3. Endp-1 with additional row of spinules on anterior surface.

P2–P4 (Fig. 6A–C) with coxa and intercoxal sclerite similar to those of P1. Basis with short row of spinules on inner margin and row of strong spinules on distal lateral corner. Exp and Endp as in P1.

P5 (Figs 7A, 9G). Baseoendopodal lobe well developed, slightly shorter than Exp. Left and right leg distinctly separated. Endopodal lobe with two pinnate, spiniform spines; outer one short, inner one ca 6× as long as outer one. Smooth, slender seta on outer margin of basis, with cuticular pore near insertion of seta. Anterior surface of baseoendopod with arched row of spinules. Exp partly fused with baseoendopod, without surface seta and with three robust pinnate spines; outermost one longest, as long as inner spine on endopodal lobe. Inner two spines as long as Exp, subequal in length.

P6 (Fig. 3B) reduced to minute prominence, forming simple plate near anterior margin of genital double-somite. With one short seta on peduncle on each side of plate.

Description of male. Body slightly smaller than in female, fusiform. Total body length, excluding caudal setae, 427–431 μm (mean = 429; *N* = 3). Preserved specimens colourless. Prosome ca 1.5× as long as urosome (Fig. 7B). Cephalothorax longer than

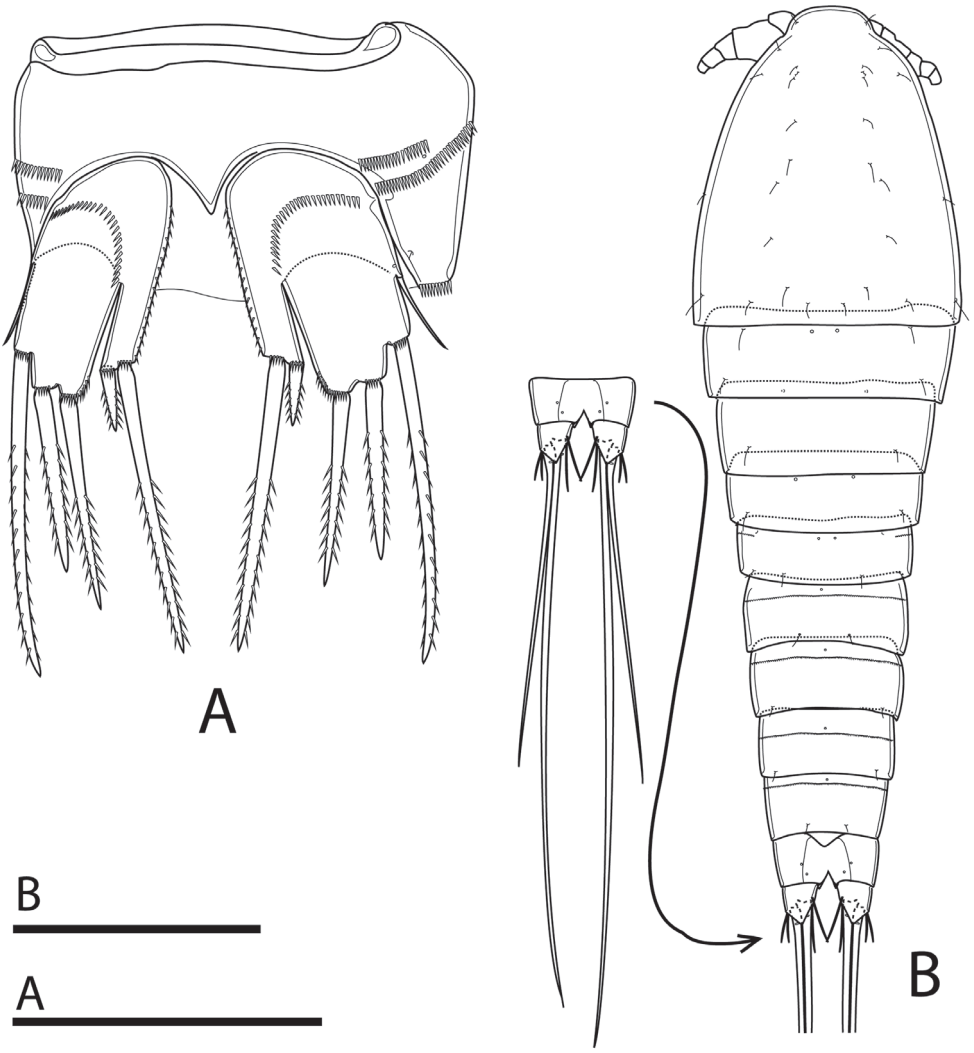

Figure 7. *Rangabradya* (*Siamorangabradya*) *wongkamhaengae* subgen. et sp. nov. female **A** P5; male: **B** habitus. Scale bars: 50 µm (**A**); 100 µm (**B**).

wide, ca 0.5× as long as length of prosome. Rostrum and surface ornamentation of prosome as in female.

Urosome (Figs 7B, 8A) five-segmented, comprising fifth pedigerous somite, genital somite and four free abdominal somites. All somites with finely spinulated hyaline frill on posterior margin, except anal somite. Fifth pedigerous somite as in female. Genital somite with continuous row of minute spinules dorsally and row of strong spinules ventrally. Cuticular pore near anterior margin mid-dorsally and pair of sensilla near posterior margin. Genital field with copulatory pore mid-ventrally. First to third abdominal somites each with row of minute spinules dorsally, continuing into row of

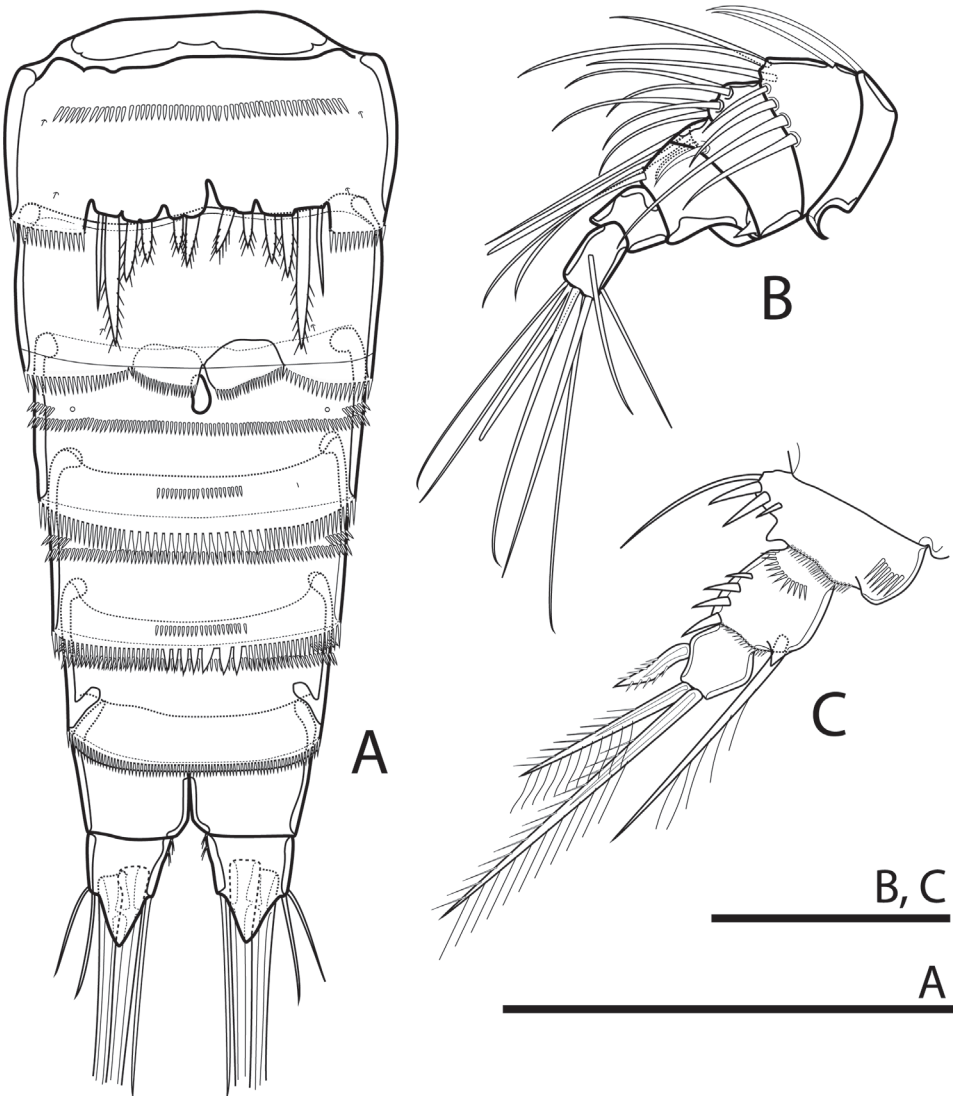

Figure 8. *Rangabradya* (*Siamorangabradya*) *wongkamhaengae* subgen. et sp. nov. male: **A** urosome, ventral view **B** antennule **C** endopod of P2. Scale bars: 50 μm.

strong spinules ventrally. Sixth thoracic somite with finely spinulated hyaline frill on posterior margin. Ornamentation of first abdominal to anal somites as in female.

Antennule (Fig. 8B) geniculate, six-segmented, with geniculated articulation between fourth and fifth segment. Third segment with apical aesthetasc on peduncle. Armature formula 1-[1], 2-[8], 3-[7 + (1 + ae)], 4-[2], 5-[0], 6-[7 + (1 + ae)]. Aesthetasc on third segment robust, reaching well beyond tip of antennule.

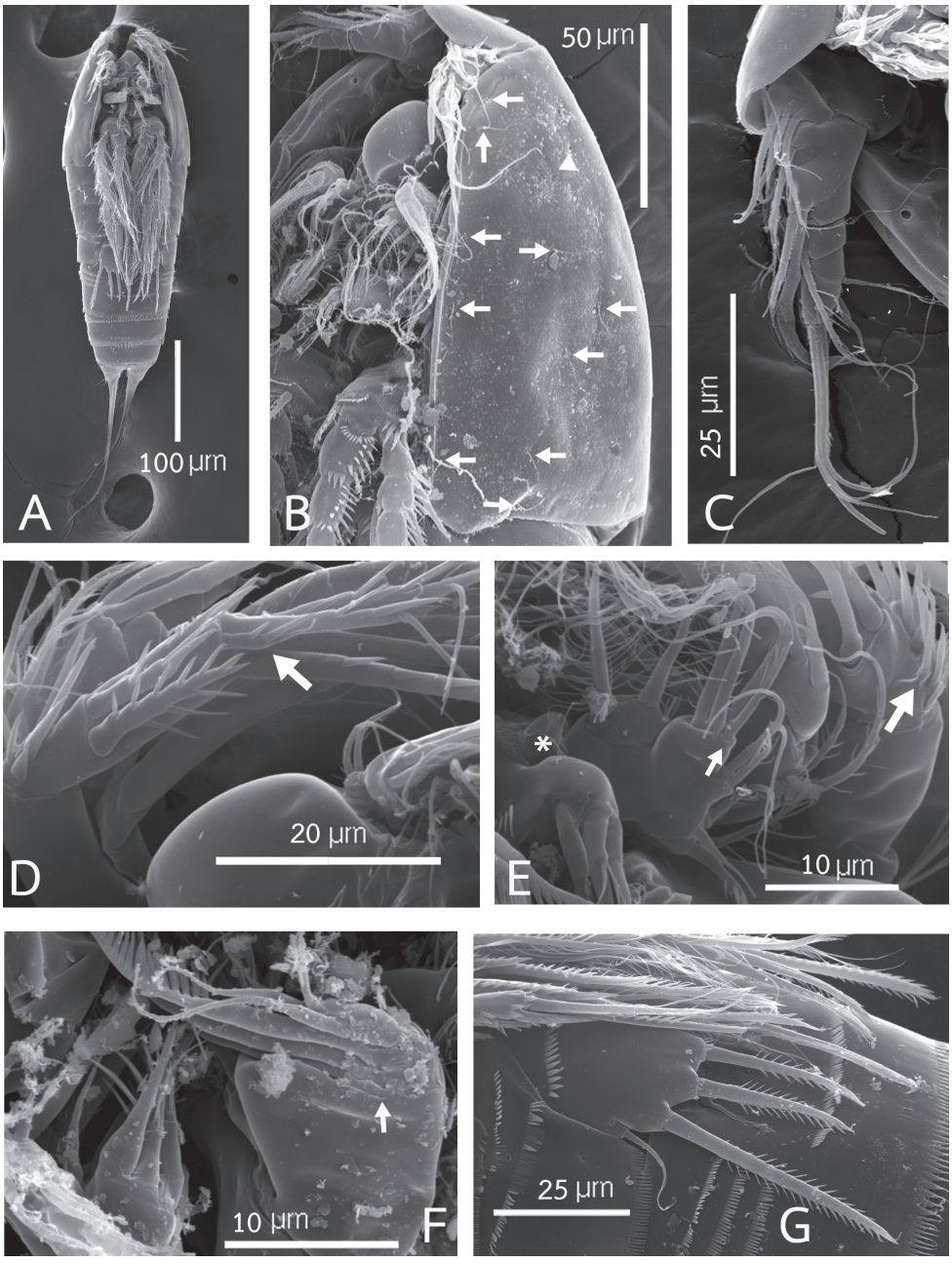

Figure 9. *Rangabradya* (*Siamorangabradya*) *wongkamhaengae* subgen. et sp. nov. Scanning electron microscope photographs **A** female habitus, ventral view **B** cephalothorax, ventrolateral view **C** antennule **D** distal segment of antenna **E** maxillule **F** maxilla **G** P5. The arrows and the triangular in figure B indicate the sensilla and integumental pore, respectively. The asterisk in figure **E** indicates coxa of the maxillule.

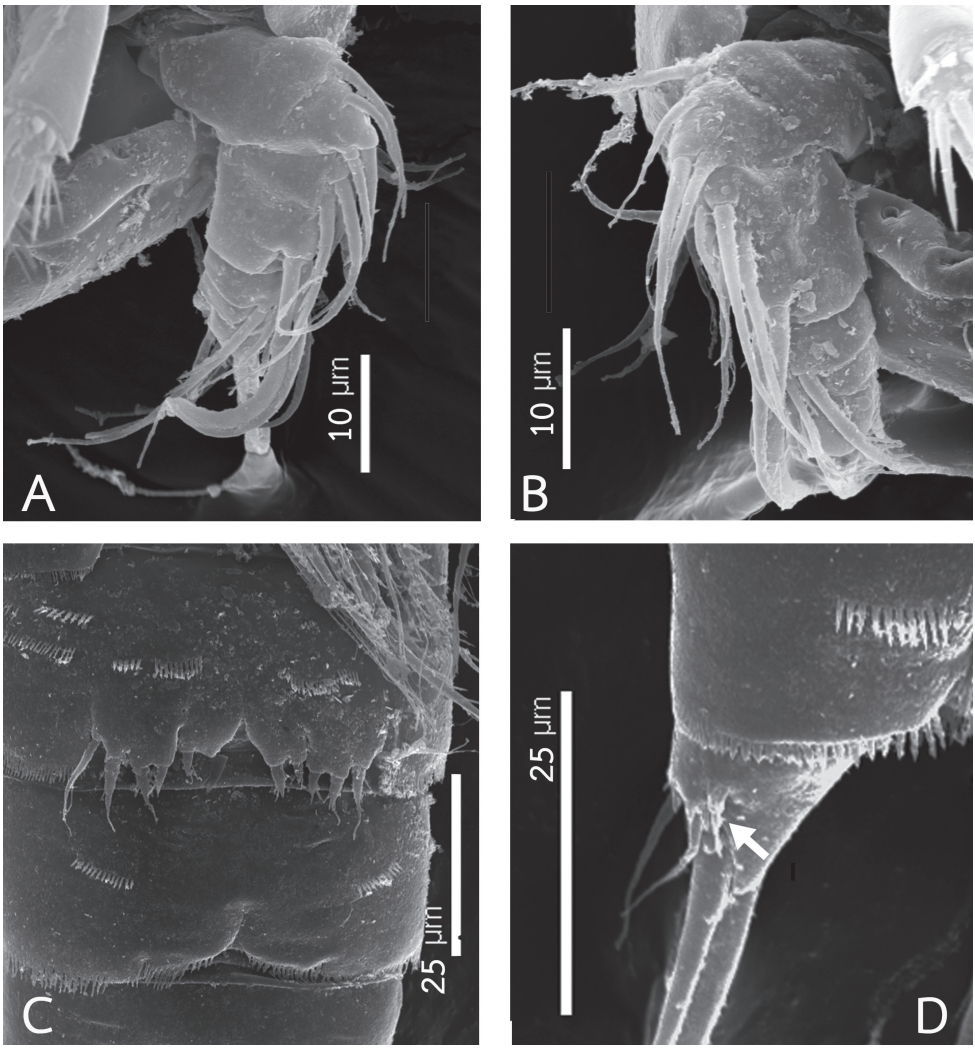

Figure 10. *Rangabradya* (*Siamorangabradya*) *wongkamhaengae* subgen. et sp. nov. Scanning electron microscope photographs, male **A** right antennule **B** left antennule **C** P5 and P6 of copepodid 5 **D** caudal ramus of copepodid 5.

Rostrum, antenna, mouthparts and P1–P4 (not figured) as in female.

P5 (Fig. 8A). with simple plate fused to somite bearing it. Left and right leg separated by cleft. Exp completely fused to baseoendopod. Smooth soft seta on outer margin of basis. Endopodal lobe with two pinnate spiniform setae apically. Inner one slightly longer than outer one. Exopodal lobe with three pinnate spiniform setae. Outermost one longest, ca 2× as long as median one, and ca 3× as long as innermost one.

P6 (Fig. 8A) reduced to simple, rectangular plate, without armature and ornamentation. Posterior margin serrated. Left leg distinct, but right leg fused to somite bearing it.

Variability. No variability was observed in the female. In one male, on the right P3 Endp were two segments only. The terminal segment short, armed with one lateral spine and two apical setae, unequal in length (Fig. 8C). In all specimens of the male, left and right P6 are asymmetrical. The left P6 is articulated, but the right P6 is completely fused to genital somite.

Etymology. The species name is a feminine noun in the genitive singular case, named after Dr Koraon Wongkamhaeng (Kasetsart University) in honour of her contribution to the research into the diversity of cave-dwelling copepods in Satun and Songkhla provinces.

Distribution. The species is known only from the type locality.

Ecology. As previously mentioned in the descriptions of *Boholina laorsriae* (Boonyanusith et al. 2020), the new species was collected from a temporary pool, where there is a small opening on the cave wall (Fig. 1C). The water temperature was 24.6 °C, pH 8.93, electrical conductivity 450 μS cm^{-1}, dissolved oxygen 5.7 mg L^{-1}, and salinity 0.2 ppt. The new species was accompanied by other species, including *Thermocyclops crassus* (Fischer, 1953), *Boholina laorsriae*, *Metacyclops* sp., *Mesocyclops* sp., and *Schizopera* sp.

Discussion

Two characters commonly used in assessing phylogenetic relationships of the family Ectinosomatidae are: 1) the shapes of the cephalothorax and habitus and 2) the orientation of the maxillary allobasis.

The recently known genera of the family can be divided into three groups, according to the shapes of the cephalothorax and habitus. The first includes six genera with a rectangular cephalothorax and a cylindrical body shape. They are comprised of: *Arenosetella* Wilson, 1932; *Ectinosomoides* Nicholls, 1945; *Glabrotelson* Huys in Kihara & Huys, 2009; *Noodtiella* Wells, 1965; *Oikopus* Wells, 1967; and *Tetanopsis* Brady, 1910. The second group includes 15 genera with a cephalothorax tapering anteriorly and a fusiform body shape: *Bradya* Boeck, 1873; *Bradyellopsis* Brian, 1925; *Chaulionyx* Kihara & Huys, 2009; *Ectinosoma* Boeck, 1865; *Ectinosomella* Sars, 1910; *Halophytophilus* Brian, 1919; *Halectinosoma* Vervoort, 1962; *Klieosoma* Hicks & Schriever, 1985; *Microsetella* Brady & Robertson, 1873; *Parahalectinosoma* George & Schwabe, 2019; *Parabradya* Lang, 1944; *Pseudectinosoma* Kunz, 1935; *Pseudobradya* Sars, 1904; *Rangabradya* Karanovic & Pesce, 2001 (including *Siamorangabradya*, subgen. nov.); and *Sigmatidium* Giesbrecht, 1881. The third group comprises genera with a cephalothorax clearly wider than the urosome and a dorsoventrally depressed prosome, including *Peltobradya* Médioni & Soyer, 1968 and *Pontobradya* Apostolov, 2011. Of the above-mentioned genera, *Halectinosoma* is most speciose with 69 valid species (Sciberras et al. 2018).

The orientation of the maxillary allobasis is another significant taxonomic character, which can be divided into two types: prehensile and non-prehensile. The maxilla of most Ectinosomatidae is geniculated, with the allobasis considerably bending medially to form a prehensile appendage. In the other genera, as well as in the new species, the

maxilla is not geniculate and an allobasis bends slightly, forming a slight angle between the syncoxa and the allobasis. A third group represented by the genus *Parahalectinosoma* has a maxilla that is strongly atrophied (George and Schwabe 2019).

Among the genera with a fusiform body, most characters of the Thai specimens match well the characteristics of *Rangabradya*. The shared characters are as follows:

1. the allobasis of the maxilla bends slightly, forming a wide angle with the syncoxa;
2. the mandibular gnathobase comprises a large convex space between the lacinia and pars incisiva;
3. the basal endite of the maxilla is situated in the first half-length of the syncoxa;
4. the allobasis of the maxilla is inserted by the medial seta at the middle of the segment;
5. P1–P4 Exp and Endp are three-segmented and the armature formula of P1–P4 Exp-3 is 5.6.6.6;
6. P5 in both sexes lacks a surface seta;
7. the female P5 Exp bears three spiniform setae and the outermost seta is the longest;
8. the male P5 Exp is completely fused to the baseoendopod;
9. the male P6 is reduced to a simple cuticular plate and has no armature element.

Of the nine shared characters, the combination of characters 6) and 7) confirms the close phylogenetic relationships between the new species from Thailand and the Indian species within the genus *Rangabradya*.

The female P5 in the new species is similar to that of *Ectinosoma* in that it has subdivided Exp and lacks a surface seta on the segment. However, the former has only three setae on Exp compared to the four reported for *Ectinosoma*. Three spiniform setae have also been observed in the female P5 Exp in *Halectinosoma*, but its representatives have a surface seta on this segment.

Karanovic and Pesce (2001) suggested that *Rangabradya* is most similar to *Halectinosoma*, one of the primitive genera of the family Ectinosomatidae. Based on this point of view, several characters present in the new species are considered primitive compared to those of *R. indica* (Table 1). The new species probably represents one of the phylogenetic transitional stages between *Halectinosoma* and *Rangabradya*. However, because there is no significant character (i.e., apomorphic character) to distinguish the new species from the genus *Rangabradya*, we suggest establishing the new subgenus *Siamorangabradya* subgen. nov. to accommodate the new stygobiotic species, *Rangabradya* (*Siamorangabradya*) *wongkamhaengae* subgen. et sp. nov. from Thailand.

After Sciberras et al. (2018) the key to genera of Ectinosomatidae includes 22 known genera. The genus *Parahalectinosoma* George & Schwabe, 2019 was later described from the Kuril Basin, Russia (George and Schwabe 2019). It has a fusiform habitus, with numerous derived characters on its buccal appendages suggesting a symbiotic mode of life. As the Thai *Rangabradya* could not be identified using this key, the following amendments were made to the key in Sciberras et al. (2018: 420) by

Table 1. Distinctive characters between *Siamorangabradya* subgen. nov. and the nominative subgenus *Rangabradya*.

Characters	***Siamorangabradya* subgen. nov.**	***Rangabradya***
Ornamentation of urosomite	present	absent/reduced
Number of setae on caudal ramus	7	6
Number of segments of antennule	6	5
Spine between pars incisiva and lacinia on mandibular gnathobase	present	absent
Number of setae on mandibular Endp	8	5
Basal seta on praecoxal arthrite	present	absent
Setal formula of maxillary syncoxal endite from proximal to distal ones	3.2.3	4.1.2
Number of setae on maxillipedal Endp	4	3
Exp and baseoendopod of female P5	subdivided	fused
Number of setae on female P6	1	absent
Number of setae on endopodal lobe of the male P5	2	1

modifying the character detailed in paragraphs 13 and 14 and adding new couplets as the last paragraphs, as follows:

Updated key to the genera of Ectinosomatidae

1 Body cylindrical with cephalothorax rectangular in dorsal aspect; body approximately the same width throughout its length **2**

– Body fusiform with cephalothorax sub-triangular in dorsal aspect; greatest body width usually at posterior margin of cephalothorax; urosome gradually tapering towards the posterior end **7**

– Body with dorsoventrally depressed prosome, clearly wider than urosome..... **20**

2 Exp of antenna two-segmented; maxilla prehensile, with major articulation between elongate syncoxa and elongate allobasis..... ***Noodtiella* Wells, 1965**

– Exp of antenna one- or three-segmented; maxilla not prehensile, with at most a slight angle between syncoxa and allobasis **3**

3 P2–P4 Endp two-segmented..... ***Ectinosomoides* Nicholls, 1945**

– P2–P4 Endp three-segmented..... **4**

4 Anal somite with dorsal armature of claws, lappets or spiniform processes around anal opening; P5 Exp with three marginal and one surface seta..... ..... ***Arenosetella* Wilson, 1932**

– Anal somite without such ornamentation..... **5**

5 Exp of antenna one-segmented ..... ***Tetanopsis* Brady, 1910**

– Exp of antenna three-segmented **6**

6 Female P5 Exp and baseoendopod with foliaceous setae, Exp with three marginal and no surface setae; male P5 Exp with four normal marginal setae .... ***Oikopus* Wells, 1967**

– P5 Exp and baseoendopod with normal setae in both sexes, Exp with three marginal and typically a surface seta [absent in *Glabrotelson soyeri* (Bodin, 1979)]..... ..... ***Glabrotelson* Huys in Kihara & Huys, 2009**

7 P1–P4 Endp two-segmented..... ***Pseudectinosoma* Kunz, 1935**

– P1 Endp two- or three-segmented, P2–P4 Endp three-segmented **8**

8 P1 Endp prehensile **9**
– P1 Endp not prehensile **12**
9 P1 Endp two-segmented **10**
– P1 Endp three-segmented ..... ***Klieosoma*** **Hicks & Schriever, 1985**
10 P1–P2 Exp-3 with two outer elements **11**
– P1–P2 Exp-3 with three outer elements ..... ***Halophytophilus*** **Brian, 1919**
11 Antennule with large spine on second segment (and often first and third segments); Exp of antenna rudimentary, with one to three small setae; P1 Endp-2 with four elements (one to two pinnate and claw-like) ..... ***Bradyellopsis*** **Brian, 1925**
– Armature elements on first to third antennulary segments setiform; Exp of antenna well developed and three-segmented; P1 Endp-2 with six elements (outer one bifid and claw-like) ..... ***Chaulionyx*** **Kihara & Huys, 2009**
12 Maxilla prehensile, with syncoxa and allobasis forming right angle; P5 Exp poorly developed, short, fused to baseoendopod in female and distinct in male, with three marginal and no surface setae; body very small (< 300 μm) ..... ***Sigmatidium*** **Giesbrecht, 1881**
– These characters not combined **13**
13 Female P5 Exp and baseoendopod fused, forming a single plate in both sexes, or partly discrete; male P6 forming a single plate or absent **14**
– Female P5 Exp and baseoendopod at least partly discrete; male P6 with armature element **15**
14 Armature formula of P1–P4 Exp-3: 5, 6, 6, 6; male P6 absent or unarmed **21**
– Armature formula of P1–P4 Exp-3: 6, 7, 8, 8; male P6 with two setae; body of female large (≥ 1200 μm); marine, usually deepwater .... ***Parabradya*** **Lang, 1944**
15 Integument of somites with distinctive sub-rectangular pores; P5 Exp with four marginal setae ..... ***Ectinosoma*** **Boeck, 1865**
– Integument of somites without distinctive sub-rectangular pores; P5 Exp with three marginal setae and one seta on anterior surface **16**
16 Mandible with rudimentary gnathobase, elongate basis and filiform rami, each terminating in two to three setae; Exp of antenna without lateral spines ..... ***Ectinosomella*** **Sars, 1910**
– These characters not combined **17**
17 Third segment of female antennule 3× as long as wide; Endp of mandible with one strong seta laterally; P1–P4 Exp-3 with two outer spines; planktonic (occasionally in sediment) ..... ***Microsetella*** **Brady & Robertson, 1873**
– These characters not combined **18**
18 Body comparatively robust with prosome–urosome separation usually distinct (exception: *Bradya kurtschminkei* Seifried & Martínez Arbizu, 2008 with dorsoventrally flattened habitus); antenna with two setae on Exp-1 and one seta on Endp-1; Exp of mandible with at least five setae; maxilliped robust with short Endp usually fused at an angle with basis and bearing four conspicuous setae ..... ***Bradya*** **Boeck, 1873**
– Body comparatively slender with no sharp separation between prosome and urosome; antenna with less than two setae on Exp-1 (except *Pseudobradya ambigua*

Sars, 1920 with two) and no seta on Endp-1; Exp of mandible generally with less than five setae; maxilliped usually slender and straight with discrete Endp bearing one small and four conspicuous setae **19**

19 Antennule with or without dark pigment spot within the proximal three segments; maxilla prehensile, allobasis usually truncate distally and carrying three-segmented Endp (although Endp sometimes very small and segmentation difficult to discern; reduced to a narrow three-segmented cylinder in *P. leptognatha* Sars, 1920); maxilliped short and robust ..... ***Pseudobradya*** **Sars, 1904**

– Antennule without pigment spot; maxilla with at most a slight angle between syncoxa and allobasis, the latter generally tapering distally, Endp three-segmented but always small, its morphology not clearly discernible; maxilliped generally slender ..... ***Halectinosoma*** **Vervoort, 1962**

20 P1 Endp three-segmented; female P5 Exp with four marginal elements .... ***Pontobradya*** **Apostolov, 2011**

– P1 Endp two-segmented; female P5 Exp with three marginal elements and one surface seta..... ***Peltobradya*** **Médioni & Soyer, 1968**

21 Exp of antenna three-segmented; maxillule and maxilla normally developed; maxilliped three-segmented; continental groundwater .... ***Rangabradya*** **Karanovic & Pesce, 2001**

– Exp of antenna one-segmented; maxillule and maxilla strongly atrophied; maxilliped two-segmented; symbiosis in echiuran coelom..... ..... ***Parahalectinosoma*** **George & Schwabe, 2019**

22 Female P5 Exp fused to baseoendopod; male P5 with one seta on baseoendopodal lobe..... ***Rangabradya*** **(*Rangabradya*) Karanovic & Pesce, 2001**

– Female P5 Exp and baseoendopod partly discrete; male P5 with two setae on baseoendopodal lobe..... ***Rangabradya*** **(*Siamorangabradya*) subgen. nov.**

Acknowledgements

This paper is a result of research project supported by a grant from the Office of the Higher Education Commission, Thailand (2558A13562002) and was funded by the Research and Academic Affairs Promotion Fund (RAAPF), Faculty of Science, Khon Kaen University, the Fiscal year 2017. The authors sincerely thank Dr Kai Horst George, Dr Anton Brancelj, and B.A. Venmathi Maran for their valuable revision of the manuscript.

References

Bodin P (1968) Copépodes Harpacticoides des étages bathyal et abyssal du golfe de Gascogne. Mémoires du Muséum national d'Histoire naturelle de Paris, n. ser. (A) 55: 1–107.

Boonyanusith C, Wongkamhaeng K, Athibai S (2020) A new species of *Boholina* (Crustacea, Copepoda, Calanoida) and a first record for stygobiotic calanoid fauna from a cave in Thailand. ZooKeys 904: 1–22. https://doi.org/10.3897/zookeys.904.37609

Boonyanusith C, Saetang T, Wongkamhaeng K, Maiphae S (2018) *Onychocamptus* Daday, 1903 from Thailand, with descriptions of two new species and two new records (Crustacea, Copepoda, Harpacticoida, Laophontidae). ZooKeys 810: 45–89. https://doi.org/10.3897/zookeys.810.29253

Boxshall GA, Halsey SH (2004) An Introduction to Copepod Diversity. The Ray Society, London.

George KH, Schwabe E (2019) A new species of Ectinosomatidae Sars (Copepoda, Harpacticoida) associated with *Pseudoikedella achaeta* (Zenkevitch, 1958) (Echiura, Bonelliida). Progress in Oceanography 173: 1–8. https://doi.org/10.1016/j.pocean.2019.02.003

Huys R, Boxshall GA (1991) Copepod Evolution. The Ray Society, London, 468 pp.

Karanovic T, Pesce GL (2001) A new genus and species of the family Ectinosomatidae (Crustacea: Copepoda: Harpacticoida) from the groundwaters of India. Annales de Limnologie 37: 281–292. https://doi.org/10.1051/limn/2001025

Kihara TC, Huys R (2009) A new genus of Ectinosomatidae (Copepoda, Harpacticoida) from sublittoral sediments in Ubatuba, São Paulo State (Brazil), an updated key to genera and notes on *Noodtiella* Wells, 1965. ZooKeys 17: 57–88. https://doi.org/10.3897/zookeys.17.202

Liu C, Li F, Wongprom P, Zheng G, Li S (2017) Eleven new species of the spider genus *Althepus* Thorell, 1898 (Araneae, Ochyroceratidae) from Thailand. Zootaxa 4350: 469–499. https://doi.org/10.11646/zootaxa.4350.3.3

Metcalfe I (1998) Palaeozoic and Mesozoic geological evolution of the SE Asian region: multidisciplinary constraints and implications for biogeography. In: Hall R, Holloway JD (Eds) Biogeography and Geological Evolution of SE Asia. Backhuys Publishers, Leiden, 25–41.

Nilsai A, Jantarit S, Satasook C, Zhang F (2017) Three new species of *Coecobrya* (Collembola: Entomobryidae) from caves in the Thai Peninsula. Zootaxa 4286:187–202. https://doi.org/10.11646/zootaxa.4286.2.3

Promdam R, Yeesin P, Ng PKL (2017) A second new species of terrestrial long-legged *Terrapotamon* Ng, 1986 (Crustacea: Brachyura: Potamidae) from karst forests in Peninsular Thailand. The Raffles Bulletin of Zoology 65: 404–415.

Sciberras M, Huys R, Bulnes VN, Cazzaniga N (2018) A new species of *Halectinosoma* Vervoort, 1962 (Copepoda: Harpacticoida) from Argentina, including a key to species with unusual leg armature patterns, notes on wrongly assigned taxa and an updated key to ectinosomatid genera. Marine Biodiversity 48: 407–422. https://doi.org/10.1007/s12526-017-0806-0

Seifried S, Plum C, Schulz M (2007) A new species of *Parabradya* Lang, 1944 (Copepoda: Harpacticoida: Ectinosomatidae) from the abyssal plain of the Angola Basin. Zootaxa 1432: 121. https://doi.org/10.11646/zootaxa.1432.1.1

Shergold J, Burrett C, Akerman T, Stait B (1988) Late Cambrian trilobites from Tarutao Island, Thailand. In: Contributions to Paleozoic Paleontology and Stratigraphy in Honor of Rousseau H. Flower. New Mexico Bureau of Mineral Resources Memoir 44: 303–320.

Sumontha M, Pauwels OSG, Suwannakarn N, Nutatheera T, Sodob W (2014) *Cyrtodactylus wangkulangkulae* (Squamata: Gekkonidae), a new Benttoed Gecko from Satun Province, southern Thailand. Zootaxa 3821: 116–124. https://doi.org/10.11646/zootaxa.3821.1.8

ZooKeys 1009: 67–79 (2021)
doi: 10.3897/zookeys.1009.57556
https://zookeys.pensoft.net

RESEARCH ARTICLE

A peer-reviewed open-access journal
ZooKeys
Launched to accelerate biodiversity research

Two new species of *Dzhanokmenia* (Hymenoptera, Eulophidae) from China, with first report on a host association for the genus

Qin Li[1,2], Chao Wang[1,2], Hong-Ying Hu[1,2]

1 *College of Life Science and Technology, Xinjiang University, 666 Shengli Road, Tianshan District, Urumqi, Xinjiang, 830046, China* **2** *Xinjiang Key Laboratory of Biological Resources and Genetic Engineering, 666 Shengli Road, Tianshan District, Urumqi, Xinjiang, 830046, China*

Corresponding author: Hong-Ying Hu (hoohyi-69@163.com)

Academic editor: K. van Achterberg | Received 12 August 2020 | Accepted 7 October 2020 | Published 4 January 2021

http://zoobank.org/6E43F3EF-02C6-4910-934A-3A21DDD1EA17

Citation: Li Q, Wang C, Hu H-Y (2021) Two new species of *Dzhanokmenia* (Hymenoptera, Eulophidae) from China, with first report on a host association for the genus. ZooKeys 1009: 67–79. https://doi.org/10.3897/zookeys.1009.57556

Abstract

Two new species of *Dzhanokmenia* Kostjukov (Hymenoptera: Eulophidae: Tetrastichinae), *D. stefaniolae* Li, Wang & Hu, **sp. nov.** and *D. yuxuannis* Li, Wang & Hu, **sp. nov.**, are described and illustrated from Xinjiang Uyghur Autonomous Region, China. *D. stefaniolae* was reared from stem-galls made by *Stefaniola* sp. (Diptera: Cecidomyiidae) on black saxaul, *Haloxylon ammodendron* (Chenopodiaceae); *D. yuxuannis* was collected by sweeping from both black saxaul and white saxaul, *H. persicum*, in Beishawo Desert near Fukang. A key to females of all known species of *Dzhanokmenia* is provided.

Keywords

Cecidomyiidae, Chalcidoidea, desert, taxonomy, Xinjiang

Introduction

Tetrastichinae is the largest subfamily of Eulophidae (Hymenoptera: Chalcidoidea). At present, this subfamily includes about 1900 species in more than 100 genera throughout the world (Noyes 2020).

Kostjukov (1977) regarded *Tetrastichus* (*Dzhanokmenia* Kostjukov), with type-species *Tetrastichus bibikovae* Dzhanokmen, as one of the 17 subgenera of the genus *Tetrastichus* Haliday (*sensu lato*). Graham (1991) revised the European Tetrastichinae, recognizing 28 valid genera including *Dzhanokmenia*, which he upgraded to genus level. The reasons why it was given a generic rank were discussed in Li et al. (2016). Kostjukov (2014) and Kostjukov and Kosheleva (2014, 2015) described three species of *Dzhanokmenia*. Li et al. (2016) described three more species of the genus during an expedition to study insect biodiversity of the Junggar Basin in northern Xinjiang Uyghur Autonomous Region (hereafter Xinjiang), China. Up to now, 13 valid species of *Dzhanokmenia* have been described from arid and semi-arid areas of southern Russia and Central Asia; however, their hosts remained unknown.

Here we describe two new species of *Dzhanokmenia* from rearings and collections, and provide a key to females of all known species of the genus.

Materials and methods

Parasitoid wasp collection and rearing

Our research group (Hong-Ying Hu, Qin Li, Wan Yin, Ya-Jie Zhu, Feng Li) collected many insects in 2015 by sweeping with a net and searching for galls on black saxaul, *Haloxylon ammodendron*, and white saxaul, *H. persicum* (Chenopodiaceae), in Beishawo Desert, near Fukang (44°22'29"N to 44°22'49"N, 87°52'57"E to 87°52'58"E, 401–446 m). These galls were reared by Qin Li in the laboratory at room temperature (20–32 °C) and 22–60% relative humidity, with natural and fluorescent lighting of approximately 13:11 L:D, at the College of Life Science and Technology, Xinjiang University, Urumqi. The emerged insects were preserved in 100% ethanol after dying naturally, without any food or water for 2–3 days usually.

Taxonomy

All the specimens were examined under a Nikon SMZ 745T stereomicroscope. The images were taken with a Nikon DS-Fi3 connected to a Nikon SMZ 25 stereomicroscope. All images were stacked with NIS-Elements software and arranged in plates using Adobe Photoshop.

Description of each new species is based on its holotype, with variation of some key morphological features in the paratypes summarized separately. Morphology and terminology follows Gibson (1997) except for the metasoma. Gibson (1997) used petiole + gaster for the metasoma. In the case of *Dzhanokmenia*, the petiole is sessile and metasoma is equal to gaster, the metasomal terga I–VII are synonym with gastral terga I–VII. Abbreviations of morphological terms used are: C3, claval segment 3; CC, length of costal cell; CL, length of clava; CW, width of clava; EH, height of eye; EL, length of eye; F1–F3, funicle segments 1–3; FWL, length of fore wing; FWW, width of fore wing; GL, length of metasoma; GW, width of metasoma; HL, head length; HW, head

width; HWL, length of hind wing; HWW, width of hind wing; MFL, length of metafemur; MFW, width of metafemur; ML, length of mesosoma; MLL, length of midlobe of mesoscutum; MLW, width of midlobe of mesoscutum; MSP, malar space; MV, length of marginal vein; MW, width of mesosoma; OOL, distance between eye and posterior ocellus; PMV, length of postmarginal vein; POL, distance between posterior ocelli; PSV, length of parastigma; SL, length of scape; SMV, length of submarginal vein of fore wing; STL, length of scutellum; STV, length of stigmal vein; STW, width of scutellum; SW, width of scape.

An acronym for the depository of parasitoids is: ICXU, Insect Collection of College of Life Science and Technology, Xinjiang University, Urumqi, Xinjiang, China. All the parasitoids were identified by the first and second authors. *Stefaniola* sp. was identified to genus by Ke-Long Jiao (Department of Plant Protection, College of Horticulture and Landscape, Tianjin Agricultural University, Tianjin, China), in whose collection some of the voucher specimens of this gall-maker are deposited; the remainder are in ICXU.

The key is an update of that in Li et al. (2016).

Results

Two new species of *Dzhanokmenia* Kostjukov are described and illustrated here. All specimens of one of the new species of *Dzhanokmenia* were reared from stem-galls made by *Stefaniola* sp. (Diptera: Cecidomyiidae) on *H. ammodendron*, which is the first host record for the genus. Specimens of the other new species were collected by sweeping on both *Haloxylon ammodendron* and *H. persicum*.

Systematics

***Dzhanokmenia* Kostjukov, 1977**

Tetrastichus (*Dzhanokmenia*) Kostjukov 1977: 189. Type-species: *Tetrastichus bibikovae* Dzhanokmen, by original designation. Subsequent references: Kostjukov 1978: 430–467 (key); Kostjukov 1984: 3435 (key).

Dzhanokmenia Kostjukov: Graham 1991: 162–163 (elevated to generic rank); Kostjukov 2014: 84 (diagnosis); Kostjukov and Kosheleva 2014: 160 (diagnosis); Kostjukov and Kosheleva 2015: 451 (diagnosis); Li et al. 2016: 448 (diagnosis, key).

Diagnosis. Antenna usually yellow, with 1–3 anelli, 3 funicle segments, and 3-segmented clava. Mesosoma convex, pronotum very short, transverse; midlobe of mesoscutum about as long as broad, with a single row of adnotaular setae on each side; scutellum with two distinct longitudinal submedian lines and two setae behind the middle; propodeum with median carina, without plica. Tegula yellow. Fore wing with marginal and stigmal veins very thick; submarginal vein with only one dorsal seta; marginal vein very short, much shorter than costal cell; apical margin without setae. Metasomal terga with yellow areas or completely dark.

Distribution. Palearctic region: China (Xinjiang), Kazakhstan, Russia, and Turkmenistan.

Host. *Stefaniola* sp. (Diptera: Cecidomyiidae); first host record for the genus.

Key to species of *Dzhanokmenia* (females)

1 Metasomal terga green, with bluish or bronze tint and metallic shine, without yellow or brownish yellow areas **2**

– Metasomal terga at least partially yellow or brownish yellow **7**

2(1) Meso- and metafemora yellow **3**

– Meso- and metafemora black or dark brown **6**

3(2) Funicular segments quadrate, as long as wide ..... ***D. antonovae*** **(Kostjukov)**

– Funicular segments longer than wide **4**

4(3) Funicular segments unequal in length ..... ***D. nikolskajae*** **(Kostjukov)**

– Funicular segments equal in length **5**

5(4) Fore wing with STV less than 0.2× as long as MV and PSV; body green, without bronze tint; apical 1/4 of procoxa and apical 2/3 of mesocoxa yellow ..... ***D. zadepskyi*** **(Kostjukov)**

– Fore wing with STV 0.3× as long as MV and PSV; body green with yellow or orange reflections; coxae green with metallic tinge ..... ***D. karamayica*** **Li, Wang & Zhu**

6(2) Funicle yellow, F2 2× as long as greatest width ..... ***D. demakovi*** **(Kostjukov)**

– Funicle brown, F2 more than 2× as long as its greatest width ..... ***D. kurdjumovi*** **(Kostjukov)**

7(1) Metasomal terga yellow; POL 9.0× OOL ..... ***D. kozlovi*** **(Kostjukov)**

– Metasomal terga only partially yellow or brownish yellow; POL at most 5.0× OOL **8**

8(7) Metasoma predominantly yellow with terga IV–VII brownish yellow **9**

– Metasoma with dark or green metallic patterns on terga **10**

9(8) Metasomal terga IV–VII brownish yellow; hind wing at least 9.0× as long as broad; mesoscutum with median line weakly expressed; metasoma as long as mesosoma ..... ***D. bibikovae*** **(Dzhanokmen)**

– Only metasomal tergum VI brownish yellow; hind wing at most 7.5× as long as broad; mesoscutum with median line distinct; metasoma 1.4× as long as mesosoma ..... ***D. evgenyi*** **Kostjukov & Kosheleva**

10(8) POL at most 1.6× OOL; mid lobe of mesoscutum with strong median line ... **11**

– POL at least 3.0× OOL; mid lobe of mesoscutum without median line **12**

11(10) Scutellum at least 1.4× as broad as long; MV at least 2.9× as long as STV; body length 1.2–1.5 mm; MV 3.7–3.75× as long as STV ..... ***D. kasparyani*** **Kostjukov & Kosheleva**

– Scutellum at most 1.25× as broad as long; MV at most 2.5× as long as STV; body length 1.9–2.0 mm; MV 3.4–3.6× as long as STV ..... ***D. sugonjaevi*** **Kostjukov**

12(10) Metasomal terga II–IV entirely yellow; metasoma longer than mesosoma (1.2×) **13**
– Metasomal terga II–IV not entirely yellow; metasoma shorter than mesosoma (less than 1.0×) **14**
13(12) Pro- and mesocoxae mostly yellow; metasoma with tergum VII with anterior triangular- to crescent-shaped area dark brown with green metallic tinge, laterally with yellow part occupying most of tergum VII; POL at least 4.5× OOL ..... ***D. yuxuannis*** **Li, Wang & Hu, sp. nov.**
– Pro- and mesocoxae mostly dark green with metallic tinge as on mesosoma; metasoma with tergum VII fully dark green with metallic tinge; POL at most 4.0× OOL ..... ***D. stefaniolae*** **Li, Wang & Hu, sp. nov.**
14(12) Vertex with a yellow area surrounding ocelli; metasomal terga I–IV laterally with round greenish-tinged spots, terga V–VI green with metallic tinge, and tergum VII yellow..... ***D. muleica*** **Li, Wang & Hu**
– Vertex without a yellow area surrounding ocelli; metasomal terga I–IV yellow, without round greenish-tinged spots, terga V–VII green with strong metallic tinge ..... ***D. gobica*** **Li, Wang & Zhu**

Species treatment

Dzhanokmenia stefaniolae **Li, Wang & Hu, sp. nov.**
http://zoobank.org/9E38CB14-AF1C-4915-A0C7-749956F29057
Figs 1–12

Description. Female (holotype, Figs 1–6). Body length 2.1 mm; Head with metallic tinge, vertex with small yellow area outside of each posterior ocellus, and with a triangular yellow T-shaped area in front of anterior ocellus; eye red; ocelli dark red; antenna with scape, pedicel and flagellum yellow; mandible dark brown. Mesosoma green with strong metallic tinge. Legs yellow except all coxae mostly dark green with metallic luster, as on mesosoma, and apical tarsomeres brown (Fig. 2). Metasoma with tergum I yellow except for metallic tinge in a triangular anteromedial area; terga II–IV entirely yellow; tergum V medially with a round green or orange metallic pattern; tergum VI mostly with green metallic tinge, laterally with small yellow part round like, yellow part not large than metallic tinge area; tergum VII fully dark green with metallic tinge. Ovipositor black with green metallic tinge; hypopygium fully black with green metallic tinge; outer plate of ovipositor mostly black.

Head (Fig. 3) 1.1× as wide as high, 1.5× as wide as midlobe of mesoscutum. Ocellar triangle surrounded by shallow grooves (vertex collapses along these lines in air-dried specimens). POL 3.8× OOL. Torulus at lower margin of eye. Malar space about 0.4× eye height. Malar sulcus strongly curved.

Antenna (Fig. 4) with scape 4.0× as long as wide, not reaching anterior ocellus; pedicel 1.6×, F1 1.6×, F2 1.5×, F3 1.0×, and clava 1.9× as long as wide; C3 short with rounded apex, without a terminal spine.

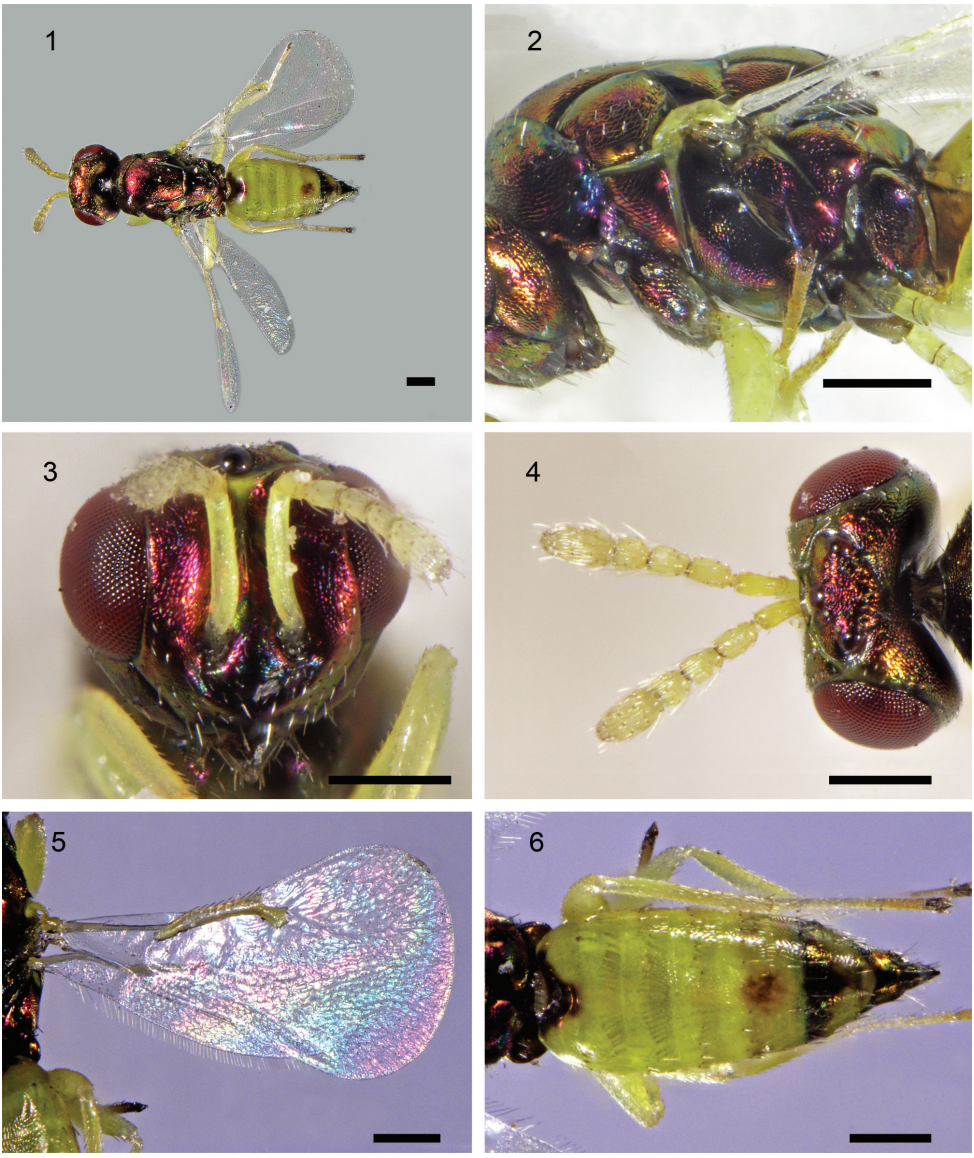

Figures 1–6. *Dzhanokmenia stefaniolae*, female (holotype): **1** habitus, dorsal **2** mesosoma, lateral **3** head, frontal **4** head, dorsal **5** wings **6** metasoma, dorsal. Scale bars: 0.2 mm.

Mesosoma 1.7× as long as wide, convex. Pronotum in dorsal view medially very short. Mesoscutum with midlobe about 1.2× as long as wide, with median line very weak, and with a single row of 3 or 4 adnotaular setae. Scutellum 1.2× as long as wide, with anterior pair of setae in posterior half, and submedian and sublateral grooves strong and parallel to each other. Propodeum medially as long as dorsellum, with a median carina but without paraspiracular carinae; callus with 4 or 5 setae; with a groove extending from spiracle to posterior margin of propodeum.

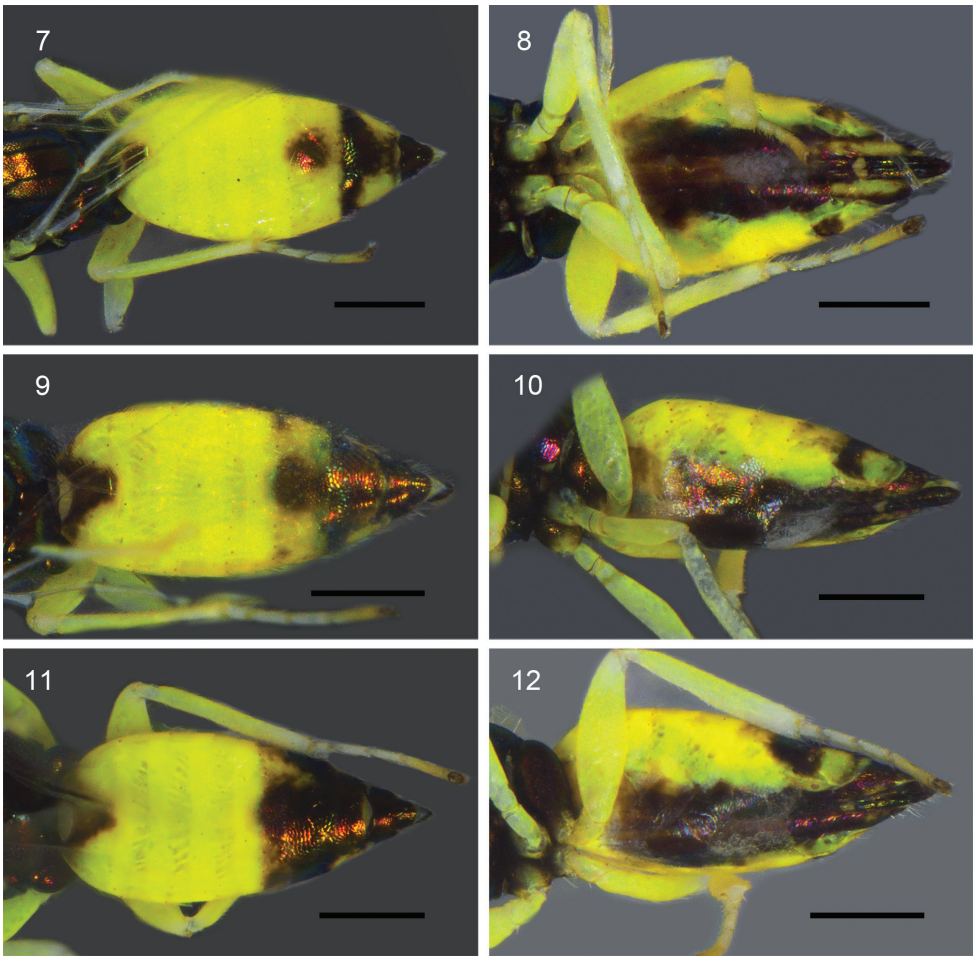

Figures 7–12. *Dzhanokmenia stefaniolae*, female (paratypes): **7, 9, 11** metasoma, dorsal **8, 10, 12** metasoma, ventral. Scale bars: 0.2 mm.

Fore wing (Fig. 5) hyaline, 1.9× as long as wide. Speculum large, extending from parastigma to stigmal vein. Discal setae short. CC 1.6× as long as MV; MV thick, 6.0× as long as wide; MV 2.4× as long as STV, with 7 marginal setae (about 0.5× as long as STV); STV rather thick; PSV not thicker than MV, short, stub-like. Hind wing rounded apically, 4.5× as long as wide.

Legs. Metafemur 3.5× as long as wide.

Metasoma (Fig. 6) 1.2× as long as mesosoma, 2.0× as long as wide; hypopygium extending to about half length of metasoma; cercal setae subequal in length; ovipositor sheath slightly protruding.

Variation (paratypes, Figs 7–12). Body length 1.9–2.1 mm. Metasomal tergum V with metallic area small to large size which occupying most of the tergum (Figs 7, 9, 11); tergum VI with metallic pattern area large to very large, relatively, with yellow

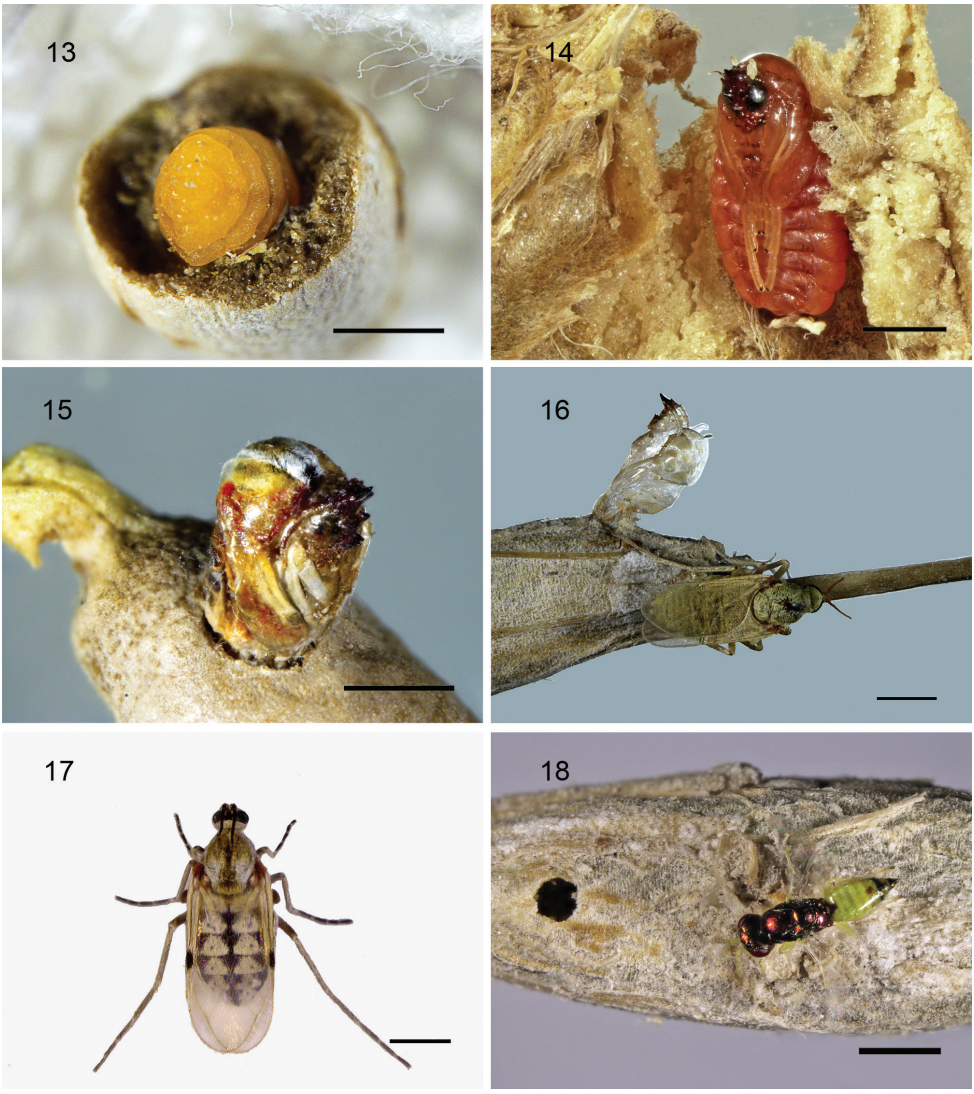

Figures 13–18. 13–17 *Stefaniola* sp.: **13** larva **14, 15** pupa **16, 17** adult **18** emergence hole of adult *Dzhanokmenia stefaniolae*. Scale bars: 1 mm.

part laterally from middle size to small (Figs 8, 10, 12); hypopygium from dark brown to black; outer plate of ovipositor mostly black to entirely black with metallic reflections (Figs 8, 10, 12). Pedicel 1.6–1.7×, F1 1.6–1.7×, F2 1.5–1.6×, F3 0.9–1.0×, clava 1.8–1.9× as long as wide. POL 3.8–4.0× OOL. EL 1.9–2.4× MSP. ML 1.6–1.7× MW. STL 1.1–1.2× STW. FWL 1.8–1.9× FWW. HWL 4.4–4.9× HWW. CC 1.5–1.6× MV. MV 2.3–2.4× STV. GL 2.0–2.3× GW. MFL 3.5–3.8× MFW.

Male. Unknown.

Etymology. The species is named after the host genus.

Type material. ***Holotype*** f# [ICXU], air-dried on card point: China, Xinjiang, Fukang, 44°22'29"N, 87°52'57"E, 466 m, reared from stem-gall of *Stefaniola* sp. on

H. ammodendron 26.iv.2015, H.-y. Hu group. ***Paratypes*:** 3 f# on card points [ICXU], same label data as holotype.

Host. An unidentified species of *Stefaniola* Kieffer (Cecidomyiidae). The larval, pupal and adult stages of *Stefaniola* sp., are shown in Figs 13–17. The emergence hole of adult *D. stefaniolae* is shown in Fig. 18.

Distribution. China: Xinjiang.

Remarks. See the remarks of the other species below.

***Dzhanokmenia yuxuannis* Li, Wang & Hu, sp. nov.**

http://zoobank.org/300330F0-A903-40A4-AD84-08240A282CB2

Figs 19–26

Description. Female (holotype, Figs 19–22). Body length 1.9 mm. Head with metallic tinge, eye red; ocelli dark red; antenna with scape, pedicel and flagellum yellow; mandible dark brown. Mesosoma with strong metallic tinge. Legs yellow except metacoxa mostly with metallic luster, as on mesosoma, and apical tarsomeres dark. Tergum I yellow except for metallic tinge in a triangular anteromedial area; terga II–IV entirely yellow; tergum V mostly yellow except medially with a faint pale brown round with faint metallic tinge; tergum VI mostly yellow, with brown stripe from anterior to posterior margins with green metallic tinge, with anterior margin brown; tergum VII with anterior triangular-shaped area dark brown with green metallic tinge, with yellow part laterally which is larger than the metallic area (Fig. 20). Ovipositor dark brown with metallic tinge; hypopygium laterally with a yellow oval area surrounded by brown to black part; upper outer plate of ovipositor with two dark brown stripe areas with metallic reflections on either side of ovipositor, and lower outer plate of ovipositor with yellow stripe-like part between dark brown stripe and ovipositor, which is linked with tergum VII.

Head (Fig. 21) 1.2× as wide as high, 1.6× as wide as midlobe of mesoscutum.

Ocellar triangle surrounded by shallow grooves. POL 5.0× OOL. Malar space about 0.4× eye height. Torulus at lower margin of eye. Malar sulcus strongly curved.

Antenna (Fig. 21) with scape 4.6× as long as wide, not reaching anterior ocellus; pedicel 2.0×, F1 1.7×, F2 1.5×, F3 1.1×, and clava 2.1× as long as wide; C3 short with rounded apex, without a terminal spine.

Mesosoma 1.8× as long as wide, convex. Pronotum in dorsal view medially very short. Mesoscutum with midlobe about 1.1× as long as wide, with median line very weak, and with a single row of 3 or 4 adnotaular setae. Scutellum 1.15× as long as wide, with anterior pair of setae in its posterior half, submedian and sublateral grooves strong and parallel to each other. Propodeum medially as long as dorsellum, with a median carina but without paraspiracular carinae; callus with 4 or 5 setae; with a groove extending from spiracle to posterior margin of propodeum.

Fore wing (Fig. 22) hyaline, 1.8× as long as wide; speculum large, extending from parastigma to stigmal vein. Discal setae short. CC 2.0× as long as MV; MV thick, 5.0× as long as wide; MV 2.2× as long as STV, with 7 marginal setae (about 0.5× as long

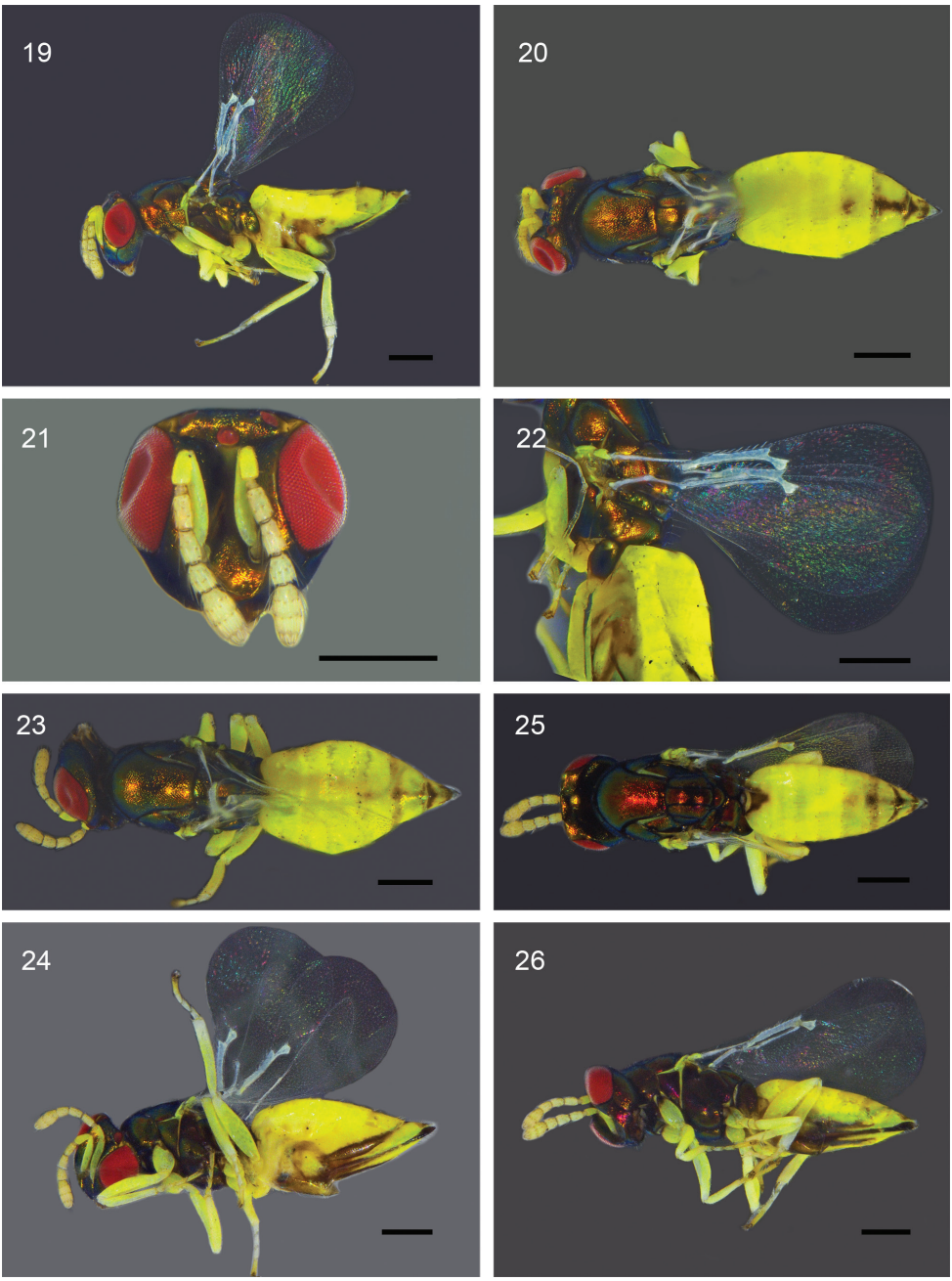

Figures 19–26. *Dzhanokmenia yuxuannis*, female (**19–22** holotype **23–26** paratypes): **19** habitus, lateral **20** body, dorsal **21** head, frontal **22** wings **23, 25** metasoma, dorsal **24, 26** metasoma, ventral. Scale bars: 0.2 mm.

as STV); STV rather thick; PSV not thicker than MV, short, stub-like. Hind wing rounded apically, 4.7× as long as wide.

Legs. Metafemur 3.3× as long as wide.

Metasoma 1.2× as long as mesosoma, 2.0× as long as wide; hypopygium extending to about half length of metasoma; cercal setae subequal in length; ovipositor sheath slightly protruding.

Variation (paratypes, Figs 23–26). Body length 1.9–2.0 mm. Metasomal tergum V with pale brown round from nearly invisible to visible (Figs 20, 23, 25); tergum VI with brown stripe small to large, anterior margin pale brown to brown; tergum VII with anterior triangular-shaped to crescent-shaped area dark brown with green metallic tinge, laterally with yellow part occupying mostly area of tergum VII. Ovipositor brown to dark brown with faint green or orange metallic tinge; hypopygium with oval shaped yellow area middle size to large, which is surrounded by brown to black part with metallic tinge; upper outer plate of ovipositor with dark brown stripes narrow to wide, relatively, lower outer plate of ovipositor with yellow stripe-like part from wide to narrow (Figs 24, 26). HW 1.1–1.2× HL. Pedicel 1.9–2.0×, F1 1.6–1.7×, F2 1.5–1.6×, F3 1.0–1.1×, clava 2.0–2.1× as long as wide. POL 4.7–5.0× OOL. EL 2.1–2.5× MSP. ML 1.7–1.8× MW. STL 1.1–1.3× STW. FWL 1.8–1.9× FWW. HWL 4.6–5.4× HWW. CC 1.7–2.0× MV. MV 2.2–2.6× STV. GL 2.0–2.2× GW. MFL 3.3–3.5× MFW.

Male. Unknown.

Etymology. The species name is a noun in apposition; it is derived from the first and second authors' son's first name, Yuxuan (Wang Yuxuan).

Type material. ***Holotype*** f# [ICXU], air-dried on card point: China, Xinjiang, Fukang, 44°22'29"N, 87°52'57"E, 466 m, sweeping on *H. ammodendron* and *H. persicum*, 26.iv.2015, H.-y. Hu group. ***Paratypes*****:** 2 f# on card points [ICXU], same label data as the holotype.

Hosts. Unknown.

Distribution. China: Xinjiang.

Remarks. This species is similar to *D. stefaniolae*, distinguished from each other by the combination of features as shown in Table 1.

Discussion

The description and illustration of the two new species from the Beishawo desert and the key to the species will contribute to our understanding of *Dzhanokmenia*. The 13 described species of *Dzhanokmenia*, show quite different colour patterns of coxae, metasomal terga and hypopygium according to Dzhanokmen (1971), Kostjukov (1977, 1978, 1984, 2014), Kostjukov and Kosheleva (2014, 2015) and Li et al. (2016). We regard the differences as interspecific characters which allow the separation of species in *Dzhanokmenia* as shown in the key.

Including two new species in this paper, 15 valid species of *Dzhanokmenia* are known from the arid to semi-arid regions of Southern Russia and Central Asia. However, hosts remain to be discovered for any of the species. Li et al. (2016) suggested that they are most likely associated with *Haloxylon* and *Tamarix* spp., feeding on them or as parasitoids of their pests. In this study, *D. stefaniolae* was reared from ball-like stem-galls of

Table 1. Summary of morphological differences between *Dzhanokmenia stefaniolae* and *D. yuxuannis*.

Species/ Characters	*D. stefaniolae*	*D. yuxuannis*
POL : OOL	3.8–4.0	4.6–5.0
Pedicel length to width	1.6–1.7	1.9–2.0
CC : MV	1.5–1.6	1.7–2.0
Coxae	All coxae mostly dark green with metallic luster, as on mesosoma.	Pro- and mesocoxae mostly yellow, metacoxa with metallic luster as on mesosoma.
Tergum V	Metasomal tergum V medially with a round green or orange metallic pattern from small to large size which occupying most of the tergum.	Metasomal tergum V mostly yellow except medially with a pale brown round from nearly invisible to visible with faint metallic tinge.
Tergum VI	Tergum VI mostly with green metallic tinge from large to very large, relatively, laterally with small yellow part round like, from middle size to small.	Tergum VI mostly yellow, with brown stripe from anterior to posterior margins with green metallic tinge small to large, with anterior margin pale brown to brown.
Tergum VII	Tergum VII fully dark green with metallic tinge.	Tergum VII with anterior triangular- to crescent-shaped area dark brown with green metallic tinge, laterally with yellow part occupying most of tergum VII.
Ovipositor	Ovipositor black with green metallic tinge.	Ovipositor brown to dark brown with faint green or orange metallic tinge.
Hypopygium	Hypopygium dark brown to black.	Hypopygium with oval shaped yellow area medium-sized to large surrounded by brown to black part with metallic tinge.
Outer plate of ovipositor	Outer plate of ovipositor mostly black to entirely black with metallic reflections.	Upper outer plate of ovipositor with narrow to wide dark brown stripes, lower outer plate of ovipositor with wide to narrow yellow stripe-like part.

Stefaniola sp. on *H. ammodendron* for the first time. *D. yuxuannis* was collected by sweeping from both *H. ammodendron* and *H. persicum* at the same collecting site. This suggests a relationship between *D. yuxuannis* and *Haloxylon* spp., but it needs further study.

Besides *D. stefaniolae*, from ball-like stem-galls of *Stefaniola* sp. on both *H. ammodendron* and *H. persicum* in the same desert localities, we also reared *Mesopolobus quadrimaculatus* Dzhanokmen (Pteromalidae), *Aprostocetus* sp. (Eulophidae), *Psyllaephagus caillardiae* Sugonjaev (Encyrtidae), and also some unidentified Eurytomidae and Platygastridae (Hymenoptera) (specimens in ICXU). The relationships among these species and *Stefaniola* sp. are not clear and need further study. Currently, the taxonomy of the Palaearctic species of *Stefaniola* is in flux, so unfortunately this *Stefaniola* sp. cannot be positively identified to species (pers. comm. by Ke-Long Jiao).

Acknowledgements

We thank Serguei V. Triapitsyn (Entomology Research Museum, Department of Entomology, University of California, Riverside, California, USA) for reviewing the earlier draft of the manuscript prior to its submission and Ke-Long Jiao (Department of Plant Protection, College of Horticulture and Landscape, Tianjin Agricultural University, Tianjin, China) for the identification of *Stefaniola* sp. This work was supported by the Xinjiang University Doctoral Starting Fund project (62031224704) and the National Natural Science Foundation of China (31900349, 31672338, U1170305).

References

Dzhanokmen KA (1971) A new species of *Tetrastichus* (Hymenoptera, Tetrastichidae) from southeastern Kazakhstan. Zoologicheskiy Zhurnal 50: 1883–1884. [In Russian]

Gibson GAP (1997) Morphology and terminology. In: Gibson GAP, Huber JT, Woolley JB (Eds) Annotated Keys to the Genera of Nearctic Chalcidoidea (Hymenoptera). National Research Council Research Press, Ottawa, 16–44.

Graham MDV (1991) A reclassification of the European Tetrastichinae (Hymenoptera: Eulophidae): revision of the remaining genera. Memoirs of the American Entomological Institute 49: 1–322.

Kostjukov VV (1977) Comparative morphology of chalcids of the subfamily Tetrastichinae and the system of the genus *Tetrastichus* Haliday, 1844 (Hymenoptera, Eulophidae). Entomologicheskoe Obozrenie 56(1): 177–194. [In Russian with English summary]

Kostjukov VV (1978) Subfam. 5. Tetrastichinae. In: Medvedev GS, Trjapitzin VA (Eds) Keys to the Insects of the European Part of the USSR – Volume III, Hymenoptera, Part 2. Nauka [Leningrad division], Leningrad, 430–467. [In Russian]

Kostjukov VV (1984) New species of the genus *Tetrastichus* Haliday, 1844 (Hymenoptera, Eulophidae) from Turkmenistan. Entomophagues of the orchards pests. Kishinev, Shtiintsa, 30–35. [In Russian]

Kostjukov VV (2014) New species of *Dzhanokmenia* Kostjukov, 1977 and *Kolopterna* Graham, 1987 (Hymenoptera, Eulophidae, Tetrastichinae) from Turkmenistan. Biological Plant Protection as the basis of ecosystem stabilization of Agroecosystems (Krasnodar) 8: 84–91.

Kostjukov VV, Kosheleva OV (2014) New species of *Dzhanokmenia* Kostjukov and *Kolopterna* Graham (Hymenoptera: Eulophidae: Tetrastichinae) from Russia. Proceedings of the Russian Entomological Society 85(1): 160–164.

Kostjukov VV, Kosheleva OV (2015) A new species of the eulophid-wasp genus *Dzhanokmenia* Kostjukov, 1977 (Hymenoptera, Eulophidae: Tetrastichinae) from Stavropol Territory. Entomologicheskoe Obozrenie 94(2): 451–454. https://doi.org/10.1134/S0013873815040144

Li Q, Wang C, Hu HY, Kostjukov VV, LaSalle J, Zhu CD (2016) Descriptions of three new species of *Dzhanokmenia* (Hymenoptera: Eulophidae) from China. Zootaxa 4121(4): 447–457. https://doi.org/10.11646/zootaxa.4121.4.5

Noyes JS (2020) Universal Chalcidoidea Database. https://www.nhm.ac.uk/our-science/data/chalcidoids/ [Accessed on: 2020-6-20]

ZooKeys 1009: 81–122 (2021)
doi: 10.3897/zookeys.1009.54303
https://zookeys.pensoft.net

RESEARCH ARTICLE

A peer-reviewed open-access journal
ZooKeys
Launched to accelerate biodiversity research

Lake Poso's shrimp fauna revisited: the description of five new species of the genus *Caridina* (Crustacea, Decapoda, Atyidae) more than doubles the number of endemic lacustrine species

Werner Klotz[1], Thomas von Rintelen[2], Daisy Wowor[3], Chris Lukhaup[4], Kristina von Rintelen[2]

1 *Wiesenweg 1, A-6063 Rum, Austria* **2** *Museum für Naturkunde, Leibniz Institute for Evolution and Biodiversity Science, Invalidenstr. 43, D-10115 Berlin, Germany* **3** *Division of Zoology, Research Center for Biology, Indonesian Institute of Sciences (LIPI), Jalan Raya Jakarta Bogor Km 46, Cibinong 16911, Indonesia* **4** *Waldstrasse 5a, D-66999 Hinterweidenthal, Germany*

Corresponding author: Werner Klotz (wklotz@aon.at)

Academic editor: I.S. Wehrtmann | Received 14 May 2020 | Accepted 20 July 2020 | Published 4 January 2021

http://zoobank.org/F0C4C58B-5F48-4CDB-A443-E258D732AC5B

Citation: Klotz W, von Rintelen T, Wowor D, Lukhaup C, von Rintelen K (2021) Lake Poso's shrimp fauna revisited: the description of five new species of the genus *Caridina* (Crustacea, Decapoda, Atyidae) more than doubles the number of endemic lacustrine species. ZooKeys 1009: 81–122. https://doi.org/10.3897/zookeys.1009.54303

Abstract

Lake Poso, an ancient lake system on the Indonesian island Sulawesi, harbours an endemic species flock of six, four lacustrine and two riverine species of the freshwater shrimp genus *Caridina*. In this study, five new lacustrine species are described, bringing the total to eleven species altogether. The number of lacustrine species is more than doubled to nine species compared to the last taxonomic revision in 2009. One of them, *Caridina mayamareenae* Klotz, Wowor & von Rintelen, **sp. nov.**, even represents the first case of an atyid shrimp associated with freshwater snails which is morphologically adapted to living in shells. An integrative approach was used by providing a combination of morphological, ecological, and molecular data. Based on standard morphological characters, distribution, substrate preferences, and colouration of living specimens in the field, five distinct undescribed species could be distinguished. To support our species-hypothesis based on the mitochondrial genes 16S and COI, a molecular phylogeny was used for all eleven species from Lake Poso. All species form a well-supported monophyletic group, but only four morphospecies consistently correspond to mtDNA clades – a possible reason could be introgressive hybridisation, incomplete lineage sorting, or not yet fixed species boundaries. These results are discussed further in

the context of adaptive radiation, which turned out to be more diverse than previously described. Finally, yet importantly, subjecting all new species to similar threats and to the same IUCN category and criterion than the previously described species from the lake is recommended.

Keywords
Adaptive radiation, ancient lake, freshwater biodiversity, Indonesia, integrative taxonomy, Sulawesi

Introduction

Lake Poso (Fig. 1) is one of the two so-called ancient lakes systems on the Indonesian island of Sulawesi. This long-lived lake probably is more than 1 million years old (Vaillant et al. 2011) and regarded as a hotspot of biodiversity (von Rintelen et al. 2012). The lake is of tectonic origin and has an area of 323.2 km^2, maximum depths of 450 m, is oligotrophic with a high transparency and low organic content (von Rintelen et al. 2012). It provides ideal conditions for the evolution of highly diverse endemic species flocks of freshwater organisms such as crustaceans, molluscs and fishes (see review in von Rintelen et al. 2012).

The endemic species flock of atyid freshwater shrimps of the genus *Caridina* in Lake Poso was first studied by Schenkel (1902) with the description of two new species from the lake itself and one riverine species from the lake's catchment. More than 100 years later, another lacustrine species was described by Cai and Wowor (2007), followed by von Rintelen and Cai (2009), who revised the entire species flock of four lacustrine and two riverine species in the lake system including the description of a new lacustrine and a new riverine species (Table 1).

Here, we use an integrative taxonomic approach to study newly collected material from Lake Poso to a) discover new, so far unknown species from the lake, b) provide a combination of morphological, ecological, and molecular data to describe the newly discovered species, c) provide two different identification keys (a regular key for preserved specimens and a key for pre-sorting living specimens in the field without having to use a microscope), and d) discuss the results in context of adaptive radiation and conservation status of the previously revised Lake Poso species flock.

Materials and methods

Specimens were caught by hand net and preserved in 75–95% ethanol during several fieldtrips to Lake Poso (Fig. 1) between 2003 and 2019 (for sampling details, see Systematic accounts). Specimens were dissected and morphometrical data were taken using a BMS 143 Trino Zoom dissecting microscope with an ocular grid. Details on setae and mouthparts were observed using a Reichert Biovar compound microscope. Rostral characters were taken from all specimens examined. Drawings were made from microphotographs using Adobe Illustrator following Coleman (2003, 2006). The se-

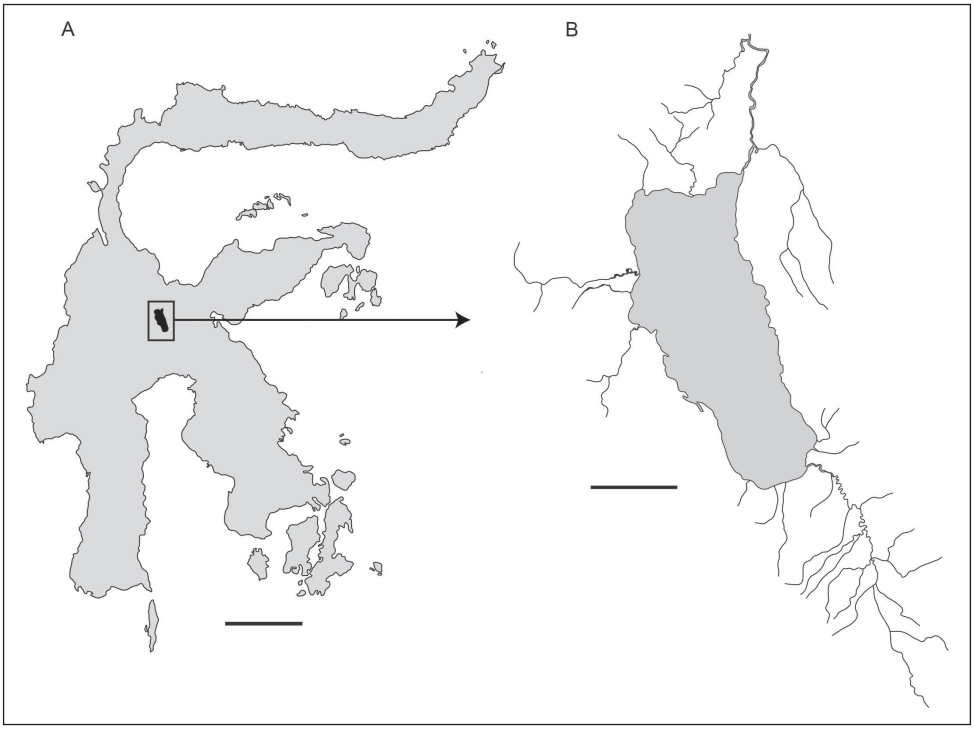

Figure 1. Lake Poso situated in the central highlands of the Indonesian island Sulawesi **A** Sulawesi (scale bar: 100 km) **B** Lake Poso and catchment area (scale bar: 10 km). Map modified from von Rintelen et al. 2007a.

tae terminology used mostly follows Short (2004). The two identification keys in this study were modified and updated from the previous keys in von Rintelen and Cai (2009). All new species were described by the first, third and last author.

All material examined is deposited in Museum Zoologicum Bogoriense, Cibinong, Indonesia (**MZB**), and the Museum für Naturkunde (Museum of Natural History), Berlin, Germany (**ZMB**). The following abbreviations are used in the text: **cl**., carapace length (measured from the postorbital margin to the posterior margin of the carapace); **ov**., ovigerous; **E**, east; **S**, south; **N**, north; **W**, west.

DNA was extracted from abdominal tissue using either a Qiagen Blood and Tissue Kit or a Qiagen BioSprint with the Plant Kit (but lysis with 10ml Qiagen Proteinase K (20mg/ml) added) according to the manufacturer's instructions. Fragments of the mitochondrial 16S rRNA (16S, ~ 590 bp) and cytochrome oxidase subunit I (COI, 861 bp) genes were amplified by polymerase chain reaction (PCR) and sequenced using primers 16S-F-Car and 16S-R-Car1 (16S), and COI-F-Car and COI-R-Car (COI) (von Rintelen et al. 2007a), or, for COI only, COI-F-Car and COI-R-H16mod3 (1087 bp fragment extending COI-F-Car/COI-R-Car fragment at 3' end; 5' CAAYKATCTGCCATTTTAGA), sometimes in combination with COI-F-Car and COI-R-int (458 bp fragment at 5' end of COI-F-Car/COI-R-Car fragment; 5' GCAATAATTATAGTTGCTGA).

Table 1. Current checklist of endemic species of the genus *Caridina* from Lake Poso, Indonesia.

Species	Remarks	Reference
Caridina acutirostris Schenkel, 1902	Exclusively riverine species, endemic to Lake Poso catchment	von Rintelen and Cai 2009
C. caerulea von Rintelen & Cai, 2009	Endemic to Lake Poso (excluding rivers)	von Rintelen and Cai 2009
C. ensifera Schenkel, 1902	Endemic to Lake Poso (excluding rivers)	von Rintelen and Cai 2009
C. fusca Klotz, Wowor & von Rintelen, sp. nov.	Endemic to Lake Poso (excluding rivers)	This study
C. lilianae Klotz, Wowor & von Rintelen, sp. nov.	Endemic to Lake Poso (excluding rivers)	This study
C. longidigita Cai & Wowor, 2007	Endemic to Lake Poso (excluding rivers)	von Rintelen and Cai 2009
C. marlenae Klotz, Wowor & von Rintelen, sp. nov.	Endemic to Lake Poso (excluding rivers)	This study
C. mayamareenae Klotz, Wowor & von Rintelen, sp. nov.	Endemic to Lake Poso (excluding rivers); hiding in empty snail shells	This study
C. poso Klotz, Wowor & von Rintelen, sp. nov.	Endemic to Lake Poso (excluding rivers)	This study
C. sarasinorum Schenkel, 1902	Endemic to Lake Poso (excluding rivers)	von Rintelen and Cai 2009
C. schenkeli von Rintelen & Cai, 2009	Exclusively riverine species, endemic to Lake Poso catchment	von Rintelen and Cai 2009

In the latter case, sequencing was done using COI-R-int and COI-R-H16mod3. Amplifications were conducted in 25 µL volumes containing 50–100 ng DNA, 1x PCR buffer, 200 mM of each dNTP, 0.5 mM of each primer, 2 mM MgCl2 and 1 U of Taq polymerase. After an initial denaturation step of 3 min at 94 °C, 35 cycles of 30 sec at 94 °C, 60 sec at 45°C (COI) or 50°C (16S) and 60 sec (16S) or 90 sec (COI) at 72 °C were performed, followed by a final extension step of 5 min at 72 °C. PCR products were sent to Macrogen Europe for purification and sequencing of both strands of the amplified gene fragments using the primers as given above.

Contigs of forward and reverse strands were assembled using Geneious Prime (v. 2019.2.1) and corrected by eye. Sequences were aligned by eye (COI) and with MAFFT (16S) (Katoh and Standley 2013). To determine the best substitution model for Bayesian inference analyses (see below), hierarchical likelihood ratio tests were carried out with jModelTest (Posada 2008) on both sequence sets. Based on the Akaike Inference Criterion (AIC), the GTR + I + G (COI) and the HKY + I + G (16S) models were chosen. The datasets were analysed further concatenated.

All new sequences (51 from Lake Poso species, 1 outgroup taxon) have been deposited in GenBank (for accession numbers and museum voucher numbers see Suppl. material 1, Table S1). Additionally, the sequences of Lake Poso species of *Caridina* published by von Rintelen et al. (2007a) have been included in the analysis and sequences from two endemic outgroup taxa from Sulawesi published in von Rintelen et al. (2010) (Suppl. material 1, Table S1).

Phylogenetic trees were reconstructed by Bayesian inference (BI; Huelsenbeck et al. 2001) using MrBayes 3.2.6 (Ronquist et al. 2012). The MCMCMC-algorithm was run with four independent chains for 20,000,000 generations, samplefreq = 500, and burnin = 25%. Maximum likelihood analyses were run with IQ-TREE (Nguyen et al. 2015) and branch support was obtained through the implemented ultrafast bootstrap (1,000 replicates; Hoang et al. 2018). BI and ML analyses were run using two gene partitions with the models specified above (for IQ-TREE, see Chernomor et al. 2016). In addition,

Maximum Parsimony (MP) analyses were performed using the heuristic search algorithm as implemented in PAUP* (Swofford 2002), with gaps treated as fifth base. Support for nodes was estimated by bootstrap analysis (1,000 fast stepwise-addition bootstrap replicates). Genetic distances were calculated using MEGA X (Kumar et al. 2018).

Results

We distinguished five morphologically distinct and undescribed species that could be separated clearly based on the examination of living specimens in the field (Figs 2E, 3A–C, E–H) and preserved in ethanol that turns specimens completely colourless. In Lake Poso, there are eleven species altogether, comprising a species flock of nine lacustrine and two riverine species (Table 1). This more than doubles the previously known lacustrine fauna of four species (von Rintelen and Cai 2009). Distribution data limited to Lake Poso and reproductive biology (few (5–36), large-sized eggs ca. 0.7–1.1 mm length of developed eggs with eyespots) indicative of direct larval development (Lai and Shy 2009) suggest endemism of all Lake Poso species (see Systematic accounts of this study; von Rintelen and Cai 2009).

Identification key to species of the genus *Caridina* from Lake Poso system

1 Tip of rostrum reaching end to distinctly overreaching end of scaphocerite (Fig. 4A, C) **2**

– Tip of rostrum not reaching end of scaphocerite (Fig. 4B) **8**

2 Tip of rostrum reaching or slightly overreaching end of scaphocerite (Fig. 4C) **3**

– Tip of rostrum reaching distinctly beyond end of scaphocerite (Fig. 4A) **4**

3 Epipods present on first and second pereiopods (Fig. 4D) .... ***C. schenkeli* von Rintelen & Cai, 2009**

– Epipod absent from all pereiopods (Fig. 4E) ..... ***C. marlenae* sp. nov**.

4 Tip of rostrum reaching beyond end of scaphocerite, ~ 0.9–1.4 times as long as carapace, long but not very slender (Fig. 4F) **5**

– Tip of rostrum reaching far beyond end of scaphocerite, ~ 1.4–2.8 times as long as carapace, long and quite slender (Fig. 4A) **6**

5 Epipod present on first pereiopod; chelae of first and second pereiopods stout, setae on tip of fingers ~ half as long as chelae (Fig. 4G) .... ***C. sarasinorum* Schenkel, 1902**

– Epipod absent from all pereiopods; chelae of first and second pereiopods very slender, setae on tip of fingers ~ as long as chelae (Fig. 4H) .... ***C. longidigita* Cai & Wowor, 2007**

6 Epipod absent from all pereiopods, vestigial epipod present on third maxilliped (Fig. 4I) ..... ***C. poso* sp. nov**.

– Epipods present on third maxilliped, first and second pereiopods (Fig. 4D) **7**

7 Rostrum 1.4–2.3 times as long as carapace, with distinctly less teeth (dorsal 9–15, ventral 16–29) (Fig. 4J); uropodal diaeresis with 9–11 spiniform setae; dactylus of third pereiopod with 6–9 spiniform setae; dactylus of fifth pereiopod with 51–57 serrate setae ..... ***C. ensifera*** **Schenkel, 1902**

– Rostrum 1.9–2.6 times as long as carapace, with distinctly more teeth (dorsal 11–20, ventral 26–48) (Fig. 4K); uropodal diaeresis with 11–14 spiniform setae; dactylus of third pereiopod with 4–5 spiniform setae; dactylus of fifth pereiopod with 27–49 serrate setae ..... ***C. caerulea*** **von Rintelen & Cai, 2009**

8 Rostrum very short, tip not reaching distal margin of eye (Fig. 7A, B) ..... ***C. lilianae*** **sp. nov**.

– Rostrum moderately short, tip distinctly overreaching distal margin of eye **9**

9 Tip of rostrum reaching end of third segment of antennular peduncle (Fig. 5A) ..... ***C. fusca*** **sp. nov**.

– Tip of rostrum reaching end of second segment of antennular peduncle (Fig. 4L) **10**

10 Rostrum high, maximum depth of rostrum more than maximum dorsoventral diameter of eye, ~ 0.17 of dorsal margin of rostrum distal without tooth (Fig. 11A, B) ..... ***C. mayamareenae*** **sp. nov**.

– Rostrum slender, maximum depth of rostrum less than maximum dorsoventral diameter of eye, ~ 0.3–0.5 of dorsal margin of rostrum distal without tooth (Fig. 4L) ..... ***C. acutirostris*** **Schenkel, 1902**

Key for pre-sorting living *Caridina* in the field (Lake Poso system)*

1 Shrimps collected from the rivers **2**

– Shrimps collected from the lake **3**

2 Rostrum approximately as long (0.9–1.1 times) as carapace; body transparently yellowish or brownish (Fig. 2A) ..... ***C. schenkeli*** **von Rintelen & Cai, 2009**

– Rostrum always distinctly shorter (0.3–0.7 times) than carapace; body transparently yellowish or brownish (Fig. 2B) ..... ***C. acutirostris*** **Schenkel, 1902**

3 Rostrum distinctly long and very slender, bent upwards, tip reaching far beyond end of scaphocerite; body rather slender and mainly transparent or with mottled pattern **4**

– Rostrum short to moderately long and not conspicuously slender, tip slightly reaching beyond end of scaphocerite or shorter; body usually more robust and less transparent **6**

4 Body showing a clearly visible red-and-white stripe pattern (Fig. 3E); tail fan with black-and-white blotches (Fig. 3F) ..... ***C. poso*** **sp. nov**.

– Body rather yellowish-transparent without stripe pattern; tail fan with colour marks **5**

* This key should not be used to identify specimens bred in captivity. Based on occasional colour hybrids not occurring in the natural environment, it could produce misleading results.

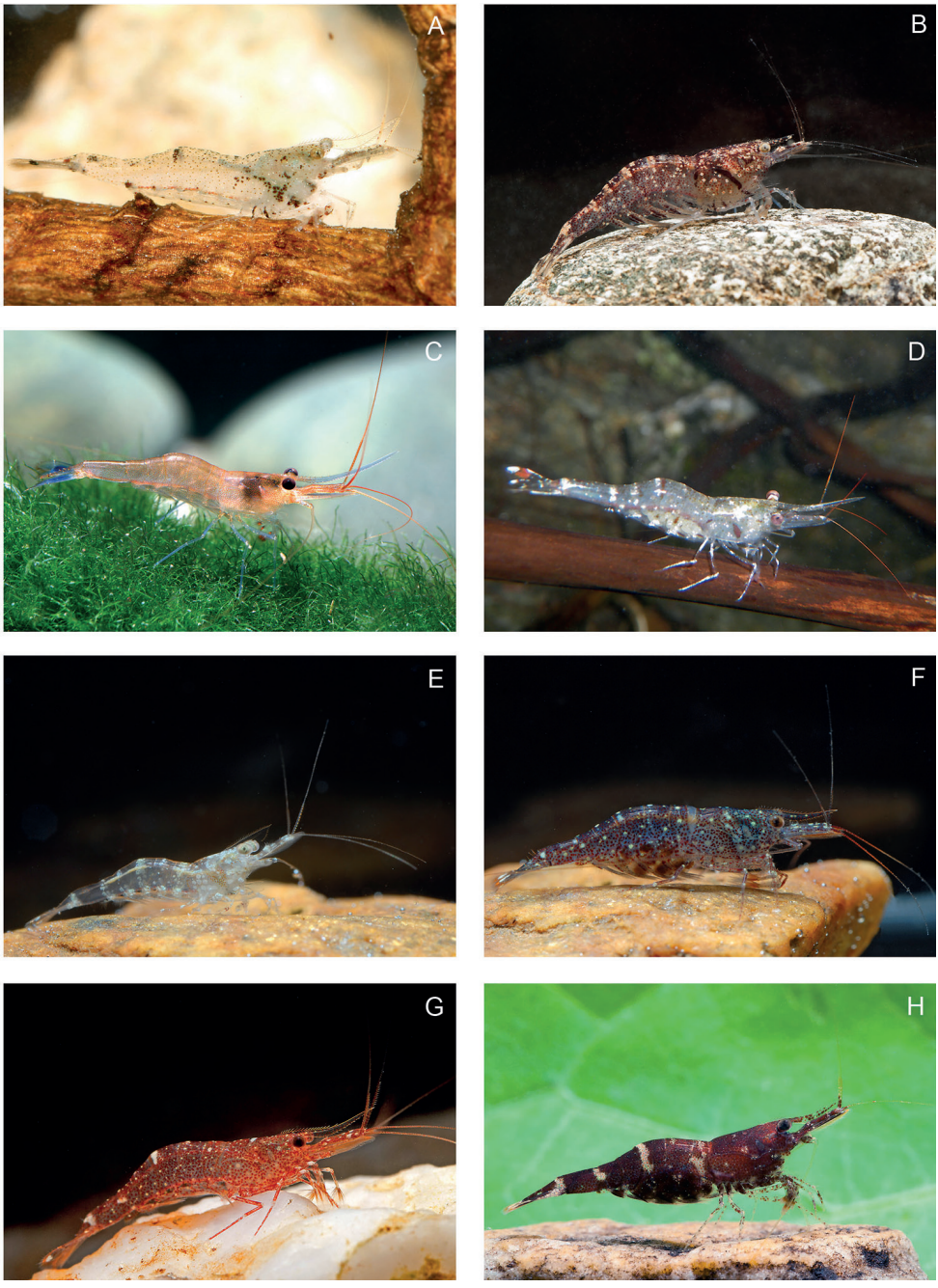

Figure 2. Living specimens of *Caridina* spp in Lake Poso 1. **A** *Caridina schenkeli* von Rintelen & Cai, 2009 **B** *C. acutirostris* Schenkel, 1902 **C** *C. caerulea* von Rintelen & Cai, 2009 **D** *C. ensifera* Schenkel, 1902 **E** *C. mayamareenae* sp. nov. male **F, G** *C. longidigita* Cai & Wowor, 2007 **H** *C. sarasinorum* Schenkel, 1902. Not to scale. Photo: C. Lukhaup (**A, C**), W. Klotz (**B, D–H**).

5 Legs and rostrum bluish; tail fan with two conspicuous blue patches (Fig. 2C) ... . ***C. caerulea* von Rintelen & Cai, 2009**
– Legs and rostrum yellowish-reddish; tail fan with two conspicuous red patches (Fig. 2D) ..... ***C. ensifera* Schenkel, 1902**
6 Rostrum conspicuously high; large females whitish, frequently with broad red stripes and blotches, eggs green (Fig. 3A, B), males mostly transparent with some white blotches (Fig. 2E); living in empty snail shells .... ***C. mayamareenae* sp. nov**.
– Rostrum not conspicuously high; usually not found in empty snail shells **7**
7 Rostrum very short, tip not reaching distal margin of eyes and body transparent-whitish (Fig. 3C); lives on very fine sand or soil in shallow water (1.5–2.5m) .... ***C. lilianae* sp. nov**.
– Rostrum distinctly longer, clearly overreaching distal margin of eyes; lives on various types of substrates **8**
8 Chelae on first two pairs of pereiopods with very long and clearly visible fingers, setae on tip of fingers as long as or longer than chelae (Fig. 2F, G, 4H) .... ***C. longidigita* Cai & Wowor, 2007**
– Chelae on first two pairs of pereiopods not conspicuously long with rather short fingers, setae on tip of fingers shorter than chelae (Fig. 4G) **9**
9 Body bright reddish with large white dots (Fig. 3G) ..... ***C. marlenae* sp. nov**.
– Body dark reddish or brown with well-defined white transversal bands **10**
10 Body dark reddish or brown with sharply defined white transversal bands on first, third, fifth and sixth abdominal segments (Fig. 3H); found under rocks .... ***C. fusca* sp. nov**.
– Body with a similar colouration and pattern, but bands less well-defined and scraggy (Fig. 2H); habitat not restricted to rocks ..... ***C. sarasinorum* Schenkel, 1902**

Systematic accounts

Atyidae De Haan, 1849
***Caridina* H. Milne Edwards, 1837**

***Caridina fusca* Klotz, Wowor & K. von Rintelen, sp. nov.**
http://zoobank.org/C6EF012A-7452-4C07-9E21-0FC6B2BC3082
Figures 3H, 5, 6

Material examined. Holotype: ov. ♀ cl. 2.9 mm (MZB Cru 5031), Indonesia, Central Sulawesi, Lake Poso, E shore, S of Tentena, dive at small cape, 15 m, 1°46.39'S, 120°38.33'E, M. Glaubrecht and T. von Rintelen leg., 12 May 2007. **Paratypes:** 1 ov. ♀ cl. 2.7 mm, 1 ♂ cl. 2.3 mm (MZB Cru 5032), 2 ♀♀ cl. 2.9 and 3.1 mm (ZMB 29518), same data as holotype; 1 ov. ♀ cl. 2.8 mm (MZB Cru 5033), Lake Poso, E shore, S of Tentena, dive at small cape, 15 m, 1°46.394'S, 120°38.327'E, coll. J. Pfaender and T. von Rintelen leg., 21 Sep. 2015; 1 ♀ cl. 2.4 mm (ZMB 29622), Lake Poso, E shore, S of Tentena, dive at small cape, 10 m, 1°46.394'S, 120°38.327'E, coll.

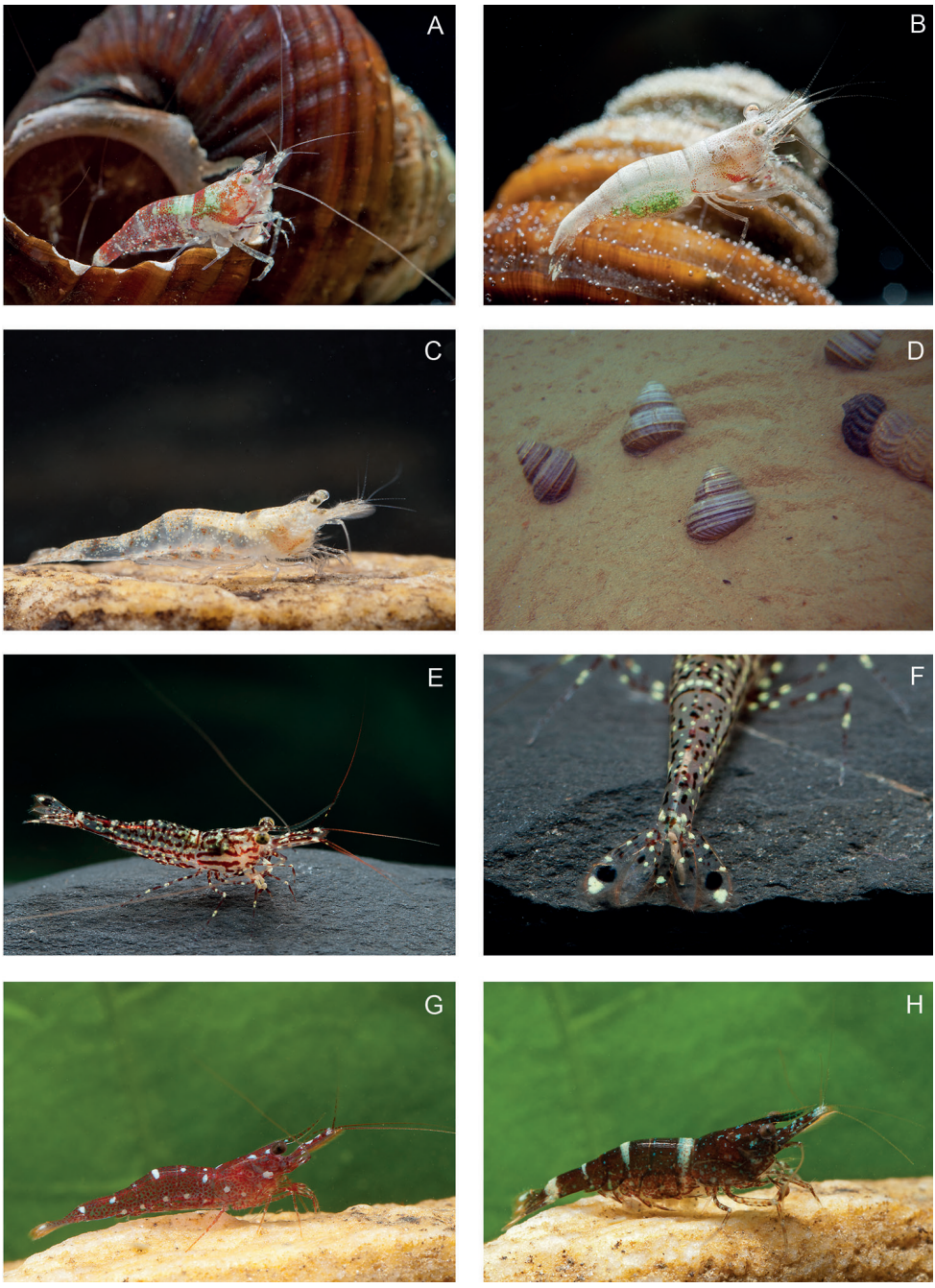

Figure 3. Living specimens of *Caridina* spp in Lake Poso 2. **A, B** *Caridina mayamareenae* sp. nov. **C** *C. lilianae* sp. nov. **D** Two snail species *Celetaia persculpta* and *Tylomelania* sp. on soft substrate. Empty shells of these species are shelter for *C. mayamareenae* sp. nov. **E, F** *C. poso* sp. nov. **G** *C. marlenae* sp. nov. **H** *C. fusca* sp. nov. Not to scale. All photographs: W. Klotz.

J. Pfaender and T. von Rintelen leg., 21 Sep. 2015; 1 ov. ♀ cl. 2.7 mm (MZB Cru 5034), 1 ♀ cl. 2.5 mm (ZMB 30223), Lake Poso, E shore, S of Tentena, dive at small cape, 15 m, 1°46.394'S, 120°38.327'E, coll. T. von Rintelen and W. Klotz leg., 12 May 2017; 1 ov. ♀ cl. 2.9 mm (ZMB 30715), Lake Poso, W shore, Bay S of cape, in ca. 6 m depth, 1°55.408'S, 120°33.315'E, coll. T. von Rintelen leg., 4 Jul. 2018. 1 ov. ♀ cl. 2.4 mm (MZB Cru 5090), Lake Poso, E shore, small bay within mouth of outlet, 1°46.30'S, 120°38.38'E, T. von Rintelen leg., 14 Jul 2019.

Description. ***Cephalothorax and cephalic appendages.*** Postorbital carapace length 2.4–2.8 mm (n = 10). Rostrum (Fig. 5A–C) moderately long, straight or slightly sigmoid, reaching to end of antennular peduncle, dorsal and ventral margin armed throughout almost to tip, 0.78–0.94 (median 0.87, n = 7) times as long as carapace, rostral formula 5–7 + 12–17 / 7–9. Antennal spine fused with or slightly separated from orbital margin. Pterygostomial angle broadly rounded. Eyes well developed with globular cornea. Antennular peduncle (Fig. 5A, C, H), 0.84–0.90 (median 0.86, n = 4) times as long as carapace, first segment 1.71–2.14 (median 1.81, n = 4) times as long as second segment, second segment 2.33–3.00 (median 2.83, n = 4) times longer than third segment. Tooth on distolateral margin of first segment of antennular peduncle acute. Stylocerite reaching to 0.85–0.89 (median 0.87, n = 4) of first segment of antennular peduncle. Scaphocerite (Fig. 5I) 3.81–4.00 (median 3.90, n = 2) times as long as wide, inner and distal margin beset with plumose setae.

Abdominal somites, telson, and uropods. Sixth abdominal somite 0.54–0.58 (median 0.56, n = 4) times carapace length, 1.53–2.21 (median 1.77, n = 4) times as long as fifth somite, 0.94–1.00 (median 0.98, n = 4) times as long as telson. Distal margin of telson (Fig. 5F, G) convex without a median projection, with three pairs of short spiniform setae dorsally and one pair of short spiniform setae dorsolaterally; distal end with six long spiniform setae, lateral pair longer than others. Preanal carina (Fig. 5D) with a hook-like spine. Uropodal diaeresis (Fig. 5E) with 11–13 short movable spiniform setae, outermost ones shorter than lateral angle.

Mouthparts and branchiae. Incisor process of mandible (Fig. 5J) ending in irregular teeth, molar process truncated. Lower lacinia of maxillula (Fig. 5K) broadly rounded, upper lacinia elongate, with numerous distinct teeth on inner margin, palp slender with few pappose setae and one conical spiniform seta near tip. Upper endites of maxilla (Fig. 5L) subdivided, palp slender, scaphognathite tapering posteriorly, fringed with long, curved setae at posterior margin. Palp of first maxilliped (Fig. 5M, N) ending in a slender triangular extension. Podobranch on second maxilliped (Fig. 5O) reduced to a lamina. Third maxilliped (Fig. 5P) with one well developed and one small arthrobranch, ultimate segment of maxilliped shorter than penultimate segment. First pereiopod with a small arthrobranch. Pleurobranchs present on all pereiopods. Epipod slightly reduced (without distal hook) on third maxilliped, absent from all pereiopods.

Pereiopods. Chelae of first and second pereiopods (Fig. 6A, B) well developed; chela of first pereiopod 2.29–2.73 (median 2.33, n = 7) times as long as wide, 1.17–1.34 (median 1.31, n = 7) times length of carpus; tips of fingers rounded, without hooks, with tufts of hairs near tip; dactylus 0.94–1.21 (median 1.11, n = 7) times as long as palm; carpus slender, hardly excavated distally, 2.33–3.00 (median 2.58, n = 7)

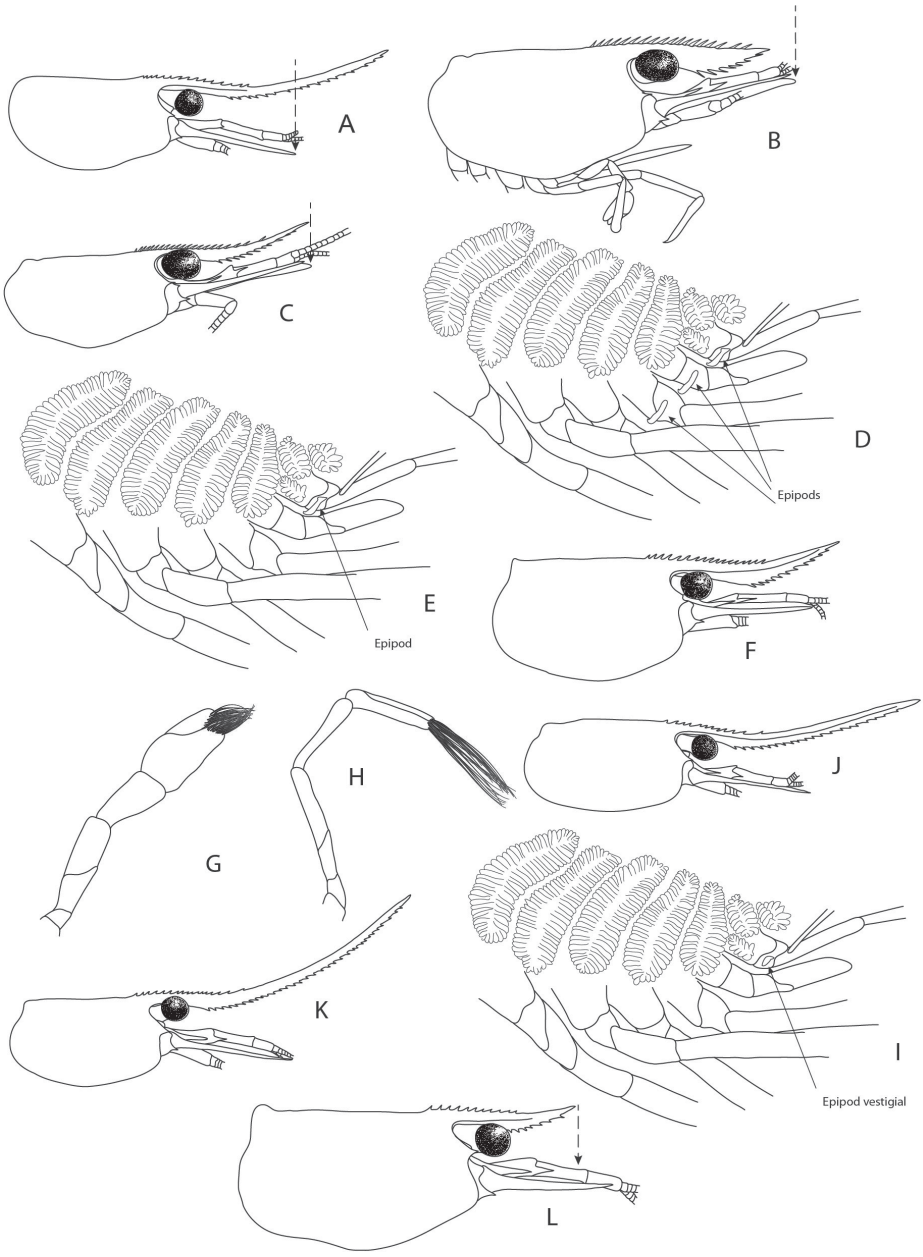

Figure 4. Morphological characters used in the identification keys **A** tip of rostrum distinctly overreaching end of scaphocerite **B** tip of rostrum not reaching end of scaphocerite **C** tip of rostrum reaching end of scaphocerite **D** epipods present on third maxilliped and first and second pereiopods **E** epipod present on third maxilliped but absent from all pereiopods **F** rostrum long but not very slender **G** chelae of first and second pereiopods stout, setae on tip of fingers approx. half as long as chelae **H** chelae of first and second pereiopods very slender, setae on tip of fingers approx. as long as chelae **I** epipod vestigial present on third maxilliped and absent from all pereiopods **J** rostrum of *C. ensifera* Schenkel, 1902 **K** rostrum of *C. caerulea* von Rintelen & Cai, 2009 **L** rostrum reaching end of second segment of antennular peduncle and slender.

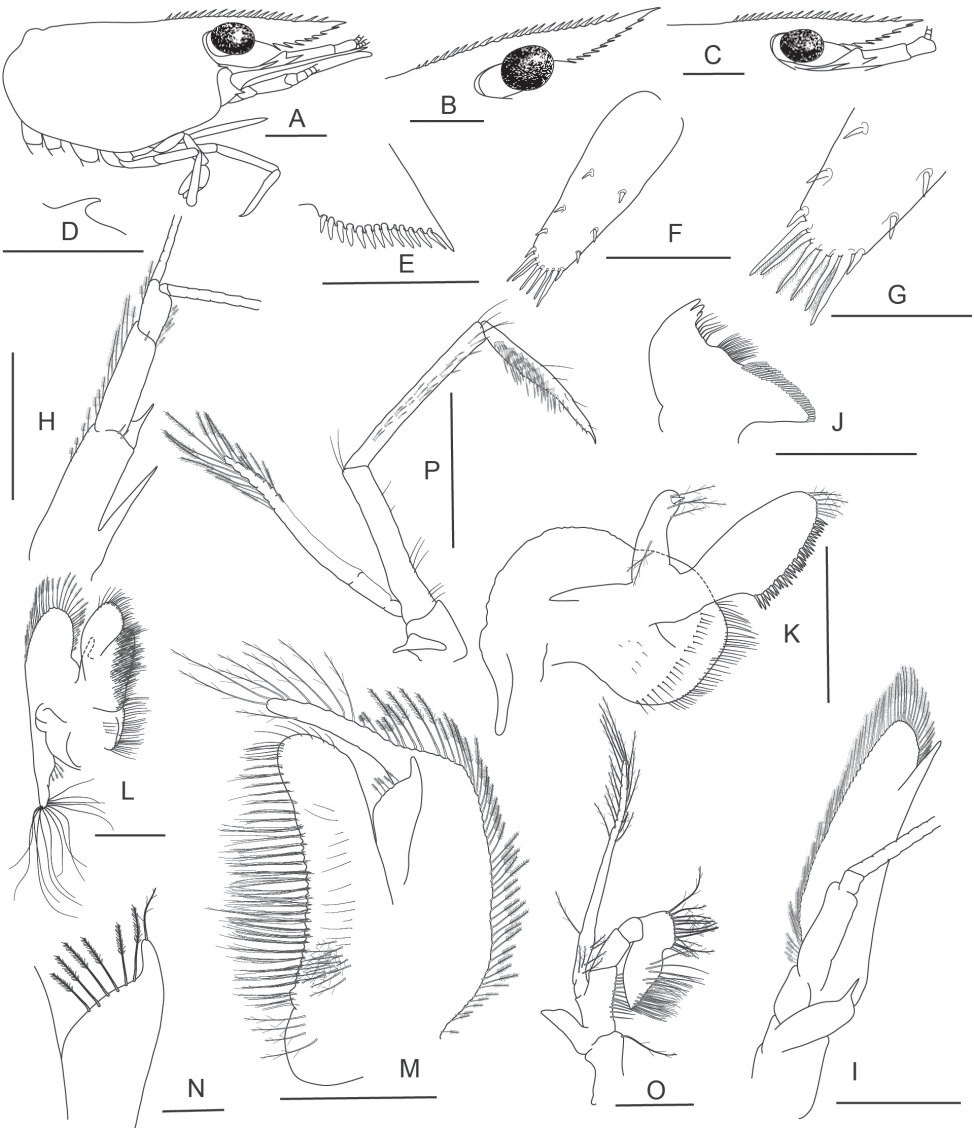

Figure 5. *Caridina fusca* sp. nov. Morphology 1. Paratype ov. ♀, cl. 2.7 mm, MZB Cru 5034 **A** cephalothorax and cephalic appendages **C** rostrum **D** preanal carina **E** uropodal diaeresis **F, G** telson **I** scaphocerite **J** distal part of mandible **K** maxillula **M** first maxilliped **N** Palp of first maxilliped **O** second maxilliped **P** third maxilliped; paratype ov. ♀, cl. 2.7 mm, MZB Cru 5032 **B** rostrum **H** antennular peduncle **L** maxilla. Scale bars: 1 mm (**A–C, F, H, I**); 0.5 mm (**D, E, G, J–M, O**); 0.1 mm (**N**).

times as long as wide, 1.21–1.32 (median 1.29, n = 5) times length of merus. Merus 2.32–3.43 (median 2.83, n = 5) times as long as wide, 0.85–0.96 (median 0.86, n = 4) times as long as ischium. Chela of second pereiopod 2.70–3.94 (median 3.31, n = 4) times as long as wide, 0.62–0.87 (median 0.74, n = 7) times length of carpus; tips of

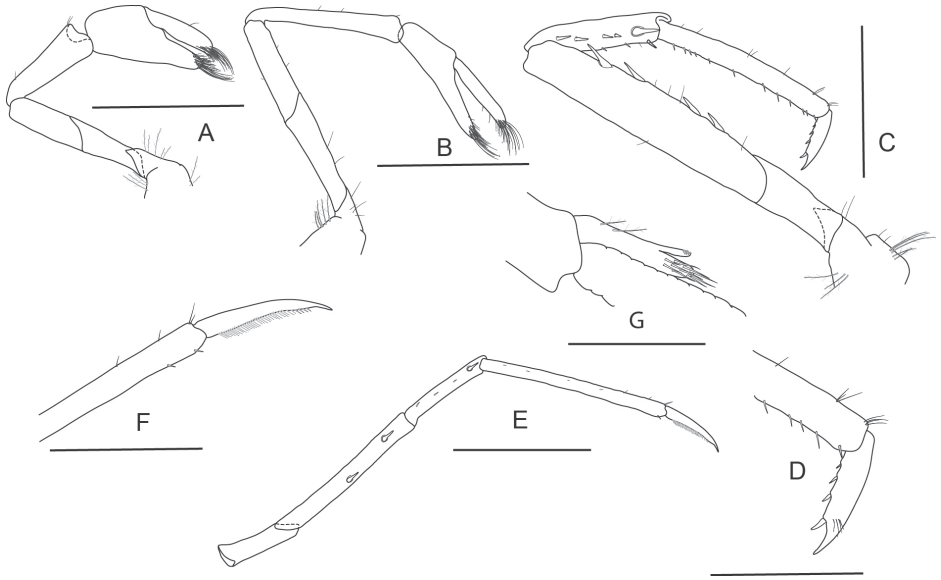

Figure 6. *Caridina fusca* sp. nov. Morphology 2. Paratype ov. ♀, cl. 2.7 mm, ZMB 30223 **A** first pereiopod **B** second pereiopod **C** third pereiopod **D** dactylus of third pereiopod; paratype ov. ♀, cl. 2.7 mm, ZMB 29518 **E** fifth pereiopod **F** dactylus of fifth pereiopod; paratype ♂, cl. 2.3 mm, MZB Cru 5032 **G** appendix masculina on male second pleopod. Scale bars: 1 mm (**A–C, E**); 0.5 mm (**D, F, G**).

fingers rounded, without hooks, with tufts of hairs near tip; dactylus 1.11–1.50 (median 1.21, n = 7) times as long as palm; carpus 4.89–7.17 (median 6.14, n = 7) times as long as wide, 1.33–1.51 (median 1.46, n = 7) times as long as merus; merus 4.00–6.40 (median 4.71, n = 7) times as long as wide, 0.82–1.06 (median 0.94, n = 4) times as long as ischium. Third pereiopod (Fig. 6C, D) not sexually dimorphic, dactylus 4.00–4.67 (median 4.13, n = 4) times as long as wide (terminal claw and spiniform setae on flexor margin included), terminating in one large claw with 3–6 stout spiniform setae on flexor margin; propodus slender, 8.40–12.00 (median 9.22, n = 4) times as long as wide, 2.63–3.24 (median 2.92, n = 4) times as long as dactylus; carpus bearing one strong and three or four small spiniform setae on posterior margin of outer surface, 4.63–5.13 (median 4.86, n = 3) times as long as wide, 0.73–0.81 (median 0.75, n = 4) times as long as propodus; merus slender, 5.84–6.70 (median 6.46, n = 3) times as long as wide, 1.97–2.05 (median 1.97, n = 4) times as long as carpus, bearing 3–5 strong spiniform setae on posterior margin of outer surface. Ischium with one spiniform seta. Fifth pereiopod (Fig. 6E, F) slender, dactylus 5.67 times as long as wide (terminal claw and serrate setae on flexor margin included), terminating in one large claw with 34–36 serrate setae on flexor margin; propodus slender, 10.89–15.43 (median 13.16, n = 2) times as long as wide, 3.18 times length of dactylus, carpus bearing one strong and three small spiniform setae on posterior margin of outer surface, 0.53 times as long as propodus; merus slender, 7.83 times as long as wide, 1.81 times length of carpus, bearing two strong spiniform setae on posterior margin of outer surface. Ischium without a strong spiniform seta.

***Pleopods*.** Appendix masculina (Fig. 6G) on male second pleopod stick-like, with long spiniform setae on inner and distal margin, few pappose setae on basal part, appendix interna reaching to ~ 0.8 of appendix masculina.

Colouration. Body dark reddish or brown with tiny light bluish dots, well-defined white transversal bands on the first, third, fifth, and sixth abdominal segments (Fig. 3H).

Reproductive biology and larval development. Ovigerous females with few eggs (35, n = 1). Size of eggs 0.77–0.81 × 0.44–0.49 mm (n = 3).

Etymology. The Latin word *fuscus* refers to the species' dark reddish or brown colouration (Fig. 3H).

Distribution. *Caridina fusca* sp. nov. is endemic to Lake Poso. Specimens were found at two localities within the lake, in a small bay south of the town of Tentena at the east shore and in a bay at the west shore.

Ecology. *Caridina fusca* sp. nov. is found under rocks in deep water (more than 5 m depth), while the morphologically similar species *C. sarasinorum* is usually found on various kinds of substrate like deposits of leaf litter, on wood or macrophytes (von Rintelen and Cai 2009).

Remarks. In life colouration, *C. fusca* sp. nov. might be confused with *C. sarasinorum*, also endemic to Lake Poso. In the latter, the transversal bands on the abdomen are less defined and scraggy compared to the sharply defined straight bands in *C. fusca* sp. nov. In preserved condition *C. fusca* sp. nov. can be differentiated from *C. sarasinorum* by the rostrum reaching to the end of the antennular peduncle, the dorsal and ventral margin armed throughout almost to the tip vs. reaching to the distal margin of the scaphocerite or beyond, unarmed in anterior one-third to half of the dorsal margin in *C. sarasinorum*. Epipods are reduced on the third maxilliped and absent on all pereiopods of *C. fusca* sp. nov. vs. well-developed on the third maxilliped and first pereiopod, absent on second to fifth pereiopods in *C. sarasinorum*. The chelae of the first pair of pereiopods are not inflated, 2.29–2.73 times as long as wide, 1.17–1.34 times as long as the carpus in *C. fusca* sp. nov. vs. slightly inflated, 1.74–2.10 times as long as wide, 1.35–1.48 times as long as the carpus in *C. sarasinorum*. The carpi of the first pair of pereiopods are more slender (2.33–4.00 times as long as wide) and hardly excavated distally vs. more stout (1.75–2.22 times as long as wide) and slightly excavated distally in *C. sarasinorum*.

Caridina lilianae Klotz, Wowor & K. von Rintelen, sp. nov.

http://zoobank.org/89F09DAB-32A3-4C99-82C7-5400C8C2632F
Figures 3C, 7, 8

Material examined. *Holotype*: ov. ♀ cl. 3.1 mm (MZB Cru 5035), Indonesia, Central Sulawesi, Lake Poso, E shore, S of Tentena, dredge in centre of bay, C. Lukhaup, T. von Rintelen, C. and F. Logemann leg., 17 Jun. 2011. **Paratypes:** 3 ov. ♀♀ cl. 2.8–2.9 mm (MZB Cru 5036), 2 ov. ♀♀ cl. 2.7 and 3.1 mm, 1 ♀ cl. 2.7 mm, 1 ♂ cl. 2.5 mm (ZMB 29807), same data as holotype; 3 ♀♀ cl. 1.7–2.6 mm, 4 ♂♂ cl. 1.9–2.2 mm (MZB Cru 5037), 1 ov. ♀ cl. 2.4 mm, 2 ♀♀ cl. 1.9 and 2.5 mm, 3 ♂♂

cl. 1.9–2.2 mm (ZMB 30197), Lake Poso, E shore, small bay within mouth of outlet, 1°46.30'S, 120°38.38'E, W. Klotz and T. von Rintelen leg., 12 May 2017; 1 ov. ♀ cl. 2.6 mm, 2 ♀♀ cl. 2.1 and 2,6 mm, 2 ♂♂ cl. 1.8 and 2.4 mm (MZB 5038), 2 ov. ♀♀ cl. 2.5 and 2.7 mm, 2 ♀♀ cl. 2.6 mm, 3 ♂♂ cl. 2.0–3.0 mm (ZMB 30713), Lake Poso, W shore, Bay N of Bancea, in 1.5–3 m depth, 1°58.91'S, 120°34.877'E, T. von Rintelen leg., 04 Aug. 2018; 1 ov. ♀ cl. 2.4 mm, 1 ♀ cl. 2.3 mm (ZMB 30755), 2 ♀♀ cl. 2.1 and 2.3 mm, 1 ♂ cl. 1.9 mm (MZB Cru 5091) Lake Poso: E shore, small bay within mouth of outlet, 1°46.30'S, 120°38.38'E, T. von Rintelen leg., 14 Jul 2019.

Description. ***Cephalothorax and cephalic appendages.*** Postorbital carapace length 1.7–3.1 mm (n = 33). Rostrum (Fig. 7A, B) very short, not overreaching distal margin of eyes, clearly convex on dorsal margin, abruptly tapering to a fine tip distally, 0.18–0.33 (median 0.26, n = 20) times as long as carapace, rostral formula 5–10 + 5–10 / 0. Antennal spine well separated from inferior orbital angle. Pterygostomial angle subrectangular. Eyes well developed with globular cornea. Antennular peduncle (Fig. 7A, G), 0.70–0.79 (median 0.75, n = 6) times as long as carapace in females, 0.92 (n = 1) times as long as carapace in male, first segment 2.08–2.70 (median 2.42, n = 7) times as long as second segment, second segment 1.67–2.75 (median 2.50, n = 7) times longer than third segment. Stylocerite reaching to 0.68–0.89 (median 0.77, n = 6) of first segment of antennular peduncle. Scaphocerite (Fig. 7H) 3.43–4.62 (median 4.02) times as long as wide.

Abdominal somites, telson and uropods. Sixth abdominal somite 0.68–0.88 (median 0.77, n = 6) times carapace length, 1.78–2.26 (median 2.00, n = 6) times as long as fifth somite, 1.08–1.29 (median 1.22, n = 6) times as long as telson. Telson (Fig. 7E, F) with distal margin rounded or convex without a median projection, with 2–4 pairs of short spiniform setae dorsally and one pair of short spiniform setae dorsolaterally; distal end with 4–8 long spiniform setae, lateral pair shorter than others. Preanal carina (Fig. 7C) with a distinct hook-like spine. Uropodal diaeresis (Fig. 7D) with seven or eight stout movable spiniform setae, outermost ones shorter than lateral angle.

Mouthparts and branchiae. Incisor process of mandible (Fig. 7I) ending in irregular teeth, molar process truncated. Lower lacinia of maxillula (Fig. 7J) ovate, upper lacinia elongate, with numerous distinct teeth on inner margin, palp slender with few pappose setae and one conical spiniform seta near tip. Upper endites of maxilla (Fig. 7K) subdivided, palp slender, scaphognathite tapering posteriorly, fringed with long, curved setae at posterior margin. Palp of first maxilliped (Fig. 7L, M) ending in blunt triangular shape. Podobranch on second maxilliped (Fig. 8A) reduced to a lamina. Third maxilliped (Fig. 8B) with one well developed and one strongly reduced arthrobranch, ultimate segment slightly shorter than penultimate segment. First pereiopod with an arthrobranch. Pleurobranchs present on all pereiopods. Epipod reduced (without distal hook) on third maxilliped, absent from all pereiopods (a vestigial epipod was seen in one of the specimens examined (Fig. 8C)).

Pereiopods. Chelae of first and second pereiopods (Fig. 8C–F) rather less developed and conspicuous small; chela of first pereiopod 3.43–4.62 (median 4.02, n = 2) times as long as wide, 0.94–0.96 (median 0.95, n = 2) times length of carpus; tips of

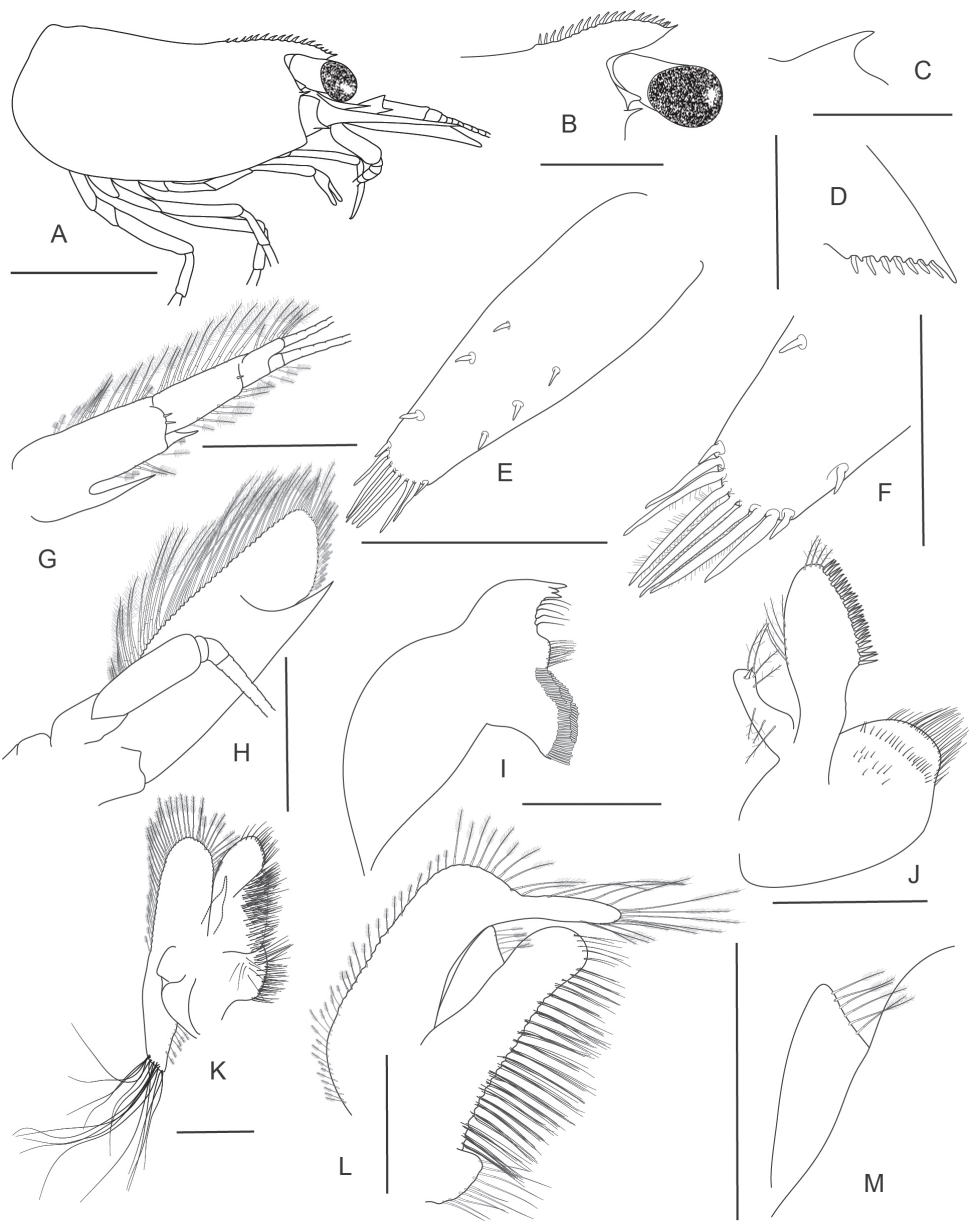

Figure 7. *Caridina lilianae* sp. nov. Morphology 1. Paratype ov. ♀, cl. 3.1 mm, ZMB 29807 **A** cephalothorax and cephalic appendages **C** preanal carina **D** uropodal diaeresis **G** antennular peduncle **H** scaphocerite **I** mandible **K** maxilla **L** first maxilliped **M** Palp of first maxilliped; paratype ♂, cl. 2.2 mm, ZMB 30197 **B** rostrum **E, F** telson **J** maxillula. Scale bars: 2 mm (**A**); 1 mm (**B, E**); 0.5 mm (**C, D, F, M**).

fingers rounded, without hooks, with scarce hairs near tip; dactylus 1.50–1.58 (median 1.54, n = 2) times as long as palm; carpus slender, hardly excavated distally, 4.55–5.33 (median 4.94, n = 2) times as long as wide, 1.32–1.33 (median 1.32, n = 2) times length

of merus. Merus 3.80–4.00 (median 3.90, n = 2) times as long as wide, as long as ischium, with few stiff simple setae. Chela of second pereiopod 4.31–4.92 (median 4.62, n = 2) times as long as wide, 0.80–0.90 (median 0.85, n = 2) times length of carpus; tips of fingers rounded, without hooks, with scarce hairs near tip; dactylus 1.67–1.80 (median 1.73, n = 2) times as long as palm; carpus 6.20–8.00 (median 7.10, n = 2) times as long as wide, 1.35–1.48 (median 1.41, n = 2) times as long as merus; merus 4.60–4.91 (median 4.75, n = 2) times as long as wide, as long as ischium, merus and ischium with long simple setae. Third pereiopod (Fig. 8G, H) slender, not sexually dimorphic, dactylus very slender 8.00–10.80 (median 9.40, n = 2) times as long as wide (terminal claw included), terminating in one large claw, without spiniform setae on flexor margin; propodus 7.25–7.56 (median 7.40, n = 2) times as long as wide, 1.26–1.45 (median 1.35, n = 2) times as long as dactylus; carpus 4.22–4.55 (median 4.38, n = 2) times as long as wide, 0.66–0.74 (median 0.70, n = 2) times as long as propodus; merus 6.33–7.43 (median 6.88, n = 2) times as long as wide, 1.31–1.53 (median 1.42, n = 2) times as long as carpus, bearing two strong spiniform setae on posterior margin of outer surface and long stiff simply setae along the entire segment. Ischium without spiniform seta but with long stiff simply setae similar to the setae on merus. Fifth pereiopod (Fig. 8I, J) slender, dactylus 10.00 times as long as wide (terminal claw and serrate setae on flexor margin included), terminating in one large claw with ~ 19 serrate setae on proximal half of flexor margin; propodus 8.00 times as long as wide, 1.33 times length of dactylus, carpus 4.17 times as long as wide, 0.63 times as long as propodus; merus 6.57 times as long as wide, 1.84 times length of carpus, bearing one strong spiniform seta on posterior margin of outer surface and long stiff simply setae along the entire segment. Ischium without spiniform seta but with long stiff simply setae similar to the setae on merus.

Pleopods. Endopod of male first pleopod (Fig. 8K) subtriangular, without appendix interna, 2.00–2.22 (n = 2) times as long as proximal width. Appendix masculina on male second pleopod (Fig. 8L) slender, 7.60–10.33 (n = 2) times as long as wide, with long spiniform setae on inner and distal margin, few pappose setae on basal part, appendix interna reaching to distal margin of appendix masculina or slightly overreaching it.

Colouration. Body colouration transparent to whitish with minute sand-coloured dots (Fig. 3C).

Reproductive biology and larval development. Ovigerous females with few eggs (35, n = 1). Size of undeveloped eggs (early stage embryos without eyespot) 0.61–0.72 × 0.37–0.39 mm, size of developed eggs (late stage embryos with eyes) 0.70–0.76 × 0.39–0.44 mm (n = 6).

Etymology. Named after the second and last authors' first daughter who is very interested in field work and helped to observe and document this species while visiting the lake in 2019.

Distribution. *Caridina lilianae* sp. nov. is endemic to Lake Poso. Specimens were found at three localities within the lake, two within a bay south of the town of Tentena at the east shore and one in a bay at the west shore.

Ecology. *Caridina lilianae* sp. nov. lives on very fine sand or silt (soft substrate) in shallow water (1.5–2.5m).

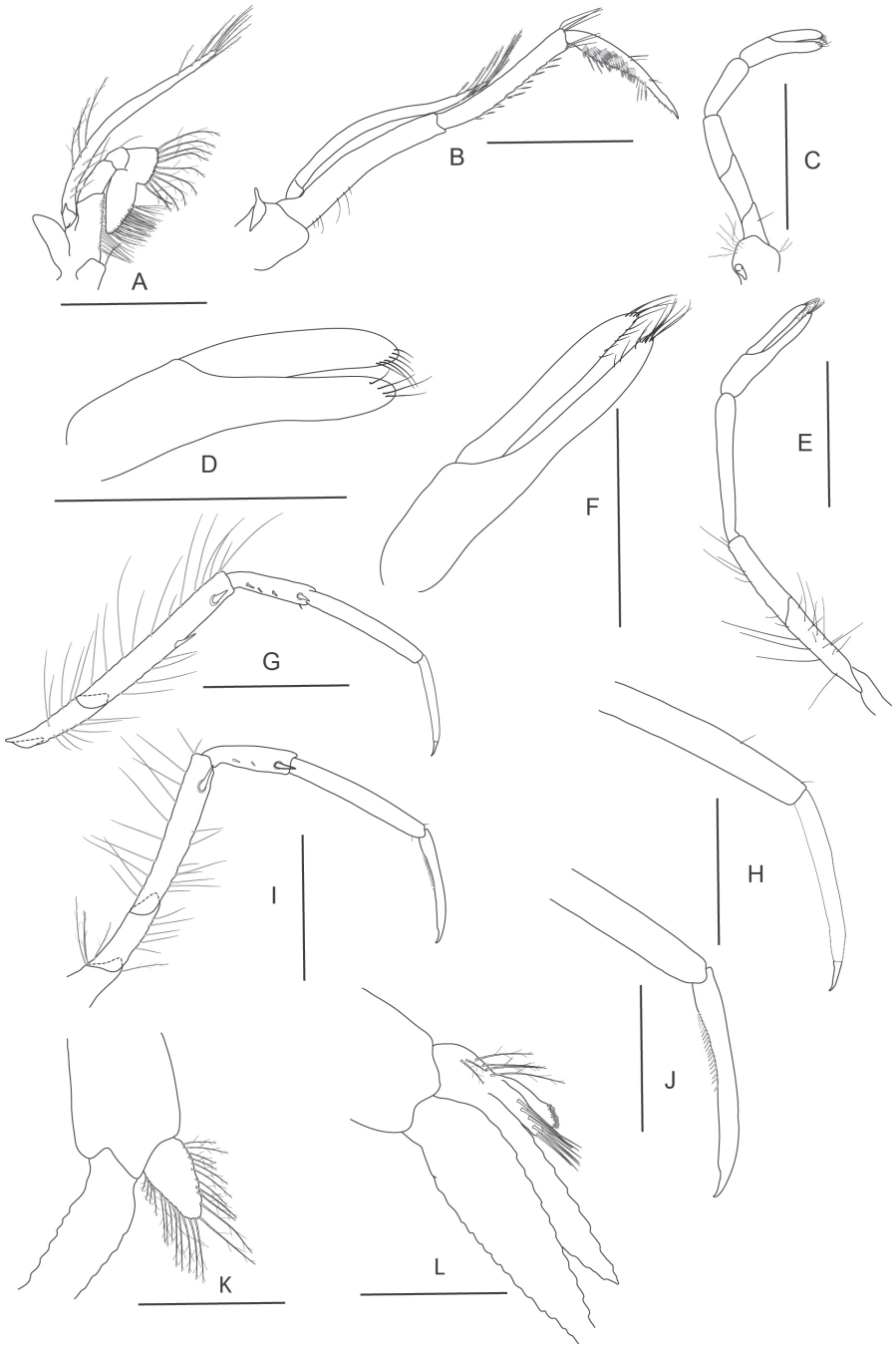

Figure 8. *Caridina lilianae* sp. nov. Morphology 2. Paratype ov. ♀, cl. 3.1 mm, ZMB 29807 **A** second maxilliped **B** third maxilliped **C** first pereiopod **D** chela of first pereiopod **E** second pereiopod **F** chela of second pereiopod **G** third pereiopod **H** dactylus of third pereiopod **I** fifth pereiopod **J** dactylus of fifth pereiopod; paratype ♂, cl. 2.2 mm, ZMB 30197 **K** endopod of male first pleopod **L** appendix masculina on male second pleopod. Scale bars: 1 mm (**A–C, E, G, I**); 0.5 mm (**D, F, H, J–L**).

Remarks. With its small size and the less developed chelae with scarce setae at the tip of the fingers, *C. lilianae* sp. nov. is similar to *C. mayamareenae* sp. nov. but can easily be distinguished from this species by the very short, convex rostrum (vs. rostrum conspicuous high, reaching to end of second segment of antennular peduncle or slightly overreaching this segment) and the slender third pair of pereiopods bearing long stiff setae on merus and ischium but without any spiniform setae on flexor margin (vs. third pereiopod very robust, without long simple setae on merus and ischium and dactylus with five or six spiniform setae on flexor margin). These characters also distinguish *C. lilianae* sp. nov. from all other *Caridina* spp. known from the Lake Poso. Although *C. lilianae* sp. nov. and *C. mayamareenae* sp. nov. occur in sympatry in the lake, the microhabitats of these species are quite different. *Caridina mayamareenae* sp. nov. lives in empty shells of aquatic snails while *C. lilianae* sp. nov. on soft substrate. The long stiff simple setae attached to the posterior segments of the chelipeds and pereiopods could be interpreted as a morphological adaption to this kind of habitat by preventing them to subside into the soft substrate. This hypothesis would need to be tested, though. In the field, the whitish or cream-coloured body colouration is indiscernible on light-coloured sandy habitats (Fig. 3D).

***Caridina marlenae* Klotz, Wowor & K. von Rintelen, sp. nov.**
http://zoobank.org/801EC24A-93F5-48EF-9394-AF0930D50E36
Figures 3G, 9, 10

Material examined. *Holotype*: ♀ cl. 2.8 mm (MZB Cru 5039), Indonesia, Central Sulawesi, Lake Poso, E shore, S of Tentena, dive at small cape, 15 m, 1°46.394'S, 120°38.327'E, T. von Rintelen and W. Klotz leg., 12 May 2017. ***Paratypes*:** 4 ♀♀ cl. 1.4–2.1 mm, 1 ♂ cl. 1.6 mm (MZB Cru 5040), 1 ♀ cl. 2.3 mm, 3 ♂♂ cl. 2.0–2.2 mm (ZMB 30199), same data as holotype; 2 ov. ♀♀ cl. 2.7 and 2.8 mm, 2 ♂♂ cl. 2.5 and 2.8 mm (MZB Cru 5041), 2 ♀♀ cl. 2.6 and 3.1 mm, 1 ♂ cl. 2.4 mm, 2 sequenced specimens without anterior pleopods cl. 2.2 and 2.9 mm (ZMB 29519), Lake Poso, E shore, S of Tentena, dive at small cape, in 15 m depth, 1°46.394'S, 120°38.327'E, M. Glaubrecht and T. von Rintelen leg., 16 May 2007; 2 ♀♀ cl. 2.1 and 2.5 mm, 1 ♂ cl. 2.0 mm, 2 juv. specimens (MZB Cru 5092), 2 ♀♀ cl. 1.9 and 2.2 mm, 1 ♂ cl. 1.8 mm, 1 juv. specimen (ZMB 31661), Lake Poso, E shore, S of Tentena, dive at small cape, in 15 m depth, 1°46.394'S, 120°38.327'E, T. von Rintelen leg., 14 Jul 2019.

Comparative material examined. *Caridina sarasinorum* Schenkel, 1902, 1 ov. ♀ cl. 3.0 mm, 1 ♂ cl. 2.6 mm (ZMB 29288), Lake Poso, E shore, 2°0.825'S, 120°42.007'E, K. Zitzler leg., 16 Aug. 2004; 2 ov. ♀♀ cl. 3.2 and 3.6 mm, 1 ♀ cl. 3.mm, 5 ♂♂ cl. 2.1–2.6 mm, 2 juv. specimens cl. 1.7 mm, 1 damaged specimen cl. 2.0 mm (ZMB 30224), Lake Poso, E shore, beach in front of Dolidi Ndano Cottages, 1°48.14'S, 120°38.043'E, W. Klotz leg., 12 May 2017.

Description. Cephalothorax and cephalic appendages. Postorbital carapace length 1.44–3.07 mm (n = 19). Rostrum (Fig. 9A, B) long and slender, curved upwards or sigmoid, reaching slightly beyond end of scaphocerite or in small specimen,

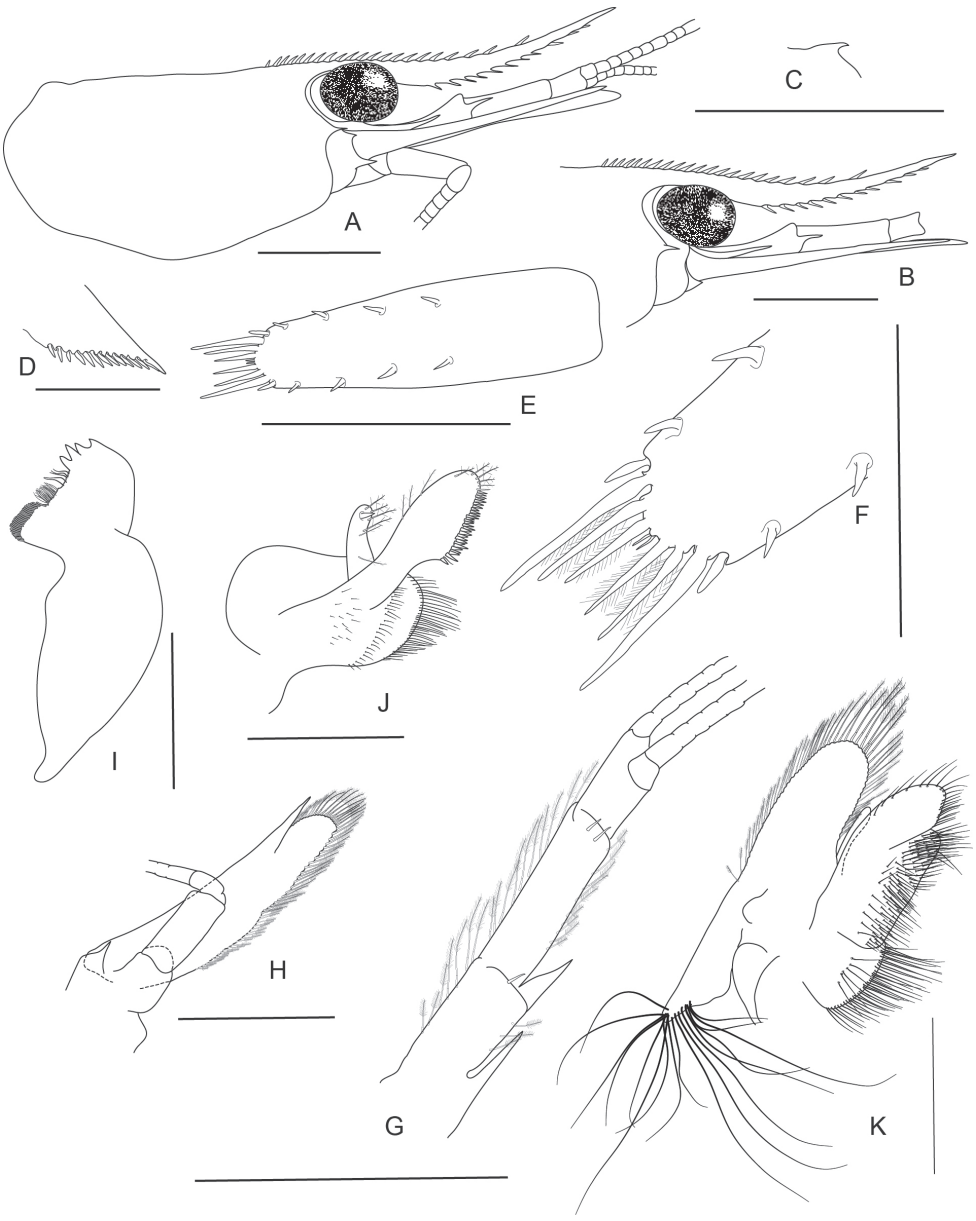

Figure 9. *Caridina marlenae* sp. nov. Morphology 1. Paratype ♂, cl. 2.2 mm, ZMB 30199 **A** cephalothorax and cephalic appendages **B** rostrum **C** preanal carina **D** uropodal diaeresis **E, F** telson **G** antennular peduncle **H** scaphocerite **I** mandible **K** maxilla; paratype ♀, cl. 2.3 mm, ZMB 30199 **J** maxillula. Scale bars: 1 mm (**A–E**); 0.5 mm (**F–K**).

to end of the antennular peduncle, distal 0.16–0.40 (median 0.38, n = 11) of dorsal margin unarmed, ventral margin armed throughout, dorsal teeth more widely spaced distally, 0.95–1.54 (median 1.20, n = 14) times as long as carapace, rostral formula 3–6 (4–6) + 10–20 / 6–18. Antennal spine slightly separated from orbital margin. Ptery-

gostomial angle broadly rounded. Eyes well developed with globular cornea. Antennular peduncle (Fig. 9A, B, G), 0.89–1.04 (median 0.96, n = 5) times as long as carapace, first segment 1.56–1.79 (median 1.71, n = 4) times as long as second segment, second segment 2.40–2.80 (median 2.58, n = 4) times longer than third segment. Tooth on distolateral margin of first segment of antennular peduncle acute. Stylocerite reaching to 0.78–0.83 (median 0.80, n = 4) of first segment of antennular peduncle. Scaphocerite (Fig. 9H) 4.10–4.25 (median 4.20, n = 3) times as long as wide.

Abdominal somites, telson and uropods. Sixth abdominal somite 0.55–0.64 (median 0.62, n = 5) times carapace length, 1.93–2.23 (median 2.15, n = 5) times as long as fifth somite, 1.00–1.13 (median 1.12, n = 4) times as long as telson. Distal margin of telson (Fig. 9E, F) convex or subtriangular without a median projection, with 3–5 pairs of short spiniform setae dorsally and one pair of short spiniform setae dorsolaterally; distal end with 7–10 long spiniform setae, lateral pair slightly longer than others, innermost pair very tiny. Preanal carina (Fig. 9C) with a hook-like spine. Uropodal diaeresis (Fig. 9D) with 11–14 stout movable spiniform setae, outermost ones shorter than lateral angle.

Mouthparts and branchiae. Incisor process of mandible (Fig. 9I) ending in irregular teeth, molar process truncated. Lower lacinia of maxillula (Fig. 9J) broadly rounded, upper lacinia elongate, with numerous distinct teeth on inner margin, palp slender with few pappose setae and one conical spiniform seta near tip. Upper endites of maxilla (Fig. 9K) subdivided, palp slender, scaphognathite tapering posteriorly, fringed with long, curved setae at posterior margin. Palp of first maxilliped (Fig. 10A, B) ending in triangular shape. Podobranch on second maxilliped (Fig. 10C) reduced to a lamina. Third maxilliped (Fig. 10D) with one well developed and one small arthrobranch, ultimate segment of maxilliped shorter than penultimate segment. First pereiopod with an arthrobranch. Pleurobranchs present on all pereiopods. Epipod slightly reduced (without distal hook) on third maxilliped, absent from all pereiopods.

Pereiopods. Chelae of first and second pereiopod (Fig. 10E, F) well developed; chela of first pereiopod 3.00–3.83 (median 3.20, n = 5) times as long as wide, 1.00–1.05 (median 1.03, n = 5) times length of carpus; tips of fingers (Fig. 10E) rounded, without hooks, with tufts of hairs near tip; dactylus 1.88–2.50 (median 2.00, n = 5) times as long as palm; carpus slender, hardly excavated distally, 3.85–4.77 (median 4.00, n = 5) times as long as wide, 1.25–1.33 (median 1.29, n = 5) times length of merus. Merus 3.80–4.25 (median 4.00, n = 5) times as long as wide, 0.89–0.95 (median 0.92, n = 4) times as long as ischium. Chela of second pereiopod 3.69–4.38 (median 3.71, n = 5) times as long as wide, 0.68–0.79 (median 0.71, n = 6) times length of carpus; tips of fingers rounded, without hooks, with tufts of hairs near tip; dactylus 1.80–2.25 (median 2.00, n = 5) times as long as palm; carpus 6.78–9.80 (median 7.60, n = 5) times as long as wide, 1.27–1.58 (median 1.47, n = 4) times as long as merus; merus 5.33–6.50 (median 6.00, n = 4) times as long as wide, 0.82–0.93 (median 0.86, n = 4) times as long as ischium. Third pereiopod (Fig. 10G, H) not sexually dimorphic, dactylus 4.40–5.33 (median 4.50, n = 5) times as long as wide (terminal claw and spiniform setae on flexor margin included), terminating in one large claw with four or five short spiniform setae on flexor margin; propodus slender, 13.67–16.25 (median 14.57, n = 5) times as long as wide, 3.56–4.06 (median 3.78, n = 5) times as

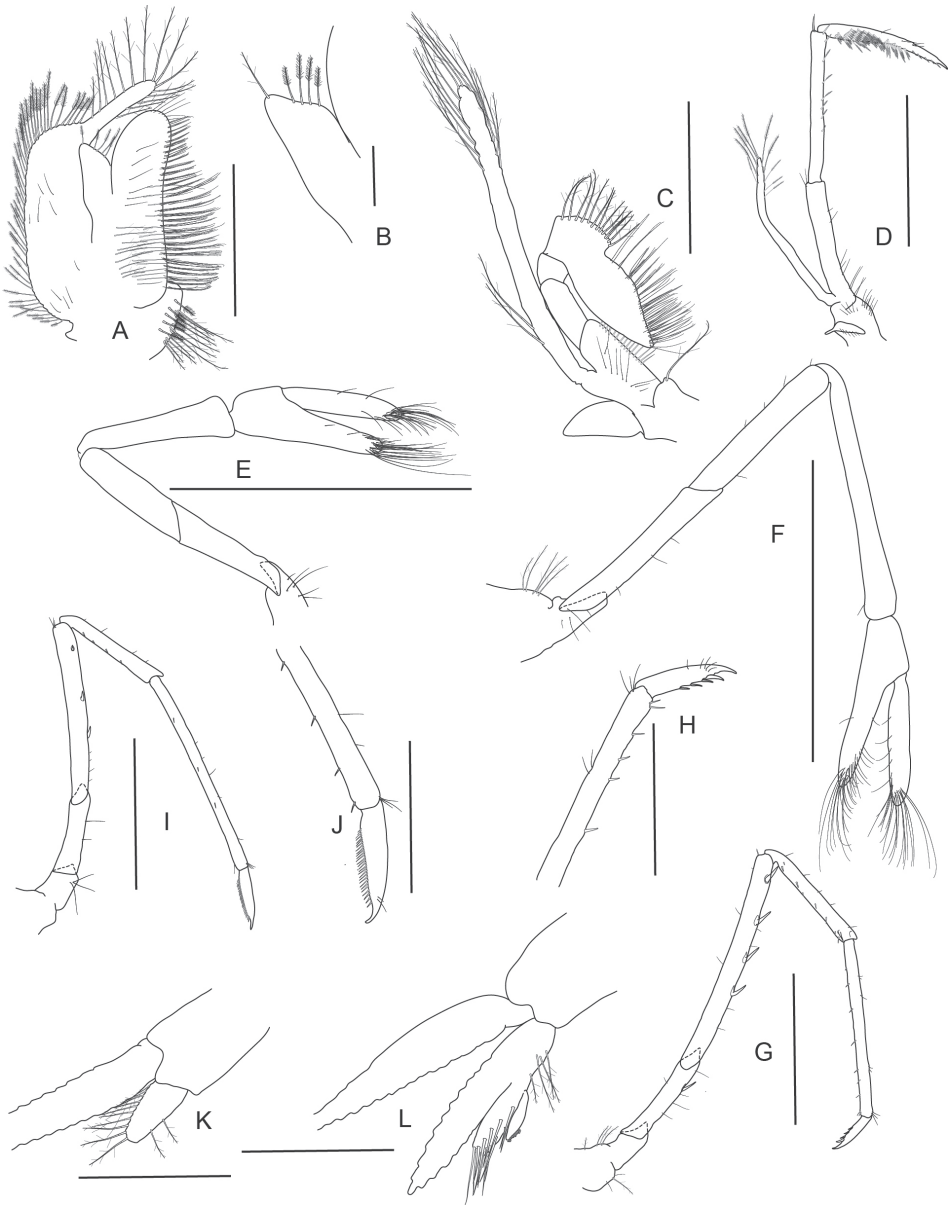

Figure 10. *Caridina marlenae* sp. nov. Morphology 2. Paratype ♂, cl. 2.2 mm, ZMB 30199 **A** first maxilliped **B** palp of first maxilliped **C** second maxilliped **D** third maxilliped **E** first pereiopod **F** second pereiopod **I** fifth pereiopod **K** endopod of male first pleopod **L** appendix masculina on male second pleopod; paratype ♀, cl. 2.3 mm, ZMB 30199 **G** third pereiopod **H** dactylus of third pereiopod **J** dactylus of fifth pereiopod. Scale bars: 0.5 mm (**A, C, H, J–L**); 0.1 mm (**B**); 1 mm (**D–G, I**).

long as dactylus; carpus bearing one strong and 6 small short spiniform setae on posterior margin of outer surface, 7.50–8.36 (median 8.00, n = 5) times as long as wide, 0.63–0.75 (median 0.68, n = 5) times as long as propodus; merus slender, 10.36–12.62

(median 11.60, n = 5) times as long as wide, 1.68–1.93 (median 1.78, n = 5) times as long as carpus, bearing 3–5 strong spiniform setae on posterior margin of outer surface. Ischium with one spiniform seta. Fifth pereiopod (Fig. 10I, J) slender, dactylus 3.50–4.86 (median 4.13, n = 4) times as long as wide (terminal claw and serrate setae on flexor margin included), terminating in one large claw with 24–31 serrate setae on flexor margin; propodus slender, 13.43–16.00 (median 14.00, n = 4) times as long as wide, 3.29–3.50 (median 3.33, n = 4) times length of dactylus, carpus bearing one strong and 5–7 small spiniform setae on posterior margin of outer surface, 7.57–9.00 (median 7.88, n = 4) times as long as wide, 0.55–0.64 (median 0.57, n = 4) times as long as propodus, 0.63–0.70 (median 0.66, n = 4) times as long as merus; merus slender, 9.20–10.67 (median 10.55, n = 4) times as long as wide, 1.44–1.53 (median 1.51, n = 4) times length of carpus, bearing three or four strong spiniform setae on posterior margin of outer surface. Ischium without a strong spiniform seta.

Pleopods. Endopod of male first pleopod (Fig. 10K) subtriangular, without an appendix interna, two pappose setae on outer, ~ eight on inner margin, 1.91–2.57 (median 2.00, n = 3) times as long as proximal width, 0.29–0.41 (median 0.29, n = 3) times as long as exopod. Appendix masculina on male second pleopod (Fig. 10L) rod-shaped, 6.00–8.40 (median 6.00, n = 3) times as long as wide, with long spiniform setae on inner and distal margin, few pappose setae on basal part, appendix interna reaching to ~ 0.72–0.80 (median 0.80, n = 3) of appendix masculina.

Colouration. Body colouration bright reddish with large white dots (Fig. 3G).

Reproductive biology and larval development. Ovigerous females with few eggs (9, n = 1). Size of eggs 0.81–0.83 × 0.48–0.0.51 mm (n = 2).

Etymology. Named after the second and last authors' second daughter who is very interested in field work and helped to observe and document this species while visiting the lake in 2019.

Distribution. *Caridina marlenae* sp. nov. is endemic to Lake Poso. Specimens were found only at one locality in a bay south of the town of Tentena at the east shore of the lake.

Ecology. *Caridina marlenae* sp. nov. is found under rocks in deep water (more than 5 m).

Remarks. With its long rostrum, approximately anterior 0.4 unarmed, *C. marlenae* sp. nov. is similar to *C. sarasinorum*, *C. schenkeli* and *C. longidigita*, all endemic to Lake Poso. In the field, body colouration alone is sufficient to differ *C. marlenae* sp. nov. from *C. sarasinorum* or *C. schenkeli* but it might be confused with reddish specimens of *C. longidigita*. *Caridina marlenae* sp. nov. is showing large bright white dots on reddish colouration of the entire body. In *C. sarasinorum*, the body is coloured dark brown with faint light transversal bands on first, third, fifth and sixth abdominal segments (W. Klotz, pers. observation on the comparative material listed above). In *C. schenkeli* the colouration of the body is mostly transparent with some brownish or whitish blotches.

In preserved condition, *C. marlenae* sp. nov. can be distinguished from *C. sarasinorum* by the more reduced epipods (slightly reduced on the third maxilliped, absent from all pereiopods vs. well developed (with distal hooks) on the third maxilliped and first pereiopod in *C. sarasinorum* and the slender chelipeds and pereiopods (in detail: chela

of first pereiopod 3.00–3.83 times as long as wide vs. 1.74–2.1 times in *C. sarasinorum*, 1.00–1.05 times as long as carpus vs. 1.35–1.48 times in *C. sarasinorum*, dactylus 1.88–2.50 times as long as palm vs. 0.83–1.05 times as long in *C. sarasinorum*, carpus 3.85–4.77 times as long as wide vs. 1.75–2.22 times in *C. sarasinorum*, merus 3.80–4.25 times as long as wide vs. 1.78–2.63 times in *C. sarasinorum*. Chela of second pereiopod 3.69–4.38 times as long as wide vs. 2.19–2.64 times in *C. sarasinorum*, dactylus 1.80–2.25 times as long as palm vs. 1.05–1.33 times as long in *C. sarasinorum*, carpus 6.78–9.80 times as long as wide vs. 4.56–5.05 times in *C. sarasinorum*, merus 5.33–6.50 times as long as wide vs. 3.60–4.29 times in *C. sarasinorum*. Dactylus of third pereiopod 4.40–5.33 times as long as wide vs. 4.0–4.20 in *C. sarasinorum*, propodus 13.67–16.25 times as long as wide vs. 10.00–11.11 in *C. sarasinorum*, 3.56–4.06 times as long as dactylus vs. 2.86–3.13 times as long as dactylus in *C. sarasinorum*. Propodus of fifth pereiopod 13.43–16.00 times as long as wide vs. 10.00–12.00 in *C. sarasinorum*).

Caridina marlenae sp. nov. can be distinguished from *C. schenkeli* by the more reduced epipods (slightly reduced on the third maxilliped, absent from all pereiopods vs. well developed (with distal hooks) on the third maxilliped and first and second pereiopod in *C. schenkeli* and the slender chelipeds and armature of the dactyli of pereiopods (in detail: chela of first pereiopod 3.00–3.83 times as long as wide vs. 1.90–3.2 times in *C. schenkeli*, dactylus 1.88–2.50 times as long as palm vs. 1.0–1.4 times as long in *C. schenkeli.* Carpus of first cheliped 3.85–4.77 times as long as wide vs. 2.1–3.2 times as long as wide in *C. schenkeli*. Dactylus of second pereiopod 1.80–2.25 times as long as palm vs. 1.2–1.4 times as long in *C. schenkeli*, carpus 6.78–9.80 times as long as wide vs. 4.5–6.5 times in *C. schenkeli.* Dactylus of third pereiopod with four or five spiniform setae on flexor margin vs. with 6–8 spiniform setae in *C. schenkeli*. Dactylus of fifth pereiopod with 24–31 serrate setae on flexor margin vs. with 57–64 in *C. schenkeli*.

Caridina marlenae sp. nov. can also be distinguished from *C. longidigita* by the type of chelae built for scraping vs. for filter-feeding in *C. longidigita* (brushes of setae short on tips of fingers of chelipeds vs. setae long, chela of first cheliped 3.00–3.83 times as long as wide vs. 4.6–6.5 times as long as wide in *C. longidigita*, dactylus 1.88–2.50 times as long as palm vs. 3.6–4.6 times as long in *C. longidigita*, carpus 3.85–4.77 times as long as wide vs. 4.8–8.1 times in *C. longidigita*; chela of second pereiopod 3.69–4.38 times as long as wide vs. 4.8–6.4 times in *C. longidigita*, dactylus 1.80–2.25 times as long as palm vs. 3.4–3.9 times as long in *C. longidigita*).

Caridina mayamareenae Klotz, Wowor & K. von Rintelen, sp. nov.

http://zoobank.org/038EA514-2161-42BF-8F93-6F8CF696B917
Figures 2E, 3A–B, 11–12

Material examined. ***Holotype*:** ov. ♀ cl. 3.0 mm (MZB Cru 5042), Indonesia, Central Sulawesi, Lake Poso, E shore, S of Tentena, dive at small cape, 15 m, 1°46.394'S, 120°38.327'E, J. Pfaender and T. von Rintelen leg., 21 Sep. 2015. ***Paratypes*:** 2 ov. ♀♀ cl. 2.6 and 2.8 mm, 4 ♀♀ cl. 2.3–3.4 mm, 3 ♂♂ cl. 1.7–2.5 mm, 1 juv. cl. 1.5

mm (MZB Cru 5043), same data as holotype; 2 ♂♂ cl. 2.5 and 2.7 mm, 1 ov. ♀ cl. 2.8 mm, 1 incomplete ♀ cl. 2.7 mm (ZMB 29627), Lake Poso, E shore, S of Tentena, dredge in centre of bay, T. von Rintelen, C. Lukhaup and F. Logemann leg., 17 Jun. 2011; 1 ♀ cl. 2.7 mm (MZB Cru 5044), Lake Poso, E shore, "Sulawesi Rock", 1°56.102'S, 120°40.402'E, J. Pfaender and T. von Rintelen leg., 22 Sep. 2015; 4 ♂♂ cl. 2.0–2.3 mm, 1 ov. ♀ cl. 2.9 mm (ZMB 29620), Lake Poso, E shore, beach in front of Dolidi Ndano Cottages, 1°48.14'S, 120°38.043'E, J. Pfaender and T. von Rintelen leg., 22 Sep. 2015; 30 ♂♂ cl. 1.5–2.7 mm, 5 ♀♀ cl. 1.6–2.9 mm, 4 ov. ♀♀ cl. 2.7–3.0 mm, 4 juv. cl. 1.4–1.7 mm (ZMB 30202), 34 ♂♂ cl. 1.5–2.6 mm, 6 ♀♀ cl. 2.0–3.0 mm, 2 ov. ♀♀ cl. 2.5 and 3.1 mm, 7 juv. cl. 1.3–1.6 mm (MZB Cru 5045), Lake Poso, E shore, beach in front of Dolidi Ndano Cottages, dive to 15 m, 1°48.14'S, 120°38.043'E, T. von Rintelen leg., 09 May 2017; 4 ov. ♀♀ cl. 2.8–2.9 mm, 8 ♀♀ cl. 1.8–2.8 mm, 6 ♂♂ cl. 3.6–3.8 mm (ZMB 30709), 4 ov. ♀♀ cl. 2.7–3.0 mm, 5 ♂♂ cl. 1.8–2.2 mm, 8 ♀♀ cl. 1.3–2.3 mm (MZB Cru 5046), Lake Poso, NW shore, westernmost cape, 15 m depth, 1°47.39'S, 120°32.641'E, T. von Rintelen leg., 03 Aug. 2018; 5 ov. ♀♀ cl. 2.8–3.0 mm, 4 ♀♀ cl. 1.5–2.8 mm, 6 ♂♂ cl. 1.9–2.1 mm (ZMB 30710), 5 ov. ♀♀ cl. 2.6–2.7 mm, 3 ♀♀ cl. 1.5–2.7 mm, 7 ♂♂ cl. 1.5–2.0 mm (MZB Cru 5047), Lake Poso, NW shore, westernmost cape, 10 m depth, 1°47.39'S, 120°32.641'E, T. von Rintelen leg., 03 Aug. 2018; 2 ov. ♀♀ cl. 2.6 and 2.7 mm, 5 ♀♀ cl. 2.0–2.6 mm, 5 ♂♂ cl. 1.5–1.8 mm (ZMB 30711), 1 ov. ♀ cl. 2.6 mm, 5 ♀♀ cl. 1.6–2.2 mm, 5 ♂♂ cl. 1.5–2.5 mm (MZB Cru 5048), Lake Poso, W shore, S corner of Siuri bay, 13–14 m depth, 1°48.35'S, 120°31.703'E, T. von Rintelen leg., 03 Aug. 2018; 3 ov. ♀♀ cl. 2.5–2.7 mm, 4 ♀♀ cl. 1.8–3.0 mm (ZMB 30714), 4 ov. ♀♀ cl. 2.2–3.0 mm, 1 ♀ cl. 3.4 mm, 1 carapace sex unknown cl. 2.7 mm (MZB Cru 5049), Lake Poso, W shore, Bay N of Bancea, 15 m depth, 1°58.91'S, 120°34.877'E, T. von Rintelen leg., 04 Aug. 2018. 1 ov. ♀ cl. 2.7 mm (MZB Cru 5093), Lake Poso, E shore, small bay within mouth of outlet, 1°46.30'S, 120°38.38'E, T. von Rintelen leg., 14 Jul 2019. 1 ♀ cl. 2.5 mm (ZMB 30388), 1 ♂ cl. 1.8 mm (MZB Cru 5097), Lake Poso, E shore, "Sulawesi Rock", 1°56.102'S, 120°40.402'E, T. von Rintelen leg., 21 Sep. 2019.

Description. ***Cephalothorax and cephalic appendages.*** Postorbital carapace length 1.3–3.8 mm (n = 220). Rostrum (Fig. 11A, B) conspicuously high, straight or slightly convex on dorsal margin, distal part of ventral margin convex, reaching to end of second segment of antennular peduncle or slightly overreaching this segment, ventral teeth placed at convex part close to the tip, 0.66–1.0 (median 0.81, n = 7) times as long as carapace, rostral formula 4–7 (5) + 10–19 (15) / 4–12 (7–9). Small antennal spine well separated from inferior orbital angle. Pterygostomial angle broadly rounded. Eyes well developed with globular cornea. Antennular peduncle (Fig. 11A, G), 0.72–0.83 (median 0.79, n = 4) times as long as carapace in females, 0.95–1.13 (median 1.09, n = 3) times as long as carapace in males, first segment 1.73–2.17 (median 2.0, n = 3) times as long as second segment, second segment 2.30–2.60 (median 2.50) times longer than third segment. Stylocerite reaching to 0.77–0.80 (median 0.77, n = 4) of first segment of antennular peduncle. Scaphocerite (Fig. 11H) 3.48–3.64 (median 3.56) times as long as wide.

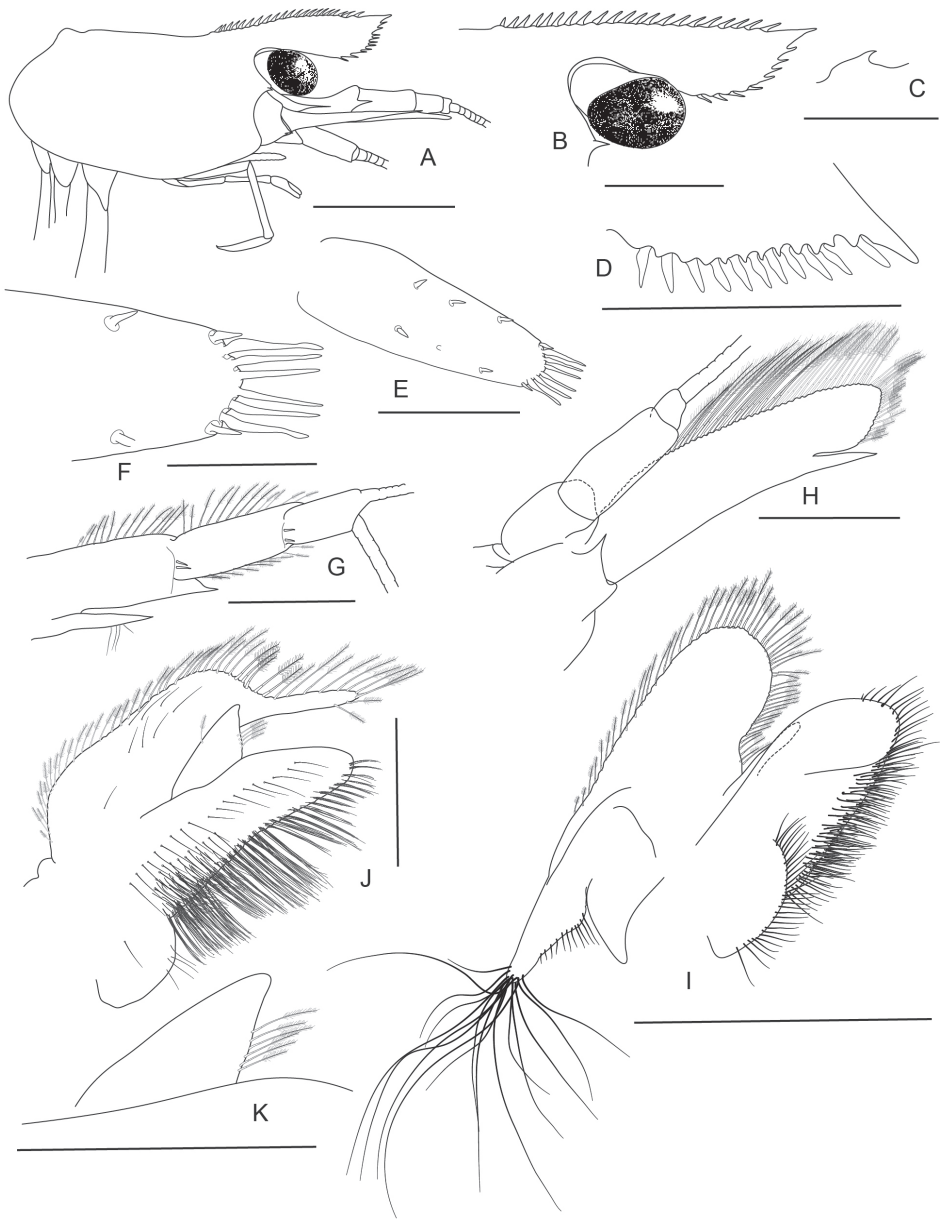

Figure 11. *Caridina mayamareenae* sp. nov. Morphology 1. Paratype ♂, cl. 2.7 mm, ZMB 29627 **A** cephalothorax and cephalic appendages **C** preanal carina **D** uropodal diaeresis **E–F** telson **G** antennular peduncle **H** scaphocerite **I** maxilla **J** first maxilliped **K** palp of first maxilliped; paratype ♀, cl. 2.7 mm, MZB Cru 5044 **B** rostrum. Scale bars: 2 mm (**A, E**); 1 mm (**B, G–I**); 0.5 mm (**C, D, F, J, K**).

Abdominal somites, telson and uropods. Sixth abdominal somite 0.46–0.71 (median 0.58, n = 8) times carapace length, 1.65–2.0 (median 1.74, n = 8) times as long as fifth somite, 0.90–1.12 (median 1.04, n = 8) times as long as telson. Telson (Fig. 11E, F) 2.45–2.64 (n = 2) times as long as proximal wide, distal margin broadly convex

without a median projection, with three or four pairs of short spiniform setae dorsally and one pair of short spiniform setae dorsolaterally; distal end with 6 long spiniform setae, lateral pair slightly longer than others. Preanal carina (Fig. 11C) with a hook-like spine. Uropodal diaeresis (Fig. 11D) with 11–13 stout movable spiniform setae, outermost ones shorter than lateral angle.

Mouthparts and branchiae. Incisor process of mandible (Fig. 12A) ending in irregular teeth, molar process truncated. Lower lacinia of maxillula (Fig. 12B) broadly rounded, upper lacinia elongate, with numerous distinct teeth on inner margin, palp slender with few simple setae and one conical spiniform seta near tip. Upper endites of maxilla (Fig. 11I) subdivided, palp slender, scaphognathite tapering posteriorly, fringed with long, curved setae at posterior margin. End of palp of first maxilliped (Fig. 11J, K) ending in blunt triangular shape. Podobranch on second maxilliped (Fig. 12C) reduced to a lamina. Third maxilliped (Fig. 12D) with one well developed and one arthrobranch reduced to a small worm-like structure. First pereiopod with an arthrobranch. Pleurobranchs present on all pereiopods. Epipod vestigial on third maxilliped, absent from all pereiopods.

Pereiopods. Chelae of first and second pereiopods (Fig. 12E–H) rather less developed and conspicuous small; chela of first pereiopod 4.00–4.17 (median 4.00, n = 3) times as long as wide, 1.07–1.14 (median 1.07, n = 3) times length of carpus; tips of fingers (Fig. 12E, F) rounded, without hooks, with scarce hairs near tip; dactylus 1.70–1.74 (median 1.73, n = 3) times as long as palm; carpus hardly excavated distally, 4.31–4.40 (median 4.31, n = 3) times as long as wide, 1.05–1.22 (median 1.22, n = 3) times length of merus. Merus 3.83–5.25 (median 4.18, n = 3) times as long as wide, as long as ischium. Chela of second pereiopod 5.00–5.27 (median 5.14, n = 3) times as long as wide, 0.73–0.81 (median 0.76, n = 3) times length of carpus; tips of fingers rounded, without hooks, with scarce hairs near tip; dactylus 1.47–1.93 (median 1.58, n = 3) times as long as palm; carpus 7.17–8.44 (median 8.17, n = 3) times as long as wide, 1.27–1.40 (median 1.34, n = 3) times as long as merus; merus 5.82–7.50 (median 6.36, n = 3) times as long as wide, as long as ischium. Third pereiopod (Fig. 12I, J) conspicuous stout, not sexually dimorphic, dactylus 3.40–4.38 (median 4.00, n = 3) times as long as wide (terminal claw and spiniform setae on flexor margin included), terminating in one large claw with five or six short spiniform setae on flexor margin; propodus stout, 5.25–7.80 (median 6.00, n = 3) times as long as wide, 2.10–2.47 (median 2.23, n = 3) times as long as dactylus; carpus 3.52–4.83 (median 3.94, n = 3) times as long as wide, 0.74–0.88 (median 0.85, n = 3) times as long as propodus; merus very stout, 4.67–6.50 (median 5.00, n = 3) times as long as wide, 1.89–2.24 (median 2.11, n = 3) times as long as carpus, bearing three strong spiniform setae on posterior margin of outer surface. Ischium without or with one spiniform seta. Fifth pereiopod (Fig. 12K, L) slender, dactylus 2.73–5.22 (median 5.00, n = 3) times as long as wide (terminal claw and serrate setae on flexor margin included), terminating in one large claw with 18–36 serrate setae on flexor margin; propodus 8.33–11.11 (median 9.09, n = 3) times as long as wide, 2.13–3.33 (median 2.50, n = 3) times length of dactylus, carpus 4.83–6.00 (median 5.17, n = 3) times as long as wide, 0.54–0.62 (median 0.58, n = 3) times as long as propodus; merus 6.93–10.00 (median 8.67, n = 3) times as long as wide, 1.68–1.85 (median 1.79, n = 3) times length of carpus, bearing 2–4 strong spiniform setae on posterior margin of outer surface. Ischium without a strong spiniform seta.

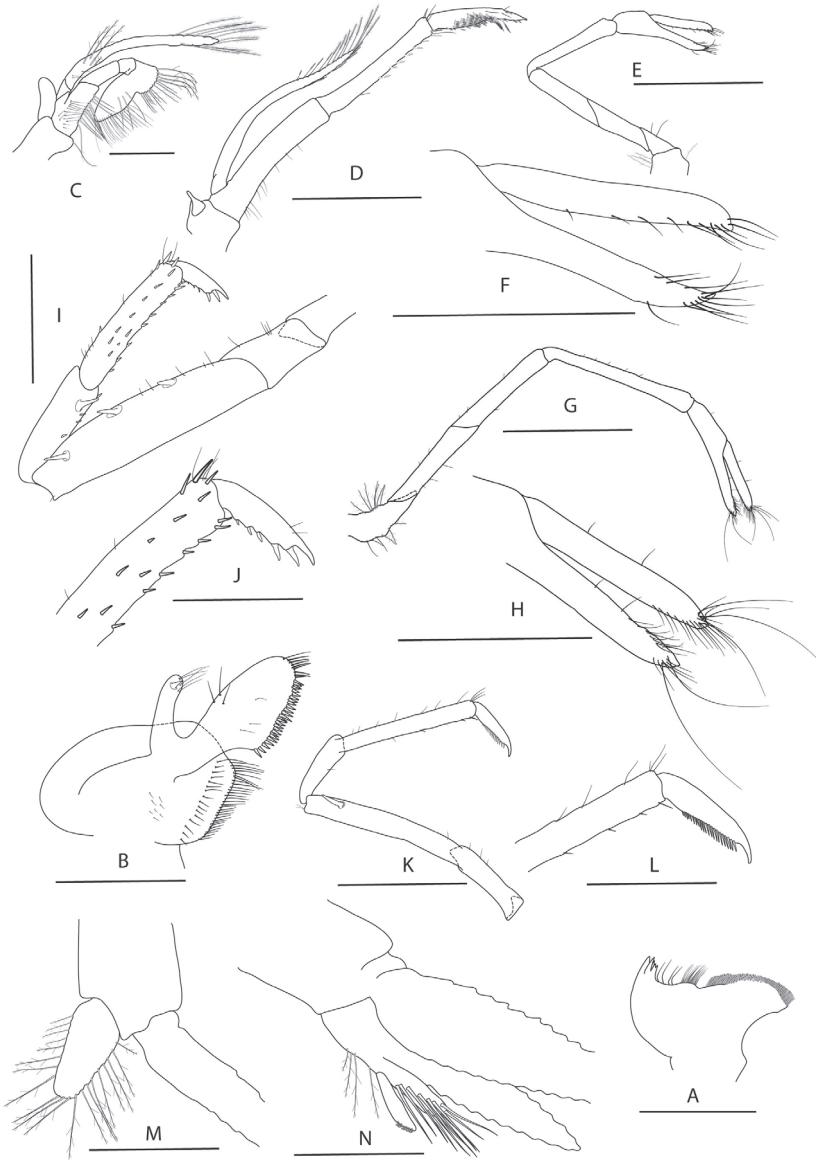

Figure 12. *Caridina mayamareenae* sp. nov. Morphology 2. Paratype ♂, cl. 2.7 mm, ZMB 29627 **A** distal part of mandible **B** maxillula **C** second maxilliped **D** third maxilliped **E** first pereiopod **F** dactyli of first pereiopod **I** third pereiopod **J** dactylus of third pereiopod **K** fifth pereiopod **L** dactylus of fifth pereiopod **M** endopod of male first pleopod **N** appendix masculina on male second pleopod; paratype ♀, cl. 2.7 mm, MZB Cru 5044 **G** second pereiopod **H** dactyli of second pereiopod. Scale bars: 0.5 mm (**A–C, F, H, J, L–N**); 1 mm (**D, E, G, I, K**).

Pleopods. Endopod of male first pleopod (Fig. 12M) subtriangular, without an appendix interna, 1.83 times as long as proximal width, 0.28 times as long as exopod. Appendix masculina on male second pleopod (Fig. 12N) slender, rod-shaped, 7.20

times as long as wide, with long spiniform setae on inner and distal margin, few pappose setae on basal part, appendix interna reaching to ~ 0.94 of appendix masculina.

Colouration. Body colouration of large females whitish, frequently with broad bright red stripes and blotches, eggs green (Fig. 3A, B), males mostly transparent with some white blotches (Fig. 2E).

Reproductive biology and larval development. Ovigerous females with few eggs (36, n = 1). Size of undeveloped eggs (early stage embryos without eyespot) 0.71–0.78 × 0.39–0.54 mm, size of developed eggs (late stage embryos with eyes) 0.78 × 0.47 mm (n = 9).

Etymology. Named after the fourth author's, daughter for her strong interest in decapod crustaceans her father is working on.

Distribution. *Caridina mayamareenae* sp. nov. is endemic to Lake Poso. Specimens were found at five localities within the lake, three in the northern part and two at the eastern and western shores in the southern part of the lake.

Ecology. *Caridina mayamareenae* sp. nov. is hiding inside empty shells of the viviparid snail *Celetaia persculpta* (P. Sarasin and F. Sarasin, 1898) and *Tylomelania* spp. (Fig. 3D), and was not observed on any other substrate. On average, 1.4 shrimps were found per shell, but there is considerable variation (0.6–2.4 shrimps per shell) among the examined sites (Table 2). Up to four specimens were found in a single shell at the Dolidi Ndano locality. *Caridina mayamareenae* sp. nov. is also confined to deeper water; shells from depths of 7 m upwards did not contain any shrimps.

Remarks. Among all species of the genus *Caridina* known from Lake Poso, *C. mayamareenae* sp. nov. is unique by its short and conspicuous high rostrum, the less developed chelipeds with scarce setae at the tip of the fingers, and the strong third pair of pereiopods. A high and rather short rostrum is an infrequent character among lacustrine species of the genus *Caridina* from the Central Lakes of Sulawesi (compare revision in von Rintelen and Cai 2009). Many lacustrine species are showing slender, styliform rostrum shapes as seen in *C. ensifera* and *C. caerulea*, the most common species in Lake Poso. The conspicuous high rostrum and the strong third pair of pereiopods adapted for clinging on hard substrate are visible characters of a high grade of specialisation to the microhabitat of this species.

Table 2. Abundance of *Caridina mayamareenae* sp. nov. in shells of aquatic snails in Lake Poso. The numbers in brackets in the "shells" column refer to numbers of shells of *Celetaia persculpta* / shells of *Tylomelania* spp.; in the "other taxa" column, the numbers are juvenile gecarcinucid crabs / n *Cirolana* spp.

Locality and depth	shells (n)	shrimps (n)	Other taxa
E shore:			
Dolidi Ndano, 15m	28*	66	-#
W shore:			
Bay N of Cape Bancea, 15m	22 (13/9)	13	6/2
NW shore:			
Cape Wotu			
10m	25 (16/9)	30	-/1
15m	27 (27/0)	35	4/8
Siuri, 13–14m	19 (4/15)	23	4/-

Key: * total snail count, not differentiated between genera; # other taxa present, but not recorded.

***Caridina poso* Klotz, Wowor & K. von Rintelen, sp. nov.**
http://zoobank.org/83931AF8-E252-4068-94D9-69C1103D42D7
Figures 3E–F, 13, 14

Material examined. *Holotype*: ov. ♂ cl. 2.7 mm (MZB Cru 5050), Indonesia, Central Sulawesi, Lake Poso, at Taipa, H-G. Evers leg., 26 Sep. 2010. **Paratypes:** 2 ov. ♀♀ cl. 2.9 and 3.1 mm, 3 ♀♀ cl. 3.0–3.1 mm, 2 ♂♂ cl. 2.6 and 2.7 mm (ZMB 29624), same data as holotype; 5 ov. ♀♀ cl. 3.2–3.4 mm, 5 ♂♂ cl. 2.7–3.2 mm (MZB Cru 5051), 5 ov. ♀♀ cl. 3.3–3.8 mm, 2 ♂♂ cl. 3.1 and 3.2 mm (ZMB 29621), Lake Poso, E shore, "Sulawesi Rock", 1°56.102'S, 120°40.402'E, J. Pfaender and T. von Rintelen leg., 22 Sep. 2015; 5 ♂♂ cl. 2.4–2.7 mm (MZB Cru 5052), 1 ov. ♀ cl. 3.1 mm, 4 ♂♂ cl. 2.6–2.9 mm (ZMB 28063), Lake Poso, W shore, 1°56.67'S, 120°33.925'E, B. Stelbrink leg., 07 Sep. 2012.

***Other material*:** 1 ♂ cl. 2.7 mm (ZMB 29766), aquarium reared specimen, preserved on 08 Oct. 2015 by W. Klotz.

Description. *Cephalothorax and cephalic appendages.* Postorbital carapace length 2.6–3.8 mm (n = 36). Rostrum (Fig. 13A-C) very long and slender, curved upwards, reaching far beyond end of scaphocerite, distal 0.5 to 0.8 unarmed, ventral margin armed throughout, most proximal tooth placed below third tooth of dorsal margin in most specimens, 1.35–2.75 (median 2.01, n = 23) times as long as carapace, rostral formula 3–5(4) + 8–14 / 19–37. Orbital margin fused with an antennal spine. Pterygostomial angle broadly rounded. Eyes well developed with globular cornea. Antennular peduncle (Fig. 13A, C), 0.97–1.03 (median 1.01, n = 4) times as long as carapace in females, 1.07–1.19 (median 1.16, n = 4) times as long as carapace in males, first segment 1.48–1.78 (median 1.55, n = 5) times as long as second segment, second segment 2.25–2.88 (median 2.44, n = 5) times longer than third segment. Stylocerite reaching to 0.78–0.88 (median 0.83, n = 4) of first segment of antennular peduncle. Scaphocerite (Fig. 13H) 4.30–5.33 (median 4.75, n = 6) times as long as wide.

Abdominal somites, telson and uropods. Sixth abdominal somite 0.60–0.76 (median 0.67, n = 12) times carapace length, 1.70–2.18 (median 1.95, n = 11) times as long as fifth somite, 0.93–1.11 (median 1.08, n = 9) times as long as telson. Telson (Fig. 13F, G) 3.19–3.83 (median 3.50, n = 3) times as long as proximal wide, 5.73–6.42 (median 6.13, n = 3) times as long as distal wide, distal margin convex without a median projection, with three or four pairs of short spiniform setae dorsally and one pair of short spiniform setae dorsolaterally; distal end with 6–8 long spiniform setae, lateral pair slightly longer than others, innermost pair very tiny. Preanal carina (Fig. 13D) with a hook-like spine. Uropodal diaeresis (Fig. 13E) with 10–12 short movable spiniform setae, outermost ones shorter than lateral angle.

Mouthparts and branchiae. Incisor process of mandible (Fig. 13I) ending in irregular teeth, molar process truncated. Lower lacinia of maxillula (Fig. 13J) broadly rounded, upper lacinia elongate, with numerous distinct teeth on inner margin, palp slender with few pappose setae and one conical spiniform seta near tip. Upper endites of maxilla (Fig. 13K) subdivided, palp slender, scaphognathite tapering posteriorly, fringed

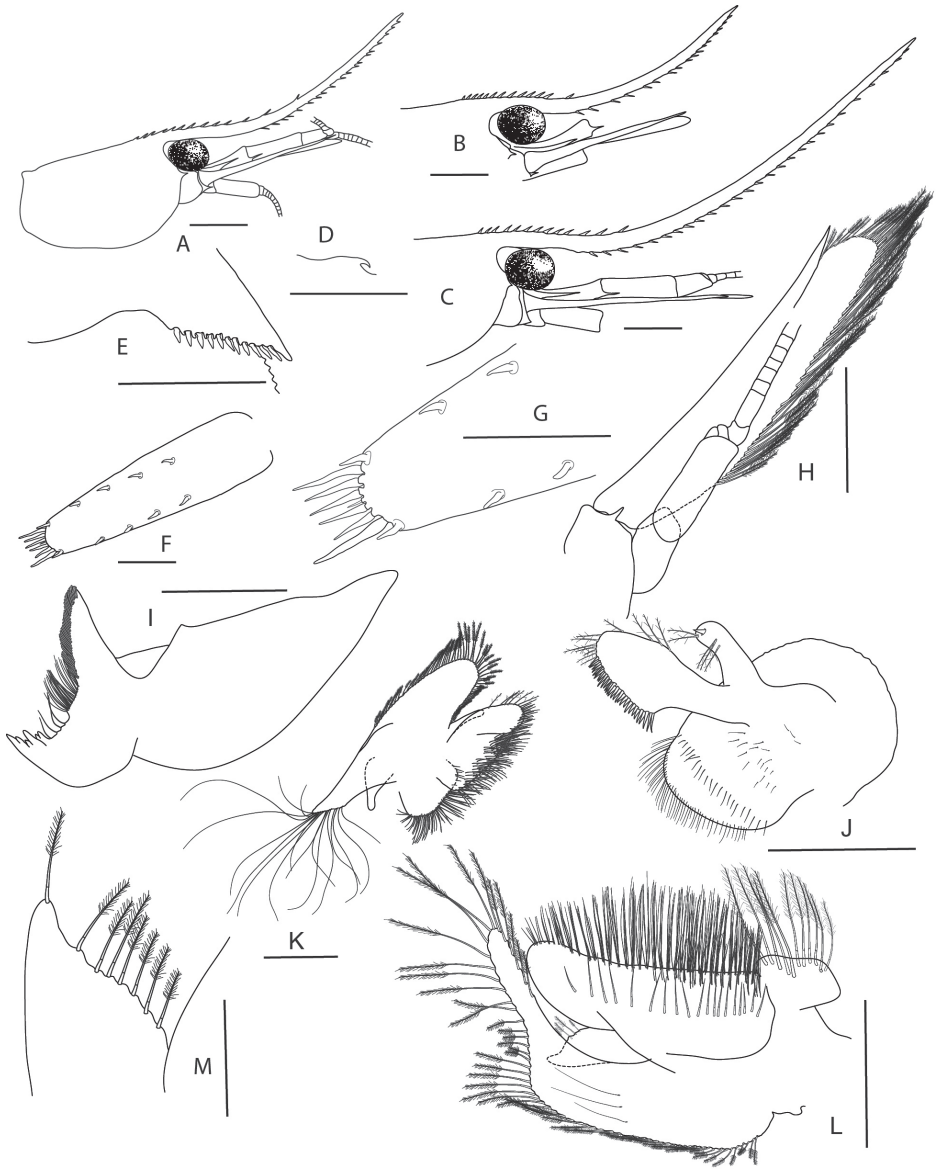

Figure 13. *Caridina poso* sp. nov. Morphology 1. ♂, cl. 2.7 mm, ZMB 29766 **A** cephalothorax and cephalic appendages **D** preanal carina **E** uropodal diaeresis **F, G** telson; paratype ♂, cl. 2.7 mm, ZMB 29624 **B** rostrum **H** scaphocerite **I** mandible **J** maxillula **K** maxilla **L** first maxilliped **M** palp of first maxilliped; paratype ov. ♀, cl. 3.4 mm, MZB Cru 5051 **C** Rostrum. Scale bars: 1 mm (**A–C, F, H, I**); 0.5 mm (**D, E, G, J–L**); 0.1 mm (**M**).

with long, curved setae at posterior margin. End of palp of first maxilliped triangular (Fig. 13L, M). Podobranch on second maxilliped (Fig. 14A) reduced to a lamina. Third maxilliped (Fig. 14B) with two arthrobranchs, ultimate segment of maxilliped shorter

than penultimate segment. First pereiopod with an arthrobranch. Pleurobranchs present on all pereiopods. Epipod vestigial on third maxilliped, absent from all pereiopods.

***Pereiopods*.** Chelae of first and second pereiopods (Fig. 14C, D) well developed; chela of first pereiopod 3.11–3.36 (median 3.13, n = 5) times as long as wide, 0.95–1.21 (median 1.13, n = 5) times length of carpus; tips of fingers (Fig. 14C) rounded, without hooks, with tufts of hairs near tip; dactylus 2.00–2.50 (median 2.00, n = 5) times as long as palm; carpus slender, hardly excavated distally, 3.13–4.33 (median 3.76, n = 5) times as long as wide, 1.29–1.56 (median 1.45, n = 5) times length of merus. Merus 3.13–3.63 (median 3.38, n = 5) times as long as wide, 0.81–0.88 (median 0.85, n = 5) times as long as ischium. Chela of second pereiopod 3.23–3.91 (median 3.71, n = 6) times as long as wide, 0.67–0.84 (median 0.76, n = 6) times length of carpus; tips of fingers rounded, without hooks, with tufts of hairs near tip; dactylus 1.47–2.29 (median 2.00, n = 6) times as long as palm; carpus 6.50–8.38 (median 7.29, n = 6) times as long as wide, 1.38–1.63 (median 1.53, n = 6) times as long as merus; merus 5.08–6.43 (median 5.71, n = 6) times as long as wide, 0.86–0.96 (median 0.87, n = 6) times as long as ischium. Third pereiopod (Fig. 14E, F) not sexually dimorphic, dactylus 3.11–4.67 (median 3.86, n = 5) times as long as wide (terminal claw and spiniform setae on flexor margin included), terminating in one large claw with 5–7 short spiniform setae on flexor margin; propodus very slender, 16.50–19.11 (median 18.71, n = 6) times as long as wide, 4.78–6.00 (median 5.12, n = 6) times as long as dactylus; carpus 8.73–10.40 (median 9.50, n = 6) times as long as wide, 0.64–0.72 (median 0.70, n = 6) times as long as propodus; merus slender, 11.25–13.93 (median 12.31, n = 6) times as long as wide, 1.54–1.71 (median 1.66, n = 6) times as long as carpus, bearing 4 strong spiniform setae on posterior margin of outer surface. Ischium with one spiniform seta. Fifth pereiopod (Fig. 14G, H) slender, dactylus 2.43–4.67 (median 3.69, n = 6) times as long as wide (terminal claw and serrate setae on flexor margin included), terminating in one large claw, with 30–34 serrate setae on flexor margin; propodus slender, 15.80–21.50 (median 16.97, n = 6) times as long as wide, 4.41–5.28 (median 4.73, n = 6) times length of dactylus, carpus 7.27–10.40 (median 8.30, n = 6) times as long as wide, 0.51–0.61 (median 0.59, n = 6) times as long as propodus; merus slender, 11.50–12.92 (median 11.74, n = 6) times as long as wide, 1.35–1.63 (median 1.50, n = 6) times length of carpus, bearing four or five strong spiniform setae on posterior margin of outer surface. Ischium without a strong spiniform seta.

***Pleopods*.** Endopod of male first pleopod (Fig. 14I) subtriangular, without an appendix interna, 1.77–2.27 (median 1.83, n = 3) times as long as proximal width, 0.21–0.27 (median 0.23, n = 3) times as long as exopod. Appendix masculina on male second pleopod (Fig. 14J) slender, rod-shaped, 7.25–10.50 (median 7.67, n = 3) times as long as wide, with long spiniform setae on inner and distal margin, a few pappose setae on basal part, appendix interna reaching to ~ 0.65–0.90 (median 0.85, n = 3) of appendix masculina.

Colouration. Body and legs mottled with reddish and white dots arranged in rows, exopod of uropods with a black and white blotch, antennae dark red, chelae white with red fingers (Fig. 3E, F).

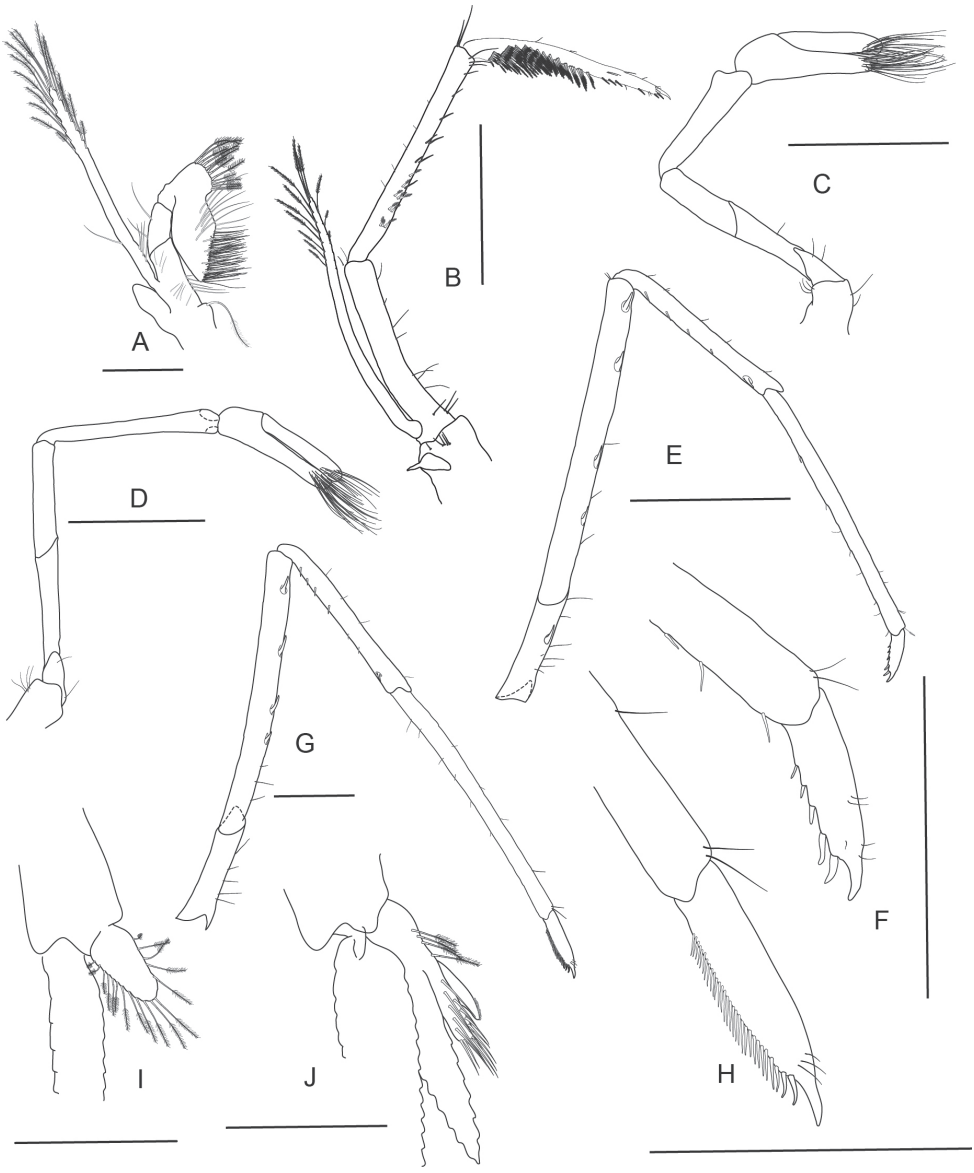

Figure 14. *Caridina poso* sp. nov. Morphology 2. Paratype ♂, cl. 2.7 mm, ZMB 29624 **A** second maxilliped **B** third maxilliped **C** first pereiopod **D** second pereiopod **E** third pereiopod **F** dactylus of third pereiopod **G** fifth pereiopod **H** dactylus of fifth pereiopod; ♂, cl. 2.7 mm, ZMB 29766 **I** endopod of male first pleopod **J** appendix masculina on male second pleopod. Scale bars: 0.5 mm (**A, F–J**); 1 mm (**B–E**).

Reproductive biology and larval development. Ovigerous females with few, large eggs (5 and 9, n = 2). Size of eggs 0.96–1.11 × 0.56–0.66 mm (n = 9).

Etymology. The specific name is a noun in apposition after the type locality, Lake Poso.

Distribution. *Caridina poso* sp. nov. is endemic to Lake Poso. Specimens were found at three localities within the lake, one at the east shore and two at the west shore.

Ecology. *Caridina poso* sp. nov. lives in packs of debris (small to medium-sized stones) close to the shore of the Lake Poso and thus could be considered a hard substrate dweller as defined in von Rintelen and Cai (2009). The species was never found on soft substrates such as dead leaves, wood or water plants.

Remarks. With its long and upturned rostrum, *C. poso* sp. nov. is similar to *C. ensifera* and *C. caerulea*, two endemic species to Lake Poso. In the field, colouration alone is sufficient to differenciate *C. poso* sp. nov. from these species. The much smaller species *C. poso* sp. nov. (carapace length 2.6–3.8 mm) is showing black and white blotches on the exopod of the uropods. In the larger species *C. ensifera* (cl. 3.5–5.3 mm), a dark red spot is seen on the exopod of the uropods. In *C. caerulea* (cl. 3.0–4.5 mm), the exopod of the uropods shows an elongate blue blotch (von Rintelen and Cai 2009).

In preserved condition, *C. poso* sp. nov. can be distinguished from *C. ensifera* by the absence of epipods on all pereiopods (a vestigial epipod is present on third maxilliped vs. epipods well developed, with distal hooks on the third maxilliped and first and second pereiopods in *C. ensifera*) and by the higher number of postorbital teeth on the rostrum (3–5 (mode 4) vs. 1–3 (mode 2) in *C. ensifera*). Further, *C. poso* sp. nov. differs by its slender chelipeds (chela of first pereiopod 3.1–3.4 times as long as high vs. 2.0–2.8 times in *C. ensifera*, dactylus of first cheliped 2.0–2.5 times as long as palm vs. 1.0–1.3 times in *C. ensifera*, dactylus of second cheliped 1.5–2.3 times as long as palm vs. 1.2–1.4 times in *C. ensifera*) and slender third pair of pereiopods (propodus 16.5–19.1 times as long as wide vs. 10–13 times in *C. ensifera*, carpus 8.7–10.4 times as long as wide vs. 4.7–6.1 times in *C. ensifera*, merus 11.3–13.9 times as long as wide vs. 9.2–11.4 times in *C. ensifera*). In contrast, the dactyli of the fifth pereiopods are shorter (dactylus 2.4–4.7 times as long as wide vs. 5.4–7.0 times in *C. ensifera*, propodus 4.4–5.3 times as long as dactylus vs. 2.5–3.0 times in *C. ensifera*). The dactyli of fifth pereiopods are armed with a smaller number of serrate setae on the flexor margin (30–34 vs. 51–57 in *C. ensifera*). *Caridina poso* sp. nov. differs from *C. caerulea* by the absence of epipods on all pereiopods (a vestigial epipod is present on the third maxilliped) vs. epipods well developed (with distal hooks) on the third maxilliped and first and second pereiopods and the higher number of postorbital teeth on the rostrum (3–5 (mode 4) vs. 2–4 (mode 2)) in *C. caerulea*; further by its shorter telson (telson 0.6–0.7 times as long as carapace vs. 0.8 times in *C. caerulea*), by the slender chelipeds (chela of first pereiopod 3.1–3.4 times as long as high vs. 1.9–2.7 times in *C. caerulea*, dactylus of first cheliped 2.0–2.5 times as long as palm vs. 1.1–1.4 times in *C. caerulea*, carpus of first cheliped 3.1–4.3 times as long as wide vs. 2.1–2.5 times in *C. caerulea*; chela of second cheliped 3.2–3.9 times as long as wide vs. 2.1–3.2 times in *C. caerulea*, dactylus of second cheliped 1.5–2.3 times as long as palm vs. 1.3–1.6 times in *C. caerulea*, carpus of second cheliped 6.5–8.4 times as long as wide vs. 4.1–5.4 times in *C. caerulea*). The third pair of pereiopods is more slender (propodus 16.5–19.1 times as long as wide vs. 12.9–16.3 times in *C. caerulea*, carpus 8.7–10.4 times as long as wide vs. 5.9–8.0 times in *C. caerulea*, merus 11.3–13.9 times as long as wide vs. 9.4–11.8 times in *C. caerulea*). Merus of fifth pereiopod slender, 11.5–12.9 times as long as wide vs. 8.5–11.3 times in *C. caerulea*.

Molecular phylogenetics

We used sequences of mitochondrial DNA to investigate the phylogenetic relationship among the species of *Caridina* from Lake Poso as described above. The resulting sequence alignments have a length of 781 bp (COI) and 540 bp (16S), respectively. In 16S, only two short and largely unambiguous indels (1–2 bp) were required to homologise positions in the alignment.

If support values are considered, the tree topologies reconstructed from 16S and COI are largely congruent (Suppl. material 2, Figs S4, S5). All well supported clades (BPP > 0.9) are found in both trees, while basal splits of both trees, particularly for 16S, are poorly supported.

The molecular phylogeny of Lake Poso species for this study and from the previous study with fewer species (von Rintelen et al. 2007a) revealed similar results: a) All 11 species from the lake as well as its catchment area (Table 1) form a well-supported monophyletic group (Fig. 15; Suppl. material 2: Figs S1–S3); b) the nine species from the lake proper do not form a monophylum but cluster in separate groups as highlighted in Figure 15, partly clustering with the riverine species *Caridina acutirostris* and *C. schenkeli*; c) the match of morphospecies and genetic clades remains as heterogeneous as in von Rintelen et al. (2007a). Only four of the eleven morphospecies consistently correspond to mtDNA clades (*C. acutirostris*, *C. caerulea*, *C. ensifera*, and *C. lilianae* sp. nov.). *Caridina mayamareenae* sp. nov. also forms a single clade but contains one specimen of *C. fusca* sp. nov. Two more species (*Caridina longidigita* and *C. sarasinorum*) form distinct clades comprising the majority of sequenced specimens, but not all. A few specimens of these two species are also found within a clade comprising all sequences of *C. marlenae* sp. nov. and *C. poso* sp. nov. as well as several specimens of *C. sarasinorum, C. schenkeli* and the second known population of *C. fusca* sp. nov. The majority of *C. schenkeli* specimens form a paraphyletic group with respect to *C. caerulea*, and this group also includes one sequence of *C. sarasinorum*.

Discussion

Lake Poso revisited – new insights from new material?

The molecular phylogeny and field observations (colour pattern, habitat, distribution, behaviour if applicable) were used to test and support the morphological studies of alcohol preserved specimens. The integrative taxonomic approach taken by von Rintelen et al. (2007a) and von Rintelen and Cai (2009) was again successfully applied in this study.

The match of morphospecies and genetic clades remains as heterogeneous as in von Rintelen et al. (2007a). Although all new species are morphologically distinguishable based on the characters described in this study, only four species form exclusively monophyletic groups (Fig. 15). The non-monophyly of the remaining species including three of the new species described here might be explained by introgressive hybridi-

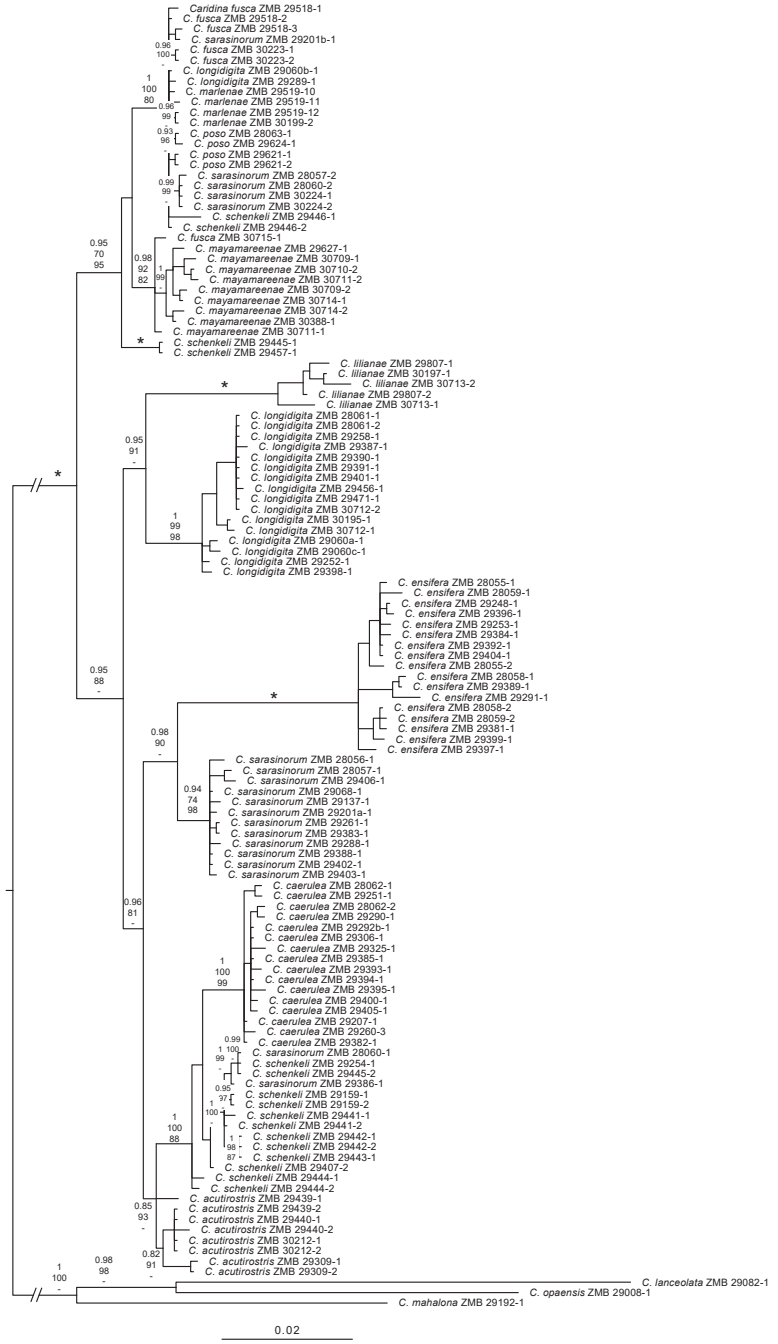

Figure 15. Molecular phylogeny of the 11 species of *Caridina* in Lake Poso. Phylogenetic relationships reconstructed by BI analyses of two mitochondrial gene fragments (topology based on concatenated 16S and COI datasets). Number of branches show, from top, Bayesian posterior probabilities (> 0.85) and ML/MP bootstrap values (> 70). An asterisk indicates nodes with full support (1/100/100). The scale bar indicates the substitution rate. See Suppl. material 1 for information on the sequenced specimens.

sation or incomplete lineage sorting as discussed for the previously described species. It remains to be seen whether the hypothesis forwarded by von Rintelen et al. (2007a) and von Rintelen and Cai (2009) that the colour patterns of the hybridising species seem to be less obvious and stable than those of the monophyletic taxa, occasionally resulting in mating errors between lake species and between riverine and lake species, holds true. Among the newly described species, *Caridina poso* sp. nov. and *C. marlenae* sp. nov. show characteristic, stable, and in the latter also rather conspicuous colour patterns. This hypothesis, however, needs further testing. Another assumption explaining the insufficient resolution by molecular data in most of the new species, which possibly also led to their late discovery, is that their species boundaries are not as fixed yet and they are still in the process of becoming proper biological species. A similar case is known from four closely related *Caridina* species from Lake Towuti, Sulawesi (von Rintelen and Cai 2009). In a future study, this assumption could be tested and distinguished from introgressive hybridisation by applying a population genomics approach such as, e.g., RAD seq, which has been applied to much the same purpose in Lake Poso ricefishes (Sutra et al. 2019).

Adaptive radiation in Lake Poso

Von Rintelen et al. (2007a) positively tested the hypothesis of an adaptive radiation in the atyid shrimp species flock in Lake Poso, which met at least three of the four criteria defined by Schluter (2000): All eleven species, including those from the catchment area, showed common ancestry, indicative of one colonisation of the entire Poso lake system, and rapid radiation. Apart from the well supported monophyly of the entire species flock, the non-monophyly of the nine lake species are congruent with the results found by von Rintelen et al. (2007a). This time again, the data failed to provide conclusive evidence for an *in situ* radiation within the lake itself. The earlier study revealed a correlation of phenotype and environment (habitat preferences and divergence in trophic morphology) in Lake Poso species. By exhibiting species-specific and unusual colour patterns, the species seemed to have reached the third stage of adaptive radiation according to Streelman and Danley (2003), i.e., sexual selection suggested as a driving force of diversification (see review in von Rintelen et al. 2020).

The new species cluster within the Poso clade (Fig. 15) are thus part of the monophyletic species flock (common ancestry) that radiated into several specialised ancestors. All new lake species also show pronounced microhabitat preferences – the most extreme example is *Caridina mayamareenae* sp. nov. (Fig. 3A, B) – along with interspecific differences in cheliped morphology (Figs 6, 8, 10, 12, 14) and species-specific colour patterns (Figs 2E, 3A, B), although not always as clear as described in von Rintelen and Cai (2009). The adaptive radiation of shrimps in Lake Poso is thus more diverse than previously assumed, not just in terms of species number, but also with respect to habitat and trophic specialisation. A parallel case of adaptive and largely microhabitat-driven radiation in *Caridina* is know from the Malili lake system of Sulawesi (von Rintelen et al. 2010; Martin and Richards 2019).

Atyid shrimps in association with other organisms

The occurrence of a Lake Poso species in empty snail shells (i.e., *Caridina mayamareenae* sp. nov.; Fig. 3A, B, D) is rather unusual, as empty shells of aquatic snails were not reported as microhabitat of atyid shrimp up to now.

In Lake Tanganyika, East Africa, Roth-Woltereck (1958) described the small atyid species *Limnocaridina iridinae* based on two ovigerous females found in the gill chamber of the bivalve *Iridina spekei*. Later, no further specimen of this shrimp species was found. Only in November 2010, the first author received a single ovigerous specimen of *L. iridinae* (now deposited in the crustacean collection of the Oxford University Museum of Natural History, collection number OUMNH.ZC.2012-05-0012) for determination. This time, it was found in an empty shell of the viviparid snail *Neothauma tanganyicense*. According to the collector, approximately 100 specimens of *Iridina spekei* were checked for specimens of shrimp without any success (Heinz Büscher, pers. comm.). This might indicate that *L. iridinae* is not only associated with bivalves but likewise seeks shelter in empty snail shells.

So far, *Limnocaridina iridinae* and the parallel case of *C. mayamareenae* sp. nov. from Lake Poso are the only cases of freshwater shrimps in general, and particularly in ancient lake species flocks, associated with molluscs. As a possibly morphological adaptation to their habitat, both species share the less developed type of chelae bearing just some scarce setae at the tips of fingers in contrast to the brush-like dense tufts of setae found in other atyids. A similar association was only described for *C. spongicola* from the Malili lake system, Sulawesi. This species is associated with an endemic freshwater sponge from Lake Towuti and one of the most extreme specialisations found in the adaptive radiation of *Caridina* in the ancient lakes of Sulawesi (Zitzler and Cai 2006; von Rintelen et al. 2007b). All three cases might be seen as an example of ecological convergence between species of all three ancient lake systems.

Conservation status and sustainability

Following the IUCN categories, all previously described species from Lake Poso and catchment (Table 1) were assessed as Vulnerable under the D2 criterion (De Grave et al. 2013a–e, Wowor et al. 2013). This was justified based on the limited occurrence of endemic populations and the presence of an introduced fish species as a plausible threat. This originally African cichlid species was again observed in Lake Poso in 2019 (KvR, TvR pers. obs.). The five new *Caridina* species are thus subjected to similar threats and have a similarly limited occurrence in the lake system as the previously described species. We therefore suggest to include the new species under the same IUCN category and criterion. Currently, the third author and Indonesian colleagues are preparing measures to protect the habitats and fauna of the ancient lakes of Sulawesi, including the atyid species flocks from Lake Poso and the Malili lakes summarised in this study and in von Rintelen and Cai (2009).

The key to pre-sorting living specimens in the field can be used easily without having to use microscopic equipment. Shrimps can, for example, be observed while swimming or snorkelling or by putting them in small fish tanks, and releasing back into the water afterwards. The key can be used for pre-sorting in the field for scientific purpose but also for sustainable capacity building or citizen science projects without having to reduce the populations. This key, however, has not fully been tested in the field and would certainly be an ideal test case for a local citizen science or student project.

Conclusions

Even in relatively well studied areas like the ancient lakes of Sulawesi, the biodiversity of freshwater shrimps has largely been underestimated. An integrative taxonomic approach is the key to the discovery of new species and to a better understanding of the evolution of Lake Poso's fauna. This new knowledge can contribute to the prevention of biodiversity and habitat loss.

Acknowledgements

This study was supported by BMBF (project INDOBIOSYS MfN Berlin, 16GW0111K) with regard to the crustacean fauna of Lake Poso. We thank Robert Schreiber (MfN Berlin) for his support of the molecular work in this study. Björn Stelbrink (currently Basel University) and Jobst Pfaender (Potsdam Natural History Museum) helped in collecting some of the samples studied. We further thank the three daughters involved who supported this study in their own way and hope that the lake's, ecosystem and endemic fauna will still be intact when they have grown up. Thanks to both reviewers, Charles Fransen and Yixiong Cai, for their valuable comments that improved the quality of the manuscript.

References

Cai Y, Wowor D (2007) Atyid shrimps from Lake Poso, Central Sulawesi, Indonesia with description of a new species (Crustacea: Decapoda: Caridea). The Raffles Bulletin of Zoology 55: 311–320.

Chernomor O, von Haeseler A, Minh BQ (2016) Terrace aware data structure for phylogenomic inference from supermatrices. Systematic Biology 65(6): 997–1008. https://doi.org/10.1093/sysbio/syw037

Coleman CO (2003) “Digital inking”: How to make perfect line drawings on computers. Organisms Diversity & Evolution 3 (4): 1–14. https://doi.org/10.1078/1439-6092-00081

Coleman CO (2006) Substituting time-consuming pencil drawings in arthropod taxonomy using stacks of digital photographs. Zootaxa 1360: 61–68. https://doi.org/10.11646/zootaxa.1360.1.4

De Grave S, Wowor D, Klotz W (2013a) *Caridina acutirostris*. The IUCN Red List of Threatened Species 2013. e.T197725A2497568.

De Grave S, Wowor D, Klotz W (2013b) *Caridina caerulea*. The IUCN Red List of Threatened Species 2013. e.T197973A2507226.

De Grave S, Wowor D, Klotz W (2013c) *Caridina ensifera*. The IUCN Red List of Threatened Species 2013: e.T197967A2506841.

De Grave S, Wowor D, Klotz W (2013d) *Caridina sarasinorum*. The IUCN Red List of Threatened Species 2013: e.T198277A2518617.

De Grave S, Wowor D, Klotz W (2013e) *Caridina schenkeli*. The IUCN Red List of Threatened Species 2013: e.T197587A2491852.

Hoang DT, Chernomor O, von Haeseler A, Minh BQ, Vinh LS (2018) UFBoot2: Improving the ultrafast bootstrap approximation. Molecular Biology and Evolution 35: 518–522. https://doi.org/10.1093/molbev/msx281

Huelsenbeck JP, Ronquist F, Nielsen R, Bollback JP (2001) Bayesian inference of phylogeny and its impact on evolutionary biology. Science, 294: 2310–2314. https://doi.org/10.1126/science.1065889

Katoh K, Standley DM (2013) MAFFT multiple sequence alignment software version 7: improvements in performance and usability. Molecular Biology and Evolution 30: 772–780. https://doi.org/10.1093/molbev/mst010

Kumar S, Stecher G, Li M, Knyaz C, Tamura K (2018) MEGA X: Molecular evolutionary genetics analysis across computing platforms. Molecular Biology and Evolution 35: 1547–1549. https://doi.org/10.1093/molbev/msy096

Lai H-T, Shy J-Y (2009) The larval development of *Caridina pseudodenticulata* (Crustacea: Decapoda: Atyidae) reared in the laboratory, with a discussion of larval metamorphosis types. The Raffles Bulletin of Zoology, Supplement 20: 97–107.

Martin CH, Richards EJ (2019) The paradox behind the pattern of rapid adaptive radiation: how can the speciation process sustain itself through early burst? Annual Review of Ecology, Evolution, and Systematics 50: 569–593. https://doi.org/10.1146/annurev-ecolsys-110617-062443

Nguyen LT, Schmidt HA, von Haeseler A, Minh BQ (2015) IQ-TREE: A fast and effective stochastic algorithm for estimating maximum likelihood phylogenies. Molecular Biology and Evolution 32: 268–274. https://doi.org/10.1093/molbev/msu300

Posada D (2008) jModelTest: phylogenetic model averaging. Molecular Biology and Evolution 25 (7): 1253–1256. https://doi.org/10.1093/molbev/msn083

Ronquist F, Teslenko M, van der Mark P, Ayres DL, Darling A, Höhna S, Larget B, Liu L, Suchard MA, Huelsenbeck JP (2012) MrBayes 3.2: efficient Bayesian phylogenetic inference and model choice across a large model space. Systematic Biology 61: 539–542. https://doi.org/10.1093/sysbio/sys029

Roth-Woltereck E (1958) *Limnocaridina iridinae*, n. sp. Eine interessante Garnele aus dem Tanganijka-See (Decapoda Atyidae). Zoologischer Anzeiger 161: 188–192.

Schenkel E (1902) Beitrag zur Kenntnis der Dekapodenfauna von Celebes. Verhandlungen der Naturforschenden Gesellschaft in Basel 13: 485–585.

Schluter D (2000) The Ecology of Adaptive Radiation. Oxford University Press, Oxford, 296 pp.

Short JW (2004) A revision of Australian river prawns, *Macrobrachium* (Crustacea: Decapoda: Palaemonidae. Hydrobiologia 525: 1–100. https://doi.org/10.1023/B:HYDR.0000038871.50730.95

Streelman JT, Danley PD (2003) The stages of vertebrate evolutionary radiation. Trends in Ecology & Evolution 18: 126–131. https://doi.org/10.1016/S0169-5347(02)00036-8

Sutra N, Kusumi J, Montenegro J, Kobayashi H, Fujimoto S, Masengi KWA, Nagano AJ, Toyoda A, Matsunami M, Kimura R, Yamahira K (2019) Evidence for sympatric speciation in a Wallacean ancient lake. Evolution 73: 1898–1915. https://doi.org/10.1111/evo.13821

Swofford DL (2002) PAUP* (version 4.0). Phylogenetic analysis using parsimony (*and other methods). Sinauer Associates, Sunderland, Massachusetts, USA .

Vaillant JJ, Haffner, GD, Cristecu, ME (2011) The ancient lakes of Indonesia: towards integrated research on speciation. Integrative and Comparative Biology 51(4): 634–643. https://doi.org/10.1093/icb/icr101

von Rintelen K, Cai Y (2009) Radiation of endemic species flocks in ancient lakes: Systematic revision of the freshwater shrimp *Caridina* H. Milne Edwards, 1837 (Crustacea: Decapoda: Atyidae) from the ancient lakes of Sulawesi, Indonesia, with the description of eight new species. The Raffles Bulletin of Zoology 57: 343–452.

von Rintelen K, von Rintelen T, Glaubrecht M (2007a) Molecular phylogeny and diversification of freshwater shrimps (Decapoda, Atyidae, *Caridina*) from ancient Lake Poso (Sulawesi, Indonesia) – the importance of being colourful. Molecular Phylogenetics and Evolution 45: 1033–1041. https://doi.org/10.1016/j.ympev.2007.07.002

von Rintelen K, von Rintelen T, Meixner M, Lüter C, Cai Y, Glaubrecht M (2007b) Freshwater shrimp-sponge association from an ancient lake. Biology Letters 3: 262–264. https://doi.org/10.1098/rsbl.2006.0613

von Rintelen K, Glaubrecht M, Schubart CD, Wessel A, von Rintelen T (2010) Adaptive radiation and ecological diversification of Sulawesi's, ancient lake shrimps. Evolution 64: 3287–99. https://doi.org/10.1111/j.1558-5646.2010.01043.x

von Rintelen T, von Rintelen K, Glaubrecht M, Schubart CD, Herder F (2012) Aquatic biodiversity hotspots in Wallacea: the species flocks in the ancient lakes of Sulawesi Indonesia. In: Gower DJ, Johnson KG, Richardson JE, Rosen BR, Rüber L, Williams ST (Eds) Biotic Evolution and Environmental Change in Southeast Asia. Cambridge University Press, Cambridge, 290–315. https://doi.org/10.1017/CBO9780511735882.014

von Rintelen K, De los Ríos P, von Rintelen T (2020) Standing waters, especially ancient lakes. In: Poore GCB, Thiel M (Eds) The Natural History of the Crustacea: Evolution and Biogeography, Volume 8. Oxford University Press, New York, 296–318.

Wowor D, De Grave S, Klotz W (2013) *Caridina longidigita*. The IUCN Red List of Threatened Species 2013: e.T197820A2501422.

Zitzler K, Cai Y (2006) *Caridina spongicola*, new species, a freshwater shrimp (Crustacea: Decapoda: Atyidae) from the ancient Malili lake system of Sulawesi, Indonesia. The Raffles Bulletin of Zoology 54: 271–276.

Supplementary material 1

Table S1. Sample provenience and accession numbers

Authors: Werner Klotz, Thomas von Rintelen, Daisy Wowor, Chris Lukhaup, Kristina von Rintelen

Data type: molecular data

Link: https://doi.org/10.3897/zookeys.1009.54303.suppl1

Supplementary material 2

Supplementary figures

Authors: Werner Klotz, Thomas von Rintelen, Daisy Wowor, Chris Lukhaup, Kristina von Rintelen

Data type: multimedia

Explanation note: **Figure S1.** Phylogenetic relationships reconstructed by BI analyses of two mitochondrial gene fragments (topology based on concatenated 16S and COI datasets). The scale bar indicates the substitution rate. Original Bayesian posterior probabilities of Fig. 13. **Figure S2.** Phylogenetic relationships reconstructed by ML analyses of two mitochondrial gene fragments (topology based on concatenated 16S and COI datasets). The scale bar indicates the substitution rate. **Figure S3.** Phylogenetic relationships reconstructed by MP analyses of two mitochondrial gene fragments (topology based on concatenated 16S and COI datasets). **Figure S4.** Phylogenetic relationships reconstructed by ML analyses of one mitochondrial gene fragments (16S). The scale bar indicates the substitution rate. **Figure S5.** Phylogenetic relationships reconstructed by ML analyses of one mitochondrial gene fragments (COI). The scale bar indicates the substitution rate.

Link: https://doi.org/10.3897/zookeys.1009.54303.suppl2

ZooKeys 1009: 123–138 (2021)
doi: 10.3897/zookeys.1009.57857
https://zookeys.pensoft.net

RESEARCH ARTICLE

A peer-reviewed open-access journal
ZooKeys
Launched to accelerate biodiversity research

Three new species of the segmented spider genus *Qiongthela* (Mesothelae, Liphistiidae) from Hainan Island, China

Li Yu[1], Fengxiang Liu[2], Zengtao Zhang[2], Daiqin Li[3], Xin Xu[1,2]

1 *College of Life Sciences, Hunan Normal University, Changsha, Hunan 410081, China* **2** *State Key Laboratory of Biocatalysis and Enzyme Engineering, and Centre for Behavioural Ecology and Evolution (CBEE), School of Life Sciences, Hubei University, 368 Youyi Road, Wuhan, Hubei 430062, China* **3** *Department of Biological Sciences, National University of Singapore, 14 Science Drive 4, Singapore 117543, Singapore*

Corresponding author: Xin Xu (xuxin@hunnu.edu.cn); Daiqin Li (dbslidq@nus.edu.sg)

Academic editor: J. Miller | Received 21 August 2020 | Accepted 9 November 2020 | Published 11 January 2021

http://zoobank.org/5CD8C660-7CDB-4664-AF88-B79090215BA3

Citation: Yu L, Liu F, Zhang Z, Li D, Xu X (2021) Three new species of the segmented spider genus *Qiongthela* (Mesothelae, Liphistiidae) from Hainan Island, China. ZooKeys 1009: 123–138. https://doi.org/10.3897/zookeys.1009.57857

Abstract

We report three new species of the segmented trapdoor spider genus *Qiongthela* Xu & Kuntner, 2015 collected from Hainan Island, China based on morphological characters: *Q. dongfang* **sp. nov.** (♂♀), *Q. nankai* **sp. nov.** (♂♀), *Q. yalin* **sp. nov.** (♂♀). We also provide the GenBank accession codes of the DNA barcode gene, cytochrome c oxidase subunit I (COI), of the type specimens of all three new species to aid future identification.

Keywords

DNA barcode, morphology, taxonomy, trapdoor spiders

Introduction

The segmented trapdoor spider genus *Qiongthela* Xu & Kuntner, 2015 is currently distributed in Hainan Island (China) and southern Vietnam (Xu et al. 2015a, b; World Spider Catalog 2020; Fig. 1). It contains 11 described species, nine of which have been recorded from Hainan Island and the remaining two, *Q. australis* (Ono, 2002) and *Q. nui*

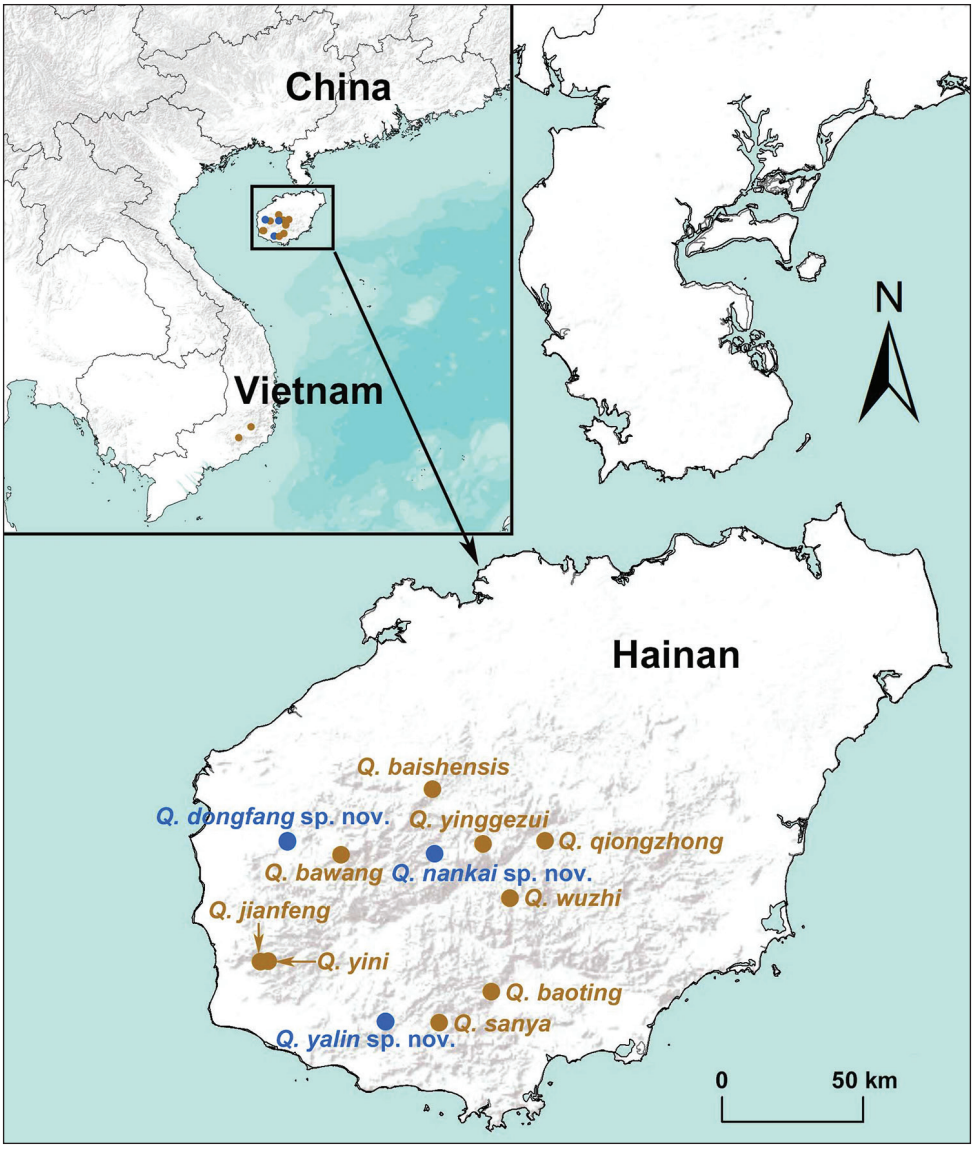

Figure 1. Map showing the type localities of fourteen *Qiongthela* species in southern Vietnam and Hainan Island, China. The type localities of 11 known species are indicated in brown solid circles, and the three new species are indicated in blue solid circles.

(Schwendinger & Ono, 2011), found in southern Vietnam (Ono 2002; Schwendinger and Ono 2011; Xu et al. 2015b; Yu et al. 2020; Word Spider Catalog 2020).

When examining the specimens collected from Hainan Island, we diagnosed three new *Qiongthela* species. Here, we describe these new species based on genital morphology of both males and females. Furthermore, we provide the genetic distances of intraspecific

and interspecific relationships with the closest species based on the DNA barcode gene, cytochrome c oxidase subunit I (COI), to support our descriptions, and also provide the COI sequences of type specimens for future identifications.

Materials and methods

All specimens in this study were collected from Hainan Island, China. We collected them alive, checked for their maturity status, removed the right four legs of adult specimens, preserved the legs in 100% ethanol, and kept them at –80 °C for molecular work. The remains were preserved in 80% ethanol as vouchers for morphological identification and examination. We took juvenile/subadult males back to the laboratory, reared them until they reached sexual maturity, removed the right four legs, and preserved them as described above. All the types and voucher specimens are deposited at the College of Life Sciences, Hunan Normal University, Changsha, Hunan Province, China.

We examined and dissected the specimens using an Olympus SZX16 stereomicroscope. We removed the soft tissues of female genitalia using 10 mg/ml trypsase (Bomei Biotech Company, Hefei, Anhui, China) for at least 3 hours at room temperature. We took photographs of male and female genitals under an Olympus BX53 compound microscope using a CCD digital camera. We conducted all measurements using an MC170HD digital camera mounted on a Leica M205C stereomicroscope and presented the measurements in millimeters. Leg and palp measurements are given in the following order: leg total length (femur + patella + tibia + metatarsus + tarsus), palp total length (femur + patella + tibia + tarsus).

Abbreviations used: ALE = anterior lateral eyes; AME = anterior median eyes; BL = body length; CL = carapace length; Co = conductor; CT = contrategulum; CW =carapace width; E = embolus; HNU = Hunan Normal University; OL = opisthosoma length; OW = opisthosoma width; PC = paracymbium; PLE = posterior lateral eyes; PME = posterior median eyes; RC = receptacular cluster; T = tegulum.

We extracted total genomic DNA from spider legs using the Animal Genomic DNA Isolation Kit (Kangwei Biotech, Beijing, China) following the manufacturer's protocols. We used the primer pair LCO1490/HCO2198 (Folmer et al. 1994) to amplify COI sequences under the following PCR reaction protocol: initial denaturation at 95 °C for 5 min; 35 cycles of denaturation at 95 °C for 1 min, annealing at 40 °C for 1 min, and elongation at 72 °C for 30 s; and final extension at 72 °C for 7 min (Xu et al. 2015c). The 25 μl PCR reactions consisted of 12.5 μl of 2×Taq MasterMix (KangWei Biotech, Beijing, China), 1 μl of each forward and reverse 10 μM primer, 1 μl of genomic DNA, and 9.5 μl of double-distilled H_2O. The PCR products were examined using agarose gel electrophoresis (1% agarose). All PCR products were purified and sequenced at Tsingke Biotechnology Company (Changsha, China). We downloaded all the COI sequences of known *Qiongthela* species from NCBI and calculated genetic distances based on the standard DNA barcode alignment using MEGA v6.0 (Tamura et al. 2013).

Taxonomy

Genus *Qiongthela* Xu & Kuntner, 2015

Type species. *Qiongthela baishensis* Xu, 2015.

Diagnosis. Males of *Qiongthela* can be distinguished from those of all other six Heptathelinae genera by the blade-like conductor narrowing towards the apex (Figs 3A–C, E, 5A–E, 7A–E), and by the tegulum with two obvious apophyses (Figs 3A–E, 5A–E, 7A–E). Females of *Qiongthela* differ from those of all other six Heptathelinae genera by the two pairs of the receptacular clusters with numerous granula (Figs 3H–K, 5H–K, 7H–M) (Xu et al. 2017; Yu et al. 2020).

Species composition. *Q. australis* (Ono, 2002), *Q. baishensis* Xu, 2015, *Q. baoting* Yu, Liu, Zhang, Wang, Li & Xu, 2020, *Q. bawang* Xu, Liu, Kuntner & Li, 2017, *Q. jianfeng* Xu, Liu, Kuntner & Li, 2017, *Q. nui* (Schwendinger & Ono, 2011), *Q. qiongzhong* Yu, Liu, Zhang, Wang, Li & Xu, 2020, *Q. sanya* Yu, Liu, Zhang, Wang, Li & Xu, 2020, *Q. wuzhi* Xu, Liu, Kuntner & Li, 2017, *Q. yinggezui* Yu, Liu, Zhang, Wang, Li & Xu, 2020, *Q. yini* Xu, Liu, Kuntner & Li, 2017.

Distribution. China (Hainan), Vietnam.

Qiongthela dongfang sp. nov.

http://zoobank.org/6A654737-8B5C-48F0-84F6-BC0C14333BAD
Figures 2, 3

Type material. ***Holotype*** ♂: China, Hainan Province, Dongfang City, between Puguang and the 14th Dongfang Farm, 19.08°N, 108.92°E, alt. 160 m, 24 August 2019, D. Li, F.X. Liu, X. Xu and L. Yu leg., XUX–2019–159 (matured on 2 October 2019 at HNU). ***Paratypes*****:** 3 ♀♀, same data as holotype, XUX–2019–156, 157, 160; 1 ♂, same locality as holotype, 5 August 2017, D. Li, F.X. Liu, Z.T. Zhang and X. Xu leg., XUX–2017–065 (♂ matured on 20 October 2018 at HNU).

Diagnosis. Males of *Q. dongfang* sp. nov. resemble those of *Q. jianfeng*, but can be distinguished from the latter by the tegular marginal apophysis with a pointed, sharp apex (Fig. 3D, E, G) and the tegular terminal apophysis with a hook-like apex (Fig. 3A, B); from those of the rest of *Qiongthela* species by the conductor base with a semioval apophysis ventrally (Fig. 3E). Females of *Q. dongfang* sp. nov. differ from those of *Q. bawang* and *Q. qiongzhong* by the receptacular clusters all similar in size and with short genital stalks (Fig. 3H–K); from those of *Q. nankai* sp. nov. by the bases of middle receptacular clusters separated from each other (Fig. 3H–K); from those of the rest of *Qiongthela* species by the two paired receptacular clusters separated from each other, and situated along the anterior margin of the bursa copulatrix and all similar in size (Fig. 3H–K).

Description. Male (holotype, Fig. 2D). Carapace light brown; opisthosoma brown, with 12 dark brown tergites, close to each other, the first 2–7 larger than the

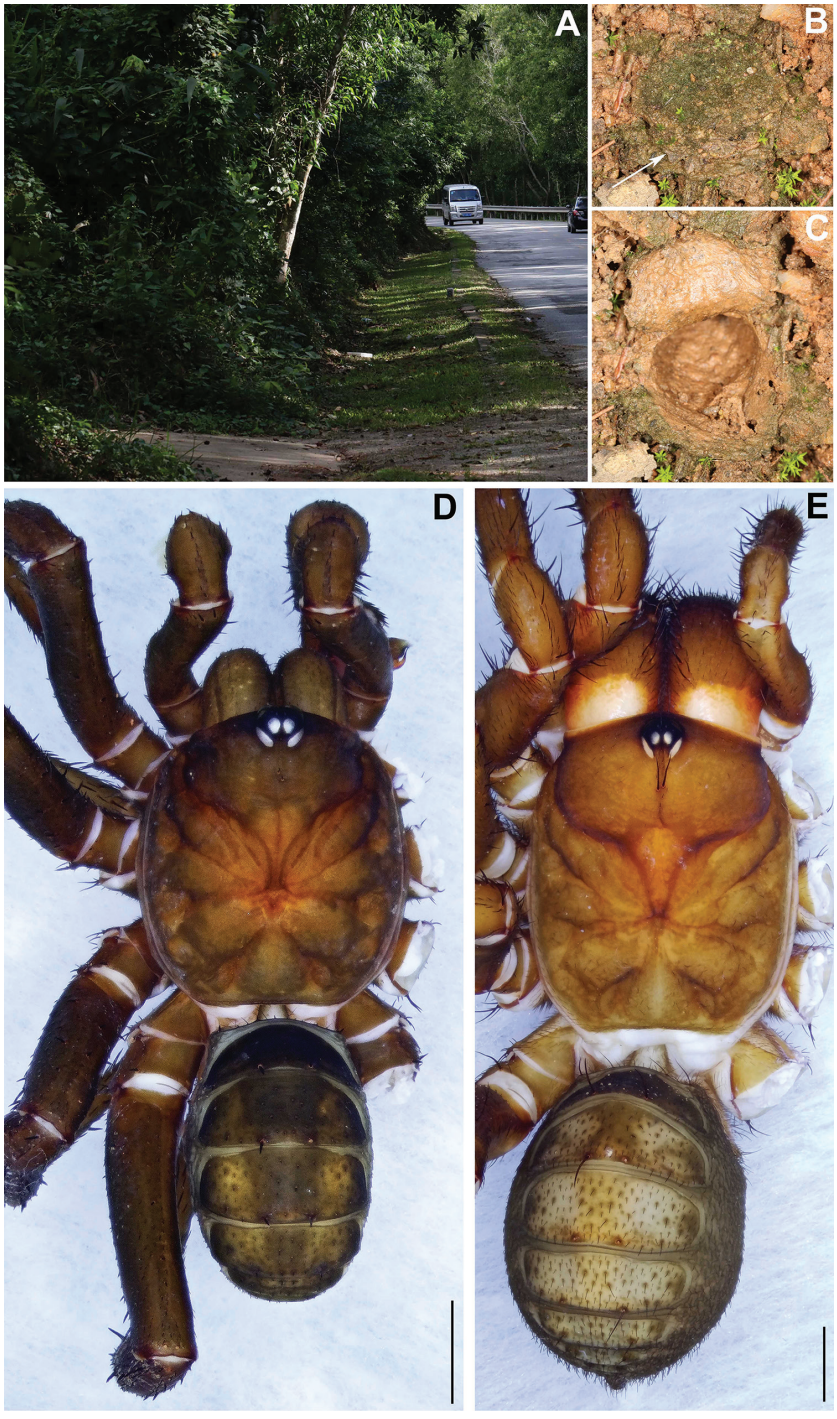

Figure 2. Microhabitat and general somatic morphology of *Qiongthela dongfang* sp. nov. **A** microhabitat **B, C** trapdoor with door closed and open **D** male (XUX–2019–159, holotype) **E** female (XUX–2019–157); Scale bars: 2 mm (**D, E**).

others, and the fourth largest; sternum narrow, much longer than wide; a few fine pointed hairs running over the ocular area; chelicerae with promargin of cheliceral groove bearing 8 denticles; legs with firm hairs and spines; 7 spinnerets. Measurements: BL 10.89, CL 5.35, CW 4.85, OL 5.26, OW 3.56; ALE > PLE > PME > AME; leg I 16.22 (4.82 + 1.45 + 3.59 + 4.33 + 2.03), leg II 15.90 (4.48 + 1.30 + 3.58 + 4.37 + 2.17), leg III 15.34 (3.83 + 1.08 + 3.25 + 4.63 + 2.55), leg IV 20.64 (4.95 + 1.10 + 4.43 + 7.00 + 3.16).

***Palp*.** Cymbium with a short projection dorsally (Fig. 3G); paracymbium unpigmented and unsclerotised prolaterally, with numerous setae at the tip (Fig. 3A–C). Contrategulum with two edges distally: the inner one finely dentate, the outer one sharp, semi-translucent (Fig. 3D–F). Marginal apophysis of the tegulum long, pointed, wide basally, with a sharp apex (Fig. 3D), proximally-directed terminal apophysis of tegulum with several denticles, narrowing to a hooked apex (Fig. 3A, B, E). Conductor situated ventro-proximally on the embolus, basal portion fused with the embolus and forming a semioval apophysis ventrally, distal portion free, narrowing to a slightly bent apex (Fig. 3A, B, E). Embolus largely sclerotised, with a wide, flat opening of the sperm duct distally (Fig. 3B, C, E).

Female (Fig. 2E). Carapace reddish brown; opisthosoma brown, with 12 light brown tergites, close to each other, the first 2–7 larger than the others, and the fourth largest; sternum narrow, much longer than wide; a few fine pointed hairs running over the ocular area; chelicerae robust with promargin of cheliceral groove containing 10 denticles of variable size; legs with firm hairs and spines; 7 spinnerets. Measurements: BL 17.47, CL 8.25, CW 6.78, OL 8.36, OW 6.43; ALE > PLE > PME > AME; palp 11.01 (3.66 + 1.40 + 2.81 + 3.14), leg I 15.16 (4.87 + 1.89 + 3.54 + 3.07 + 1.79), leg II 14.86 (4.78 + 1.85 + 3.20 + 3.15 + 1.88), leg III 15.37 (4.37 + 1.94 + 3.04 + 3.74 + 2.28), leg IV 22.99 (6.70 + 2.58 + 4.55 + 6.06 + 3.10).

***Female genitalia*.** Two pairs of similar-sized receptacular clusters along the anterior margin of the bursa copulatrix, with short genital stalks (Fig. 3H–K).

Variation. Males and females vary in body size. Range of measurements in males (N = 2): BL 10.89–14.76, CL 5.35–7.20, CW 4.85–6.50, OL 5.26–7.18, OW 3.56–4.58; in females (N = 3): BL 12.63–17.47, CL 6.00–8.25, CW 5.46–6.78, OL 6.19–8.36, OW 4.93–6.43.

Etymology. The species epithet, a noun in apposition, refers to the type locality.

Distribution. Hainan (Dongfang), China

GenBank accession number. XUX–2019–159: MT900751.

Remarks. The maximum and mean intraspecific genetic distances of *Q. dongfang* sp. nov. are 0.3% and 0.2% based on Kimura 2-parameter (K2P) model, respectively (N = 5). We calculated the interspecific genetic distance between the holotypes of the two closest species. The genetic distances between *Q. dongfang* sp. nov. and *Q. jianfeng* (GenBank accession code: KP229838 (paratype); we used the sequence of paratype because the DNA barcodes of the holotype and paratype are identical; Xu et al. 2017), *Q. nankai* sp. nov., and *Q. yalin* sp. nov. are 7.7%, 15.7%, and 9.1% based on K2P, respectively.

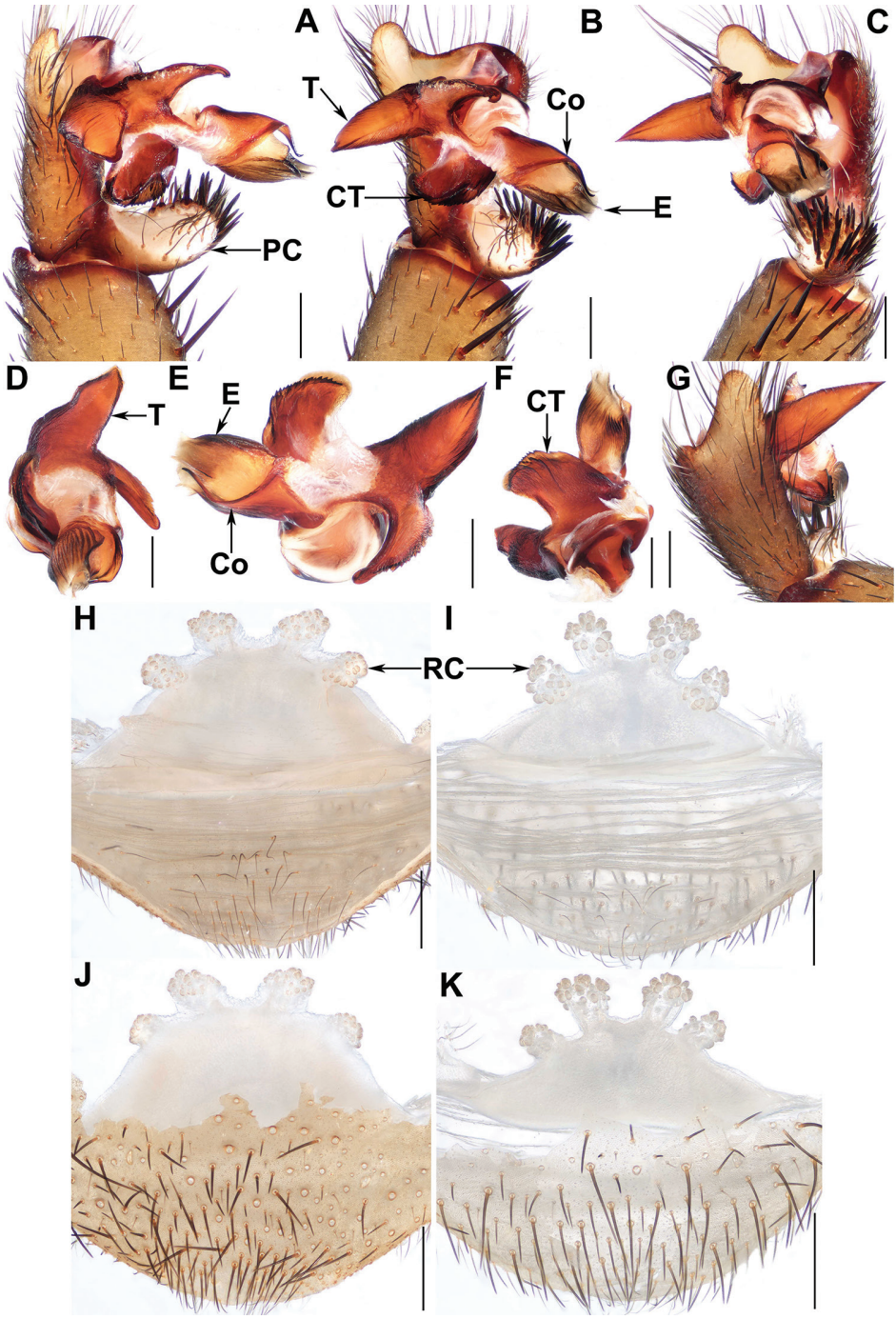

Figure 3. Male and female genital anatomy of *Qiongthela dongfang* sp. nov. **A** left palp, prolateral view **B, E** left palp, ventral view **C** left palp, retrolateral view **D** left palp, distal view **F, G** left palp, dorsal view **H, I** vulva, dorsal view **J, K** vulva, ventral view **A–C, G** XUX–2019–159 (holotype) **D–F** XUX–2017–065 **H, J** XUX–2019–157 **I, K** XUX–2019–160; Scale bars: 0.5 mm.

***Qiongthela nankai* sp. nov.**
http://zoobank.org/7A75CB1F-E032-40BC-906D-F79CEAC64B96
Figures 4, 5

Type material. ***Holotype*** ♂: China, Hainan Province, Baisha City, Nankai Town, Nankai Village, 19.04°N, 109.39°E, alt. 300 m, 26 August 2019, D. Li, F.X. Liu, X. Xu and L. Yu leg., XUX–2019–174 (matured on 10 September 2019 at HNU). ***Paratypes*:** 1 ♂, 2 ♀♀, same data as holotype, XUX–2019–172, 173, 175.

Diagnosis. Males of *Q. nankai* sp. nov. can be distinguished from those of *Q. qiongzhong*, *Q. yalin* sp. nov. and *Q. yinggezui* by the straight tegular marginal apophysis (Fig. 5A, D), and the cymbial projection short and thick (Fig. 5G); from those of *Q. australis* by the conductor with a bent apex (Fig. 5C, E, G), and the longer tegular marginal apophysis (Fig. 5A, C, D, F); from those of *Q. dongfang* sp. nov., *Q. jianfeng* and *Q. sanya* by the tegular terminal apophysis with an abruptly narrowed and hooked apex (Fig. 5A–E); from those of *Q. nui* by the tegular marginal apophysis with a blunt edge (Fig. 5A–G); from those of the rest of *Qiongthela* species by the contrategulum with two distal edges (Fig. 5A, D). Females of *Q. nankai* sp. nov. differ from those of *Q. dongfang* sp. nov. and *Q. wuzhi* by the middle receptacular clusters situated close to each other (Fig. 5H–K); from those of *Q. bawang* and *Q. qiongzhong* by the two pairs of receptacular clusters similar in size and shape (Fig. 5H–K); from those of the rest of *Qiongthela* species by similar-sized receptacular clusters, and all situated along the anterior margin of the bursa copulatrix (Fig. 5H–K).

Description. Male (holotype, Fig. 4D). Carapace reddish brown; opisthosoma brown, with 12 yellow tergites, close to each other, the first 2–7 larger than the others, and the fourth largest; sternum narrow, much longer than wide; a few fine pointed hairs running over the ocular area; chelicerae with promargin of cheliceral groove bearing 11 denticles of variable size; legs with firm hairs and spines; 7 spinnerets. Measurements: BL 11.44, CL 5.31, CW 5.12, OL 5.63, OW 3.62; ALE > PLE > PME > AME; leg I 14.01 (3.91 + 0.95 + 3.18 + 3.94 + 2.03), leg II 14.76 (4.05 + 1.30 + 3.28 + 4.00 + 2.13), leg III 15.64 (3.94 + 1.53 + 3.09 + 4.61 + 2.47), leg IV 21.12 (5.48 + 1.34 + 4.56 + 6.43 + 3.31).

***Palp*.** Cymbium with a short projection dorsally (Fig. 5G); paracymbium unpigmented and unsclerotised prolaterally, with numerous setae at the tip (Fig. 5A–C). Contrategulum with an irregular dentate edge proximally and two edges distally: the inner one dentate, and the outer one sharp, semi-translucent (Fig. 5A, D, F). Marginal apophysis of tegulum long, with a blunt apex distally, distal portion of similar width as basal portion (Fig. 5A, D), a proximally directed terminal apophysis of the tegulum with few denticles, abruptly narrowing to a hooked apex (Fig. 5A–E). Conductor situated ventro-proximally on the embolus, the basal portion fused with the embolus, distal portion free, narrowing to a bent apex (Fig. 5A–E). Embolus largely sclerotised, smooth ventrally, with several longitudinal ribs retrolaterally, and with a wide, flat opening of the sperm duct distally (Fig. 5A, D, E).

Female (Fig. 4E). Carapace and opisthosoma color like in male, 12 opisthosoma tergites, close to each other, the first 2–7 larger than the others, and the fourth largest;

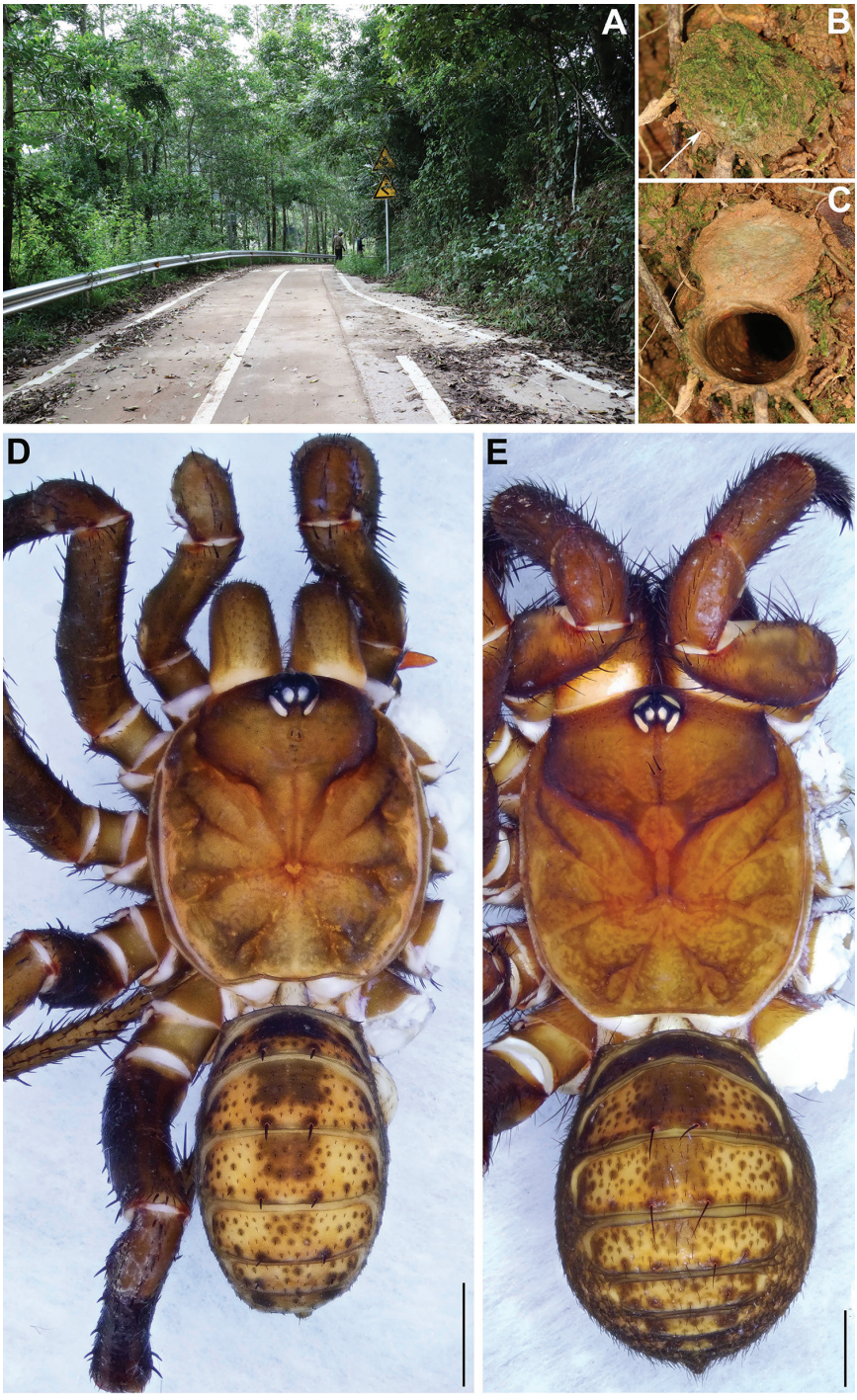

Figure 4. Microhabitat and general somatic morphology of *Qiongthela nankai* sp. nov. **A** microhabitat **B, C** trapdoor with door closed and open **D** male (XUX–2019–174, holotype) **E** female (XUX–2019–173); Scale bars: 2 mm (**D, E**).

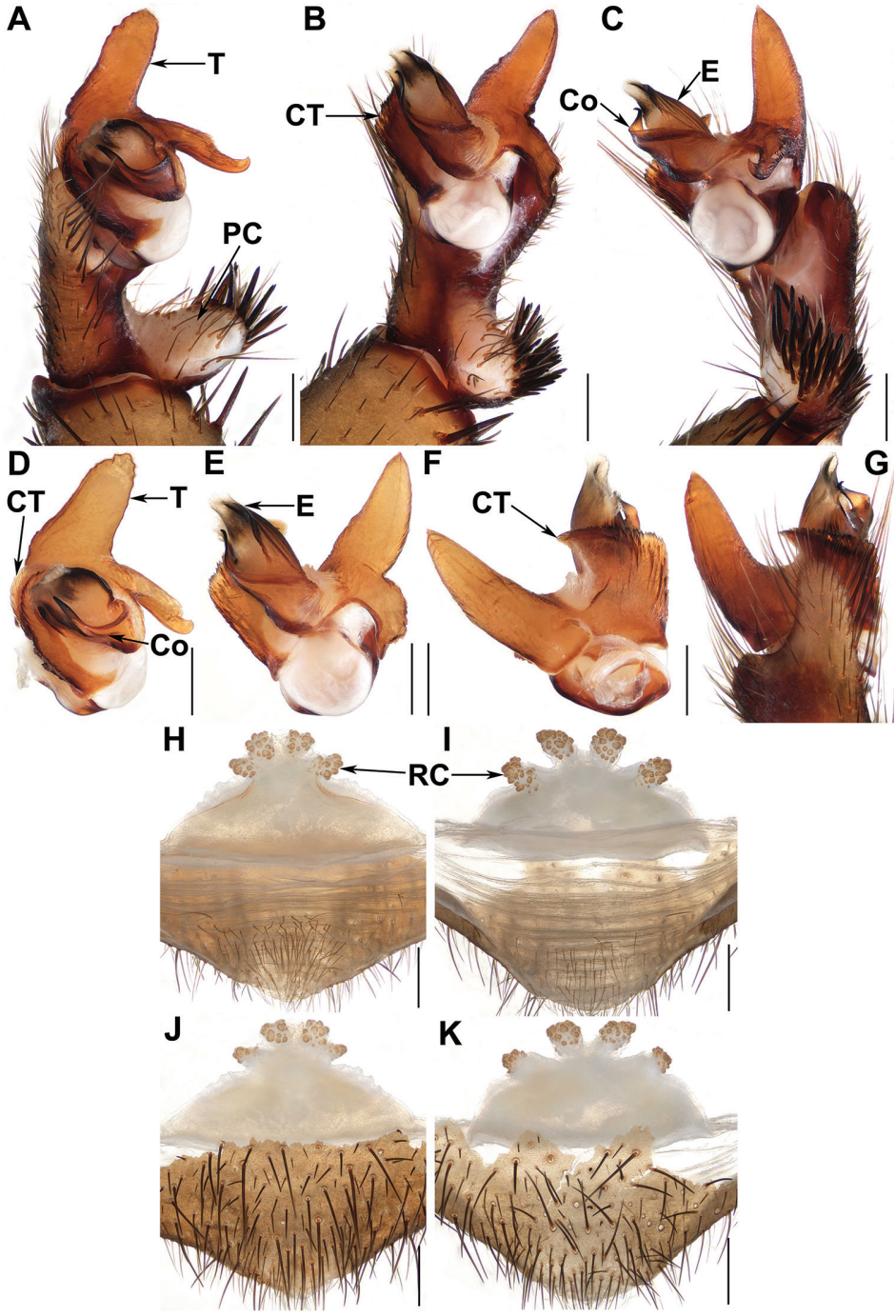

Figure 5. Male and female genital anatomy of *Qiongthela nankai* sp. nov. **A** left palp, prolateral view **B, E** left palp, ventral view **C** left palp, retrolateral view **D** left palp, distal view **F, G** left palp, dorsal view **H, I** vulva, dorsal view **J, K** vulva, ventral view **A–C, G** XUX–2019–174 (holotype) **D–F** XUX–2019–172 **H, J** XUX–2019–173 **I, K** XUX–2019–175; Scale bars: 0.5 mm.

sternum narrow, much longer than wide; a few fine pointed hairs running over the ocular area; chelicerae robust with promargin of cheliceral groove containing 10 denticles of variable size; legs with firm hairs and spines; 7 spinnerets. Measurements: BL 17.48, CL 8.45, CW 7.56, OL 8.47, OW 6.49; ALE > PLE > PME > AME; palp 14.11 (5.02 + 1.93 + 3.41 + 3.75), leg I 15.49 (4.90 + 1.72 + 3.72+ 3.21 + 1.94), leg II 15.79 (4.91 + 1.97 + 3.41 + 3.38 + 2.12), leg III 16.31 (4.64 + 1.93 + 3.50 + 4.00 + 2.24), leg IV 23.11 (6.47 + 2.18 + 5.08 + 6.21 + 3.17).

***Female genitalia*.** Two pairs of receptacular clusters along the anterior margin of the bursa copulatrix, of similar size and shape, and the middle ones close to each other, with very short genital stalks (Fig. 5H–K).

Variation. Males and females vary in body size. Range of measurements in males (*N* = 2): BL 11.44–12.13, CL 5.31–5.65, CW 5.12–5.56, OL 5.63–6.35, OW 3.62–4.69; in females (*N* = 2): BL 13.09–17.48, CL 6.63–8.45, CW 6.04–7.56, OL 6.32–8.47, OW 5.05–6.49.

Etymology. The species epithet, a noun in apposition, refers to the type locality.

Distribution. Hainan (Baisha), China

GenBank accession number. XUX–2019–174: MT900752.

Remarks. The maximum and mean intraspecific genetic distances of *Q. nankai* sp. nov. are 0.6% and 0.3% based on K2P, respectively (*N* = 4). The interspecific genetic distances between *Q. nankai* sp. nov., *Q. baishensis* (GenBank accession code: KP229805), and *Q. yalin* sp. nov. are 10.3% and 16.1% based on K2P, respectively.

***Qiongthela yalin* sp. nov.**

http://zoobank.org/FDD06B09-7B47-4055-84F4-4BD552242BD2

Figures 6, 7

Type material. ***Holotype*** ♂: China, Hainan Province, Sanya City, Yalinling, 18.51°N, 109.24°E, alt. 220 m, 22 August 2019, D. Li, F.X. Liu, X. Xu and L. Yu leg., XUX–2019–140 (matured on 2 October 2019 at HNU). ***Paratypes*:** 1 ♂, 2 ♀♀, same data as holotype; XUX–2019–138 (♂ matured on 6 November 2019 at HNU), XUX–2019–139, 141; 1 ♀; same locality as holotype, 18.50°N, 109.23°E, alt. 240 m, 1 August 2017, D. Li, F.X. Liu, Z.T. Zhang and X. Xu leg., XUX–2017–033.

Diagnosis. Males of *Q. yalin* sp. nov. resemble those of *Q. sanya*, but can be distinguished from the latter by the narrower conductor base (Fig. 7A, D) and by the cymbium with a longer and more slender projection (Fig. 7G); from those of *Q. dongfang* sp. nov. by the tegular marginal apophysis slightly longer and with a blunt apex (Fig. 7A, D), and the cymbium with an elongated projection (Fig. 7G); from those of the rest of *Qiongthela* species by the contrategulum with a smooth edge proximally (Fig. 7F, G). Females of *Q. yalin* sp. nov. differ from those of *Q. sanya* by the middle receptacular clusters having short, indistinct genital stalks (Fig. 7I, L); from those of *Q. australis*, *Q. yini* and *Q. yinggezui* by the smaller middle receptacular clusters compared with the lateral ones (Fig. 7H–M); from those of the rest of *Qiongthela* species

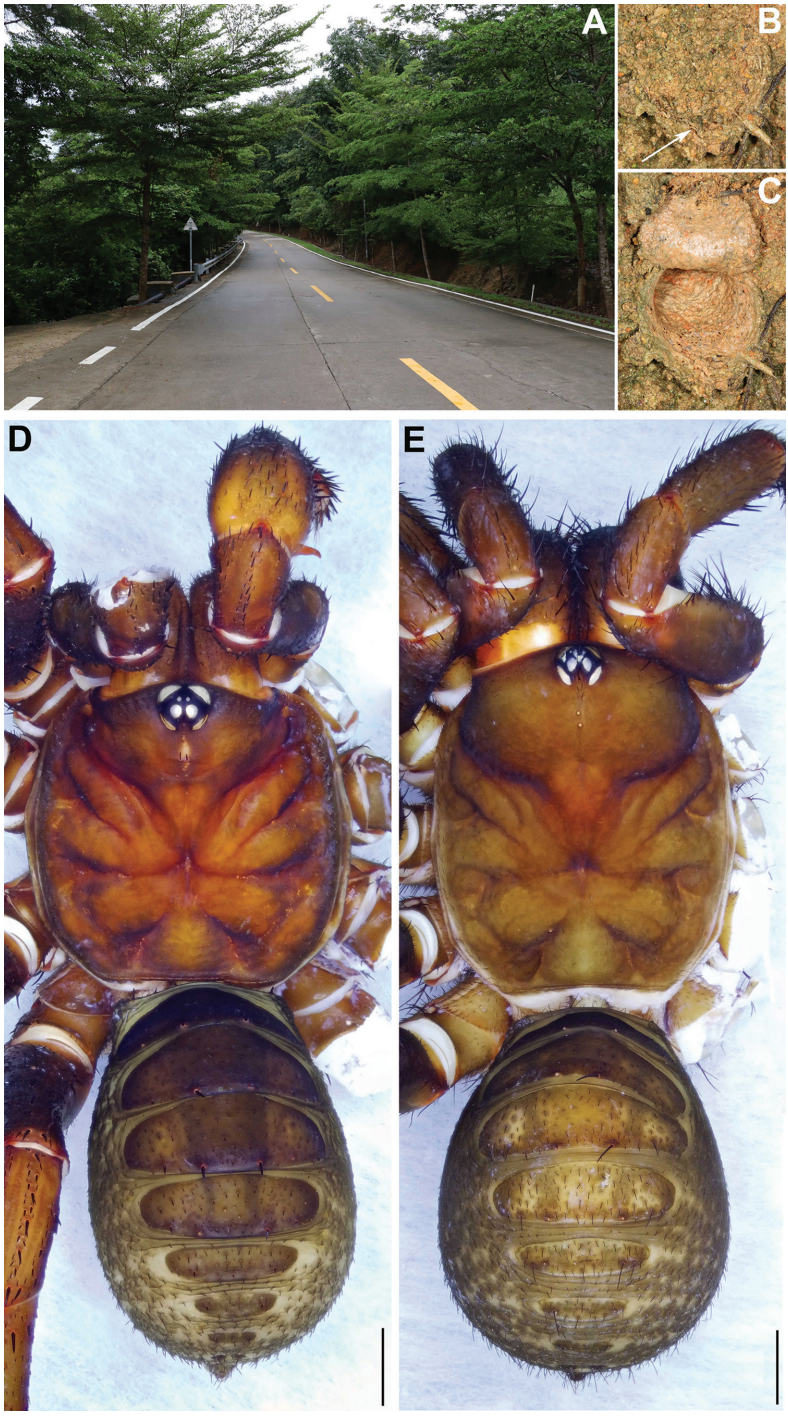

Figure 6. Microhabitat and general somatic morphology of *Qiongthela yalin* sp. nov. **A** microhabitat **B, C** trapdoor with door closed and open **D** male (XUX–2019–140, holotype) **E** female (XUX–2019–139); Scale bars: 2 mm (**D, E**).

by the middle receptacular clusters situated along the anterior margin of the bursa copulatrix, the laterals located slightly on the dorsal wall of the bursa copulatrix, and the trapezoidal bursa copulatrix (Fig. 7H–M).

Description. Male (holotype, Fig. 6D). Carapace reddish brown; opisthosoma brown, with 12 dark brown tergites, close to each other, the first 2–7 larger than the others, and the fourth largest; sternum narrow, much longer than wide; a few fine pointed hairs running over the ocular area; chelicerae with promargin of cheliceral groove bearing 9 denticles of variable size; legs with firm hairs and spines; 7 spinnerets. Measurements: BL 16.80, CL 7.52, CW 7.72, OL 9.13, OW 6.52; ALE > PLE > PME > AME; leg I 26.07 (7.40 + 1.96 + 6.12 + 7.23 + 3.36), leg II 25.66 (7.00 + 1.92 + 5.81 + 7.21 + 3.72), leg III 25.51 (6.06 + 1.70 + 5.40 + 8.10 + 4.25), leg IV 33.43 (8.64 + 2.44 + 7.18 + 10.26 + 4.91).

***Palp*.** Cymbium with a slender projection dorsally (Fig. 7G); paracymbium unpigmented and unsclerotised prolaterally, with numerous setae at the tip (Fig. 7A–C). Contrategulum with a smooth edge proximally and two edges distally: the inner one with fine, small denticles, the outer one smooth, sharp, semi-translucent, fused with the inner at the middle of the contrategulum (Fig. 7A, D, F). Tegulum with a long, slightly curved, distally blunt marginal apophysis (Fig. 7A, D), the proximally directed terminal apophysis with a dentate margin, continuously narrowing to a rounded, hooked apex (Fig. 7A–E). Conductor situated ventro-proximally on the embolus, fused with the embolus at the basal portion, distal portion free, narrowing to a slightly bent apex (Fig. 7A–E). Embolus largely sclerotised, with a wide, flat opening of the sperm duct distally, ventrally smooth, retrolaterally with several longitudinal ribs (Fig. 7B, C, E).

Female (Fig. 6E). Carapace light brown; opisthosoma brown, with 12 brown tergites, separate from each other, the first 2–7 larger than the others, and the fourth largest; sternum narrow, nearly twice as long as wide; a few fine pointed hairs running over the ocular area; chelicerae robust with promargin of cheliceral groove containing 9 denticles of variable size; legs with firm hairs and spines; 7 spinnerets. Measurements: BL 18.31, CL 8.60, CW 7.47, OL 9.16, OW 7.52; ALE > PLE > PME > AME; palp 14.72 (5.12 + 1.88 + 3.53 + 4.19), leg I 17.23 (5.56 + 2.14 + 3.82 + 3.61 + 2.10), leg II 16.69 (5.46 + 2.22 + 3.42 + 3.33 + 2.26), leg III 17.17 (5.32 + 2.40 + 3.07 + 3.97 + 2.41), leg IV 24.44 (7.27 + 2.34 + 5.28 + 6.25 + 3.30).

***Female genitalia*.** The middle receptacular clusters along the anterior margin of the bursa copulatrix, the lateral ones located slightly on the dorsal wall of the bursa copulatrix; the middle ones smaller than the lateral ones, with indistinct genital stalks; bursa copulatrix trapezoidal (Fig. 7H–M).

Variation. Males and females vary in body size. Range of measurements in males (N = 2): BL 15.76–16.80, CL 6.92–7.52, CW 6.18–7.72, OL 7.48–9.13, OW 5.89–6.52; in females (N = 3): BL 18.31–29.27, CL 8.60–14.19, CW 7.47–11.67, OL 9.16–13.68, OW 7.52–11.08.

Etymology. The species epithet, a noun in apposition, refers to the type locality.

Distribution. Hainan (Sanya), China

GenBank accession number. XUX–2019–140: MT900753.

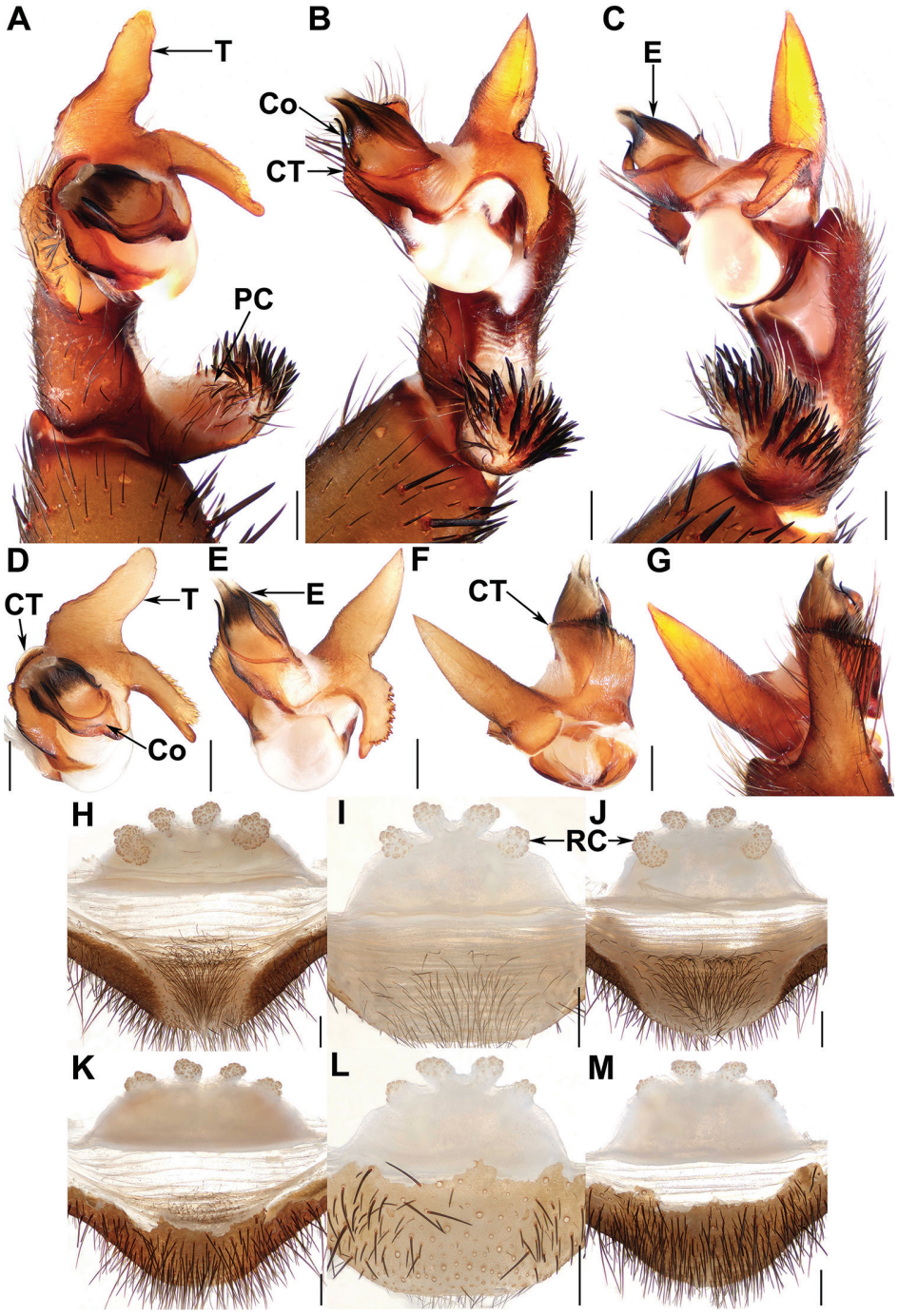

Figure 7. Male and female genital anatomy of *Qiongthela yalin* sp. nov. **A** left palp, prolateral view **B, E** left palp, ventral view **C** left palp, retrolateral view **D** left palp, distal view **F, G** left palp, dorsal view **H–J** vulva, dorsal view **K–M** vulva, ventral view **A–C, G** XUX–2019–140 (holotype) **D–F** XUX–2019–138 **H, K** XUX–2017–033 **I, L** XUX–2019–139 **J, M** XUX–2019–141; Scale bars: 0.5 mm.

Remarks. Both maximum and mean intraspecific genetic distances of *Q. yalin* sp. nov. are 0% based on K2P ($N = 5$). The interspecific genetic distance between *Q. yalin* sp. nov. and *Q. sanya* (GenBank accession code: MN911990) is 7.2% based on K2P.

Acknowledgements

This study was supported by the National Natural Sciences Foundation of China (NSFC-31601850; NSFC-32070430; NSFC-31272324), the Hunan Provincial Natural Science Foundation of China (2017JJ3202), and the Singapore Ministry of Education AcRF Tier 1 grant (R-154-000-A52-114). We thank Dengqing Li and Zhaoyang Chen for their assistance in rearing spiders in the laboratory. We also thank Hirotsugu Ono and Rebecca Godwin for their valuable comments on the manuscript. We are grateful to the Animal Nutrition and Human Health Laboratory, Mineral Nutrition Laboratory as well as Plant Development Laboratory of the College of Life Sciences, Hunan Normal University for supporting the molecular work.

References

Folmer O, Black M, Hoeh W, Lutz R, Vrijenhoek R (1994) DNA primers for amplification of mitochondrial cytochrome c oxidase subunit I from diverse metazoan invertebrates. Molecular Marine Biology and Biotechnology 3: 294–299.

Ono H (2002) Occurrence of a heptatheline spider (Araneae, Liphistiidae) in Lam Dong province, Vietnam. Bulletin of the National Museum of Nature and Science Tokyo (A) 28: 119–122.

Schwendinger PJ, Ono H (2011) On two *Heptathela* species from southern Vietnam, with a discussion of copulatory organs and systematics of the Liphistiidae (Araneae: Mesothelae). Revue Suisse de Zoologie 118: 599–637. https://doi.org/10.5962/bhl.part.117818

Tamura K, Stecher G, Peterson D, Filipski A, Kumar S (2013) MEGA6: Molecular evolutionary genetics analysis version 6.0. Molecular Biology and Evolution 30(12): 2725–2729. https://doi.org/10.1093/molbev/mst197

World Spider Catalog (2020) World spider catalog, Version 21.5. Natural History Museum Bern. http://wsc.nmbe.ch [access on 16 December 2020]

Xu X, Liu FX, Cheng RC, Chen J, Xu X, Zhang ZS, Ono H, Pham DS, Norma-Rashid Y, Arnedo MA, Kuntner M, Li D (2015a) Extant primitively segmented spiders have recently diversified from an ancient lineage. Proceedings of the Royal Society of London B: Biological Sciences 282(1808): e20142486. https://doi.org/10.1098/rspb.2014.2486

Xu X, Liu FX, Chen J, Ono H, Li D, Kuntner M (2015b) A genus-level taxonomic review of primitively segmented spiders (Mesothelae, Liphistiidae). ZooKeys 488: 121–151. https://doi.org/10.3897/zookeys.488.8726

Xu X, Liu FX, Chen J, Li D, Kuntner M (2015c) Integrative taxonomy of the primitively segmented spider genus *Ganthela* (Araneae: Mesothelae: Liphistiidae): DNA barcoding

gap agrees with morphology. Zoological Journal of the Linnean Society 175(2): 288–306. https://doi.org/10.1111/zoj.12280

Xu X, Liu FX, Kuntner M, Li D (2017) Four new species of the primitively segmented spider genus *Qiongthela* from Hainan island, China (Mesothelae, Liphistiidae). ZooKeys 714: 1–11. https://doi.org/10.3897/zookeys.714.19858

Yu L, Liu FX, Zhang ZT, Wang Y, Li DQ, Xu X (2020). Four new species of the primitively segmented spider genus *Qiongthela* from Hainan Island, China (Mesothelae, Liphistiidae). ZooKeys 911: 51–66. https://doi.org/10.3897/zookeys.911.48703

ZooKeys 1009: 139–151 (2021)
doi: 10.3897/zookeys.1009.61515
https://zookeys.pensoft.net

RESEARCH ARTICLE

A peer-reviewed open-access journal
ZooKeys
Launched to accelerate biodiversity research

Notes on the genus *Xestopus* from China, with description of a new species (Carabidae,Sphodrini, Dolichina)

Pingzhou Zhu[1,2], David H. Kavanaugh[3,4], Hongbin Liang[1]

1 *Key Laboratory of Zoological Systematics and Evolution, Institute of Zoology, Chinese Academy of Sciences, Beijing 100101, China* **2** *College of Life Science, University of Chinese Academy of Sciences, Beijing 100049, China* **3** *Department of Entomology, California Academy of Sciences, Golden Gate Park, San Francisco, CA 94118, USA* **4** *Research Professor, Biology, San Francisco State University, San Francisco, California, USA*

Corresponding author: Hongbin Liang (lianghb@ioz.ac.cn)

Academic editor: T. Assmann | Received 1 December 2020 | Accepted 27 December 2020 | Published 11 January 2021

http://zoobank.org/3E78899F-3A6F-4C21-A690-4375A15EA34A

Citation: Zhu P, Kavanaugh DH, Liang H (2021) Notes on the genus *Xestopus* from China, with description of a new species (Carabidae, Sphodrini, Dolichina). ZooKeys 1009: 139–151. https://doi.org/10.3897/zookeys.1009.61515

Abstract

The genus *Xestopus* Andrewes, 1937 in China is reviewed, with the description of a new species: *X. gutangensis* Zhu & Kavanaugh, **sp. nov.** (type locality: Xizang: Mêdog, 29.46414°N, 95.73563°E). The male of *X. cyaneus* Sciaky & Facchini, 1997 is described for the first time, and the first record of this species in Yunnan, China, represents an eastward range extension for the species. A key is provided for the eight known species of the genus.

Keywords

China, Dolichina, endophallus, key, new species, *Xestopus*

Introduction

Xestopus Andrewes, 1937 (Sphodrini, Dolichina) is a small genus previously comprised of seven species, all distributed along the Himalaya (Nepal, Bhutan, China, and Myanmar). This genus is differentiated from related genera mainly by its larger size (15 mm > BL > 25 mm) and the hooked right paramere of the male genitalia (Sciaky and Wrase 1998).

Before the present study, only one species, *Xestopus cyaneus* Sciaky & Facchini, 1997, had been recorded from China. This species is distinct among *Xestopus* species, with its bluish elytra, absence of the anterior pair of supraorbital setae, full-sized hind wings, and smaller size (16 mm) (Sciaky and Facchini 1997). In recent expeditions to Xizang, China, specimens of *X. cyaneus* and a new species were collected. The new species is very similar to *X. cyaneus*, except for the presence of the anterior pair of supraorbital setae.

In this article, we (1) describe the new species, (2) provide additional morphological data for *X. cyaneus*, including the first descriptions of male and female genitalia, (3) discuss previous erroneous distributional records, and (4) provide a revised key to all known species of genus *Xestopus*.

Materials and methods

Specimens examined during our study are deposited in the following collections:

CAS California Academy of Science, San Francisco, USA;
CCCC Collection of Changchin Chen, Tianjin, China;
CRS Collection of Riccardo Sciaky, Milano, Italy;
IZAS Institute of Zoology, Chinese Academy of Sciences, Beijing, China;
NZSI Zoological Survey of India, National Zoological Collection, Calcutta, India.

Abbreviations for measurements used in the paper are as follows: body length (**BL**) was measured from the apical margin of the labrum to the elytral apex; body width (**BW**) was measured across the elytral greatest width (**EW**). Pronotum width (**PW**) was measured across its greatest width; basal width (**PBW**) was measured along its basal margin; apical width (**PAW**) was measured between the apices of the anterior angle, pronotum length (**PL**) was measured along its median line. Elytra length (**EL**) was measured along the suture from the base of the scutellum to the elytra apex. The methods of dissection, illustrations, and measurements mainly follow our previous work (Shi et al. 2013; Shi and Liang 2015).

Taxonomy

Genus *Xestopus* Andrewes, 1937

Andrewes 1937: 59; Morvan 1979: 41 (mentioned only); Casale 1981: 389 (key to species); Morvan 1982: 45 (described new species); Casale 1988: 138 (placed in Dolichina); Sciaky and Facchini 1997: 235 (described new species); Sciaky and Wrase 1998: 223 (key to genera of Dolichina); Lorenz 1998: 373 (catalogue); Hovorka and Sciaky 2003: 530 (catalogue); Lorenz 2005: 399 (catalogue); Hovorka 2017: 769 (catalogue); Schmidt and Will 2020: 336 (diagnosis).

Synonym: *Nepalocalathus* Habu, 1973: 100, type species *Calathus kumatai* Habu, 1973; Habu 1978: 302 (raised to genus rank and transferred to Dolichina); Casale 1981: 389 (synonymized with *Xestopus*).

Synonym: *Wittmerosphodrus* Morvan, 1978: 100, type species *Wittmerosphodrus walteri* Morvan, 1978; Morvan 1979: 36 (described a new species); Casale 1981: 389 (synonymized with *Xestopus*).

Type species. *Pristonychus alticola* Fairmaire, 1889 (type locality: Mountain Yeomatong, North Myanmar; holotype in NZSI), by monotypy.

Diagnosis. Among the seven genera of Dolichina, *Xestopus* can be distinguished from others by the following character combination: third antennomere very long, usually longer than the first two antennomeres combined; tooth of mentum bifid; pronotum more or less cordiform; elytra with microsculpture nearly isodiametric, parascutellar seta present, elytral disc without setigerous pores; lateral grooves absent on metatarsomeres I–IV; males with right paramere hooked at apex; female apical gonocoxite with one ensiform seta at external margin (in most specimens) and sensory pit absent. Detailed descriptions and a key to the genera in the subtribe Dolichina have been provided by Casale (1981) and Sciaky and Wrase (1998).

Comparisons. This genus is most similar to the genus *Dolichus* Bonelli, sharing the large body size (>15 mm), but its members differ from those of the latter in having the tooth of the mentum bifid, the pronotum cordiform, elytral interval 3 without setigerous pores, and the right paramere of male genitalia apically hooked.

Distribution. This genus includes eight species distributed along the Himalayas (two in Nepal, three in Bhutan, two in China, and one in Myanmar).

Remarks. The type species of this genus, *Xestopus alticola* (Fairmaire, 1889) was described from Mount Yeomatong, northern Myanmar. In the two versions of the *Catalogue of Palearctic Coleoptera* (Hovorka and Sciaky 2003; Hovorka 2017), the distribution of this species includes Sichuan and Sikkim and both these two are doubtful. The record for Sikkim was added by Andrewes (1937); however, this locality and the type locality are extremely distant from each other for a species with apterous members. In addition, the record for Sikkim maybe a different species (Morvan 1979; Casale 1981). No other literature records have reported *X. alticola* from Sichuan, and, in fact, no *Xestopus* specimens have been found in that province during our many expeditions in Sichuan, so we also doubt the reliability of this distributional record.

Casale (1981) pointed out that the three species from Bhutan (*X. walteri* (Morvan, 1978), *X. bhutanensis* (Morvan, 1979), and *X. cordicollis* (Morvan, 1979)) may represent three subspecies of a single species or eventually be combined into one species when abundant materials are available. Conversely, the male allotype and female holotype of *X. nepalensis* probably represent two different species, in our opinion, based on the original description and figures. The male differs from the female in having elytra with (1) rufous color in the scutellar region and along the sutural margin to mid-length, (2) the humeri more rounded, (3) the basal margination markedly sinuate, and (4) the apices more rounded and slightly oblique medially. Thus, a revision appears necessary to deal with this situation.

***Xestopus gutangensis* Zhu & Kavanaugh, sp. nov.**
http://zoobank.org/9BF90A02-37CD-4FF6-B5A2-5EF5F4C90A3D
Figures 1, 3–7, 8–10, 19

Type locality. China, Xizang: Mêdog (29.46414°N, 95.73563°E), altitude 2025 m.

Type material. ***Holotype.*** Male (IZAS), body length = 16.9 mm, board mounted, genitalia dissected and glued on plastic film pinned under specimen, "Xizang, Nyingchi Prefecture, Mêdog County, Gutang Township, Xingkai village, 29.46414°N, 95.73563°E"; "2025 m, 2019.VIII.15 N, Liang H.B. & Xu Y. lgt., Institute of Zoology, IZAS"; "HOLOTYPE ♂ *Xestopus gutangensis* sp. nov. des. ZHU & KAVANAUGH 2020" [red label]. ***Paratypes*** (34 males and 45 females): one female (IZAS), "CHINA, Yunnan, Gongshan County, Dulongjiang Township, Bapo, 1412 m, 27.73902°N, 098.34975°E, 26 October 2004, Stop # LHB-2004-033, H.-B. Liang collector"; 14 males and 13 females (CAS, IZAS), "CHINA, Yunnan, Gongshan County, Dulongjiang Township, Bapo, Mulangdang, 1355 m, 27.75256°N, 098.34745°E, 4 November 2004, Stop # LHB-2004-046, H.-B. Liang collector"; one male and three females (CAS, IZAS), "CHINA, Yunnan, Gongshan County, Dulongjiang Township, 0.6 km N of Dizhengdang village on Dulong Jiang, 28.08442°N, 098.32652°E, 1880 m, 29 October 2004, Stop # DHK-2004-061B, D.H. Kavanaugh, G. Tang & D.-Z. Dong collectors"; three females (CAS, IZAS), "CHINA, Yunnan, Gongshan County, Dulongjiang Township, 0.6 km N of Dizhengdang village on Dulong Jiang, 28.08442°N, 098.32652°E, 1880 m, 30 October 2004, Stop # DHK-2004-064, D.H. Kavanaugh, G. Tang & D.-Z. Dong collectors"; one male and three females (CAS, IZAS), "CHINA, Yunnan, Gongshan County, Dulongjiang Township, west bank of Dulong Jiang at Elideng village, 1640 m, 28.00287°N, 098.32145°E, 3 November 2004, Stop # DHK-2004-073, D.H. Kavanaugh, G. Tang & D.-Z. Dong collectors"; one male (CAS), "CHINA, Yunnan, Gongshan County, Dulongjiang Township, 0.5 km N of Kongdang, 1500 m, 27.88111°N, 098.34063°E, 25 October 2004, Stop # DHK-2004-057B, D.H. Kavanaugh , H.-B. Liang & D.-Z. Dong collectors"; two males and three females (CAS, IZAS), "CHINA, Yunnan, Gongshan County, Dulongjiang Township, 0.5 km N of Kongdang, 1500 m, 27.88111°N, 098.34063°E, 25 October 2004, Stop # DHK-2004-057C, D.H. Kavanaugh, Q.-B. Hou, H.-B. Liang, D.-Z. Dong & G. Tang collectors"; six males and eight females (CAS, IZAS), "CHINA, Yunnan, Gongshan County, Dulongjiang Township, Dulong Jiang at Xianjiudang village, 1580 m, 27.94092°N, 098.33340°E, 4 November 2004, Stop # DHK-2004-074, D.H. Kavanaugh, M.A. Dixon, G. Tang & D.-Z. Dong collectors"; one male and five females (IZAS), the same collecting data as holotype; six males and four females (IZAS, CAS), "CHINA, Tibet, Bomi, Yi'ong, Tangmai bridge, Beach of Yi'ong Zangbo, 30.09633°N, 95.06577°E"; "2035 m, 2006.8.30 N, Liang H.B., Song Z.S., Institute of Zoology, Chinese Acad. of Sciences"; one male and one female (IZAS), "CHINA, Xizang, Nyingchi, Bomi, Yi'ong, Tangmai bridge, Beach of Yi'ong Zangbo, 30.09633°N, 95.06577°E"; "2035m, 2020.VIII.31 N, Liang H.B. & Zhang N. lgt., Institute of Zoology, Chinese Acad. of Sciences"; one male and one female (IZAS), "CHINA, Xizang, Nyingchi, Bomi, Yi'ong, Tangmai bridge, Beach of Yi'ong Zangbo, 30.09633°N, 95.06577°E"; "2035 m,

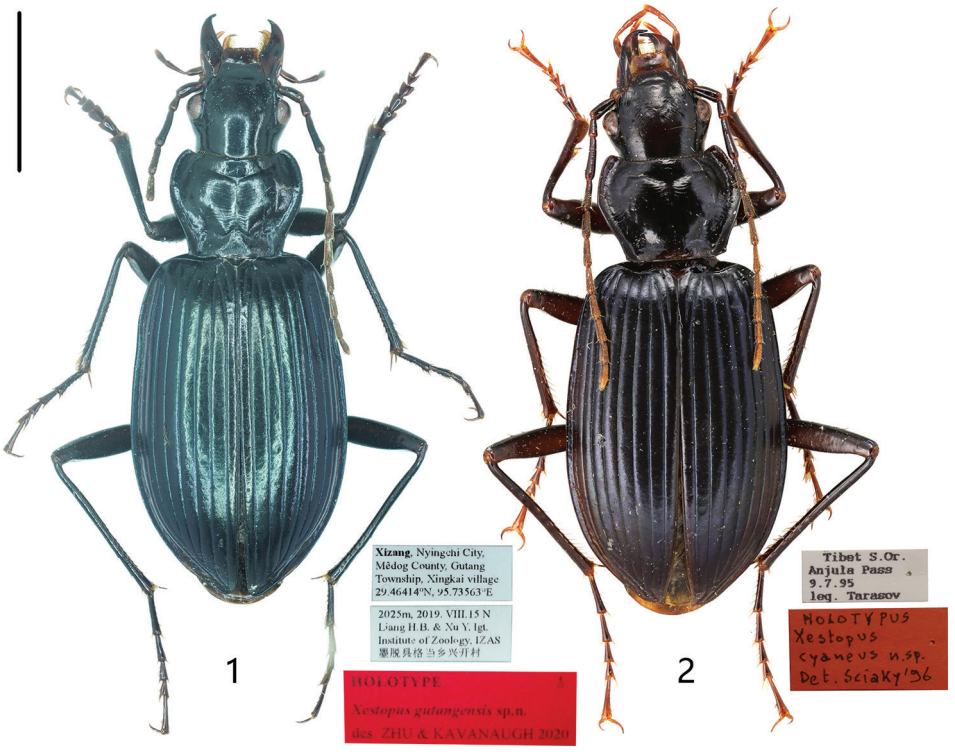

Figures 1, 2. Holotypes of *Xestopus* spp. **1** *X. gutangensis* Zhu & Kavanaugh, sp. nov. (male, Xizang, IZAS) **2** *X. cyaneus* Sciaky & Facchini, 1997 (female, Xizang, CRS). Scale bar: 5.0 mm.

2020.IX.1 N, Liang H.B. & Zhang N. lgt., Institute of Zoology, Chinese Acad. of Sciences"; All paratypes also bear the following label: "PARATYPE *Xestopus gutangensis* sp. nov. des. ZHU & KAVANAUGH 2020" [red label].

Diagnosis. Dorsum black, elytra with more or less bluish metallic luster. Anterior supraorbital setae present. Pronotum with lateral margins faintly sinuate before posterior angles. Apices of elytra rounded (Fig. 6). Hind wings full-sized. Metepisternum long and narrow.

Comparisons. This new species is most similar to *Xestopus cyaneus*, sharing the bluish elytra and full-sized hind wings, which are distinctive features in the genus. *X. gutangensis* sp. nov. can be readily distinguished from *X. cyaneus* by: (1) anterior pair of supraorbital setae present; (2) apices of elytra rounded; (3) apical lamella of median lobe strongly bent ventrally like a hook; (4) endophallus without a densely setose area on left side; (5) gonocoxite II of female ovipositor very long. Supernumerary setae have been found in some *X. gutangensis* specimens in the area of the posterior supraorbital setae, on the pronotal lateral margins and posterior angles, and on the external margin of gonocoxite II (as ensiform setae). These additional setae were not observed on any of the specimens of *X. cyaneus* that we examined.

Description. BL = 15.7–18.0 mm, BW = 6.4–7.8 mm. Dorsum (Fig. 1) black, elytra with more or less bluish metallic luster, very faint in some specimens; appendages dark, antennomeres 4–11, labial and maxillary palpi, apex of mouthparts and tarsomeres dark brown; venter black, without metallic luster. Head, pronotum and elytra with strong isodiametric microsculpture.

Head with vertex smooth; frontal impressions shallow and curved, in front of eyes; clypeus with anterior margin faintly emarginate; labrum with anterior margin straight; temporae slightly swollen behind eyes; both anterior and posterior pairs of supraorbital setae present (two pairs of posterior supraorbital setae present in a few specimens); antennae long and slender, extended to basal one-third of elytra.

Pronotum cordiform, slightly transverse, PW/PL = 1.38–1.55, widest near anterior quarter; anterior margin markedly concave, slightly wider than basal margin, PAW/PBW = 1.13–1.33, lateral margins broadly rounded before middle, then distinctly narrowed to base, faintly sinuate before posterior angles, PW/PBW = 1.31–1.50, lateral margins with one pair of setae at widest points and posterior angles respectively (with an additional seta on one or both sides and at either or both widest points and posterior angles), basal margin straight; anterior angles rounded, moderately extended forward, posterior angles distinctly obtuse; disc glabrous, gently convex; median line fine but clearly defined; basal fovea large and deep, without punctures but with some wrinkles; lateral explanations very wide and impunctate.

Elytra wide, EL/EW = 1.44–1.59, moderately dilated towards apex, widest near posterior third, apices rounded; basal margination complete and straight; humeral angles rounded, without teeth; intervals moderately convex, striae shallow and impunctate; parascutellar striae well developed and short, between suture and stria 1; parascutellar pores present; interval 3 without setigerous pores; umbilicate series on interval 9 composed of approximately 25 setigerous pores, continuous in middle. Hind wings fully sized.

***Venter*.** Propleuron, mesoepisternum, and metepisternum glabrous, metepisternum long and narrow; all abdominal sternites with a few shallow wrinkles laterally.

Legs long and slender, all tarsi smooth, claws distinctly denticulate in basal half.

***Male genitalia*.** Median lobe (Figs 3, 7) long, slender, and straight but slightly bent ventrally; apical orifice opened dorsally, very long and wide, from basal bulb to apical lamella; in dorsal view (Fig. 3A), left and right margins both straight, apical lamella long, length about twice its basal width, apex rounded; in left lateral view (Fig. 3B), ventral margin weakly expanded in the middle, apical portion slightly bent dorsally and then strongly bent ventrally like a hook at apex. Left paramere (Fig. 5) large and round, with a membranous filament at apex. Right paramere (Fig. 4) markedly styloid and curved, the angle between basal portion and apical portion near 90°; apical portion moderately bent ventrally, apical hook rounded. Endophallus (Fig. 7) simple, with only a single large lobe, straight, extended right at an angle of about 30° relative to longitudinal axis of the median lobe in dorsal view (Fig. 7D); surface smooth, without setae or scales; gonopore and gonopore lobe folded in this specimen.

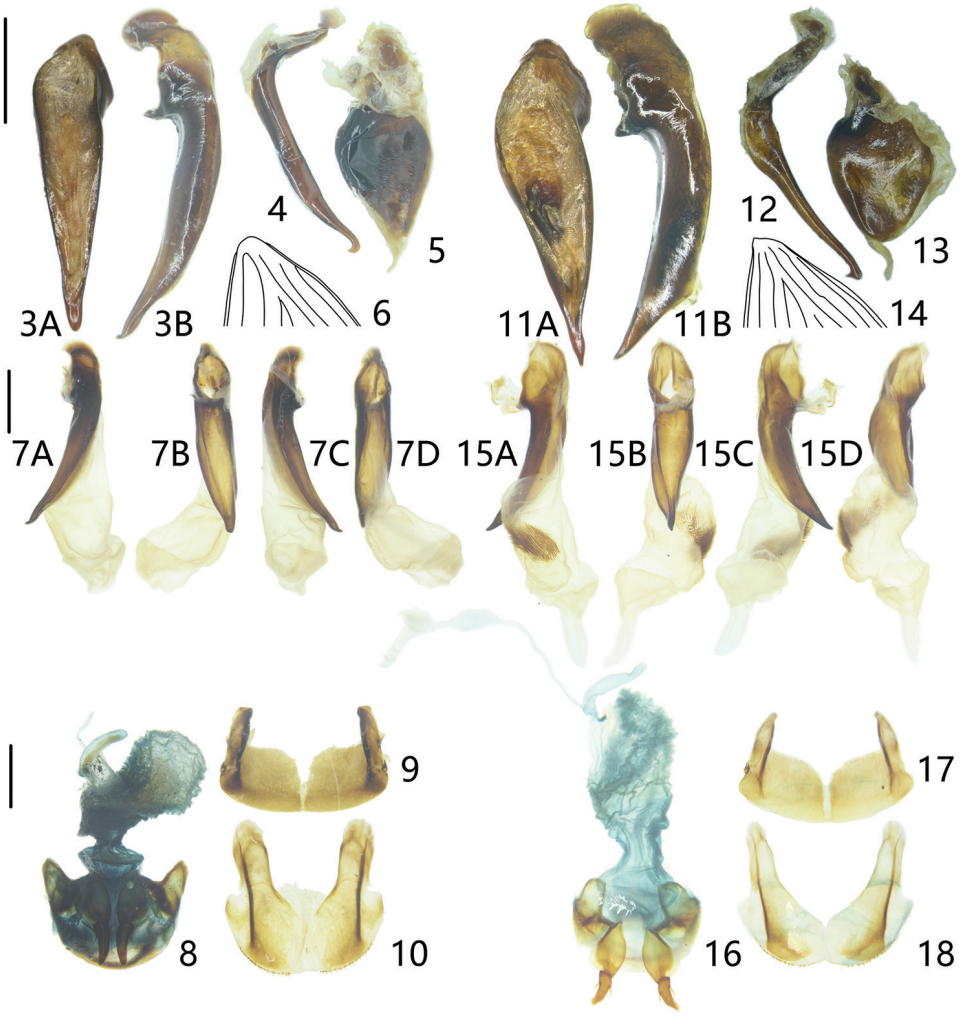

Figures 3–18. Morphological features of *Xestopus* spp. **3–6** holotype of *X. gutangensis* Zhu & Kavanaugh, sp. nov. **7–10** paratype of *X. gutangensis* Zhu & Kavanaugh, sp. nov. **11–18** *X. cyaneus* Sciaky & Facchini, 1997 **3, 11** median lobe of aedeagus **A** dorsal view **B** left lateral view **4, 12** right paramere **5, 13** left paramere **6, 14** apex of left elytron **7, 15** endophallus **A** left lateral view **B** ventral view **C** right lateral view **D** dorsal view **8, 16** female reproductive system **9, 17** female tergum VIII **10, 18** female sternum VIII. Scale bars: 1.0 mm.

Female genitalia (Figs 8–10). Gonocoxite II of ovipositor very long, length about four times basal width, with one ensiform seta at external margin in most specimens (two ensiform setae in a few specimens and ensiform seta very small in some specimens), sensory pit of apical gonocoxite absent. Bursa copulatrix very large, rounded. Spermatheca moderately long and tube-like, length about five times maximum width.

Distribution (Fig. 19)**.** This species is known from Bomi and Mêdog counties, Xizang, and from the northern part of the Dulongjiang valley in Gongshan County, Yunnan.

Etymology. The new species is named for Gutang Township, where the type locality, Mêdog, is located.

Affinities. Among all *Xestopus* species, only *X. gutangensis* and *X. cyaneus* have the bluish elytra and full-sized hind wings. Thus, a close relationship of these two species is likely, and the absence of anterior supraorbital setae in the latter is clearly apomorphic within the genus.

Xestopus cyaneus Sciaky & Facchini, 1997

Figures 2, 11–18, 19

Xestopus cyaneus Sciaky & Facchini, 1997: 235 (type locality: Anjula Pass, SE Tibet, China; holotype in CRS); Lorenz 1998: 373 (catalogue); Hovorka and Sciaky 2003: 530 (catalogue); Lorenz 2005: 399 (catalogue); Hovorka 2017: 769 (catalogue).

Material examined. Total 196 specimens. ***Holotype*** of *Xestopus cyaneus* Sciaky & Facchini, 1997, by monotypy (CRS): female, body length = 16.1 mm, board mounted, "Tibet S. Or. Anjula Pass 9.7.95 leg. Tarasov", "HOLOTYPUS Xestopus cyaneus n. sp. Det. Sciaky 1996" [red label]. One male and one female (CRS), "China, Tibet, Motuo co., Hanmi, VI.2013"; one male and one female (CRS), "China, Tibet, Motuo co., Hanmi, VIII.2013"; one male and three females (CRS), "China, Tibet, Linzhi area, Linzhi, 2000 m, VIII–IX.2019"; three females (CRS), "China, Tibet, Linzhi area, Mt. Serkyla, 3000–4000 m, VIII.2018"; four females (CRS), "China, Tibet, Bomi county, 2500 m, VIII.2019"; one female (IZAS), "China, Yunnan, Fugong, Lishadi Town, 4km below Shibali Road, 27.15727°N, 98.79784°E, 2280 m, 2005.VIII.11 N, Tang G lgt."; two males and three females (CAS, IZAS), "CHINA, Yunnan, Fugong County, Lishadi Township, 4 km E of Shibali on Shibali Road, 2280 m, 27.15727°N, 098.79784°E, 11 August 2005, Stop# DHK-2005-076A, D. Z. Dong collector"; five males and two females (CAS, IZAS), "CHINA, Yunnan, Fugong County, Lishadi Township, Shibali Road from Galadi village to 2.5 km W, 27.13863°N, 098.82174°E to 27.14286°N, 098.82001°E, 1845–1940 m, 9 August 2005, Stop #DHK-2005-071, D.H. Kavanaugh, H.B. Liang, & D. Z. Dong collectors"; one female (IZAS), "CHINA, Yunnan, Fugong County, Lishadi Township, Yamu He at Shikuliudi village, 27.11876°N, 098.83118°E, 1800 m, 26 April 2004, Stop #LHB-2004-008B, Liang H.-B. collector"; one female (CAS), "CHINA, Yunnan, Fugong County, Lumadeng Township, 4 km E of Lao Shibali on Lao Shibali Road, 2120 m, 27.09700°N, 098.80570°E, 21 August 2005, Stop# DHK-2005-101, D. Z. Dong collector"; three males and three females (CAS, IZAS), "CHINA, Yunnan, Fugong County, Lumadeng Township, 1.5 km above confluence of North and South Forks of Yamu He on Lao Shibali Road, 1825 m, 27.11992°N, 098.83150°E, 15 August 2005, at night, Stop# LHB-05-55, H.B. Liang collector"; three females (IZAS), "China, Yunnan, Gongshan,

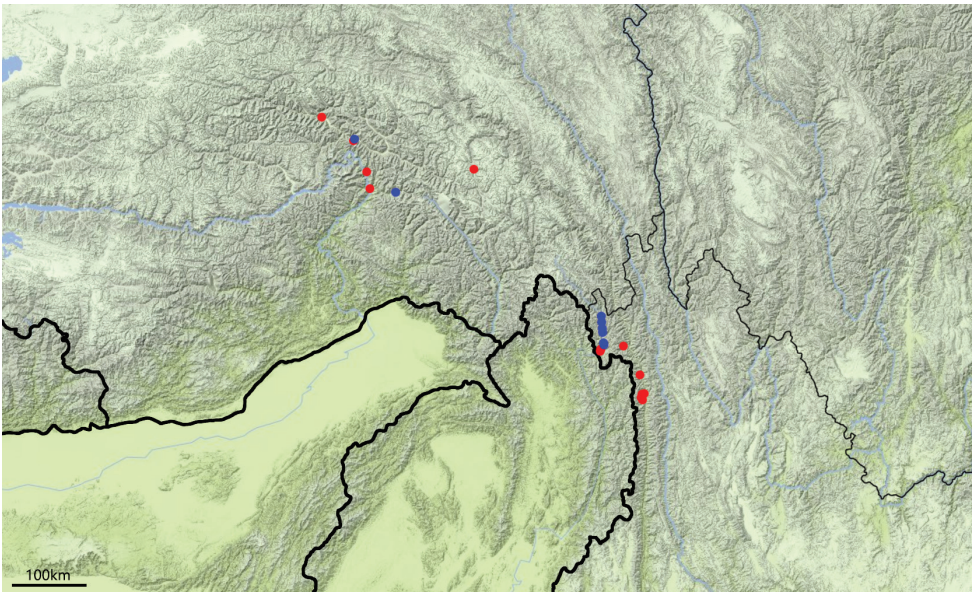

Figure 19. Distribution map for *Xestopus* from China: *X. gutangensis* sp. nov. (blue); *X. cyaneus* (red).

Dulongjiang, Maku village, 27.684453°N, 98.30547°E, 1691 m, 2019. VIII.21 N, Liang HB & Xu Y lgt."; one female (IZAS), "CHINA, Yunnan, Gongshan County, Dulongjiang Township, Maku, 1823 m, 27.68553°N, 098.30425°E, 2 November 2004, Stop # LHB-2004-042, H.-B. Liang collector"; three males and three females (CAS, IZAS), "CHINA, Yunnan, Gongshan County, Dulongjiang Township, Maku village, 1800 m, 27.68498°N, 098.30299°E, 28 August 2006, Stop #DHK-2006-100, D.H. Kavanaugh, J.A. Miller, & D.Z. Dong collectors"; 43 males and 35 females (CAS, IZAS), "CHINA, Yunnan, Gongshan County, Dulongjiang Township, Maku village, 27.68545°N, 098.30419°E, 1815 m, 2 September 2006, Stop #DHK-2006-119, Y. Liu & D. Z. Dong collectors"; ten males and nine females (CAS, IZAS), "CHINA, Yunnan, Gongshan County, Dulongjiang Township, 0.1 airkm NW of Maku Yakou, 1880 m, 27.67937°N, 098.29617°E, 31 August 2006, Stop #DHK-2006-110, Y. Liu collector"; nine males and seven females (CAS, IZAS), "CHINA, Yunnan, Gongshan County, Dulongjiang Township, 0.5 air km WSW of Maku village on trail to Maku Yakou, 1845 m, 27.68310°N, 098.30038°E, 29 August 2006, Stop #DHK-2006-103, D. H. Kavanaugh collector"; eight males and five females (CAS, IZAS), "CHINA, Yunnan, Gongshan County, Dulongjiang Township, 0.5 air km WSW of Maku village on trail to Maku Yakou, 1845 m, 27.68310°N, 098.30038°E, 29 August 2006, Stop #DHK-2006-108, D.H. Kavanaugh, J.A. Miller, D.Z. Dong, & Y. Liu collectors"; two males (CAS, IZAS), "CHINA, Yunnan, Gongshan County, Dulongjiang Township, 0.5 airkm WSW of Maku village on trail to Maku Yakou, 1845 m, 27.68310°N, 098.30038°E, 29 August 2006, Stop #DHK-2006-116, D. Z. Dong collector"; one female (CAS), "CHINA, Yunnan Province, Gaoligong Shan, Nujiang Prefecture, Nu-

jiang State Nature Reserve, Qiqi area, 10.3 air km W of Gongshan, 27.71542°N, 98.56529°E, 2010 m, 9–14 July 2000, Stop#00-22C, D.H. Kavanaugh, C.E. Griswold, Liang H.-B., D. Ubick, & Dong D.-Z. collectors"; one male (IZAS), "China, Tibet, Bomi, Yi'ong, Tongmai bridge, 30.09633°N, 95.06577°E, 2035m, 2006.VIII.30 N, Liang HB & Song ZS lgt."; one male (IZAS), "CHINA, Xizang, Nyingchi, Bomi, Yi'ong, Tangmai bridge, Beach of Yi'ong Zangbo, 30.09633°N, 95.06577°E, 2035 m, 2020.VIII.31 N, Liang H.B. & Zhang N. lgt."; one female (IZAS), "CHINA, Xizang, Nyingchi, Bomi, Yi'ong, Tangmai bridge, Beach of Yi'ong Zangbo, 30.09633°N, 95.06577°E, 2035 m, 2020.IX.1 N, Liang H.B. & Zhang N. lgt."; one male (IZAS), "China, Tibet, Mêdog, Dagmo road to Gutang, 29.5150°N, 95.4642°E, 1679 m, 2016.VIII.16, Qiu TF lgt."; one female (IZAS), "China, Xizang, Zhamo-Mêdog road 78K, light trap, 29.66570°N, 95.49577°E, 2104 m, 2017.VIII.15 N, Liang HB lgt."; three males and three females (IZAS), "China, Xizang, Nyingchi City, Mêdog County, Dagmo Township, Zhamo-Mêdog road 80K, 29.657947°N, 95.489994°E, 2073.40 m, 2020.IX.17 N, Liang H.B. & Xu Y. lgt."; one male (IZAS), "China, Xizang, Nyingchi City, Mêdog County, Dagmo Township, Zhamo-Mêdog road 80K, 29.657947°N, 95.489994°E, 2073.40 m, 2020.IX.17 N, Zhang Neng lgt.";one female (CCCC), "China, Xizang, Bomi, Tongmai, 2262 m, 2016.VII.24, Lu YQ lgt."; two males and two females (CCCC), "China, Xizang, Bomi, Yi'ong, 2380 m, 2016. VII.26, Lu YQ lgt."; one male and two females (CCCC), "China, Xizang, Mêdog, 80K, 2350 m, 2016.VII.30, Lu YQ lgt.".

Diagnosis. Dorsum (Fig. 2) black, elytra with more or less bluish metallic luster. Anterior pair of supraorbital setae absent (an anterior supraorbital seta present on one or both sides in a very few specimens). Pronotum with lateral margins very faintly sinuate before posterior angles. Apices of elytra acute (Fig. 12). Hind wings full-sized. Metepisternum long and narrow.

Supplementary description. BL = 15.4–18.6 mm, BW = 6.2–7.4 mm. PW/PL = 1.37–1.54. PW/PBW = 1.40–1.59. PAW/PBW = 1.19–1.44. EL/EW = 1.51–1.68.

***Male genitalia*.** Median lobe (Figs 11, 15) long, stout and straight but slightly bent ventrally; apical orifice broadly open dorsally, very long and wide, from basal bulb to apical lamella; in dorsal view (Fig. 11A), left and right margins both straight, apical lamella very long, length about three times as its basal width, moderately dilated in the middle, apex acute; in left lateral view (Fig. 11B), ventral margin straight, not expanded in the middle, apical portion slightly bent ventrally, apical lamella thick and straight. Left paramere (Fig. 13) large and round, with a membranous filament at apex. Right paramere (Fig. 12) strongly styloid and curved, the angle between basal portion and apical portion nearly 100°; apical portion straight, apical hook acute. Endophallus (Fig. 15) simple, only a single large lobe, straight, extended left at an angle of about 45° relative to longitudinal axis of the median lobe in dorsal view (Fig. 15D); surface with a densely setose area present on left side, without scales; gonopore lobe long and narrow, located at apex of endophallus, gonopore directed toward apex.

Female genitalia (Figs 16–18). Gonocoxite II of ovipositor moderately long, length about three times basal width, with one ensiform seta at external margin, sen-

sory pit of apical gonocoxite absent. Bursa copulatrix large and elongate. Spermatheca moderately long and tube-like, length about five times maximum width.

Distribution (Fig. 19). This species is known from Xizang (Bomi and Mêdog counties) and Yunnan (Gongshan and Fugong, new provincial record). The records from Sichuan cited by Hovorka and Sciaky (2003) and Hovorka (2017) is clearly wrong.

Remarks. The number of pairs of supraorbital setae is a very important character within Carabidae for both classification and systematics. In most members of the tribe Harpalini, only one pair of supraorbital setae is present at a middle position in relation to the diameter of the eyes, while most other ground beetles have two pairs of supraorbital setae. A few non-harpaline carabids lack one pair of supraorbital setae, but the other pair is present either in an anterior or a posterior position relative to the eyes instead of at the middle position as in Harpalinae. It is, therefore, usually easy to determine whether it is the anterior or posterior pair of supraorbital setae that is missing. Variation in this apparently apomorphic feature does not appear to have much value in high-level phylogeny. For example, members of genus *Reflexisphodrus* Casale, 1988 and genus *Eosphodrus* Casale, 1988 (Sphodrini, Sphodrina) lack the posterior pair of supraorbital setae while those of *Pterostichus* subgenus *Unitrichus* Sciaky, 1997 (Pterostichini) lack the anterior pair just like most members of *Xestopus cyaneus*. The single species of *Unitrichus*, *Pterostichus platyops* Sciaky, 1997, from Yunnan, China, is distinguished from members of other subgenera of *Pterostichus* by the absence of the anterior pair of supraorbital setae and the presence of many setae at the middle of mentum. We have found a second, undescribed species from Yunnan, China with the similar appearance of *P. platyops* and many setae present at the middle of mentum, but with the anterior pair of supraorbital setae present (unpublished data), as in *Xestopus gutangensis* Zhu & Kavanaugh, sp. nov. These two examples show that differences in the number of supraorbital setae between closely related species is possible, even if it is rarely seen.

In our examination of 260 specimens of *X. cyaneus* and *X. gutangensis* Zhu & Kavanaugh, sp. nov., we found only five that had abnormal numbers of supraorbital setae for their species assignment based on other characters. All were clearly *X. cyaneus* based on the shape of the elytral apex and features of either male or female genitalia. Three of these, including one male from Xizang and one male and one female from Yunnan, had an anterior supraorbital seta present on one side but absent from the other. In addition, we found one female from Xizang and one female from Yunnan that had anterior supraorbital setae present on both sides. Consequently, the presence or absence of anterior supraorbital setae is slightly less reliable for distinguishing these two species than are the shapes of the elytral apices and male and female genitalia.

Key to species of genus *Xestopus* Andrewes, 1937

1 Elytra with more or less bluish metallic luster; metepisternum long and narrow; hind wings full-sized **2**

– Elytra black or brown, without metallic luster; metepisternum short and wide; hind wings atrophied **3**

2 Anterior pair of supraorbital setae present; apices of elytra rounded ..... ***X. gutangensis* sp. nov.**

– Anterior pair of supraorbital setae absent; apices of elytra acute ..... ***X. cyaneus* Sciaky & Facchini, 1997**

3 Pronotum with lateral margins slightly rounded at middle; eyes small; 18 mm..... ***X. alticola* (Fairmaire, 1889)**

– Pronotum with lateral margins distinctly rounded at middle; eyes large..... **4**

4 Apical lamella of median lobe rounded at tip; 15–18 mm..... ***X. kumatai* (Habu, 1973)**

– Apical lamella of median lobe truncated at tip; 18–23 mm..... **5**

5 Pronotum with lateral margins markedly sinuate before posterior angles; 20 mm..... ***X. cordicollis* (Morvan, 1979)**

– Pronotum with lateral margins faintly sinuated before posterior angles..... **6**

6 Apices of elytra rounded or slightly oblique; 18–20 mm..... ***X. nepalensis* Morvan, 1982**

– Apices of elytra truncate; 19–23 mm **7**

7 Apices of elytra markedly truncate; pronotum longer, anterior angles more extended anteriorly, posterior angles more rounded; apical hook of right paramere more developed; apical lamella of median lobe narrower; 20–23 mm... ***X. walteri* (Morvan, 1978)**

– Apices of elytra moderately truncate; pronotum wider, anterior angles less extended anteriorly, posterior angles more acute; apical hook of right paramere less developed; apical lamella of median lobe wider; 19–20 mm ..... ***X. bhutanensis* (Morvan, 1979)**

Acknowledgements

We thank Mr Changchin Chen (CCCC) for his assistance in granting us the access to the material under his care and for depositing types of the new species in the IZAS collection. We thank Dr Riccardo Sciaky for providing us the photo of the holotype of *Xestopus cyaneus*. Gratitude is also extended to Mrs Yuan Xu, Mr Yanquan Lu, Mr Zhishun Song, and Mr Tengfei Qiu for their help in collecting specimens for the study. This work was supported by grants from the Second Tibetan Plateau Scientific Expedition and Research Program (STEP) (grant no. 2019QZKK0501) and the National Natural Science Foundation of China (grant no. 31970400).

References

Andrewes HE (1937) Keys to some Indian genera of Carabidae (Col.). VIII. The genera of the Sphodrini group. The Proceedings of the Royal Entomological Society of London (B) 6: 59–63. https://doi.org/10.1111/j.1365-3113.1937.tb00297.x

Casale A (1981) Carabidae dell'Himalaya Nepalese. Sphodrini nuovi o poco noti (Insecta: Coleoptera). Senckenbergiana Biologica 61[1980]: 383–395.

Casale A (1988) Revisione degli Sphodrina (Coleoptera, Carabidae, Sphodrini). Museo Regionale di Scienze Naturali (Torino), Monografie 5: 1–1024.

Fairmaire L (1889) [new species] Bulletin des Séances et Bulletin bibliographique de la Société Entomologique de France (6) 9: [part] Bulletin des Seances: xv–xvii.

Habu A (1973) On a collection of Carabidae from Nepal made by the Hokkaido University Scientific Expedition to Nepal Himalaya, 1968 (I). The Bulletin of the National Institute of Agricultural Sciences (C) 27: 81–132.

Habu A (1978) Fauna Japonica. Carabidae: Platynini (Insecta: Coleoptera). Keigaku Publishing Co., Tokyo, 447 pp. [xxxvi pls.]

Hovorka O (2017) Subtribe Dolichina Brullé, 1834. In: Löbl I, Löbl D (Eds) Catalogue of Palearctic Coleoptera (Vol. 1. 2nd Edn.). Brill, Leiden and Boston, 768–769.

Hovorka O, Sciaky R (2003) Subtribe Dolichina Brullé, 1834. In: Löbl I, Smetana A (Eds) Catalogue of Palaearctic Coleoptera (Vol. 1). Archostemata–Myxophaga–Adephaga. Apollo Books, Stenstrup, 529–530.

Lorenz W (1998) Systematic List of Extant Ground Beetles of the World. Wolfgang Lorenz, Tutzing, 502 pp.

Lorenz W (2005) Systematic List of Extant Ground Beetles of the World (Insecta Coleoptera Geadephaga: Trachypachidae and Carabidae incl. Paussinae, Cicindelinae, Rhysodinae), second edition. Wolfgang Lorenz, Tutzing, 530 pp.

Morvan P (1978) Ergebnisse der Bhutan-Expedition 1972 des Naturhistorischen Museums in Basel. Coleoptera: fam. Carabidae, tribus Pterostichini und Sphodrini. Entomologica Basiliensia 3: 87–102.

Morvan P (1979) Ergebnisse der Bhutan-Expedition 1972 des Naturhistorischen Museums in Basel. Coleoptera: Fam. Carabidae, tribus Sphodrini. Entomologica Basiliensia 4: 31–42.

Morvan P (1982) Contribution à la connaissance des coléoptères Carabidae du Népal (7ème note) (Coleoptera Carabidae, Anchomenini et Sphodrini). Miscellanea Entomologica 49: 37–48.

Schmidt J, Will K (2020) A new subgenus for "*Acalathus*" *advena* (LeConte, 1846) and the challenge of defining Calathina based on morphological characters (Coleoptera, Carabidae, Sphodrini). Zootaxa 4722 (4): 326–338. https://doi.org/10.11646/zootaxa.4722.4.2

Sciaky R (1997) New subgenera and new species of Pterostichini from China (Coleoptera Carabidae). Bollettino del Museo Civico di Storia Naturale di Venezia 47: 153–176.

Sciaky R, Facchini S (1997) *Xestopus cyaneus* new species from Cina (Coleoptera Carabidae). Bollettino della Società Entomologica Italiana 129: 235–240.

Sciaky R, Wrase DW (1998) Two new genera of Sphodrini Dolichina from China (Coleoptera Carabidae). Bolletino della Società Entomologica Italiana 130: 221–232.

Shi HL, Liang HB (2015) The genus *Pterostichus* in China II: the subgenus *Circinatus* Sciaky, a species revision and phylogeny (Carabidae, Pterostichini). ZooKeys 536: 1–92. https://doi.org/10.3897/zookeys.536.5982

Shi HL, Sciaky R, Liang HB, Zhou HZ (2013) A new subgenus *Wraseiellus* of the genus *Pterostichus* Bonelli (Coleoptera, Carabidae, Pterostichini) and new species descriptions. Zootaxa 3664 (2): 101–135. https://doi.org/10.11646/zootaxa.3664.2.1